THE UNIVERSITY
of EDINBURGH

The Functional Role of HCMV miRNAs

Jonathan Andrew Pavelin

Thesis presented for the degree of

Doctor of Philosophy

University of Edinburgh

2015

Declaration

I declare that the research and analysis presented in this thesis is my own unless otherwise stated. This work has not been submitted for any other degree and this thesis was composed entirely by myself.

Jonathan A. Pavelin

March 2015

Abstract

miRNAs are a species of small-regulatory RNA that post-transcriptionally regulate gene expression *via* the RNA induced silencing complex (RISC). They are encoded ubiquitously among animals and plants, and have recently been shown to be encoded by the majority of herpesviruses. It seems likely that herpesvirus encoded miRNAs have evolved as a tool for the manipulation of host-cellular and viral-gene expression during infection.

Human cytomegalovirus (HCMV) is a clinically important herpesvirus that represents a significant cause of morbidity and mortality in the immune-compromised. HCMV encodes as many as 25 miRNAs during infection, but the function of the majority of these is not known.

Identifying the targets of HCMV miRNAs will not only establish a basis for understanding the role of miRNAs within the context of HCMV infection, but also provide a means for discovering novel host-virus interactions. Using RISC immunoprecipitation and siRNA screening, host-cellular targets of viral miRNAs that play important roles in the biology of HCMV were identified. ATP6VOC, a key component of the vacuolar-ATPase, was shown to be a target of miR-US25-1 and subsequent siRNA knockdown of ATP6VOC resulted in the almost complete inhibition of infectious virion production. Despite this, ATP6VOC knock-down did not inhibit viral entry, DNA synthesis, or gene expression, highlighting a possible role for ATP6VOC in the assembly and egress of HCMV.

A critical step in HCMV assembly and egress is the formation of the juxtanuclear virion assembly compartment (VAC). The HCMV VAC is derived from host-cellular endocytic and secretory vacuoles, and is crucial for the efficient nuclear egress of nucleocapsids, cyotplasmic tegumentation, final envelopment, and the egress of mature virions. Using siRNA knock-down, immunofluorescence-microscopy, and western-blot analysis, a crucial role for ATP6VOC and v-ATPase function in the formation of the VAC was demonstrated. siRNA knock-down of ATP6VOC resulted in a failure in the reorganisation of trans-golgi and early-endosomal compartments during infection, resulting in a failure in VAC formation.

These findings demonstrate a crucial role for ATP6VOC during infection, and in so doing identify a novel host factor that is required for HCMV assembly.

Acknowledgements

Firstly, I would like to offer my sincerest thanks to Dr Finn Grey for giving me the opportunity to work on this project. This rescued me from a thoroughly unfulfilling career working in Big Pharma, which without his confidence in my potential, I may have been forced to continue to pursue. He has been an excellent mentor and a good friend. Finn has allowed me to take complete ownership of my work, while always making himself available to discuss the matters at hand, which I understand from previous experience is a hard balance to achieve. He has also been a near limitless source of constant entertainment, and without him my PhD would not have been as fun as it has been.

Thanks also to my forever patient wife, who has put up with my excited ramblings using acronyms that she doesn't understand for the past 4 years, and for her willingness to allow me to sacrifice my weekends and evenings to science (long may it continue says she...).

Finally, thanks also to current and past members of the Grey, Fazakerley, Dalziel, Simmonds, and Digard groups for being a constant and reliable source of knowledge, reagents, caffeine and baked goods.

Table of Contents

List of Figures

List of Tables

List of abbreviations

cCMV	chimpanzee cytomegalovirus
CLASH	cross linking and sequencing of hybrids
CDS	coding sequences
DNA	deoxyribonulceic acid
DMEM	Dulbecco's modified eagle's medium
EBV	Epstein Barr virus
FBS	fetal bovine serum
gB/o/l/h/n/m	glycoprotein
g	gravity
gpCMV	guniae pig cytomegalovirus
HA	haemaglutinin
HSV	herpes simlex virus
HITS CLIP	high-throughput RNA sequencing by cross-linking and immunoprecipitation
hpi	hours post infection
HCMV	human cytomegalovirus
HEK	human embryonic kidney
HHV	human herpes virus
HIV	human immunodeficiency virus
ID	identification
IE	immediate early
IP	immunoprecipitation
IL-6	interleukin-6
IRL	internal repeat long
IRS	internal repeat short
KSHV	Kaposi's sarcoma virus
kb	kilobases
lncRNA	long non-coding RNA
Mann II	Mannosidase II
mTOR	mammalian target of rapamycin
mRNA	messenger RNA
miRNP	micro ribonucleoprotein
µL	microlitre
µM	micromolar
miRNA	microRNA
mCMV	murine CMV
nmol	nano moles
NHDF	normal human dermal fibroblasts
nt	nucleotide
OHV-2	Ovine herpesvirus 2

PBS	phosphate buffered saline
PAR CLIP	photo-activatable ribonucleoside cross-linking and immunoprecipitation
PAGE	polyacrylamide gel electrophoresis
rhCMV	rhesus cytomegalovirus
RNA	ribonucleic acid
RNP	ribonucleoprotein
RISC-IP	RNA induced silencing complex immunoprecipitation
SCID	severe combined immunodeficiency
TRL	terminal repeat long
TRS	terminal repeat short
TNF-α	tumour necrosis factor α
UL	unique long
US	unique short
VAC	virion assembly compartment
VZV	varicella zoster virus
vs	versus

1. Introduction

1.1. Human Cytomegalovirus

Herpesviridae is a family of large DNA viruses that infect fish, birds, and mammals. Over 100 herpesviruses have been identified to date and they share a number of key morphological, genetic, and biological features [1-3]. Herpesviruses are structurally and functionally complex. The herpesvirus genome consists of a large linear double-strand of DNA between 110 kb to 240 kb [1]. Viral DNA replicates in the host cell nucleus, facilitated by a combination of host and viral encoded proteins, and is loaded into an icosohedral nucleocapsid before traversing the nuclear membrane [4-8]. Once in the cytoplasm, the nucleocapsid is surrounded by a plethora of tegument proteins that possess a multitude of functions ranging from viral assembly to host immune suppression [9-13]. Finally, herpesviruses are enclosed in a host acquired lipid envelope prior to egress, containing a variety of viral glycoproteins that are critical for the binding and entry of progeny virus [14-17].

Within the host, herpesviruses typically infect a wide variety of cells and tissues during acute infection (with several notable exceptions, eg. Epstein Barr virus), and then establish a lifelong persistent, latent infection in specific cell types [18].

Based on species specificity, host cell tropism, and genome content the *Herpesviridae* have been further divided into three distinct sub-families (α, β, and γ). Of these, 8 are known to infect humans, (Human herpes virus 1-8).

Human herpes virus 5, more commonly known as HCMV, is the prototypical human β-herpesvirus [2, 3, 18].

HCMV is a clinically important pathogen. It is readily transmissible and infection is prevalent in populations worldwide with infection rates of >95% of adults in developing countries, and <30% of adults in the USA and western Europe [19-23]. Acute infection with HCMV is frequently asymptomatic in immune-competent individuals, although may be associated with mild mononucleosis-like symptoms. Despite a robust immune response, the host fails to completely clear HCMV, and the virus remains latent in a sub-population of cells, likely within the myeloid lineage. The clinical consequences within the immune-competent are thought to be minor, although it has been suggested that the disease burden of HCMV persistence may have links to cancer and immune-senescence in the elderly [24-26]. In immune-compromised individuals, HCMV acute infection and reactivation from latency represents a global healthcare burden and is a significant cause of morbidity and mortality worldwide [18].

1.2. Clinical manifestations

HCMV is capable of infecting a wide range of host cell types during acute infection. HCMV is transmitted *via* infected body fluid, typically urine or saliva, and is able to infect fibroblast, epithelial, endothelial, mesenchymal, macrophage, and smooth muscle cells *in vivo*, causing widespread infection of the liver, lung, kidney, pancreas, retina, and gastrointestinal tract [19, 27-29]. Despite the broad tropism of primary HCMV infection, acute infection is typically asymptomatic in the immune-competent, and is rapidly cleared by the host innate and adaptive immune response.

HCMV represents a significant cause of morbidity and mortality of immune-compromised hosts in whom it is capable of causing severe disease. These include individuals with acquired immune deficiency syndrome (AIDS), allograft recipients, and neonates.

Individuals co-infected with HCMV and HIV experience a loss of $CD4^+$ lymphocyte adaptive immune function with the progression of disease which can cause the reactivation of lytic HCMV replication and systemic, acute infection in these individuals. This can result in severe disease, including colitis, retinitis, oesophagitis, and encephalitis [19, 22, 30-32]. These conditions are a significant contributor to morbidity and mortality in end-stage AIDS patients.

HCMV acute infection and reactivation represent significant hurdles to the success of solid organ transplants. Transplant recipients receive powerful immune-suppressive drugs in order to prevent host *vs* graft disease. This leads

to an increase in susceptibility to the risk of acute CMV disease in these individuals, either by reactivation or by de-novo infection. Chronic HCMV infection is thought to contribute directly to vascular disease and inflammation in kidney, heart, and liver grafts and this leads to a heightened risk of organ rejection [19, 33-35]. Estimates put HCMV chronic infection as contributing to the failure of between 5% and 20% of all solid organ transplants [19, 35].

Finally, HCMV infection in neonates is the leading cause of congenital birth defects in the developed world, affecting as many as 2% of live births [19, 36]. Both the transient and permanent outcomes of intra-uterine infection can be severe. Intrauterine infection of newborns can occur as a result of reactivation in HCMV positive mothers, or more commonly, as a result of primary infection of HCMV naive mothers. Approximately 10% of neonates that contract HCMV *in utero* are symptomatic at birth, with a further 15% developing symptoms in later life. Transient outcomes of infection include growth retardation, pneumonitis, hepatomegaly, splenomegaly, and seizures. Permanent outcomes include motor disabilities, mental retardation, hearing and vision loss, seizures, and death. The fact that this disease typically occurs as a result of primary infection of naive mothers means that this is of particular concern in developed countries, where the likelihood of mothers being HCMV naive is much higher than in developing countries [36].

Despite historical and more recent efforts, attempts at developing an effective HCMV vaccine has not been successful and this is due in part to the complexity of host-virus interactions during infection [37-39]. In terms of licensed

therapeutics for the treatment of acute HCMV infection, clinicians have several options; ganciclovir, valganciclovir, foscarnet, and cidofovir. However, the side effects of these treatments can be severe, and resistant strains quickly arise in subjects treated with these drugs [40, 41].

1.3. HCMV genome organisation and strain variability

The HCMV genome is approximately 240 kb in length, and this is the largest among herpesviruses. The genome structure of HCMV is distinct from other β-herpesviruses. The HCMV genome consists of two unique regions: Unique Long (UL); Unique Short (US), which, unlike other β-herpesviruses, are each flanked by terminal and internal repeats: Terminal Repeat Long/Internal Repeat Long (TRL/IRL) and Terminal Repeat Short/Internal Repeat Short (TRS/IRS). Throughout these regions, genes are distributed across the genome in both orientations, and each gene has been designated sequentially based on genomic location. Similar to other herpesviruses, this genomic location has no apparent bearing on expression kinetics during infection [18].

Thanks to the annotation of HCMV genome sequences and the advent of bacterial artificial chromosome (BAC) technology, it has been possible to generate genetically homogenous virus preparations for several strains, which is critical in functional studies of HCMV and host cell biology during infection [42]. However, HCMV has the capacity to readily adapt to its host. This adaptability extends to cell-culture, and repeated passage of HCMV has resulted in polymorphisms in these experimental strains which need to be taken account in studies of HCMV infection. HCMV strains can be broadly divided into two categories: high passage laboratory adapted strains, and low passage clinical strains. Some lab adapted strains, such as AD169 and Towne, were initially conceived as potential vaccine candidate strains and obtained by serial passage of clinical isolates in fibroblasts. Due to favourable growth kinetics, and the ease

of creating high titre cell free virus stocks, AD169 in particular has been widely adopted for *in vitro* experimentation. However, this adaptation for growth in fibroblasts has resulted in regions of the HCMV genome being permuted. Compared to low passage CMV isolates, both AD169 and Towne have large deletions (22 and 19 ORFs, respectively) and have a variety of sense and non-sense mutations throughout the genome [15, 43-45]. As such, low passage strains of HCMV such as Merlin, and TR are important for studies in epithelial and endothelial cells *in vitro*, and should be used to supplement experimentation using lab adapted strains to rule out strain specific artifacts [42, 46]. A middle ground has been established with the isolation of the TB40 virus strain, which was established by high passage of clinical isolates on endothelial and fibroblast cells, and selected for broad tropism *in vitro* [47]. BAC derived TB40 is more intact genetically compared with other lab adapted strains, but shares many of the beneficial characteristics that makes them well suited for *in vitro* experimentation [47].

1.4. The HCMV replicative cycle

1.4.1. Entry and penetration

HCMV binds to the surface of cells *via* heparan sulphate on the host cell plasma membrane, likely *via* gB and gM/gN [48-50]. Entry of the attached virion occurs by interaction between viral glycoprotein complexes gH/gO/gL (trimer) or gH/gL/UL128-131 (pentamer) with host cell receptors, which facilitate fusion of the viral envelope with the plasma membrane, or triggers endocytic uptake of the virion, respectively [14, 45]. Entry into endothelial and epithelial cells relies on the pentamer complex and occurs in a low pH dependent manner *via* endocytosis [44]. Entry into fibroblast cells relies predominantly on the trimer complex and is pH independent [48]. Penetration of the cytoplasm, therefore, occurs either immediately post entry in fibroblast cells, or upon fusion of the viral envelope with the endocytic membrane in endothelial and epithelial cells. The mechanisms at play and the role of tegument proteins in the trafficking of the HCMV capsid to the nuclear membrane have not been well characterised. However, in HSV-1 infection several roles have been ascribed to tegument proteins that have orthologues in HCMV. The HSV1 protein UL36 (orthologous to HCMV UL48) is responsible for the trafficking of capsids along the microtubule network. UL48 has been shown to be critical for HCMV immediate early (IE) gene expression, so it may be that the roles of these proteins are similar [51-53]. HSV1 protein UL25 (orthologous to the critical gene HCMV UL77 [51, 54]) has been shown to be important in the delivery of viral genomes to the nucleus [55]. Once the capsid reaches the nuclear membrane, it is not

clear how the HCMV genome penetrates the nucleoplasm. There is evidence of other herpesviruses interacting with components of the nuclear pore complex, and it has been shown that capsids do not enter the nucleus. As such it seems likely that viral proteins interact with the nuclear pore and facilitate the ejection of the viral DNA genome into the nucleoplasm [56]. However, the specific viral and host-cellular machinery involved in this process are not known for HCMV.

1.4.2. HCMV gene expression and DNA replication and packaging

The HCMV genome is in the region of 240 kb in length and encodes approximately 200 canonical ORFs [57]. However, recent analysis of the HCMV transcriptome has raised the possibility that the protein coding capacity of the HCMV genome might far exceed this estimate *via* non-canonical translation from upstream ORFs, alternative splicing, and anti-sense transcription, although these observations have not yet been validated [3, 46, 58].

Once the viral genome is unpackaged in the nucleus, HCMV gene expression takes place in a temporal cascade that can be simplistically divided into three categories; immediate early (IE), early, and late [59]. Transcription of the viral genome is dependent on host-cellular RNA polymerase II in addition to transcription factors such as IE72 and IE86 for the generation of viral RNA species, including mRNAs, miRNAs, and lncRNAs [58, 60].

Transcription of the UL122-123 major immediate early region encodes an 18 kb transcript that produces several distinct mRNA species. This includes mRNAs for the immediate early proteins IE72 and IE86 which act synergistically to

activate the expression of host-cellular transcription factors, and viral transcription factors that together facilitate the initiation of the lytic viral gene expression cascade [61-64]. Immediate early events activate the expression of early and delayed early gene expression and these genes encode proteins critical for viral DNA replication such as: UL54 the DNA polymerase; UL44 the DNA processivity factor; UL57 the single stranded DNA binding protein; and UL70/102/150 the helicase-primase complex. Other important early genes that have been characterised have roles in manipulating the host immune response: US2, US3, US6, and US11 interfere with MHC class I presentation; UL83, TRS1/IRS1, US2, and US3 circumvent the cellular response to IFN-α -β -γ stimulation; UL111A, UL146, UL33, UL78, US27, and US28 mimic chemokines or chemokine receptors to inhibit cell mediated immunity and the inflammatory response [65, 66]. Finally the late genes, which depend on the expression of IE genes and the initiation of viral DNA replication, encode the majority of the structural proteins and those involved in assembly and maturation of the HCMV virion [18, 60].

Replication of the viral DNA genome is primarily facilitated by virus encoded machinery, with a viral DNA polymerase, processivity factor, and helicase synthesised early in infection. Initiation of viral DNA replication is dependent on the circularisation of the parent DNA, and proceeds bi-directionally in a rolling circle, producing concatemers which are inverted and cleaved prior to packaging into nucleocapsids [18, 51]. The 162 capsomeres that make up the HCMV nucleocapsid consist primarily of the major capsid protein (UL86), 2

copies of the minor capsid protein (UL48-49), and 1 copy of the minor capsid binding protein (UL46) [67]. Cleavage of the newly synthesised genome and packaging into the capsid occur in concert, *via* the activities of UL89, UL56, and UL51, through the UL104 portal protein [67-69].

1.4.3. Nuclear egress

While still in the nucleus the nucleocapsid becomes partially tegumented, acquiring proteins such as pp150 [70, 71]. Egress of the nucleocapsid through the nuclear membrane is thought to occur *via* the activity of the nuclear egress complex, consisting of UL50/UL53 which span the inner nuclear membrane, and UL97, a kinase that phosphorylates host nuclear protein Lamin A/C. Together these proteins act to destabilise the inner nuclear membrane [5, 6, 67, 72]. It is not entirely clear how the nucleocapsid traverses the inner nuclear membrane and escapes the outer nuclear membrane to penetrate the cytoplasm, but it is likely to occur by a similar method to that seen in HSV1. In HSV1, the nucleocapsid traverses the inner nuclear membrane, and acquires a primary envelope in the process. The capsid then passes through the perinuclear space, the envelope fuses with the outer nuclear membrane, and the naked capsid egresses to the cytoplasm [73]. However, the viral and host proteins involved in HCMV nuclear egress remain elusive.

1.4.4. HCMV assembly, and egress

Secondary tegumentation and acquisition of the final envelope occurs in a juxtanuclear occlusion of host-cellular membranes that forms the virion

assembly compartment (VAC). The HCMV VAC is derived from host-cellular trans-golgi and endosomal compartments, the markers of which colocalise with viral tegument proteins and glycoproteins at late stages during infection [74-77]. The process of final envelopment also appears to occur within the VAC, and egress may occur *via* multivesicular bodies [78-80].

The viral tegument proteins have diverse functions at time-points both pre- and post-immediate early gene expression. These functions include: apoptosis regulation (UL36, UL38); immune evasion (UL83 [pp65], IRS1/TRS1, UL82 [pp71]); capsid trafficking (UL32 [pp150]); DNA release from the capsid (UL47, UL48); activation of gene expression (UL35, UL82 [pp71], US24); nuclear export of unspliced mRNAs (UL69); and virion assembly (IRS1/TRS1, UL32 [pp150], UL99 [pp28]) [11]. Studies have shown that many of these tegument proteins are not explicitly required, although only pp65 and UL36 are entirely dispensable for replication *in vitro.* Several of these proteins are essential to HCMV replication and these include pp150, UL48, UL77, UL94, and pp28. Characterising the functions of tegument proteins *in vitro* has proven difficult as they frequently perform multiple roles throughout the replicative cycle. Functional roles have typically been ascertained by performing deletion and complementation analyses and this makes secondary roles of tegument proteins at late time-points difficult to resolve [11-13, 81].

1.5. HCMV latency

Despite a robust immune response in infected individuals, the host is not able to completely eradicate HCMV infection, and HCMV persists in the host by establishing latency in specific cell types. In these latently infected cells, the HCMV gene expression program is restricted and the gene expression cascade does not progress as in lytic infection. The viral genome is maintained in the absence of virion production, and is able to initiate the lytic gene expression program in response to certain stimuli [82-84].

The factors that are required for the establishment and maintenance of HCMV latency have not been well characterised and the sites of HCMV latency *in vivo* have not been definitively identified. This is due to a combination of several factors: an inability to study the virus within the natural host; the lack of a representative animal model; and the lack of consistency between observations in *ex vivo* latently infected cells and *in vitro* models of latency.

A definitive confirmation of the site of latency can be made when a) cells from naturally infected hosts can be shown to latently carry virus, b) these cells can be stimulated to induce the reactivation of lytic gene expression, c) these cells support *de novo* infection, and d) the virus can establish latency in these cells after *de novo* infection. Viral genomes have been isolated from several tissue types from HCMV sero-positive, but otherwise healthy donors, indicating that these cell types may be sites of HCMV latency *in vivo*.

Low copy numbers of HCMV genomes and viral antigens have been detected in endothelial and smooth-muscle cells isolated from otherwise healthy individuals, indicating that these cell types might represent an important site of HCMV latency, and possibly persistence [83, 85, 86]. However, other studies were unable to detect HCMV in endothelial and smooth-muscle cells from saphenous tissue from triple bypass patients, indicating that physical location within the host may also play a role in the establishment of latency in these cell types [87]. HCMV positive cells have also been isolated from bone marrow stroma from healthy donors, and these cells were able to support productive infection [88]. Bone marrow stroma is a heterogenous tissue, containing multiple cell types, including myeloid lineage cells. Myeloid lineage cells seem likely to represent an important reservoir of HCMV latency [85, 89]. $CD14^+$ myeloid precursors isolated from healthy donors contain low copy numbers of viral genomes, and critically, viral replication can be reactivated as a result of differentiation of these cells *ex vivo* [85, 89, 90].

The majority of cultured cells that can be infected experimentally do not become latently infected. However, an experimental latency model has been established in naive $CD34^+$ myeloid precursor cells *in vitro*. These cells have the pluripotent potential to give rise to many of the cell types from which latent HCMV has been recovered *in vivo*. Evidence put forward by several groups have put forward a model that $CD34^+$ cells represent the major site of latent carriage, and that differentiation to terminal cell fates can stimulate the reactivation of HCMV viral replication [82, 83, 87, 91]. If this is the case it has still not been

established why all lineages that are derived from $CD34^+$ precursors do not carry latent HCMV genomes. It may be that latent carriage of HCMV limits pluripotent potential, forcing development of these cells down specific lineages. These putative factors that potentially regulate the differentiation of latently infected stem cells remain elusive.

Our understanding of HCMV, and other human β-herpesvirus latency is limited by our inability to effectively study these viruses in their natural hosts, and the lack of appropriate animal models that faithfully recapitulate elements of human infection and disease. Herpesviruses are notorious for their diversity, and their evolutionary divergence means that there are substantial differences between CMVs that infect closely related species. Despite this, we have been able to glean some understanding from animal homologues, such as murine CMV (mCMV), rat CMV (rCMV), guinea pig CMV (gpCMV), chimpanzee CMV (cCMV) and rhesus CMV (rhCMV). These homologues continue to be useful for our understanding of HCMV, but they have a number of limitations. rhCMV and cCMV are most similar in terms of sequence homology to HCMV, but they have limited use as animal models due to the expense, ethical implications, and restrictions on the use of primates in research. As such, most comparative studies utilise rodent based models. Rodent CMVs, while divergent from HCMV, have been useful for studying some aspects of HCMV biology. mCMV is capable of establishing latency in cells of the myeloid lineage, and as such has been used for studies of latency and reactivation. rCMV is capable of causing vascular disease and as such has been useful for the study of the involvement of CMV

infection in allograft rejection. gpCMV is capable of intrauterine transmission and has been used to increase our understanding of congenital CMV [92-95]. However, none of these models individually is able to faithfully recapitulate HCMV disease in humans, and the interpretation of data from experiments using these models is complicated by the incomplete structural and functional homology between genes encoded by HCMV and rodent CMVs [96]. Recently, several 'humanised' mouse models for HCMV have emerged. In essence, these models involve the xenograft of populations of HCMV infected myeloid precursor cells into severe combined immunodeficiency (SCID) mice. In these mice, HCMV can establish latency in transplanted monocytes and macrophages, which disseminate throughout the mouse into numerous organ tissues. Crucially, HCMV is capable of then reactivating in these tissues [97, 98]. The potential to study latent and lytic HCMV infection in human cells within the context of a systemic infection represents a promising avenue for future studies of all aspects of HCMV biology *in vivo*.

1.6. miRNAs and the RNA induced silencing complex (RISC)

The HCMV genome encodes a multitude of miRNAs, and although our functional understanding of their roles in infection is in its infancy, the fact that miRNA coding capacity is retained across the *Herpesviridae* is suggestive that they play an important role in herpesvirus biology.

miRNAs are a small RNA species between 21 and 24 nucleotides in length, that are capable of regulating gene expression. They were originally identified as novel developmental regulators in the nematode *Caenorhabditis elegans*. The lin-4 gene in *C. elgeans* encodes an miRNA that negatively regulates lin-14 gene expression by binding to the 3'UTR of the mRNA. This results in a temporal decrease in lin-14 expression which is critical in the development of the worm [99-101]. Initially considered somewhat of a novelty, they are now known to be ubiquitously expressed in animals and plants, and their effect on the regulation of gene expression is widespread. For example, in humans, over 60% of mRNAs are predicted to be regulated by miRNAs [102].

The majority of mature miRNAs are transcribed as primary transcripts (pri-miRNAs) by RNA polymerase II. These transcripts are typically in excess of 1 kb in length, and form multiple hairpin structures by Watson-Crick base pairing [103]. These hairpins are recognised and cleaved by the RNase-III endonuclease, Drosha, to form precursor transcripts (pre-miRNAs), which are then processed in the cytoplasm by the components of the RISC. The pre-miRNA is bound by TRBP (a double strand RNA binding protein) and cleaved by another RNase-III endonuclease, Dicer, in the cytoplasm to generate a

~22 nucleotide long duplex [104, 105]. The strand with the least stable 5' end is loaded into Argonaute 2, a key catalytic component of the RNA induced silencing complex (RISC). This microRNA ribonucleoprotein complex (miRNP) is guided to transcripts based on sequence complementarity of the miRNA to the target mRNA [106]. These miRNP complexes then bring about the post-transcriptional down-regulation of specific target transcripts *via* the activity of RISC [107-109].

miRNP complexes bring about translational repression in a number of ways. Exact complementarity to the miRNA seed sequence results in Ago-2 mediated mRNA cleavage. This type of regulation of transcription is common in plants, but in animals the majority of miRNAs do not share exact complementarity with their target transcripts, and target recognition is driven by a motif known as the seed sequence. This seed sequence consists of the 5' nucleotides of the miRNA between positions 2 and 8, and these are a strong predictor of miRNA targeting. Despite this, interactions frequently occur *via* mis-matches in the seed region and with interaction between miRNA and mRNA outside of the seed region [110].

miRNA regulation of target transcripts is frequently associated with mRNA decay, which is independent of Ago-2 mediated cleavage [102, 110, 111]. Current evidence points to this being a result of miRNP mediated translational repression, *via* recruitment of RNA helicases eIF4A2 and DDX6, and subsequent de-adenylation of the mRNA, rendering the mRNA vulnerable to degradation by exoribonucleases in the cell [112].

Target sites for miRNAs were initially thought to lie exclusively within the 3'UTRs of host transcripts [101]. However, recent advances in miRNA target identification has allowed for extensive mapping of targets sites by deep sequencing, and it appears that miRNAs frequently regulate transcripts *via* target sites in the 3'UTR, CDS, and 5'UTR, and individual miRNAs exhibit targeting bias to specific regions of transcripts .

The emerging role of miRNAs in mammalian gene expression is that of a micromanager; fine tuning the levels of the majority of transcripts in the cell to maintain an optimal protein mileu. As such, the majority of individual miRNP:mRNA interactions bring about marginal changes in target transcript levels [102, 110, 111, 113, 114]. However, there are also scenarios where the impact of miRNA regulation can have a more profound effect. The redundant nature of miRNA;mRNA interactions means that individual miRNAs, can target multiple transcripts within biological pathways, and multiple miRNAs can regulate individual transcripts [115, 116].

This can make the field of miRNA research especially challenging; traditional loss or gain of function studies result in either marginal phenotypes due to the minor effect of an individual miRNA on transcript levels, or no phenotype due to the inherent redundancy in eukaryotic pathways.

1.7. The identification of miRNAs and their targets

1.7.1. miRNA identification

The identification of miRNAs is the first step in characterising their biological role, and represents a foundation of miRNA research. Initial techniques utilised a combination of biochemistry and bioninformatics to identify novel miRNAs, and these approaches have become more complex as high-throughput next generation sequencing techniques have been developed. There are several hurdles to the identification of novel miRNAs by biochemical methods that arise from their intrinsic biological properties. Their short length, functional redundancy, and low levels of expression mean that these techniques can lack sensitivity. As such, increasingly complex bioinformatic prediction algorithms have become an important tool in miRNA discovery.

Biochemical methods for miRNA discovery can be divided into three categories; forward genetics, miRNA cloning, and next-generation sequencing. Initial studies in *Caenorhabditis elegans* used phenotype driven forward genetics approaches to identify lin-4 and let-7 miRNAs. These miRNAs were knocked out in nematodes, and this resulted in defective developmental phenotypes which were subsequently identified to be the result of defective down-regulation of lin-14, and lin-41/57, respectively [100, 101, 117, 118]. These phenotype driven approaches proved extremely time consuming, expensive, and laborious owing to the effort required to identify the genes responsible for a given phenotype. This goes some way to explain the seven year gap between the identification of the first and second miRNA in *C. elegans*. A significant step forward was made

with the approaches that allowed for the cloning of small RNAs from cDNA libraries [119]. This process involves extracting total RNA, and fractionating these RNAs by size using polyacrylamide gel electrophoresis (PAGE). Linkers are then ligated to these small RNAs, allowing for reverse transcription, PCR amplification, and sequencing. It was these approaches that first allowed for the identification of miRNAs in viruses, animals, and plants [120-122]. Although this technique is undoubtedly powerful, it has limited sensitivity as small RNA species isolated by this technique are skewed towards those that are highly expressed, and it is not able to detect miRNAs that are expressed under specific biological conditions. These liabilities have been somewhat circumvented by the development of next-generation sequencing approaches which have massively increased the sensitivity of small RNA sequencing approaches, allowing for the reliable genome wide identification of miRNAs [123].

Bioinformatic approaches have been at the forefront of efforts to annotate novel miRNAs in animals and plants. These bioinformatic tools vary in complexity, but in essence all share the ability to annotate miRNAs based on structural criteria from observed miRNAs, with varying sensitivities [124]. Early methods relied on the conservation of pre-miRNA stem loop structures to annotate putative miRNAs in closely related species (such as MiRScan and MiRseeker). These tools proved extremely useful in early studies in *Caenorhabditis* and *Drosophila* [125, 126]. However, they are relatively insensitive as they are unable to identify divergent miRNA sequences. These shortcomings led to the development of evermore sophisticated tools that are able to annotate miRNAs using complex

algorithms that predict the RNA structural features of pre-miRNAs. Tools such as ProMIR use machine learning approaches that are able to designate criteria that differentiate miRNA encoding stem-loops by comparing them to a dataset of random stem loops from throughout the genome, the majority of which do not encode miRNAs. After candidate stem loops are identified, a series of restriction criteria are applied in order to identify pre-miRNAs. These include structure, sequence composition, sequence conservation, thermodynamic stability, and structural conservation [127]. Despite the stringency of these criteria, these methods still identify many stem loop structures that don't encode miRNAs, and they require a positive dataset with a sufficient number of validated miRNA sequences in order to confidently identify novel sequences.

Together, bioinformatic and biochemical approaches have led to the identification of 24521 putative miRNA loci from 206 species encoding 30424 mature miRNAs, according to the last update of the miRBase miRNA sequence repository [128].

1.7.2. miRNA target identification

A major focus within the field of miRNA research has been the identification of target transcripts. Seed sequence complementarity is a strong predictor of miRNA:mRNA interactions and as such several bioinformatic tools have been conceived that are capable of predicting these canonical interactions. These include miRanda [129], mirSVR [130], PicTar [131], TargetScan [132], TargetScanS [133], RNA22 [134], PITA [135], DIANA-microT [136], and RNAHybrid [137]. These computational approaches apply different criteria to

identify targets. Sequence complementarity, binding energy, target site accessibility, and evolutionary conservation are among the restriction criteria employed. However, it is now clear that a large proportion of miRNA regulation occurs *via* non-canonical interactions with target transcripts, and these are very difficult to predict [110]. As such the relevance of these tools is currently under review within the field. Indeed, analyses of the efficacy of these target prediction algorithms when compared with validated target data, have estimated the false positive rate for the most sophisticated algorithms at 50-70% [113, 138]. This renders these tools unsuitable for systematic screens of miRNA targets. However, these tools continue to be extremely useful in identifying canonical target sites when combined with biochemical analyses that directly identify the targets of miRNAs.

With inherent flaws in the bioinformatic prediction of miRNA targets, techniques that allow for the unbiased identification of miRNA:mRNA interactions are critical. There are several techniques available to researchers that allow for the direct identification of miRNA target transcripts that vary in their complexity, but share a similar basic premise. These techniques utilise the miRNP complex in order to pull-down miRNAs and their target transcripts which can then be isolated and analysed by high-throughput transcriptome analyses. The simplest of these techniques is RISC immunoprecipitation (RISC-IP or RIPCHIP). In RISC-IP miRNP complexes are isolated by immunoprecipitation *via* antibodies against components of RISC, or molecular tags on components of RISC or transfected miRNAs , which allows for the

isolation of a population of RNAs that are enriched for the targets of miRNAs. These RNA samples can then be analysed using microarray, and compared to total RNA to ascertain which transcripts are targeted by miRNAs [139, 140]. An evolution of this technique are high-throughput RNA sequencing by cross-linking and immunoprecipitation (HITS CLIP) and photo-activatable ribonucleoside CLIP (PAR CLIP). These techniques cross-link miRNPs to their target mRNAs using UV radiation prior to immunoprecipitation, which prevents any post-lysis interactions and enables the identification of unstable or transient target interactions. Given the stability of these cross-linked complexes it is also possible to RNAse digest transcripts allowing for the identification of the region which contains the target site by deep sequencing [141, 142]. A further evolution of this is the cross linking and sequencing of hybrids (CLASH) technique, which employs a molecular ligation step to fuse miRNAs to their target mRNAs. This creates a hybrid miRNA:mRNA molecule, representing the candidate miRNA ligated to the binding site of the mRNA. In this way CLASH allows for the direct identification of target transcripts, the candidate miRNA that is responsible for targeting, and the target sites within these transcripts by deep sequencing [143]. This technique is extremely powerful in that it is able to reveal non-canonical interactions that would otherwise be very difficult to predict.

1.8. Viral encoded miRNAs

miRNAs represent a powerful biological tool for micro-managing the cellular environment. As such, it is particularly interesting that several virus families have been shown to encode miRNAs. Adenovirus, torque-teno virus, and polyomavirus family members encode miRNAs in their DNA genomes, and several retroviruses encode miRNAs in their RNA genomes [144-147]. However, the vast majority of viral miRNAs identified to date are encoded by herpesviruses (93% [432/463]), including HCMV which encodes as many 25 mature miRNAs from 15 precursors [128, 148].

Despite the conservation of this capacity to encode miRNAs, miRNA sequence conservation is not observed between herpesvirus family members (with the exception of the EBV and rhesus lymphocryptovirus, and human and chimp CMV) [128, 149, 150]. However, as we learn more about herpesvirus miRNAs targets it is becoming clear that there may be functional conservation or convergence within the family, with orthologous miRNAs regulating the same genes or distinct miRNAs regulating genes within related pathways [151-154]. It also interesting to note that viral encoded miRNAs are predominantly associated with viruses capable of lifelong persistence or latency. During latency, the viral genome must be maintained in a restricted state, yet still responsive to external stimuli that allow for lytic reactivation, all without being detected by the immune system. The ability of the virus to manipulate the host cell despite severe restriction of the viral gene expression program is crucial. In theory, miRNAs represent a 'weapon of choice' for this type of low profile

regulation of host-cellular and viral gene expression during latency. Individual miRNAs are capable of regulating multiple transcripts within diverse cellular pathways, making them genetically economic. Critically, miRNAs can do this without eliciting an immune response, as there is no known pattern recognition receptor that can differentiate viral from host transcribed miRNA, meaning that they are likely non-immunogenic.

The identification and functional characterisation of herpesvirus miRNA targets is still in its infancy and as such their role is not entirely clear. Despite this, there is an emerging picture from functional studies to date that miRNAs facilitate lytic replication and maintain latent persistence in a number of ways: manipulating the host cell innate immune response; manipulating host cell processes to facilitate virus replication; manipulating virus gene expression cascade; and mimicking host cell miRNAs to drive proliferation.

1.8.1. Herpesvirus miRNAs facilitate innate immune evasion

There are several examples of herpesviruses using miRNAs to manipulate cell-mediated innate immune responses in the host. Natural killer (NK) cells are an important component of the innate immune response to viral infection, and circumventing the killing of infected cells by NK cells is a well utilised strategy for viruses to persist [155-157]. As such, it is interesting that activating ligands for NK cells are conserved targets of herpesvirus miRNAs. HCMV encoded miRNA UL112-1, KSHV miRNA K12-7, and EBV BART-2-5P regulate the expression of MHC class I related-sequence B (MICB) during lytic and latent infection [151-153]. MICB encodes a natural killer (NK) cell activating ligand,

which activates cytolytic NK activity, resulting in the killing of infected cells. Herpes virus miRNAs can also regulate the inflammatory response to sites of infection. HCMV miR-UL148D-1 can regulate CCL5, which encodes RANTES, a secreted chemokine that attracts leukocytes to sites of inflammation and also has a role in signaling for the proliferation and activation of NK cells [158]. Clearly, tempering NK cell cytolytic activity and inhibiting the inflammatory response are desirable during lytic replication, and during latency may facilitate the survival of persistently infected cells.

Apoptosis is another well utilised innate immune response to viral infection [159]. Multiple pathways in the cell detect cell stress associated with viral infection and initiate programmed cell death to eradicate infected cells. KSHV miR-K10a contributes to circumventing this response by regulating the expression of tumour necrosis factor like weak inducer of apoptosis receptor protein (TWEAKR) during latent infection [160]. TWEAK signaling induces caspase activation and apoptosis, as well as the induction of pro-inflammatory cytokine expression, both of which are important components of the host innate immune response. Another regulator of apoptotis, Bcl associated factor-1 (Bclaf1), is regulated by HCMV miR-UL112-1 and KSHV miRs-K12-5, -9, -10a, and 10b during lytic HCMV infection, and lytic and latent KSHV infection [161, 162]. The exact role of Bclaf1 in infection is not clear. It has reported pro- and anti-apoptotic functions, and has been shown to be required for T-cell activation [163]. In HCMV infection, Bclaf1 prevents the accumulation of IE1 expression at early time-points as part of the cell's innate restriction of viral infection. As

such, it is possible that down regulation of Bclaf1 is important to de-repress IE expression in latently infected cells. Indeed, observation that miRNA regulation of Bclaf1 facilitates lytic reactivation in KSHV suggest that this might be the case [161, 162, 164].

1.8.2. Herpesvirus miRNAs manipulate host cell gene expression to create an environment conducive with replication during the lytic cycle

Herpesvirus miRNAs have also been shown to manipulate the cellular environment in order to facilitate viral genome replication and viral assembly during lytic replication. HCMV miR-US25-1 regulates cell cycle regulator cyclin E2 (CCNE2) and RNA polymerase II transcriptional regulator TRIM28 during infection [165]. HCMV manipulation of the cell cycle has been well documented, with cell cycle arrest at the G1/S phase boundary creating optimal conditions in the host cell for the replication of the viral genome and generation of progeny virus [166, 167]. At early time-points in infection, HCMV induces CCNE2 expression, which is then down-regulated by miR-US25-1 at late time-points. It may be that un-checked cyclin E expression throughout virus replication would disrupt this favourable host-cellular environment. TRIM28 encodes a component of a transcriptional co-repressor complex that is able to inhibit viral gene expression [168, 169], and recent observations have demonstrated that TRIM28 mediates RNA polymerase II pausing and progression at intrinsic sites in the genome [170]. Interestingly, HCMV encoded UL79 performs a similar role in the transcription of the viral genome by RNA polymerase II. It is plausible that UL79 confers a distinct functionality to RNA polymerase II that is critical to

HCMV genome transcription, and competition with TRIM28 could be deleterious [171].

Perhaps the most dramatic role identified to date for herpesvirus miRNAs during lytic infection is the coordinated regulation of multiple endocytic pathway genes during HCMV infection which are required to facilitate assembly. miRs-US5-1, -US5-2, and -UL112-1 down-regulate VAMP3, RAB5C, RAB11A, SNAP23, and CDC42 to facilitate the aggregation of endocytic compartments to form the VAC, and this is critical for the production of functional virions [172]. Interestingly individual knockout of these miRNAs had marginal effects on viral phenotype, with the defect in the formation of the VAC only apparent after knockout of all of these miRNAs. This study is ground breaking as it demonstrates that viral miRNAs have evolved to regulate the expression of multiple genes within complex biological pathways to facilitate a crucial process in the viral replication cycle. It also highlights that the importance of regulation of individual miRNA targets may not be apparent when considered in isolation, due to redundancy in miRNA regulation.

1.8.3. Herpesvirus miRNAs restrict the viral lytic gene expression program

One strategy employed by herpesviruses to maintain latency is the restriction of the immediate-early viral transactivators by targeting either viral or host-cellular transcription factors. The ability to restrict the lytic gene cascade by direct miRNA mediated regulation of viral transcriptional transactivators appears to be conserved in herpesviruses and conceivably has a role in both the

establishment and maintenance of latency: HCMV encoded miR-UL112-1 targets IE72; HSV1 miR-H2-3p and HSV2 miR-III target ICP0; KSHV encoded miR-K12-5, 7-5p, -9 , EBV encoded BART6-5p, and OHV-2 miR-5 regulate the expression of ORF50 (RTA). In HSV1, HSV2, KSHV, EBV, OHV-2 these miRNAs are expressed during experimental latency, and it seems that these miRNAs likely act to restrict the lytic cycle, and subdue reactivation of lytic infection during latency [173-180].

Host-cellular transcription factors are also important in the initiation of viral lytic gene expression. In KSHV latency, ORF50, which encodes the RTA protein, is down-regulated by NFkB expression [181]. NFkB expression is typically inhibited by IkBa expression. However, during KSHV latency miR-K12-1 down-regulates IkBa expression, which results in the de-repression of NFkB thus facilitating the restriction of ORF50 [182]. Similarly another NFkB antagonist, nuclear factor I/B (NFIB) is regulated by KSHV miR-K12-3 which down-regulates ORF50 during latency [175]. This is another example of distinct miRNAs regulating the same effector *via* distinct intermediaries in a redundant fashion.

1.8.4. Herpesvirus miRNAs mimic host-cellular miRNAs during latency to facilitate persistence

γ-herpesviruses are distinct among herpesviruses possessing a well documented ability to promote the proliferation of latently infected cells, which allows the virus to spread. This transformative capability results can result in tumours in the host. KSHV is the causative agent of Kaposi's sarcoma and

associated with primary effusion lymphoma and some forms of multi-centric Castleman's disease, while EBV is associated with Burkitt's lymphoma, Hodgkin's lymphoma, and nasopharyngeal carcinoma, and MDV causes T-cell lymphoma in chickens.

During normal development, host-cellular miR-155 is involved in regulating the development and differentiation of lymphatic cells and aberrant over-expression of miR-155 is associated with lymphoproliferative cancers. Interestingly, γ-herpesviruses appear to disrupt the miR-155 axis in order to facilitate the proliferation of latently infected cells. KSHV encodes a miR-155 functional orthologue, miR-K12-11, which shares many targets of miR-155 in B cells *in vitro* [183, 184]. Significantly, miR-K12-11 expression *in vivo* results in B-cell proliferation in a humanised mouse model and is able to rescue defective B-cell phenotypes associated with miR-155 knockout [185, 186]. MDV also encodes a miR-155 functional orthologue, miR-M4, and this has provided a rare opportunity to examine the consequences of the regulation of multiple host-cell transcripts by conserved herpesvirus miRNAs within the context of a natural host. Observations for miR-M4 function showed similarity in function to miR-K12-11, with a miR-M4 knock-out exhibiting a reduction in transformative ability which could be somewhat rescued by complementation with miR-155 [187].

1.9. Preface: A global screen to identify the host cellular targets of HCMV miRNAs in acute infection[1]

As a prelude to the work presented in Chapters 2, 3, and 4, preliminary experiments were performed to identify the host cellular transcripts that are targeted by HCMV encoded miRNAs. The results of these experiments are presented in Section 1.9.2, 1.9.3, and 1.9.4, and these findings are discussed in Section 1.9.5 and 1.9.6.

1.9.1. RISC immunoprecipitation and microarray for identifying the targets of HCMV miRNAs in acute infection *in vitro*

RISC immunoprecipitation (RISC-IP) is a powerful biochemical technique for identifying the targets of miRNAs. During miRNA mediated gene regulation, target transcripts are stably associated with RISC. Using antibodies or molecular tags on miRNAs or RISC, it is possible to immunoprecipitate miRNPs allowing for the isolation of target transcripts [139, 140]. As such this technique was selected for use in this screen. As discussed in Chapter 1.3 the AD169 strain has been widely adopted by the research community and has proved a useful tool for the study of HCMV. However, serial passage has led to the deletion of 22 ORFs that are not required for replication in fibroblast cells, most notably in the genome region between UL128 and UL150 [44, 57, 188]. Of particular relevance for this study, this region is known to encode a single miRNA, HCMV miR-UL148-D1. Therefore, in order for this screen to be representative, it was

[1] Data presented in this section were from experiments performed in their entirety by Finn Grey

crucial to include a genetically competent strain of HCMV. The low passage clinical strain TR was therefore also used in this screen in order to circumvent any potential bias resulting from strain dependent variation in miRNA expression.

Fibroblast cells were infected with AD169 or TR at an MOI of 3, and lysates were harvested at 72 hours post infection (hpi). Three separate pools of RNA were then isolated from these lysates. Total RNA was isolated to ascertain total transcript abundance, and two immunoprecipitated RNA fractions were isolated: a specific RISC pull down using an Ago2 antibody; and a pull down using pre-bleed serum as a control for non-specific binding. In order to establish a baseline which allowed for transcripts targeted by host-cellular miRNAs to be discounted, identical RISC-IPs were performed on lysate from uninfected fibroblast cells. For each RNA sample, the abundance of over 24000 transcripts were analysed using the Illumina HumanRef-8 microarray platform.

In order to specifically identify the targets of viral miRNAs from the microarray data, a series of calculative steps were required (Figure 1.1). In brief, this calculation enabled the identification of transcripts that were proportionally over represented in the infected RISC-IP sample when compared with the uninfected RISC-IP sample, taking into account a) virus induced transcriptional changes during infection and b) non-specific pull-down of transcripts.

Step 1: Normalise against viral induced host cell gene regulation

Enrichment = (IP RNA/Total RNA)

This calculation took into account the global changes in host-gene expression that take place during HCMV infection [167].

Step 2: Normalise against non-specific pull-down in IP samples

Corrected Enrichment = (Enrichment-[Pre bleed IP/Total RNA])

A second calculation was performed to control for non-specific pull-down of transcripts by subtracting the enrichment values from the pre-bleed IP from those using the Ago2 antibody.

Step 3: Normalise against transcripts targeted by host-cellular miRNAs

Corrected Infected Enrichment - Corrected Uninfected Enrichment

Finally, a calculation was performed to normalise against host-cellular miRNA target transcripts in the RISC-IP sample.

^{inf} (IP/Tot) / ^{uninf}(IP/Tot) = Enrichment

^{pre}(IP/Tot) / ^{uninf}(IP/Tot) = correction value

Enrichment – correction value = Corrected enrichment

ATP6V0C	Infected	Total	= 652	
		IP	= 15620	
		IP/Total Ratio	= 23.9	
	Uninfected	Total	= 886	
		IP	= 720	
		IP/Total Ratio	= 0.81	
		Enrichment	= 23.9/0.8	= 29.4
	Pre-serum	Total	= 1090	
		IP	= 1364	
		IP/Total ratio	= 1.25	
		Enrichment	= 1.25/0.8	=1.53
Corrected enrichment			= 29.4 – (1.53-1)	= 28.8
PSG6	Infected	Total	= 146	
		IP	= 158	
		IP/Total Ratio	= 1.07	
	Uninfected	Total	= 1844	
		IP	= 354	
		IP/Total Ratio	= 0.19	
		Enrichment	= 1.07/0.19	= 5.6 – False positive
	Pre-serum	Total	= 152	
		IP	= 167	
		IP/Total ratio	= 1.09	
		Enrichment	= 1.09/0.19	= 5.7
Corrected enrichment			= 5.6 – (5.7-1)	= .088

Figure 1.1 Example of enrichment calculation from RISC-IP and microarray

Examples of calculations for ATP6VOC, a genuinely enriched transcript from the screen, and PSG6, a false positive that was corrected by normalising against the pre-bleed serum IP enrichment value.

1.9.2. RISC-IP and microarray: AD169 *versus* TR

The data from RISC-IP and microarray are summarised in Figure 1.2. Over 96% of transcripts in AD169 infected fibroblast cells and 98% in TR infected fibroblast cells were not enriched by RISC-IP compared with the negative control IPs, which was consistent with the hypothesis that viral miRNAs regulate the expression of a specific subset of host-cellular genes during infection. Enrichment levels were as high as 28 fold in the AD169 infected RISC-IPs, and 19 fold in the TR infected RISC-IPs compared with the negative control IPs (Figure 1.2 **A** and **B** and Table 1.1). The distribution of enrichment values for the top 50 transcripts demonstrated that, overall, higher levels of enrichment were observed in AD169 infected fibroblast cells compared with TR infected fibroblast cells. This is likely a result of AD169 being capable of reaching higher titres in cultured fibroblast cells than TR, which results in a higher abundance of miRNAs [44]. Despite these differences, of the 686 unique transcripts identified in AD169 infected fibroblast cells and 442 transcripts in TR infected fibroblast cells that were enriched over 2 fold by RISC-IP, 222 of these transcripts overlapped (Figure 1.2**D**). This overlap was statistically significant ($p=<0.001$ by chi-squared test), and provided a high degree of confidence that the transcripts that were enriched were genuine viral miRNA targets.

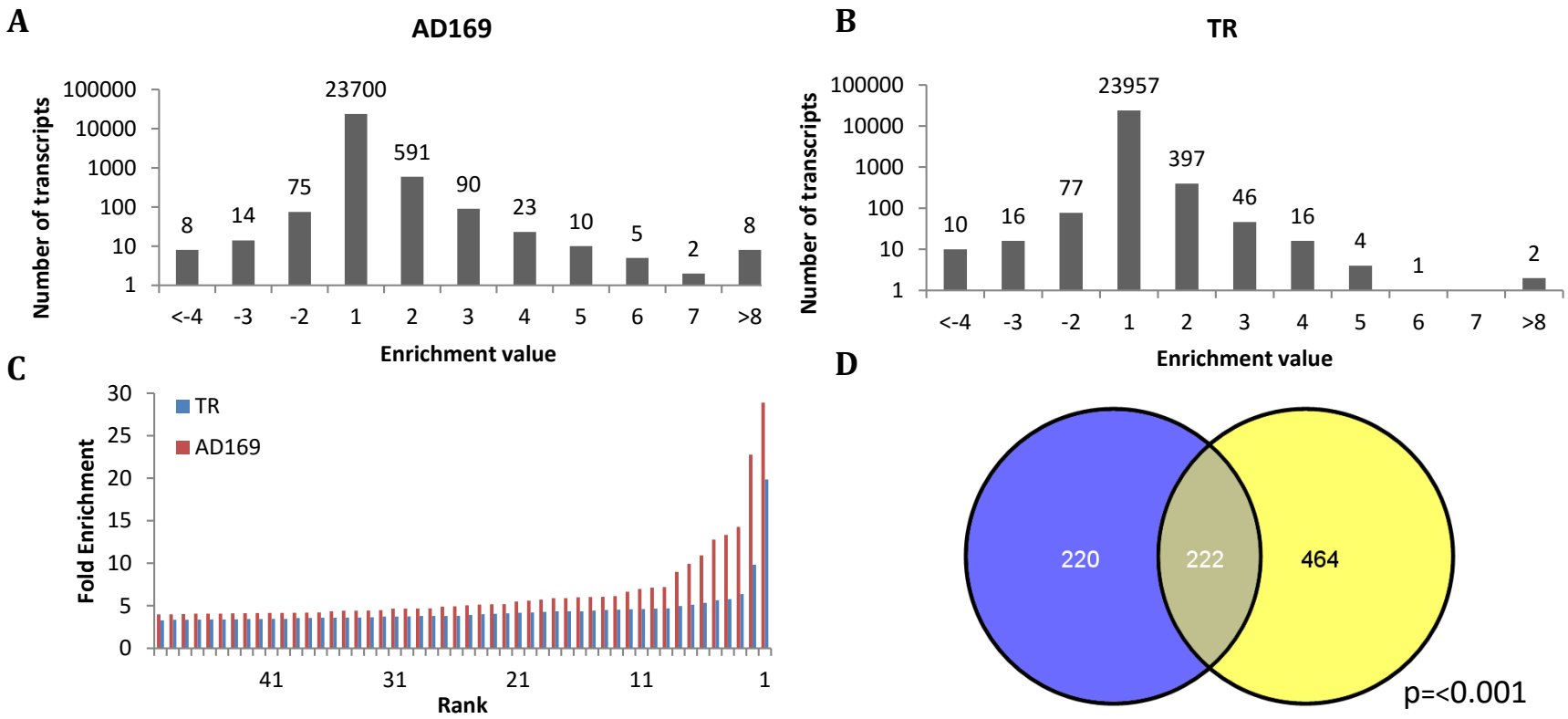

Figure 1.2 Distribution and overlap of normalised enrichment values in AD169 and TR infected fibroblast cells
A. Distribution of fold enrichment in AD169 infected fibroblast cells (N=1). **B.** Distribution of fold enrichment in TR infected fibroblast cells (N=1). **C.** Distribution by gene rank and fold enrichment of the top 50 transcripts in AD169 and TR infected fibroblast cells. **D.** Overlap of transcripts enriched over 2 fold between AD169 and TR infected fibroblast cells. Fibroblast cells were infected with AD169 or TR at an MOI of 3, and at 72 hpi cell lysates were obtained. RNA was fractioned, and RISC-IP performed. Total RNA, RISC-IP RNA and control-IP RNA were extracted and analysed by microarray.
Note: The sum of the values in Figure 1.2**A** and **B** do not match the values in **D** (in Figure 1.2**A** and **B**, 729 and genes are enriched over 2 fold, where as the value is 686 in Figure 1.2**B**). This is the result of the duplication of specific probes for transcripts within the microarray, and these duplicates are subtracted from the alignment analysis in Figure 1.2**B**.

1.9.3. RISC-IP and microarray: Choosing targets of interest from the screen

The RISC-IP and microarray provided nearly 700 transcripts that are potentially regulated by HCMV miRNAs during infection. Prior to this study, others had used similar approaches and observed that highly enriched transcripts were more likely to be genuine targets of viral and host-cellular miRNAs [189, 190]. As such, an assumption was made that transcripts with higher levels of enrichment represented targets with a higher probability of being significantly regulated by HCMV miRNAs during infection, and these transcripts were deemed to be of particular interest.

Due to the higher levels of enrichment in the AD169 infected RISC-IPs and the minimal strain dependent variation between RISC-IP datasets (Table 1.1 and Figure 1.4), the AD169 strain was chosen for further study. The 30 most highly enriched putative targets in AD169 infected fibroblast cells are summarised in Table 1.1.

Table 1.1 Summary of top 30 transcripts from RISC-IP in AD169 and TR infected fibroblast cells

Gene ID	AD169	TR	Definition
ATP6V0C	28.9	9.8	ATPase, H+ transporting, lysosomal
GRN	22.8	2.4	granulin
COMMD10	14.3	19.9	COMM domain containing 10
CTRB2	13.3	6.4	chymotrypsinogen B2
SGSH	12.8	3.4	N-sulfoglucosamine sulfohydrolase
LGALS3	10.9	3.6	galactoside-binding, soluble, 3 (galectin 3)
PIGH	9.9	3.7	phosphatidylinositol glycan anchor biosynthesis
BSG	9.0	1.7	basigin
LEPRE1	7.2	2.4	leucine proline-enriched proteoglycan
LIN28B	7.1	2.9	lin-28 homolog B
SRPRB	7.0	3.8	signal recognition particle receptor
PDIA5	6.6	4.2	protein disulphide isomerase family A
CCNE1	6.1	5.7	cyclin E1
FLJ39061	6.1	3.2	FLJ39061
NUCB1	6.0	0.9	nucleobindin 1
PRSS8	6.0	4.6	protease, serine, 8
BCKDHA	5.9	1.8	branched chain keto acid dehydrogenase E1
C1ORF35	5.9	4.7	chromosome 1 open reading frame 35
TMEM74	5.7	2.4	transmembrane protein 74
NUCB2	5.6	3.1	nucleobindin 2
DSC2	5.5	2.0	desmocollin 2
FALZ	5.2	2.1	fetal Alzheimer antigen
CCNE2	5.2	2.6	cyclin E2
STX10	5.1	3.5	syntaxin 10
COL1A1	5.0	3.4	collagen, type I
KRTAP10-7	4.9	4.1	keratin associated protein 10-7
FAM38A	4.9	2.3	family with sequence similarity 38
ACP2	4.7	1.8	acid phosphatase 2, lysosomal
ATP1A3	4.7	4.2	ATPase, Na+/K+ transporting
PROK2	4.7	4.4	prokineticin 2

Source: Appendix Table 7.1 and Table 7.2.

To identify the miRNAs responsible for targeting the transcripts identified by RISC-IP, the bioinformatic tool RNAHybrid was used [137]. Seed sequence complementarity was analysed within the 3'UTR, ORF, and 5'UTR of the top 30 targets from the AD169 RISC-IP, for the 14 HCMV miRNAs most abundant

during infection [150]. These data are summarised in Figure 1.3. HCMV miRNA seed complementarity was found for 27 out of 30 of the putative targets. Interestingly, the majority of the miRNA target sites were located in the ORF of transcripts with only 14 of 30 predicted to target the 3'UTR. Until recently it was assumed that cellular miRNA targeting was tightly restricted to the 3'UTRs of transcripts [133]. However, a recent study has debunked this assumption, and demonstrated directly that miRNA target sites are distributed across 5'UTR, ORF, and 3'UTR [110]. The data presented in Figure 1.3 support these observations.

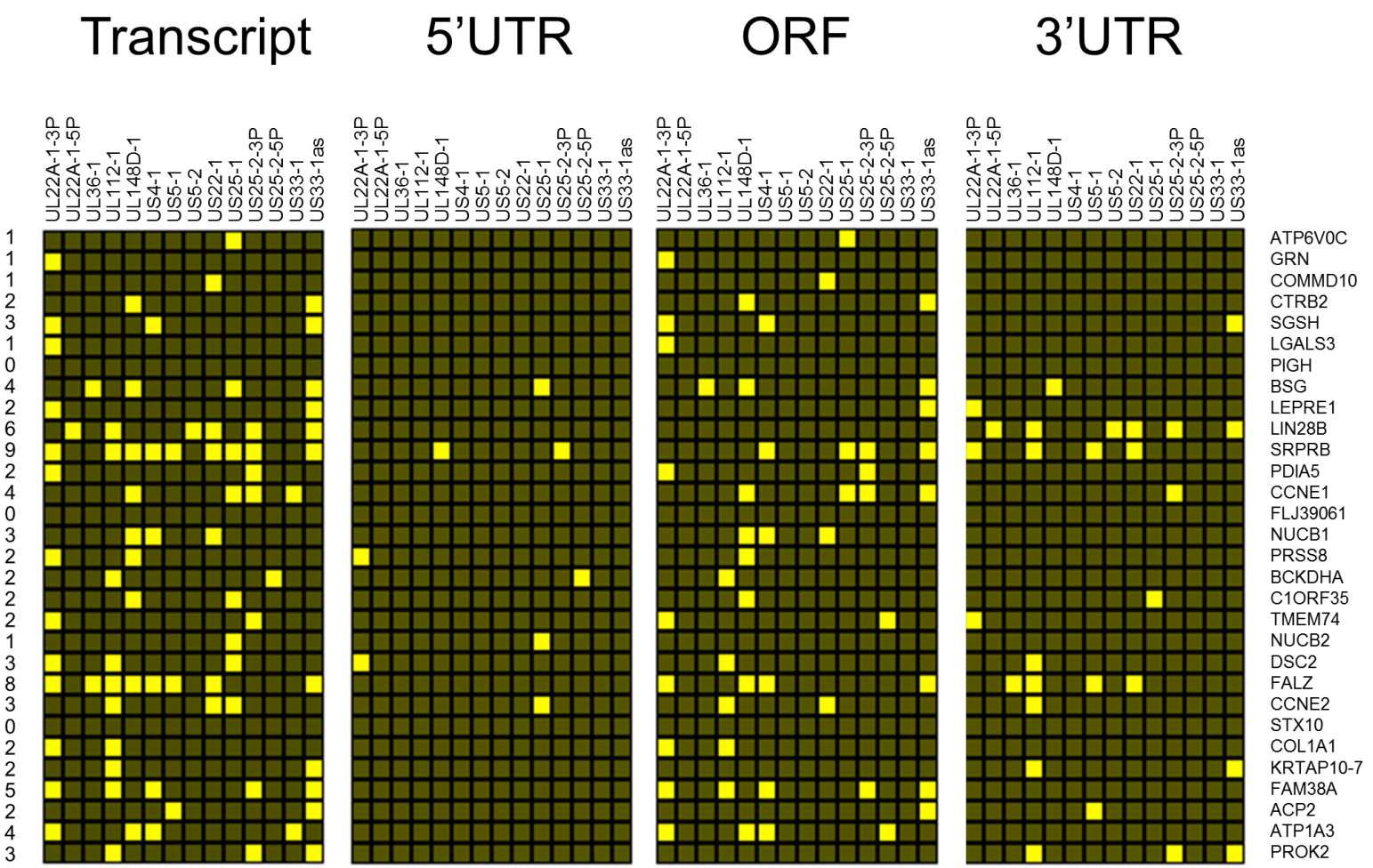

Figure 1.3 Bioinformatic target prediction for the 14 most abundant HCMV miRNAs against the top 30 putative target transcripts identified by RISC-IP and microarray in AD169 infected fibroblasts

5'UTR, ORF, and 3'UTR sequences for the top 30 putative targets of HCMV miRNAs were analysed for seed-sequence complementarity (with sequence constraint between nucleotide 1-7 and 2-8) against the 14 most abundant HCMV miRNAs.

1.9.4. RISC-IP and micro-array: AD169 *vs* miR-US25-1

Prior to these studies in infected cells, RISC-IPs had been performed using individual miRNAs outside of the context of infection. HEK-293 cells were transfected with a biotinylated miRNA mimic or a plasmid expressing HCMV miR-US25-1, and immunoprecipitations were performed using myc-tagged Ago-2 or *via* the biotin tag [165]. As a high proportion of the most highly enriched targets identified from RISC-IP in AD169 infected cells (8/30) were predicted to be targeted by miR-US25-1, the results of these RISC-IPs were compared to the AD169 infected dataset to determine whether there was any correlation. These datasets are presented in full in Appendix Table 7.3, and a summary of the overlap with the top targets from the infected RISC-IPs is presented in Figure 1.4. Of the top 30 targets from the AD169 and miR-US25-1 RISC-IPs, 6 out of 30 overlapped (Figure 1.4**B**). With the exception of LGALS3, all of these targets had high confidence predicted target sites for HCMV miR-US25-1, including ATP6VOC, the most highly enriched target transcript from AD169 RISC-IP and second most highly enriched transcript from the TR RISC-IP (Figure 1.3).

miR-US25-1 is one of the most highly expressed HCMV miRNAs during infection [150]. Assuming that miRNA abundance is likely to be proportionally associated with target transcript regulation, miR-US25-1 represented a particularly relevant focus for further study.

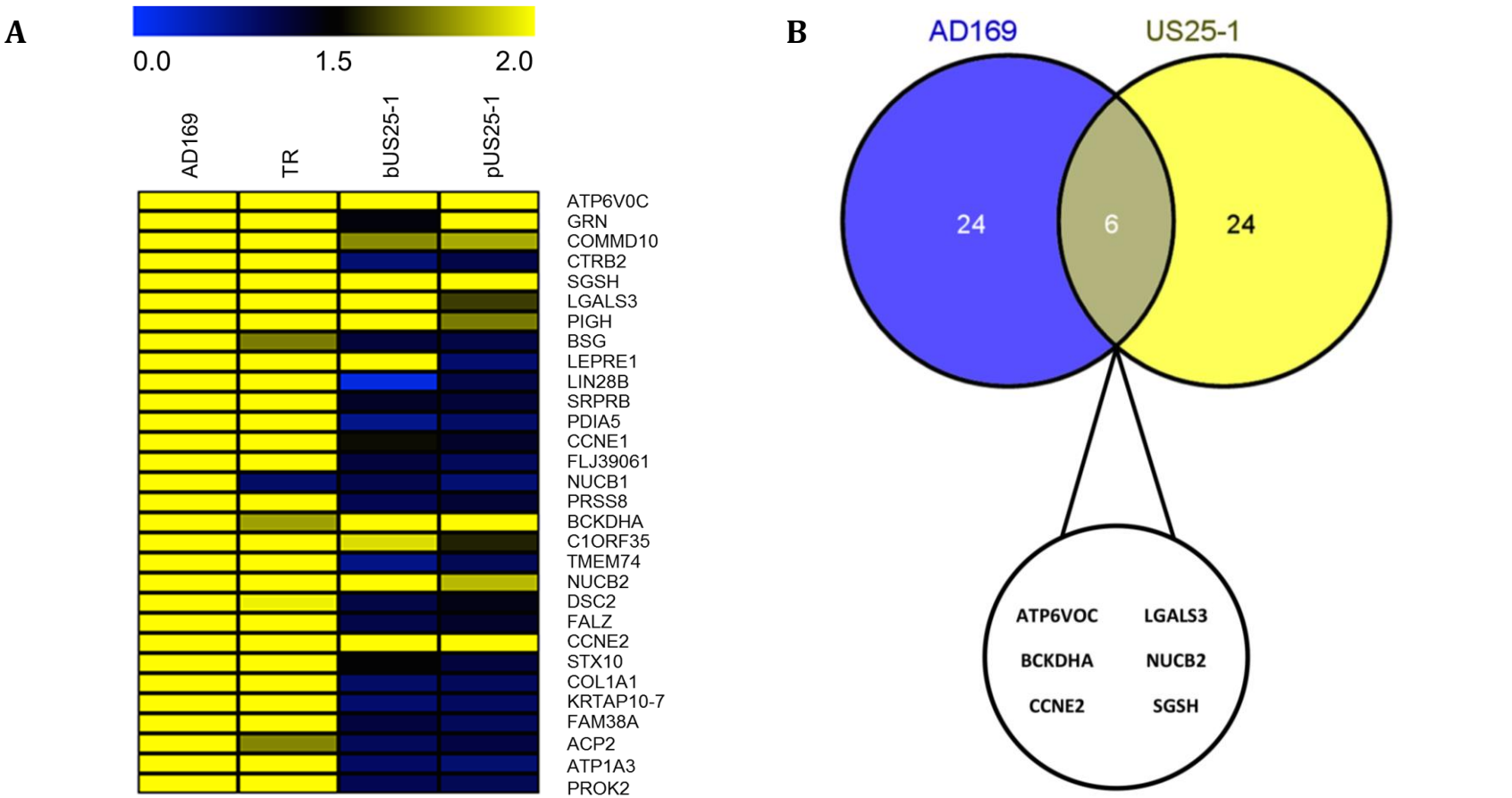

Figure 1.4 Overlap between top targets in AD169 and miR-US25-1 RISC-IP pull downs (AD169 N=1; TR N=1; bUS25-1 N=2; pUS25-1 N=2)

A. Heat map showing enrichment levels of 30 top targets from AD169 and TR infected RISC-IPs, biotinylated miR-US25-1 pull-downs, and myc-Ago pull downs in 293s expressing miR-US25-1.

B. Venn diagram showing overlap between the 30 top transcripts from AD169 and the consensus of the miR-US25-1 RISC-IPs.

1.9.5. Comparison of putative HCMV miRNA targets to other herpesvirus miRNA target studies

Relatively few host-cellular transcripts have been identified as targets of HCMV miRNAs (as discussed in Chapter 1.8) [152, 158, 172, 191]. The few that have been identified have been shown to regulate innate immune pathways, transcription, and endocytosis.

miR-UL112-1 targets MICB, which is an MHC-class 1-like ligand required for the activation of natural killer (NK) cells [152]. miR-UL-148D-1 targets RANTES, a TNFα and IL-1α stimulated pro-inflammatory chemotactic cytokine, that is involved in the recruitment of immune cells to sites of infection [158]. BclaF1, a transcription factor that restricts HCMV replication, is dynamically regulated during infection, first by viral proteins delivered in the tegument, and at later time-points by miR-UL112-1 [191]. Most recently, miR-UL112-1, US5-1, and US5-2 have been shown to target multiple factors within the endocytic pathway [172].

MICB and the majority of the endocytic genes identified by Hook *et al* were enriched in the AD169 and TR RISC-IPs, giving additional confidence in the validity of this screen. BclaF1 was not enriched, but this could be due to the relatively late time-point of miR-UL-112 regulation of BclaF1 [191]. RANTES was also not enriched and this may be a result of strain or cell line dependent variation in miRNA targeting [158].

It is particularly interesting that of the top 30 targets identified by RISC-IP in HCMV infected fibroblast cells, only CCNE2 has been identified as being dysregulated during HCMV infection (as a prelude to the work presented here [165]). Looking more broadly at pathways that one would predict viral miRNAs to regulate, only 3 of the top 30 candidates have been identified as having roles in immunity; BSG, GRN and LGALS3. BSG encodes basigin (a.k.a. CD147), a member of the immunoglobulin superfamily that may have roles in IL-8 production [192]. GRN encodes granulin, which has recently been shown to act as a chaperone for unmethylated CpG DNA, which acts as an agonist for TLR9 signaling, and down stream NFkB gene expression [193]. LGALS3 encodes galectin-3, a member of a family of galactoside binding proteins that regulates the innate immune response [194, 195]. It is feasible that down-regulation of each of these transcripts could be beneficial to HCMV replication.

Several transcripts identified in the screen (ATP6VOC, TMEM74, STX10, and ACP2) have functions within the endocytic and exocytic pathways [196-198], which is particularly interesting in light of recent findings by Hook *et al* [172]. These findings are considered in greater detail in Chapter 4.1. This leaves the majority of the targets identified in the screen (23/30) that have not been shown to have roles in infection, and several of which are poorly characterised in the literature.

In other miRNA encoding human herpesviruses, there have been a small number of systematic studies of the host-cellular targets of viral miRNAs, with few targets identified, and even fewer validated targets identified to date [199-

203]. Of the high confidence targets that have been identified in these studies, there is no overlap with the high confidence HCMV miRNA targets that were identified in this screen. This is not particularly surprising, as there is little conserved miRNA sequence homology between human herpesvirus family members. However, there is some evidence of functional homology in miRNA targeting across *Herpesviridae.* Membrane trafficking processes have been implicated as a target of viral miRNA regulation from systematic analyses of KSHV and EBV, although the functional role of this regulation is currently unknown [202, 203]. Similarly, the results presented here from RISC-IP in HCMV infected fibroblast cells, and observations by Hook *et al* suggest that membrane trafficking processes may also be an important target of HCMV miRNAs. It may be that membrane trafficking processes play an important role in herpesvirus biology.

1.9.6. Caveats in the interpretation of RISC-IP data: Technical and analytical shortcomings of RISC-IP and microarray

The RISC-IP technique is a powerful tool for the systematic screening of miRNA targets, and has proven useful in the field of viral miRNA target analysis [139, 140, 203, 204]. Procedurally, it is far less complex and time consuming compared to other biochemical techniques, such as HITS-CLIP, PAR-CLIP, and CLASH. The efficiency of the pull-down means that less input material is required, which is highly advantageous when analysing infected cells. Also, microarray data are quicker and easier to interpret compared to deep sequencing data. However, the RISC-IP and microarray do have several inherent

shortcomings that need to be accounted for when interpreting data from screens using these methods.

Potential sources of false positives

One shortcoming is that the process for obtaining input material for the immunoprecipitations involves cell lysis, and this has the potential for creating associations between miRNAs and transcripts that are normally segregated by physical barriers within the cell, creating false positives for interactions that do not take place within the context of cell biology [205]. Other techniques circumvent this by cross linking miRNPs prior to cell lysis, which prohibits post lysis mRNA:miRNP interactions [110, 141, 142].

One major benefit of the RISC-IP method is the efficiency of the pull-down, which is beneficial for obtaining large amounts of RISC associated transcripts from a small input volume. However, this is associated with a relatively low stringency in RISC-IP (similarly in HITS/PAR CLIP) when compared to CLASH. In CLASH it is possible to use multiple wash steps under denaturing conditions to remove non-specific RISC associated transcripts. As such, the likelihood for false positives as a result of these non-specific interactions is increased in RISC-IP. However, efforts were made in this screen to mitigate this effect, with Ago2 IPs normalised against total RNA and pre-bleed serum IPs (as described in Chapter 1.9.1).

Within the context of HCMV infection, there are further considerations to be made when interpreting the data from RISC-IP. It is possible that several host-cellular miRNAs may be up-regulated during infection. Similarly, there is a

possibility that changes in the host-cellular gene expression mileu during infection might result in the stabilisation of specific transcripts that are targeted by host-cellular miRNAs. Both of these scenarios would specifically increase the abundance of these transcripts which has the potential to create false positive enrichment.

Potential sources of false negatives

The requirement of a stable interaction between RISC and target transcripts in RISC-IP means that transcripts that do not stably associate with miRNPs can not be identified by this method. A large proportion of these targets are likely to be those that are rapidly degraded by RISC due to exact miRNA:mRNA sequence complementarity. While this type of targeting is relatively common in plants, it accounts for only a small proportion of the miRNA regulated 'targetome' in mammals [206], and the majority of predicted host-cellular targets do not share exact complementarity with viral miRNAs [141, 172, 200-202, 207]. As such, while not discounting the possibility, one would assume that the majority viral miRNA target transcripts are not regulated in this way, and as such the screen presented here is still likely to be largely representative.

Also of note, using microarray as a platform for the analysis of the RISC-IP samples has its shortcomings. False positives and negatives can arise due to erroneous annotation, or cross reactivity of gene specific probes within the array. Finally, unlike next generation sequencing data, microarray data is restricted by the probes that are included on the chip.

1.10. Hypothesis and overall aims

HCMV is a clinically important human pathogen, capable of causing severe disease in the immune-compromised and in neonates [30, 32]. It has also been implicated in other chronic disease processes and it may be that HCMV persistent or latent infection imparts a lifelong burden on the immune system of infected individuals [24, 25, 33]. Therapeutic options for the prevention and treatment of HCMV infection are limited and despite concerted efforts there is no vaccine available [37-41]. This highlights the requirement for the establishment of a greater understanding of the vastly complex interactions that take place between HCMV and the host during infection, with the scope for development of novel therapeutics for HCMV infection greatly increasing as our knowledge of host-virus interactions improves.

The discovery of HCMV encoded miRNAs adds another layer of complexity to the conundrum of virus-host interactions during HCMV infection. These regulatory small RNAs have the capacity to broadly manipulate the transcriptional landscape within the infected cell. However, we are only beginning to understand the potentially far reaching roles that miRNAs play in HCMV biology. The identities of the vast majority of HCMV encoded miRNA targets are unknown, and the function that the regulation of these genes play within the context of infection is unclear. In order to obtain a complete understanding of the virus -host interactions that occur during HCMV infection it is critical that we first elucidate the host-cellular targets of HCMV encoded

miRNAs. Once these targets are identified, it will then be possible to characterise their functional role during infection.

Here, it is hypothesised that HCMV miRNAs have evolved to regulate host-cellular genes that are crucial for HCMV biology. Using a combined approach of miRNA target analysis and phenotypic screening of these targets, the aim of the work presented in this thesis was to identify and characterise the host cellular targets of HCMV miRNAs during infection.

2. Validating the top host-cellular targets of HCMV miRNAs

2.1. Chapter 2: Hypothesis and aims

The results of the systematic screen of the host-cellular targets of HCMV miRNAs (Chapter 1.9) provided nearly 700 transcripts enriched >2 fold, which may be regulated during infection. Of the top 30 transcripts identified in infected fibroblast cells, 8 were bioinformatically predicted to be targeted by HCMV miR-US25-1 (Figure 1.3**A**), and a total of 12 were enriched in two independent miR-US25-1 pull downs (Figure 1.4**A**). It has been shown that miR-US25-1 is expressed at high levels during lytic infection [150, 208]. As such, it was hypothesised that the regulation of host-cellular transcripts by miR-US25-1 may be particularly important in HCMV biology.

As discussed previously, analysing viral miRNAs in isolation may not be an effective strategy for characterising host-cellular targets due to inherent redundancy in eukaryotic pathways and miRNA targeting. In support of this hypothesis, several transcripts identified in Chapter 1.9 were predicted to be targeted by multiple miRNAs during infection (Figure 1.3) and several targets may have redundant functionality within the same biological pathways (Table 1.1). If these interactions were to be taken out of the context of infection, understanding the functional role of the regulation of these transcripts may be difficult, if not impossible. To this end, miRNA knockout viruses were used to validate the targets of miR-US25-1 within the context of infection.

The aims of the work presented in this chapter were to:

1. Validate the enrichment of the top HCMV miRNA targets identified by RISC-IP and microarray.
2. Confirm the regulation of putative target transcripts at the RNA and protein level.

2.2. HCMV miR-US25-1 regulates the expression of multiple host-cellular transcripts during infection at an RNA level[2]

Using bacterial artificial chromosome (BAC) mutagenesis two mutants of AD169 were created which lacked the expression of miR-US25-1 (Chapter 6.3.6). In one mutant (here on in denoted AD169 25-1KO) the region encoding the miR-US25-1 pre-miRNA was deleted, and in the second mutant (here on in denoted AD169 25-1/2KO) the entire miR-US25 region was deleted from the pAD CRE AD169 BAC [209]. A schematic showing the miR-US25-1 region and the BAC mutagenesis in more detail are shown in (Figure 2.1). Viral growth curve analyses demonstrated that these virus strains did not exhibit any growth defect at a given MOI [165]. RISC-IP was performed on fibroblast cells infected with either wild-type AD169, AD169 25-1KO, or AD169 25-1/2KO, or mock infected. Immunoprecipitated RNA and total RNA fractions were isolated and reverse transcribed. The abundance of the transcripts of interest was ascertained by qRTPCR using gene specific primer probe assays (Table 6.1). Enrichment of each transcript of interest was calculated by using the ΔΔct method, and was normalised to GAPDH [210]. An example of the ΔΔct calculation is provided in Figure 2.2.

[2] The AD169 miR-US25-1KO mutant virus was generated by Finn Grey, and the AD169 miR-US25-1/2KO mutant virus was generated by Natalie Reynolds. RISC-IP was performed by Natalie Reynolds and Jon Pavelin.

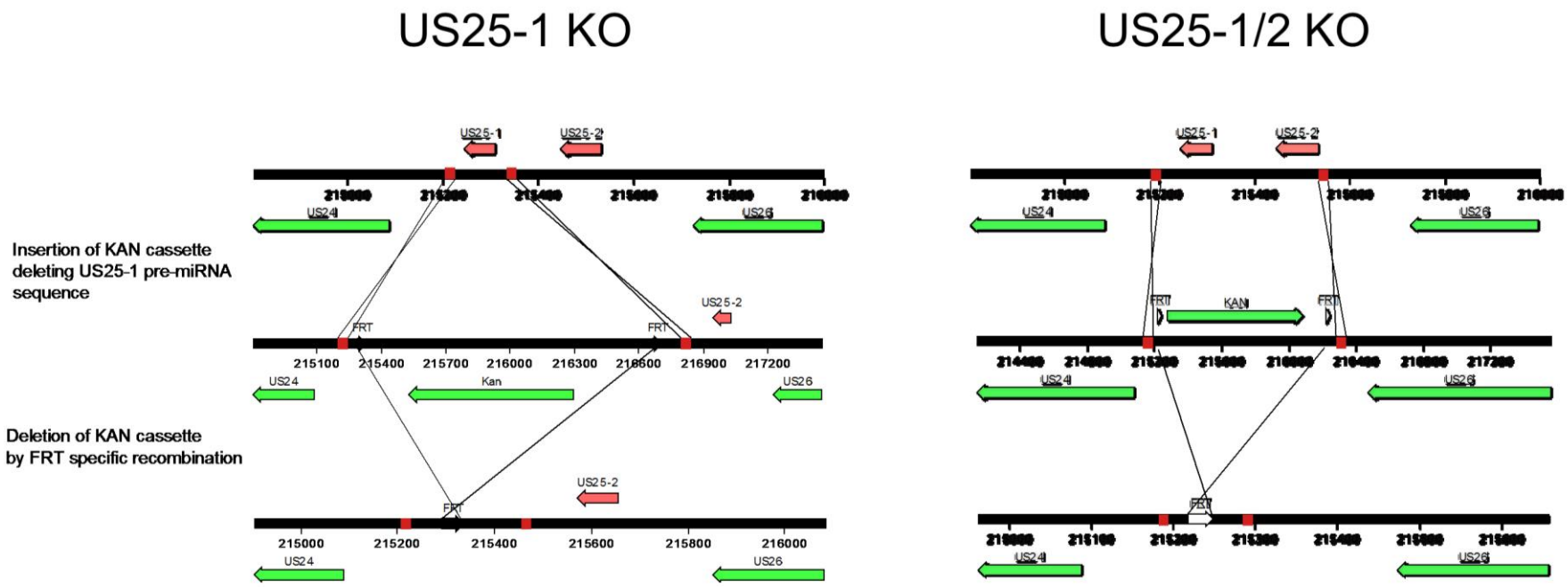

Figure 2.1 Schematic of BAC mutagenesis strategy for the generation of miR-US25-1 KO and miR-US25-1/2 KO strains of AD169.

The miR-US25-1 and miRUS25-1/2 regions were deleted from the pAD CRE AD169 BAC as described in Chapter 6 [209].

$$\underline{\text{Enrichment Value}} = 2^{-([\text{IP RNA} - \text{GAPDH}] - [\text{Total RNA} - \text{GAPDH}])}$$

or

$$\underline{\text{Enrichment Value}} = 2^{-\Delta\Delta cT} = 2^{-((\Delta cT\ \text{IP}) - (\Delta cT\ \text{Total}))}$$

Figure 2.2 RNA levels of putative miR-US25-1 target transcripts in HEK-293 cells transfected with miR-US25-1 (20 nM) (72 hours post transfection) (N=2, n=2)

The enrichment of the transcripts of interest are represented as a percentage of the enrichment in the AD169 infected sample Figure 2.3.

Enrichment profiles for the genes of interest fell into one of three distinct categories:

1. Transcripts targeted solely by miR-US25-1.
2. Transcripts targeted by miR-US25-1 in addition to other HCMV miRNAs.
3. Transcripts not targeted by miR-US25-1 that may be targeted by other HCMV miRNAs.

Transcripts targeted solely by miR-US25-1

The enrichment levels for ATP6VOC, CCNE2, BCKDHA and LGALS3 were high in the RISC-IP samples from wild-type AD169 infected fibroblast cells, indicating that HCMV miRNAs target these transcripts (29.8, 51.8, 4.9, and 12.8 fold over total RNA, respectively)(Figure 2.3). In stark contrast, the enrichment levels for these genes in the RISC-IP samples from AD169 US25-1KO and US25-1/2KO infected fibroblast cells were significantly lower when compared with those infected with wild-type AD169 ($p=0.0039$), and crucially these enrichment values were similar to those seen in uninfected fibroblast cells. Taken together, these data indicate that ATP6VOC, CCNE2, BCKDHA and LGALS3 are likely to be targeted solely by HCMV miR-US25-1 during infection.

Transcripts targeted by miR-US25-1 in addition to other HCMV miRNAs

The enrichment levels for SGSH, NUCB2, CCNE1, LEPRE1 and PIGH were high in the RISC-IP samples from wild-type AD169 infected fibroblast cells, indicating that HCMV miRNAs target these transcripts (7.5, 12.8, 29.3, 11.7, 7.2. and 22.2 fold over total RNA, respectively)(Figure 2.3). Enrichment levels in RISC-IP samples from AD169 US25-1KO and US25-1/2KO infected fibroblast cells were lower than those observed in the wild type infected cells. However, enrichment levels were still significantly higher than those observed in uninfected fibroblast cells ($p=0.0039$). These data indicate that SGSH, NUCB2, CCNE1, LEPRE1 and PIGH are likely targeted by miR-US25-1 in addition to other HCMV miRNAs during infection.

Transcripts not targeted by miR-US25-1 that may be targeted by other HCMV miRNAs

Enrichment levels for BSG, NUCB1, LIN28B, and GRN were significantly higher in the RISC-IP samples from wild-type AD169 infected fibroblasts when compared with uninfected fibroblast cells ($p=0.0039$ [with the exception of LIN28B, which is induced upon HCMV infection so is not expressed in uninfected fibroblast cells])(Figure 2.3). However, there was no significant difference observed between enrichment levels from RISC-IPs in either the AD169 miR-US25-1 KO or miR-US25-1/2KO infected fibroblast cells when compared with the wild-type AD169 infected sample indicating that miR-US25-1 is not responsible for regulating these transcripts during infection. For BSG and NUCB1 this was clear, with enrichment values numerically similar in RISC-IP samples from wild-type AD169, miR-US25-1KO, and miR-US25-1/2KO infected fibroblasts cells. For LIN28B and GRN, a numerical difference was observed between the samples from infected fibroblasts but this was not statistically significant.

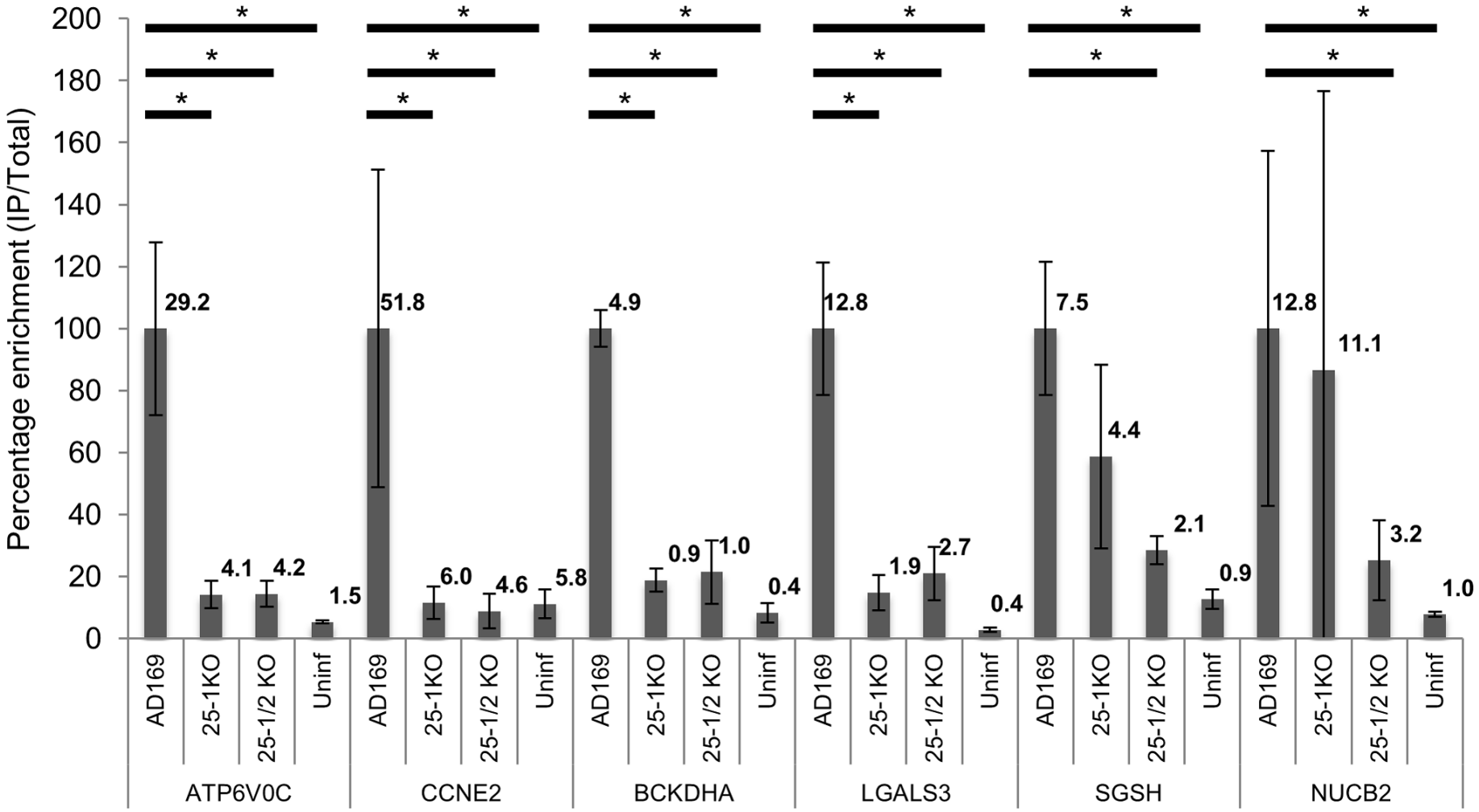
Percentage enrichment (IP/Total)
200
180
160
140
120
100
80
60
40
20
0
*
29.2
4.1
4.2
1.5
51.8
6.0
4.6
5.8
4.9
0.9
1.0
0.4
12.8
1.9
2.7
0.4
7.5
4.4
2.1
0.9
12.8
11.1
3.2
1.0
AD169
25-1KO
25-1/2 KO
Uninf
ATP6V0C
CCNE2
BCKDHA
LGALS3
SGSH
NUCB2

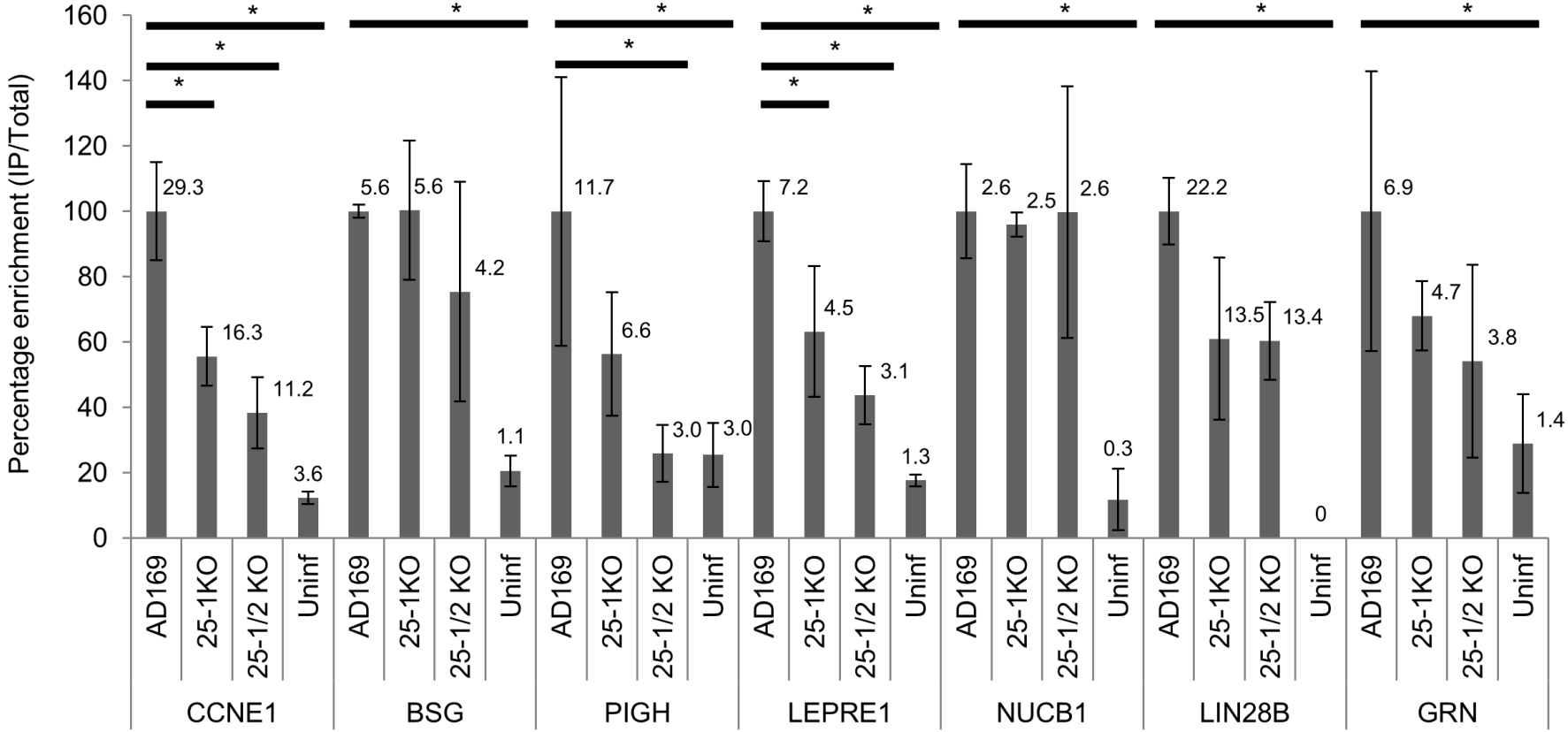

Figure 2.3 RISC-IP and qRTPCR against putative HCMV miRNA targets in fibroblast cells infected with AD169, AD169 25-1KO, or AD169 25-1/2 KO, and uninfected fibroblast cells at 72 hpi (N=2, n=6) (MOI = 3)

***** = p = <0.01 ascertained by Mann Whitney u-test; **N** = Number of technical replicates; **n** = Number of analytical replicates. RISC-IP was performed on fibroblast cells infected with AD169, AD169 miR-US25-1KO, or AD169 miR-US25-1/2KO viruses, and on uninfected cells. RNA was extracted and qRTPCR was performed using specific primer probes. Error bars represent the standard-deviation from the mean.

The HCMV miR-US25-1 pre-miRNA is a polycistronic transcript that gives rise to two other mature miRNAs that are expressed at lower levels during acute infection, miR-US25-2-3p and miR-US25-2-5p. In order to confirm that miR-US25-2-3p and miR-US25-2-5p did not contribute to the differential enrichment of ATP6VOC, CCNE2, BCKDHA, LGALS3, NUCB2 and SGSH observed in the infected pull-downs, RISC-IPs were performed in fibroblast cells transfected with miRNA mimics for miR-US25-1, 25-2-3p, and 25-2-5-p (20 nM) (Figure 2.4). As an additional control, a seed mutant miR-US25-1 was designed, in which 6 bases of the seed sequence were mutated (Figure 2.6**B**).

The enrichment of ATP6VOC, CCNE2, BCKDHA, LGALS3, NUCB2 and SGSH in fibroblast cells transfected with miR-US25-1 was significantly higher compared with negative control siRNA transfected fibroblast cells. For each of these genes, the enrichment levels in fibroblast cells transfected with miR-US25-2-3p, miR-US25-2-5p, and the negative control siRNA were similar.

These data demonstrated that miR-US25-1 was able to target these transcripts, where as miR-US25-2-3p and miR-US25-2-5p were not. As such, the differential enrichment observed within the context of infection was not the result of regulation by miR-US25-2-3p or -5P (Figure 2.4). A significantly higher level of enrichment was also observed in miR-US25-1 transfected fibroblast cells compared to those transfected with the miR-US25-1 seed mutant for all genes ($p=0.0039$). This demonstrates that the 2-8 base miR-US25-1 seed sequence is critical for the targeting of these transcripts. One possible exception is SGSH which still showed a high level of enrichment in fibroblast cells transfected with

the miR-US25-1 seed mutant. This may be the result of a non-canonical interaction between miR-US25-1 and SGSH outside of the seed region.

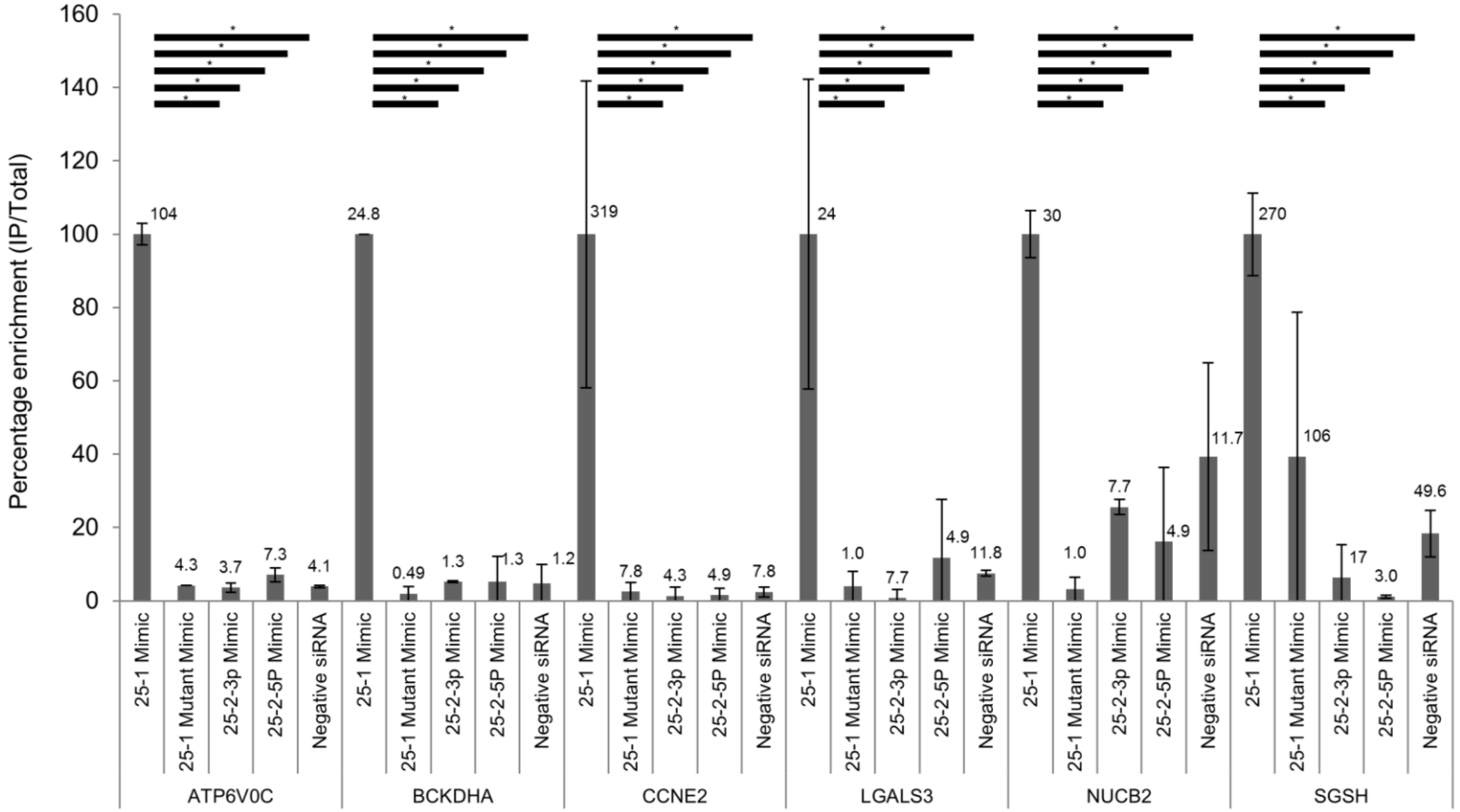

Figure 2.4 RISC-IP and qRTPCR of putative miR-US25-1 targets in fibroblast cells transfected with miR-US25-1, miR-US25-1 seed mutant, miR-US25-2-3p, and miR-US25-2-5p miRNA mimics (20 nM) (N=2, n=6)

* = p = <0.01 ascertained by Mann-Whitney u-test; N = Number of technical replicates; n = Number of analytical replicates. RISC-IP was performed on fibroblast cells transfected with miR-US25-1, 25-1 seed mutant, 25-2-3p, 25-2-5p, or a negative control siRNA 72 hours post transfection. RNA was extracted and qRTPCR was performed using specific primer probes. Error bars represent the standard-deviation from the mean.

2.3. Luciferase assay confirms regulation of ATP6VOC and CCNE2 by miR-US25-1[3]

In order to validate that the bioinformatically predicted target sites within the transcripts of interest were sufficient and required for down-regulation by miR-US25-1, luciferase assays were performed. Regions of the ATP6VOC (ORF), BCKDHA (5'UTR), CCNE2 (5'UTR), LGALS3 (5'UTR), NUCB2 (5'UTR), and SGSH (5'UTR) containing the bioinformatically predicted target sites were cloned into vectors upstream of a luciferase reporter gene. These regions are described schematically in Figure 2.5. Approximately 500bp long regions BCKDHA, CCNE2, LGALS3, NUCB2, and SGSH 5'UTRs were amplified by PCR from genomic DNA using the oligonucleotides listed in , and cloned upstream of the firefly luciferase reporter gene in the pGL4 luc2 construct. The pRL® renilla luciferase construct was used as a control. For ATP6VOC, the region of the ORF containing the miR-US25-1 target site was synthesized using custom oligonucleotides as described in Chapter 6.3.5. For the ATP6V0C and CCNE2 seed mutant constructs, custom oligonucleotides were synthesized and the miR-US25-1 target sites were replaced with BAMHI restriction sites.

HEK 293 cells were then co-transfected with the luciferase expressing vectors (200 nmol) and a miR-US25-1 mimic (20 nM).

[3] CCNE2 and CCNE2 mutant luciferase constructs were designed and cloned by Finn Grey. BCKDHA, LGALS3, NUCB2, and SGSH luciferase constructs were designed by Natalie Reynolds and the experiments were performed by Jon Pavelin.

In cells co-transfected with ATP6VOC or CCNE2 luciferase constructs and miR-US25-1, luciferase expression was reduced to 31% and 38% expression, respectively, compared with cells transfected with the negative control siRNA (Figure 2.6**A**). In cells co-transfected with BCKDHA, LGALS3, NUCB2 or SGSH luciferase constructs and miR-US25-1, there was no consistent decrease in luciferase expression, compared with cells transfected with the negative control siRNA (Figure 2.6**A**). A luciferase construct containing an exact complimentary sequence to miR-US25-1 was used a positive control, and the empty luciferase vector was used as a negative control (Figure 2.6**A**).

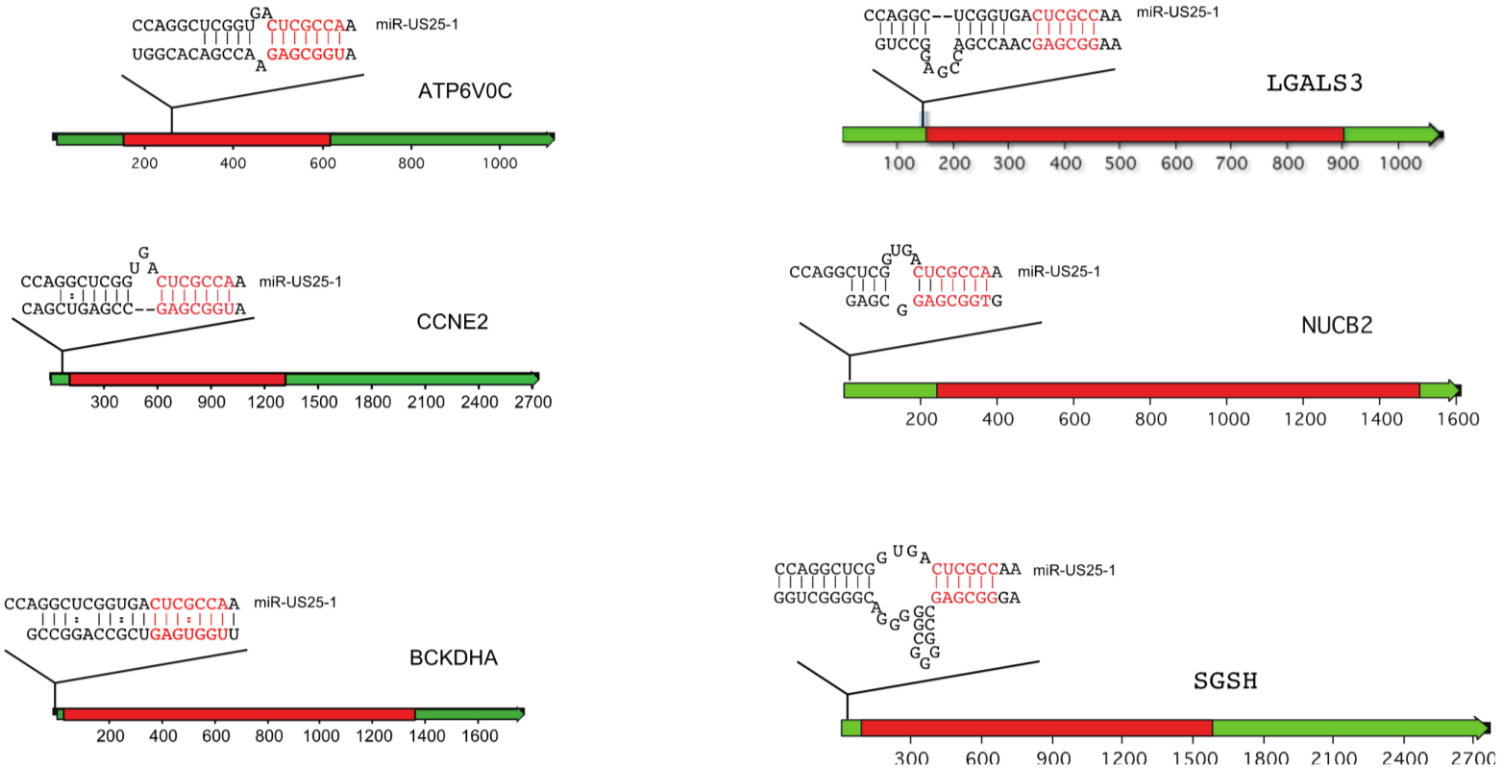

Figure 2.5 Schematic representation of the bioinformatically predicted target sites of miR-US25-1 for ATP6VOC, BCKDHA, CCNE2, LGALS2, NUCB2, and SGSH

miR-US25-1 target sites and binding in ATP6VOC, BCKDHA, CCNE2, LGALS3, NUCB2, and SGSH transcripts as predicted by RNA hybrid.

Based on these data, the bioinformatically predicted target sites for ATP6VOC and CCNE2 luciferase constructs were *sufficient* for the targeting of these transcripts by miR-US25-1, where as those predicted for BCKDHA, LGALS3, NUCB2, and SGSH appeared to be insufficient.

In order to ascertain whether the bioinformatically predicted target sites for ATP6VOC and CCNE2 were *required* for knockdown of these transcripts, seed mutant luciferase constructs and corresponding seed mutant miR-US25-1 mimic were created (Figure 2.6**B**). When the ATP6VOC and CCNE2 seed mutant constructs were co-transfected with miR-US25-1, luciferase expression was de-repressed, to 103% and 73%, respectively (3 fold and 2 fold increase in luciferase expression, respectively compared with the wild type ATP6VOC and CCNE2 luciferase constructs).

The mutant miR-US25-1 mimic was unable to down-regulate ATP6VOC linked luciferase expression (103% when compared with negative control siRNA). Conversely, the mutant miR-US25-1 mimic was able to down-regulate ATP6VOC seed mutant linked luciferase expression (22% when compared to cells transfected with the negative control siRNA) (Figure 2.6**C**).

Taken together, these findings demonstrate that the bioinformatically predicted target sites are both sufficient and required for the regulation of ATP6VOC and CCNE2 by miR-US25-1.

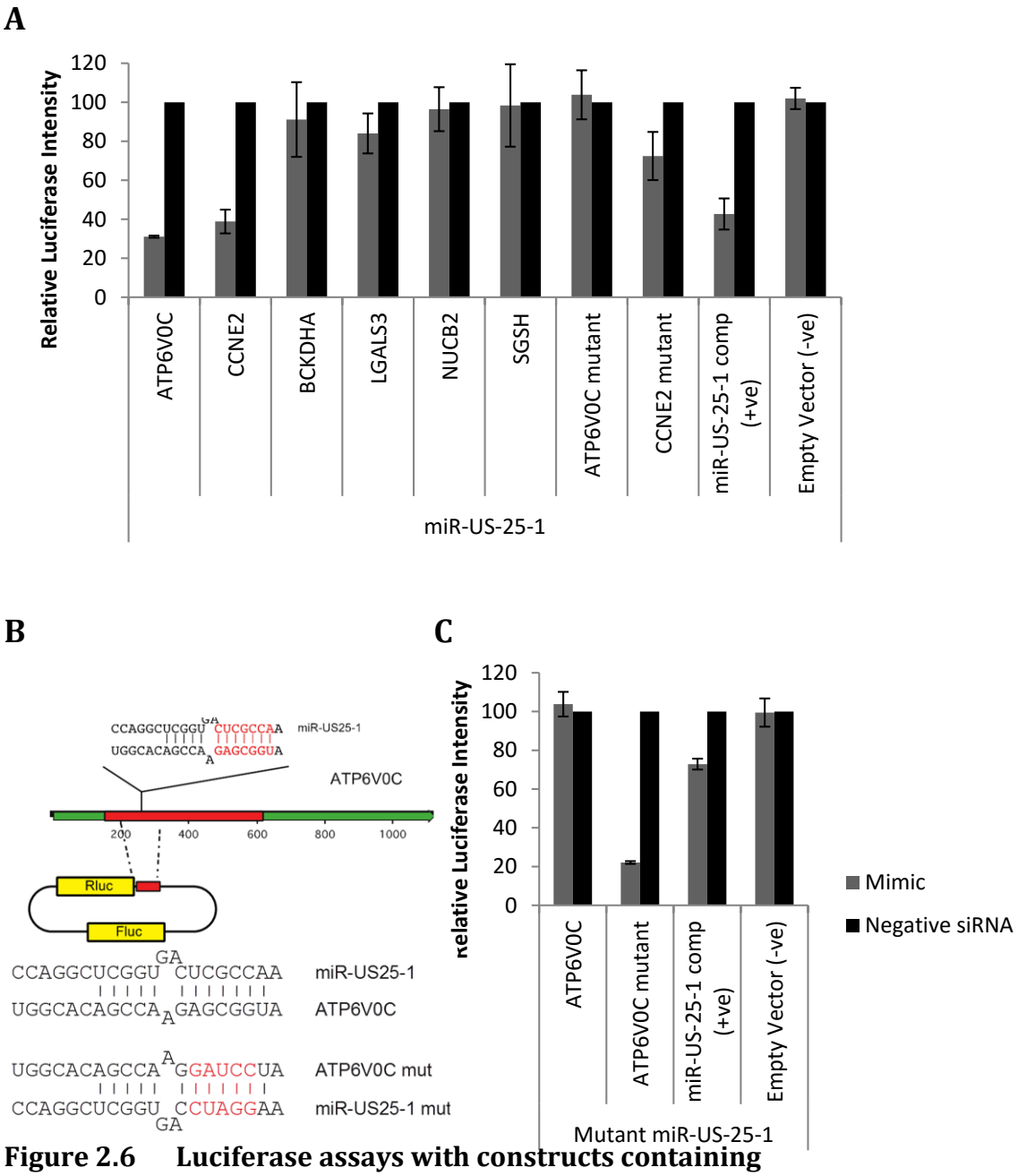

Figure 2.6 Luciferase assays with constructs containing bioinformatically predicted miR-US25-1 target sites (N=3)

A. Luciferase assays with miR-US25-1 against constructs expressing regions of ATP6VOC, BCKDHA, CCNE2, LGALS3, NUCB2, and SGSH containing predicted target sites. ATP6VOC or CCNE2 seed mutants, and an empty vector were used as negative controls. A miR-US25-1 seed match construct was used as a positive control. **B.** Schematic of ATP6VOC luciferase construct, ATP6VOC seed mutant, and mimic seed mutants. **C.** Luciferase assays with miR-US25-1 seed mutant mimic. HEK 293 cells were co-transfected with luciferase construct (200 nmol) and miRNA mimics (20 nM) using lipofectamine 2000. At 48 hours post transfection, cells were lysed and luciferase expression was quantified *via* plate reader. Error bars represent the standard-deviation from the mean.

2.4. Regulation of transcripts by HCMV miR-US25-1 results in changes at the RNA level

The results of the RISC-IPs confirm that the putative target transcripts are bound by HCMV miRNA RISC complexes. The main aim of this study was to identify miRNA targets actively regulated by HCMV during infection. As such, total transcript levels for each of the putative targets of miR-US25-1 were assayed in HEK-293 cells transfected with either a miR-US25-1 mimic or a negative control siRNA (20 nM) (Figure 2.7). Transcript levels for β-Actin and NUCB1 were assayed as negative controls for miR-US25-1 targeting. These data demonstrate that ATP6VOC, CCNE2, NUCB2, BCKDHA, and LGALS3 transcripts decrease in abundance as a result of miR-US25-1 activity. The transcript levels for SGSH increased 2 fold upon transfection with miR-US25-1, which was counter-intuitive based on previous data suggesting that miR-US25-1 targets SGSH. Total RNA data from the pUS25-1 RISC-IP showed no difference in SGSH expression in negative control and miR-US25-1 transfected cells, so this did not appear to be the result of an upstream target of miR-US25-1 (Appendix Table 7.3). It is possible that this increase in transcript levels was a result of stabilisation of the SGSH transcript by the miRNP complex. However, this was not clear and this phenomenon requires further investigation.

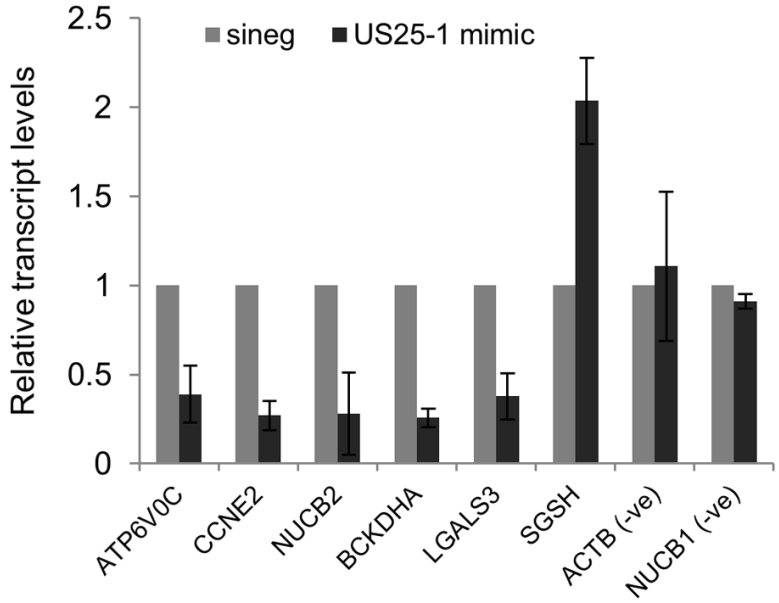

Figure 2.7 RNA levels of putative miR-US25-1 target transcripts in HEK-293 cells transfected with miR-US25-1 (20 nM) (72 hours post transfection) (N=2, n=2)

N = Number of technical replicates. n = Number of analytical replicates within each technical replicates. HEK-293 cells were transfected with miR-US25-1, or a negative control siRNA and RNA was harvested 72 hours post transfection. Gene expression was analysed by qRTPCR using specific primer probe sets. Error bars represent the standard-deviation from the mean.

2.5. Regulation of transcripts by HCMV miR-US25-1 results in changes at the protein level

In order to ascertain whether the targeting of host-cellular transcripts by miR-US25-1 resulted in an associated change in protein levels, western blot analyses were performed against ATP6VOC, BCKDHA, CCNE2, LGALS3, NUCB2, and SGSH in fibroblast cells infected with wild type AD169 or AD169 miR-US25-1/2 KO (MOI=1) (Figure 2.8).

Using specific antibodies against ATP6VOC, CCNE2, BCKDHA, LGALS3, NUCB2, and SGSH, the protein expression levels in fibroblast cells infected with either wild type AD169 or AD169 miR-US25-1/2 KO, and uninfected cells was assayed by western blot analysis. In order to confirm that bands observed in the western blot were specific for the genes of interest, protein samples were isolated from fibroblast cells transfected with specific siRNAs against ATP6VOC, BCKDHA, CCNE2, LGALS3, NUCB2, or SGSH, as a negative control.

For all of the genes of interest, protein levels changed following infection with HCMV. ATP6VOC, CCNE2, and BCKDHA appeared to be induced upon infection whereas LGALS3, NUCB2 and SGSH were down-regulated. When infected with the AD169 miR-US25-1/2KO virus, expression levels of ATP6VOC, CCNE2, BCKDHA, and LGALS3 were higher compared to fibroblast cells infected with wild-type AD169, indicating that miR-US25-1 mediated regulation was responsible for changing the expression levels for these proteins (Figure 2.8). NUCB1 and SGSH protein levels were similar in fibroblast cells infected with

both wild type AD169 and the miR-US25-1KO virus. It may be that regulation of these genes by other HCMV processes or miRNAs obscures the effects of miR-US25-1 knock-out.

These data demonstrate that miR-US25-1 mediated regulation of ATP6VOC, CCNE2, BCKDHA, and LGALS3 transcripts resulted in a decrease at the protein level during infection.

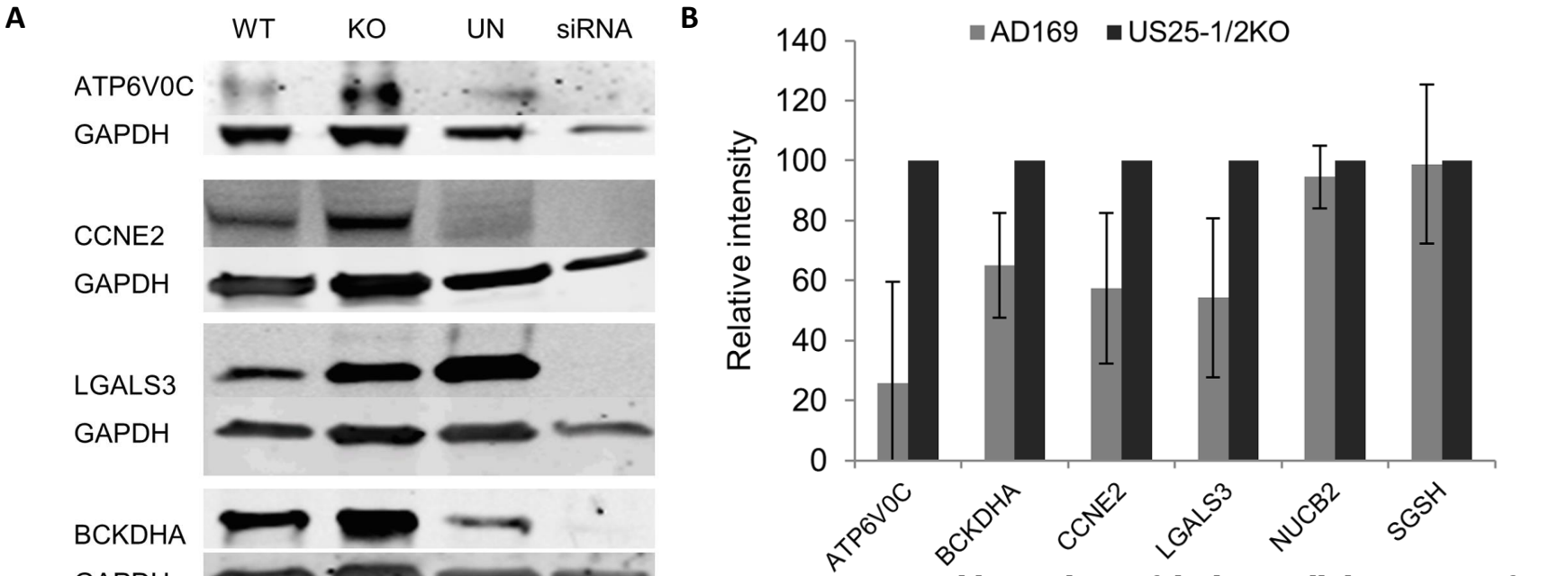

Figure 2.8 Western blot analysis of the host-cellular targets of HCMV miR-US25-1

A. Representative western bots against putative miR-US25-1 targets. Fibroblasts were infected with AD169 or miR-US25-1/2 KO virus, or were transfected with siRNA. 72 hours post infection/transfection, cell lysates were harvested in laemmli buffer and western blot analyses were performed using specific primary antibodies, and LiCOR secondary antibodies. **B.** Licor western blot quantification comparing wild type AD169 infected fibroblast cells with AD169 25-1/2KO infected fibroblast cells. Protein levels were quantified using LiCOR Odyssey software. Error bars represent the standard-deviation from the mean.

2.6. Discussion

The data presented here (published in Pavelin *et al*, PLOS Pathogens, 2013, Figures 4-6 [204]) validate several of the host-cellular transcripts identified in Chapter 1.9 as being targeted by HCMV miRNAs during infection. Furthermore, miR-US25-1 was identified as the candidate miRNA responsible for regulating several of these genes during infection. miR-US25-1 appears to be the sole HCMV miRNA responsible for regulating ATP6VOC, BCKDHA, CCNE2, and LGALS3 transcripts during infection. The bioinformatically predicted target sites for two of these genes, ATP6VOC and CCNE2, were validated as being sufficient and required for miR-US25-1 mediated regulation. Lastly, and critically, miR-US25-1 was shown to be capable of regulating ATP6VOC, BCKDHA, CCNE2, and LGALS3 expression at the RNA level outwith infection, and at the protein level within the context of infection. These data confirm that the presence of these transcripts in the AD169 and TR RISC-IP microarray datasets, and the subsequent RISC-IP and qRTPCR datasets, was not the result of post-lysis interactions between miRNPs and these transcripts. These data also validate that these transcripts are regulated by miR-US25-1 within the context of infection.

2.6.1. Validation of targets of miR-US25-1 during infection

Using RISC-IP in fibroblast cell infected AD169 miR-US25-1 knockout viruses, it was possible to validate the bioinformatically predicted targeting of miR-US25-1 within the context of infection for several of the transcripts presented in Figure 1.3; ATP6VOC, BCKDHA, NUCB2, CCNE2, and CCNE1.

Interestingly, miR-US25-1 appeared partly responsible for the regulation of several transcripts for which there were no predicted target sites; PIGH, which had no predicted HCMV miRNA target sites; and LGALS3, SGSH and LEPRE1, were predicted to be targeted by other HCMV miRNAs. LGALS3 is the most striking of these, as it appears to be solely regulated by miR-US25-1 during infection. These findings are reflective of the difficulties involved in accurately predicting targets of miRNAs. It has recently become apparent that canonical miRNA binding sites make up only 40% of all miRNA:mRNA interactions, with 60% of interactions containing mismatched bases, bulges, and significant binding outside of the seed region [110]. Indeed, when the stringency of bioinformatic prediction was relaxed (allowing 6-mer sites, nucleotide mismatches, and loops), non-canonical target sites were identified within each of these genes (Appendix Table 7.5).

The lack of sensitivity of bioinformatic prediction of miRNA target sites were also reflected in the results of the luciferase assays, where it was only possible to validate regulation by miR-US25-1 for ATP6VOC and CCNE2. In removing the regions containing the target sites for BCKDHA, LGALS3, NUCB2, and SGSH out of their normal context, RNA secondary structure that might facilitate miRNA binding to target sites may have been disrupted. Taking this into account, while the data presented in Figure 2.6 confirm the bioinformatically predicted target sites within ATP6VOC and CCNE2, they do not preclude the possibility that the bioinformatically predicted target sites for BCKDHA, LGALS3, NUCB2, and SGSH

are responsible for their regulation by miRUS25-1 within the context of infection.

2.6.2. COMMD10: An example of why thorough validation of transcripts identified in miRNA target screens is critical

As can be seen in Table 1.1, COMMD10 was the most highly enriched transcript from the TR RISC-IP and microarray, and was the third most highly enriched transcript from the AD169 RISC-IP and microarray. However, when validating this targeting using RISC-IP and qRTPCR, COMMD10 was not enriched in infected cells when compared to uninfected cells (Section 2.6.2). The reason for this discrepancy between the RISC-IP and microarray and qRTPCR was likely due to flaws in the microarray. As discussed in Chapter 1.9.6, incorrect annotation of probes or cross-hybridisation between transcripts and probes can be a source of false positives and negatives in microarray experiments, and this appears likely to have been the case here. This finding highlights the importance of proper validation of transcripts identified in screens of miRNA targets.

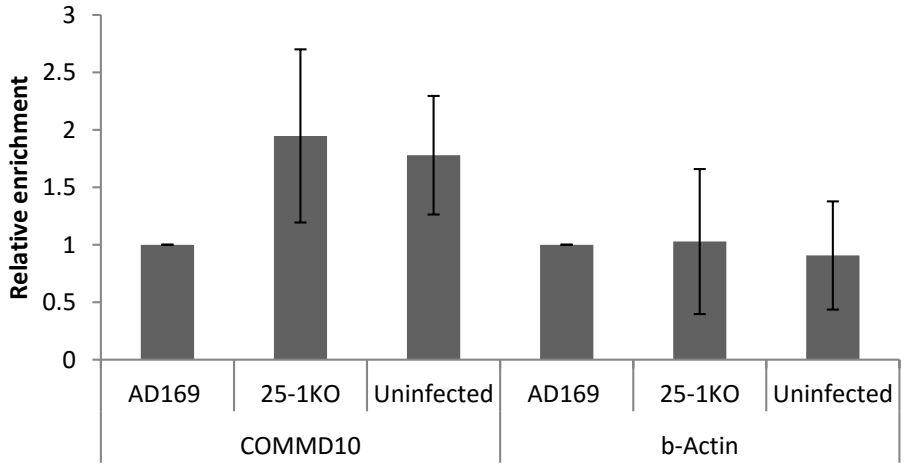

Figure 2.9 RISC-IP and qRTPCR of COMMD10 and b-Actin in fibroblast cells infected with AD169, AD169 25-1 KO, or uninfected cells (N=3)
RISC-IP was performed on fibroblast cells infected with AD169, miR-US25-1KO, or miR-US25-1/2KO viruses, and on uninfected cells. RNA was extracted and qRTPCR was performed using specific primer probes. Error bars represent the standard-deviation from the mean.

2.6.3. Implications of the regulation of the host-cellular targets of miR-US25-1

As demonstrated in Figure 2.7 miR-US25-1 is responsible for changes in ATP6VOC, BCKDHA, CCNE2, LGALS3, NUCB2, and SGSH expression at the RNA level. For all of these genes except SGSH, this change resulted in a decrease in the abundance of these transcripts, to 20-40% when compared to a negative control. For SGSH, there was a consistent 2 fold increase in the levels of SGSH transcript in cells transfected with miR-US25-1 mimic. Taken at face value, while this result is counter-intuitive with regards to canonical miRNA regulation of transcripts, it is not unprecedented as there have been several examples reported of miRNA targeting resulting in the stabilisation of transcripts [211, 212].

The down-regulation of ATP6VOC, BCKDHA, and CCNE2 by miR-US25-1 at a protein-level during infection occurs on a backdrop of being robustly up-regulated in response to infection. LGALS3 protein expression, appears to be down-regulated during infection by other viral processes and supplemented by miR-US25-1 action. Both NUCB2 and SGSH are effectively down-regulated by viral processes during infection, and it may be that regulation of these factors by miR-US25-1 and other miRNAs is redundant, or may be required in different cell types, or under certain conditions within the cell (Figure 2.8). It could be that within the context of infection, the up-regulation of these factors is anti-viral and that their down-regulation is required for viral propagation. In order to assess this possibility, the function of these genes needs to be considered.

When the changes in levels of these proteins shown in Figure 4.11 were compared with existing proteomics data in HCMV infected cells, the observed patterns are consistent for BCKDHA, LGALS3, and NUCB2 which provides further confidence in the findings presented in this chapter [59]. In studies of the host cell proteome during HCMV infection it should be noted that ATP6VOC and CCNE2 were not detected, and the data for SGSH were inconclusive due to the low number of SGSH peptides that were identified by mass spectrometry [59].

ATP6VOC

ATP6VOC is a critical component of the vacuolar ATPase, which is responsible for the acidification of vacuoles within the secretory and endocytic pathways. Acidification of these vacuoles is crucial for the progression of the endocytic

pathway, and for membrane trafficking processes in the cell. It is also important in degradative pathways within the cell, with the activity of lysosomal degradative enzymes dependent on an acidic luminal pH [213]. As such it is conceivable that the up-regulation of ATP6VOC may result in defects in the entry of HCMV, subsequent penetration, and assembly of progeny virions. Interestingly, several other genes within the endosomal pathway have been shown to be regulated by other HCMV miRNAs during infection, which adds weight to this hypothesis [172].

BCKDHA

BCKDHA encodes branched chain keto-acid dehydrogenase, an enzyme that is required for the metabolism of the branched chain amino acids (BCAAs); leucine, isoleucine, and valine. These are also known as the 'essential amino acids', because they cannot be synthesised *de novo* within the cell. Interestingly, BCAAs are important regulators of mammalian target of rapamycin (mTOR) [214]. mTOR is a key sensor of cell stress and is important in the regulation of innate and adaptive immune signaling. mTOR activity is also critical for the maintenance of host-cellular and viral gene expression during infection [215-217]. It may be that miR-US25-1 regulation of BCKDHA feeds into maintaining mTOR activity, by preventing the breakdown of BCAAs and thus preventing amino acid starvation and the subsequent inhibition of mTOR.

CCNE2

CCNE2 encodes cyclin E2, a key regulator of the cell cycle. Cyclin E2 binds to CDK2, which in turn inhibits cyclin D, allowing for the progression of the cell

cycle from G_1 to S phase [218]. HCMV has been shown to induce changes in the cell cycle during infection, and manipulates cell cycle progression in order to facilitate replication [219, 220]. It seems likely that HCMV first induces CCNE2 expression, and then HCMV miR-US25-1 regulation of CCNE2 contributes to the block of cell cycle progression at the G_1/S phase boundary. This establishes a cellular environment in the cell that is conducive with the replication of viral DNA. The data shown here recapitulate previous reports of HCMV miR-US25-1 regulating CCNE2 during infection [165]. Interestingly cyclin E1 was also confirmed as being regulated by several HCMV miRNAs, including miR-US25-1. Cyclin E1 and E2 have redundant functionality within the cell cycle, which suggests that coordinated regulation of both of these genes may be required to effectively manipulate the cell cycle during infection.

LGALS3

LGALS3 encodes galectin 3, a member of a family of β-galactoside binding proteins that have roles in cell adhesion and transmembrane signaling. Other galectin family members have been shown to have both enhancing and inhibitory roles in pathogen entry, replication, and pathogenesis [221-224]. Specifically, galectin-3 has been implicated within the endosomal pathway as being a detector of pathogen entry induced vacuole breakdown, binding host ligands normally presented in the lumen of endosomes [225]. Galectin-8 has been shown to have a similar activity and has also been shown to be a regulator of autophagy [223]. There is evidence that a downstream effect of galectin-3 knockdown is the down-regulation of pro-inflammatory cytokines [226]. It is plausible that miR-US25-1 might down-regulate these activities during infection

in order to prevent detection of HCMV and to inhibit the immune response. However, the role of galectin-3 in viral infection has not yet been characterised.

NUCB2

NUCB2 encodes nucleobindin-2, a poorly characterised protein with possible functions in calcium metabolism that has been identified as a biomarker for prostate cancer [227, 228]. A predicted family member, nucleobindin-1 was also identified as a target of HCMV miRNAs, raising another possibility that HCMV miRNAs may be regulating multiple redundant genes within biological pathways.

SGSH

SGSH encodes N-sulphoglucosamine sulphohydrolase, an enzyme that is required for the lysosomal degradation of heparan sulphate. Mutation of SGSH has been identified as the cause of Sanfilippo syndrome, a lysosomal storage disorder. There are no reports of SGSH being implicated in infection. However, the regulation of heparan sulphate is particularly relevant to HCMV infection as it is a key receptor that facilitates HCMV binding to the cell surface, which enables viral entry *via* viral glycoproteins interacting with the plasma membrane [45, 49]. As SGSH is regulated by HCMV post entry, it is possible that it may have another role. It may be that the degradation of heparan sulphate by SGSH has a role in inhibiting the release of viral ligands, which might affect MHC class I and class II presentation [45]. It is conceivable that this would be of benefit to HCMV during infection.

3. siRNA screening of HCMV miRNA targets identifies ATP6VOC as a host factor that is critical for viral replication

3.1. siRNA screen methodology

The data presented in Chapters 1.9 and 2 reveal multiple host-cellular transcripts that are regulated by HCMV miRNAs during infection, several of which are targeted solely by HCMV miR-US25-1. In order to identify critical host factors for HCMV biology among these targets, a phenotype driven siRNA screen was conceived.

Traditionally, virus replication is assayed by plaque analysis. However, for an siRNA screen of this scale this would not have been practical. The HCMV lifecycle is long, meaning that there are numerous time-points that require harvesting. Taking into account the number of replicates, and the number of siRNAs in the sceen, the expense of reagents and the manpower required would have been prohibitive. As such, a more direct approach for assaying viral fitness was devised. Fibroblast cells were transfected with siRNAs against the top targets of the HCMV miRNAs, and were infected with TB40E-eGFP, a strain of HCMV that constitutively expresses eGFP (here on in simply denoted TB40E), at an MOI of 1. Twenty-four hours later the inoculum was removed, and viral replication was measured over the course of infection *via* GFP intensity, which was monitored by plate reader. Genes that caused a viral phenotype when knocked down were validated using de-convoluted siRNA pools.

3.2. Hypotheses and aims

Through millions of years of coevolution of virus and host, it is likely that HCMV miRNAs have evolved to regulate the gene expression of factors that are important to HCMV biology. In Chapters 1.9 and 2 a number of host-cellular targets of HCMV miRNAs were identified. Monitoring changes in viral replication as a result of the knock-down of these genes should identify factors that are critical in HCMV biology.

The aims of the work presented in this chapter were to:

1. Identify host-cellular targets of HCMV miRNAs that are critical in HCMV biology by analysing viral growth kinetics.
2. Validate critical genes using de-convoluted pools of siRNAs.
3. Investigate viral phenotype using plaque analysis, microscopy, and viral gene expression analysis.

3.3. Establishing the efficacy of siRNAs for use in subsequent screens

In order to design an effective siRNA screen against viral phenotypes, it was critical to establish both the efficacy of the knockdown of the desired transcripts, and the optimum time-point post transfection to infect. To ascertain this, the efficacy of a selection of pre-validated commercial siRNAs was tested at 24, 48, and 72 hours post-transfection using qRTPCR (Figure 3.1). For the majority of the genes tested the knock-down increased with time post-transfection. GRN and NUCB1 expression levels were higher at 48 hours than at 24 hour post transfection. This may have been due to replicative variability, as the margin of error at these time points was high. However, the variation between replicates was smallest, and the knock-down of protein expression was highest, at 72 hours post transfection, therefore this time-point was selected.

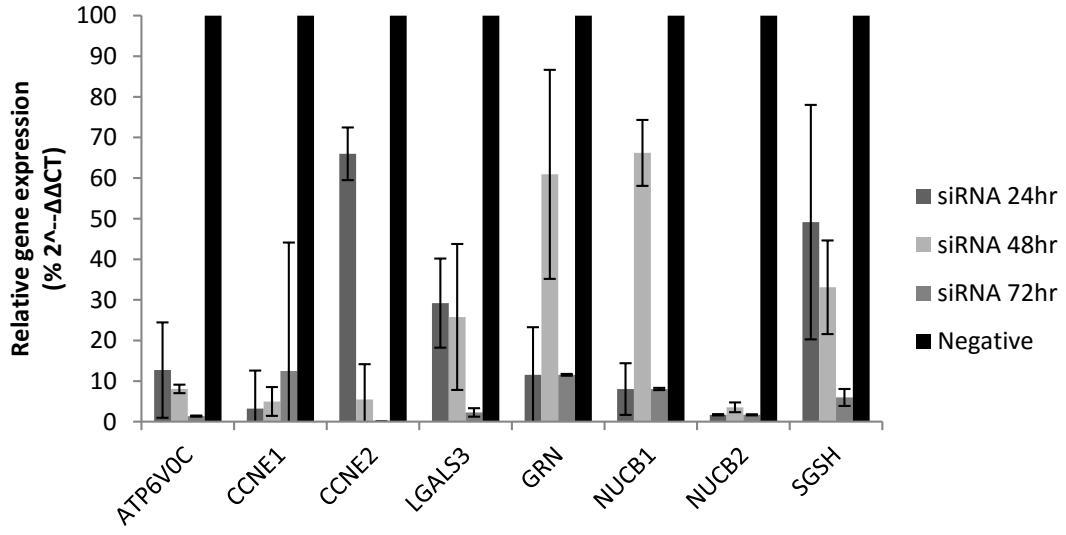

Figure 3.1 Efficacy test of commercial siRNAs for use in siRNA screen (20 nM) (N=2, n=4)
N = Number of technical replicates. n = Number of analytical replicates.

Fibroblast cells were transfected with siRNAs and lysates harvested at 24, 48, and 72 hours post-transfection. RNA was extracted and gene expression levels were ascertained by qRTPCR using specific primer probes. Error bars represent the standard-deviation from the mean.

3.4. siRNA knockdown of host-cellular targets of HCMV miRNAs affects viral replication

Fibroblast cells were transfected with siRNAs against the top host-cellular targets of HCMV encoded miRNAs (20 nM), and 72 hours later cells were infected with TB40E (MOI=1). Initially, the validated targets of HCMV miR-US25-1 were screened; ATP6VOC, BCKDHA, CCNE2, LGALS3, NUCB2, and SGSH.

In phenotypic screens, redundancy within host-cellular pathways has the potential to mask critical interactions. As such, possible redundant co-factors that were identified as targets of HCMV miRNAs from RISC-IP in AD169 infected fibroblasts were also selected; NUCB1 and CCNE1.

The GFP intensity over time in TB40E infected fibroblast cells transfected with siRNAs against ATP6VOC, BCKDHA, CCNE1, CCNE2, CCNE1&2, LGALS3, NUCB1, NUCB2, NUCB1&2, and SGSH is shown in Figure 3.2. The knockdown of the majority of these genes resulted in marginal effects on viral replication as measured by GFP intensity. However, ATP6VOC was a clear exception with HCMV replication inhibited by between 2-4 fold between 120 and 168 hpi.

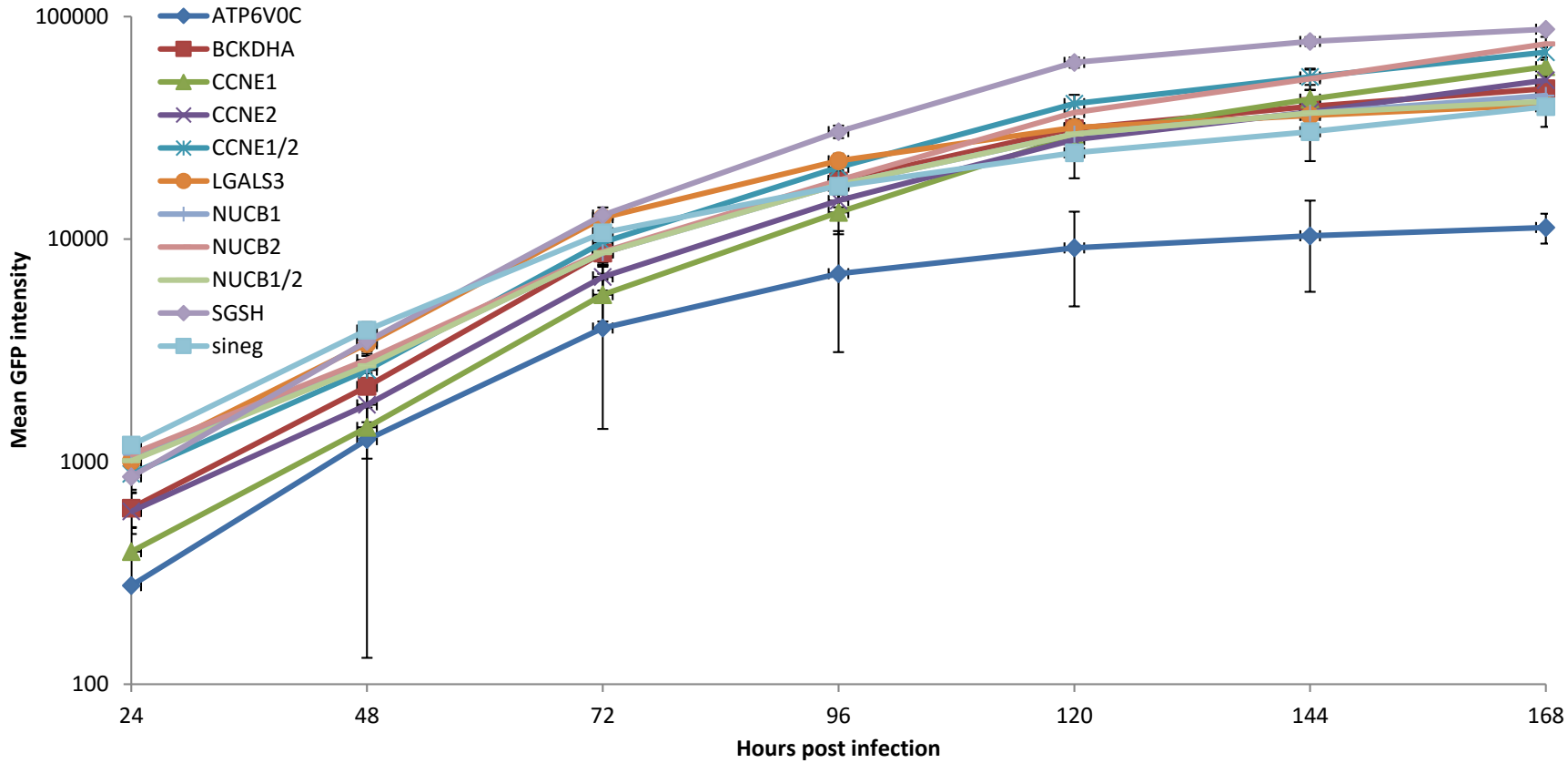

Figure 3.2 siRNA screen: TB40E GFP expression profile in fibroblast cells transfected with siRNAs against the validated targets of miR-US25-1 (MOI=1)(20 nM)(N=3)

Fibroblast cells were transfected with siRNAs and 72 hours post transfection were infected with TB40E. Virus replication was monitored *via* GFP plate reader. Error bars represent the standard-deviation from the mean.

The screen was expanded to include the top 30[4] most highly enriched targets identified from RISC-IP in AD169 infected fibroblasts. The GFP intensity at 144 hpi are summarised in Figure 3.3 and TB40E GFP expression profiles are presented in full in Chapter 7. These data demonstrate that there was little difference (less than 0.5 fold change) in viral replication after knock-down of the majority of the putative miRNA targets.

An arbitrary threshold of +/- 1.5 fold of the GFP intensity of fibroblast cells transfected with negative control siRNA was set for identifying induction or inhibition of viral replication. Four genes inhibited HCMV replication when knocked down: ATP6VOC, NUCB1, GRN, and PRSS8, and two genes induced HCMV replication when knocked-down: DSC2 and FAC1.

Again, the largest observed change in viral replication as determined by GFP intensity was observed with knock-down of ATP6VOC, which was the most highly enriched transcript in the infected RISC-IPs, and has been validated as being targeted solely by HCMV miR-US25-1 during infection.

[4] The top 30 became 28, as there were no commercially available siRNAs for FALZ, and COMMD10 was confirmed as being a false positive in the first screen.

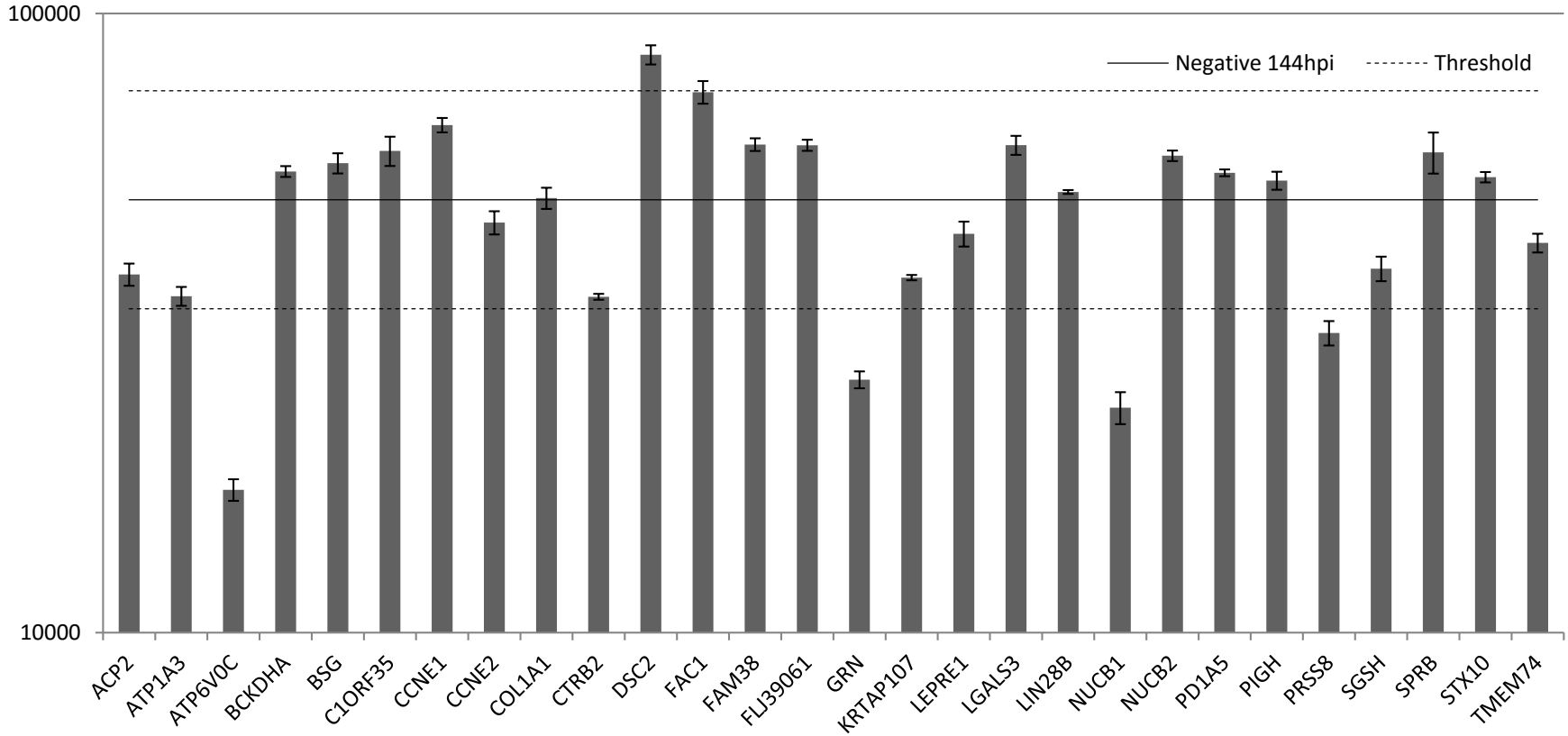

Figure 3.3 siRNA screen: TB40E GFP expression profile in fibroblast cells transfected with siRNAs against the top 30 host-cellular targets of HCMV miRNAs (20 nM)(144hpi)(N=3)

Fibroblast cells were transfected with siRNAs and 72 hours post transfection were infected with TB40E. Virus replication was monitored *via* GFP plate reader. Negative control siRNA is represented as a solid black line and the 0.5 and 1.5 fold thresholds are represented as dashed lines.

The three genes that produced the biggest phenotypic effect on HCMV replication when knocked-down were chosen for further study: ATP6VOC, DSC2, and NUCB1. A de-convoluted pool of distinct pre-validated siRNAs was used to ensure that the observed viral phenotypes were not due to off target effects of the siRNA. While the vendors of these siRNAs validate the knockdown of target genes, and screen for common adverse phenotypes that might indicate off-target effects, these experiments will not have been performed within the context of infection. As such, extra caution is required in this type of study to validate the effect of siRNAs on viral replication. The results of the assessment of the de-convoluted pools of ATP6VOC, DSC2, and NUCB1 siRNAs are summarised in Figure 3.4. The ATP6VOC siRNAs, and to a lesser degree NUCB1 siRNAs, produced a consistent decrease in TB40E replication. This gave confidence that the decreases observed in TB40E replication was not the result of an off target effect. The increase observed in TB40E replication with DSC2 siRNA in the initial screen, was not recapitulated with the de-convoluted siRNA pool. This indicates that the result for DSC2 in the initial screen was likely due to an off-target effect of the siRNAs.

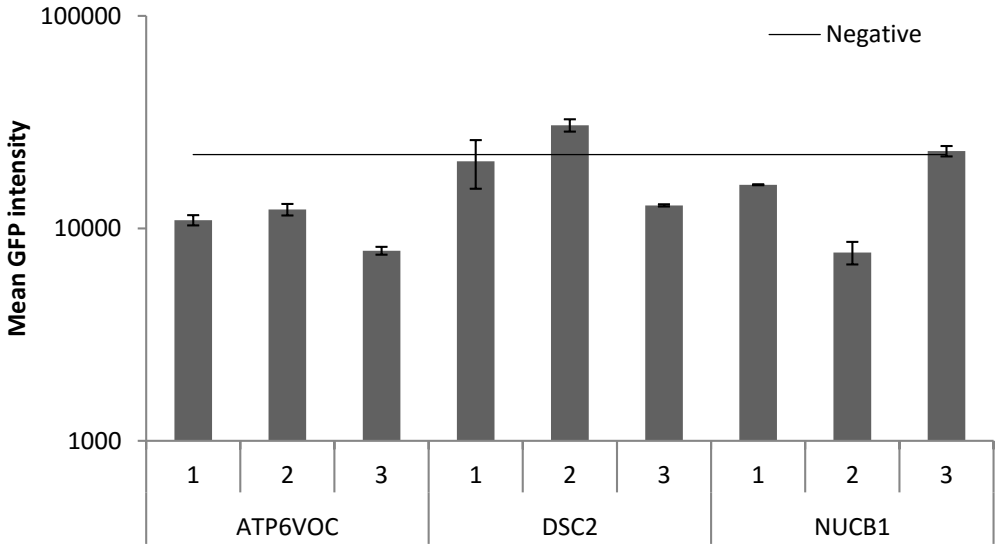

Figure 3.4 TB40E GFP expression profiles in fibroblast cells transfected with deconvoluted pool of ATP6VOC, DSC2, and NUCB1 siRNAs (20 nM)(120hpi)(N=3)
Fibroblast cells were transfected with siRNAs and 72 hours post transfection were infected with TB40E. Virus replication was monitored *via* GFP plate reader. Error bars represent the standard-deviation from the mean.

Finally, the possibility that the observed defect in viral replication was a non-specific consequence of a loss of cell-viability or IFNβ induction was ruled out. There was no change in cell viability or IFNβ induction in fibroblasts after ATP6VOC knock-down, when compared with the negative control (Appendix Figure 7.4 and Figure 7.5).

3.5. ATP6VOC expression is not required for entry and viral gene expression, but is critical for the formation of functional HCMV virions

In order to further characterise the defect in viral replication after knock-down of ATP6VOC in fibroblast cells, it was necessary to dissect where in the HCMV viral lifecycle this defect occured. To this end, fibroblast cells were infected with TB40E after ATP6VOC knock-down, and defects in entry, penetration, and un-packaging were assayed using fluorescent microscopy and qRTPCR against viral genes during infection (Figure 3.5 and Figure 3.6). Defects in assembly and egress of the virus, were assayed using viral genome copy number analyses and plaque analyses (Figure 3.7).

There was no apparent reduction in the proportion of GFP positive fibroblast cells after ATP6VOC knock-down when compared with the negative control siRNA transfected fibroblast cells, with 100% of cells GFP positive at 24 hpi (MOI=1) (Figure 3.5).

Viral gene expression levels were calculated using the ΔΔct method, and normalised to the gene expression level in the 2 hpi negative control sample, to provide a relative measure of gene expression over time. Viral gene expression profiles were intact in fibroblast cells after ATP6VOC knock-down. Interestingly, between 24 and 72 hpi, there was a marginal (2 to 3 fold) increase in the expression of IE86 in fibroblast cells after ATP6VOC knock-down. However, at the majority of time-points viral gene expression was equivalent in fibroblast cells after ATP6VOC knock-down, when compared with negative control transfected fibroblast cells, for immediate early (IE86), late (UL83), and true

late (gH: UL75) genes (Figure 3.6). Taken together, these data demonstrate that ATP6VOC knock-down in fibroblast cells: does not prevent the entry of HCMV into fibroblast cells; does not prevent either intracellular trafficking of the virion or genome penetration; and does not affect viral gene expression, with viral mRNA transcribed as normal.

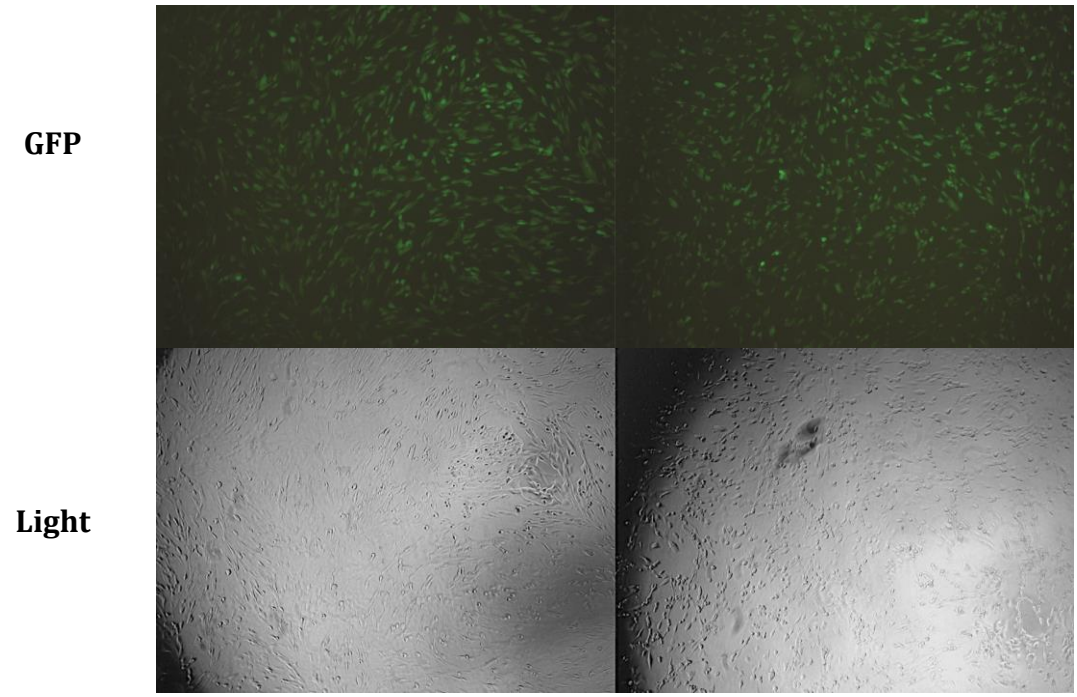

Figure 3.5 Fluorescence microscopy of fibroblast cells transfected with ATP6VOC siRNA and infected with TB40E (MOI=1) (24hpi) (10X magnification)

Fibroblasts were transfected with ATP6OC siRNA, or a negative control siRNA. 72 hours post transfection, cells were infected with TB40E at an MOI of 1, and were imaged by fluorescence microscopy at 24 hours post infection.

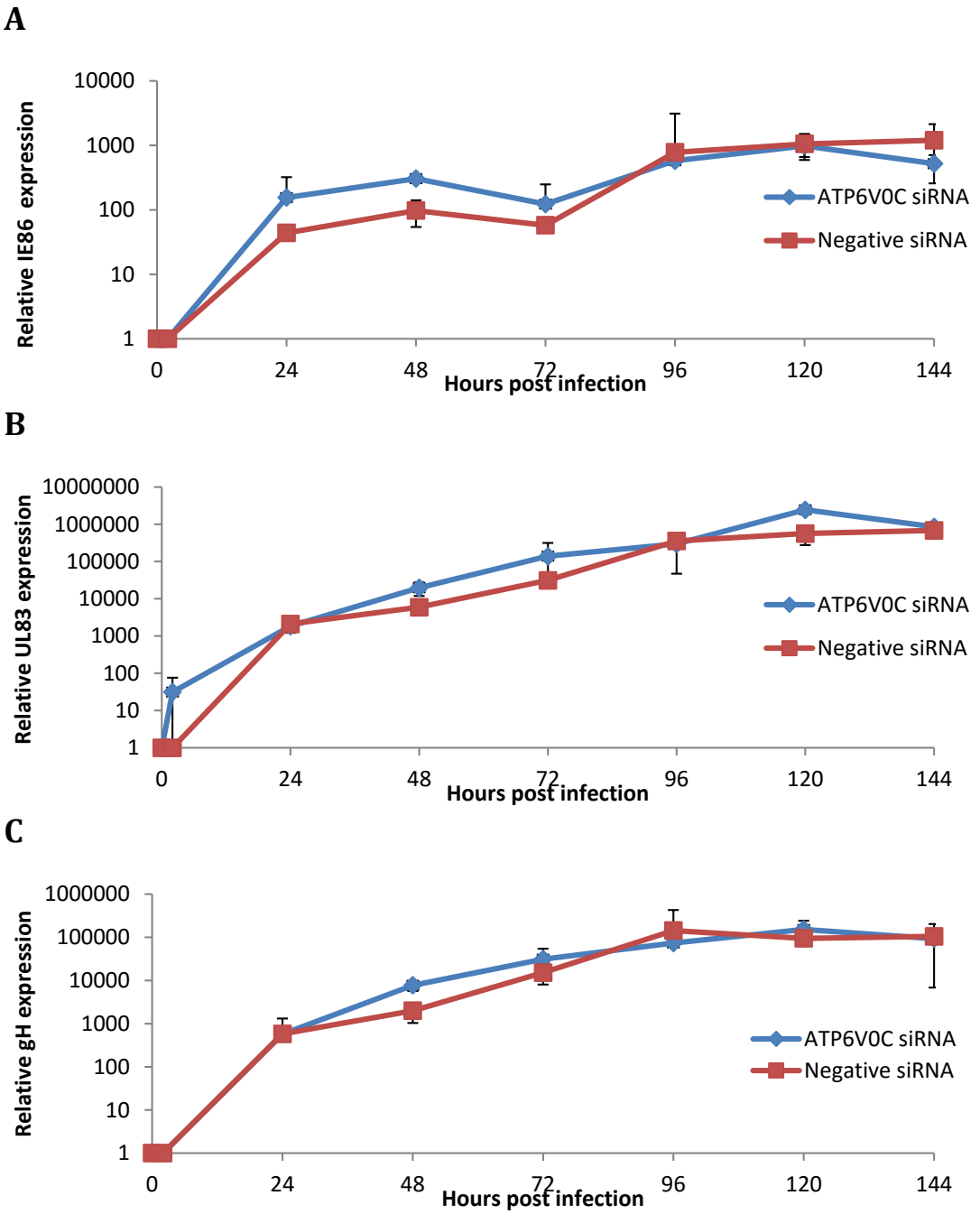

Figure 3.6 Viral gene expression in fibroblast cells transfected with ATP6VOC siRNA and infected with AD169 (N=2)

A. IE86 gene expression **B.** UL83 gene expression **C.** gH gene expression. Fibroblast cells were transfected with ATP6VOC siRNA or a negative control siRNA and at 72 hours post transfection were infected with AD169 at an MOI of 1. Infected cells were harvested and genomic DNA isolated. Viral gene expression was calculated by the ΔΔct method, normalised to expression levels in the 2 hpi negative control sample. Error bars represent the standard-deviation from the mean.

Despite the apparent lack of effect on viral gene expression, there was a striking difference in the production of progeny virions in fibroblast cells after ATP6VOC knock-down compared with negative control siRNA transfected fibroblast cells (Figure 3.7). There was a decrease in the number of plaque forming units (PFU) of between 2 and 4 $\log^{10}$ (100 and 10000 fold) between 72 and 144 hpi in fibroblast cells after ATP6VOC knock-down compared with negative control transfected fibroblast cells, while a similar number of viral genomes were detected at each time point (Figure 3.7**A** and **B,** respectively). The relative 'infectivity' of the progeny virus from these cells is given as a ratio in Figure 3.7**C**, with a higher ratio indicating more infectious units per detected genome.

A

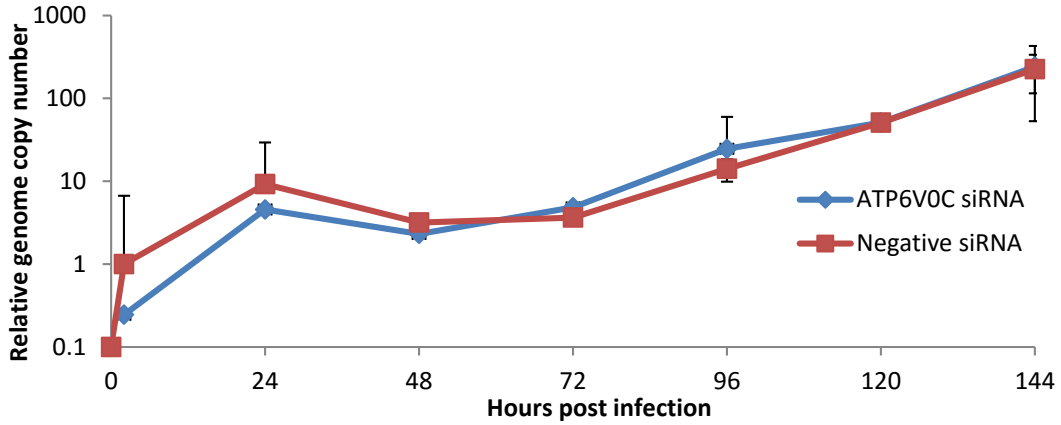

B

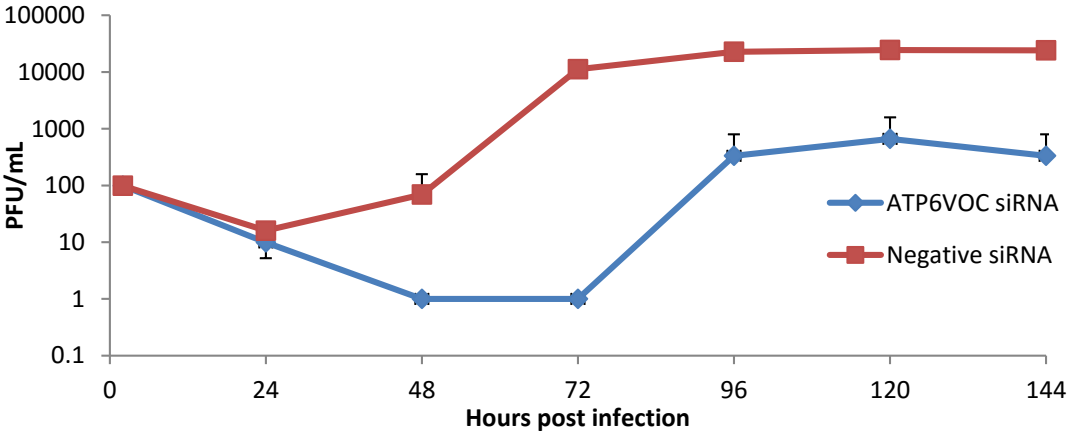

C

	2hpi	24hpi	48hpi	72hpi	96hpi	120hpi	144hpi
ATP6VOC siRNA	1:10	1:0.2	1:0.4	1:69	1:27	1:13	1:1.4
Negative siRNA	1:16	1:7.5	1:3540	1:6250	1:1610	1:480	1:107

Figure 3.7 Relative viral genome copy number, PFU/mL, and genome copy number : PFU ratios from lysates of fibroblast cells transfected with ATP6VOC siRNA of negative control siRNA and infected with TB40E (N=3) (MOI=1)

A. Genome copy number **B**. PFU/mL **C**. Genome copy number : PFU ratio Fibroblast cells were transfected with ATP6VOC siRNA or a negative control siRNA and at 72 hours post transfection were infected with AD169 at an MOI of 1. Infected cells were harvested by scraping into media, and were fractioned. Genomic DNA was isolated, and analysed for genome copy number by qRTPCR using gH and UL83 primer probes. Lysates of infected cells were analysed by plaque assay. Error bars represent the standard-deviation from the mean.

3.6. Discussion

The data presented in this chapter identify the miR-US25-1 target ATP6VOC as a critical host factor that is required for HCMV replication in fibroblast cells *in vitro*. Marginal changes (<1.5 fold) in viral replication were observed for the majority of the validated and putative HCMV miRNA targets that were screened using siRNA knock-down (Figure 3.2). The biggest decreases in viral replication were observed in fibroblast cells transfected with siRNAs against ATP6VOC and NUCB1, and the biggest increases were observed in fibroblast cells transfected with DSC2 and FAC1. Of these, ATP6VOC knock-down was validated as being responsible for inhibiting viral replication using a de-convoluted pool of siRNAs.

Further examination confirmed a post-entry defect, as both GFP expression and viral gene expression profiles were similar in fibroblast cells after ATP6VOC knock-down when compared with negative control transfected fibroblast cells. However, there was a striking difference in the progeny virus produced by cells transfected with ATP6VOC siRNA: despite similar numbers of viral genomes being produced in fibroblast cells after ATP6VOC knock-down when compared with negative control transfected fibroblast cells, there was a 2-4 fold decrease in the number of plaque forming units produced.

3.7. siRNA screening to identify novel host-virus interactions

Several other groups have used similar approaches, either screening the entire host genome, select pathways, or druggable targets, in order to identify critical host-factors for several alphaviruses, influenza A virus, HCV, HIV and HPV [229-240]. The real power and novelty in the screen presented here is that rather than blindly screening for host-cell factors that are involved in virus replication, this screen focused on genes that appear to be actively regulated during infection by HCMV miRNAs. While this approach proved fruitful in this instance, there are several changes in experimental design that might have improved the sensitivity of the screen in identifying critical factors.

One consideration to be made is that the artificial conditions experienced by infected cells *in vitro* may obscure important host factors. It is possible that certain pathways regulated by HCMV miRNAs may only be relevant under certain biological conditions and that the serum and nutrient rich cell-culture environment may obscure these interactions. BCKDHA and CCNE1/2 may represent examples of this. BCKDHA function is only likely to be relevant in an environment where BCAAs are depleted. CCNE1/2 inhibition may only be applicable in conditions of cell stress where the cell cycle is arrested. In these cases it would be informative to test the effect of BCKDHA knock-down in BCAA starved conditions, and CCNE1/2 in serum starved conditions. As discussed in Chapter 1 and 2, there is also a likelihood that miRNA function may well be cell specific, as is evident for other HCMV gene products. As such, it would be informative to repeat this screen in endothelial and epithelial cells.

Within the context of miRNA regulation of host-cellular genes, the use of an siRNA screen is perhaps not as representative as a screen that would allow for the overexpression of these factors. However, within the scope of this study, this would not have been practical. Recently, other groups have developed lenti-viral libraries that allow the overexpression of factors to analyse their relevance within the context of infection. This has been particularly informative for analysing the effect of interferon-stimulated genes on innate immune responses to several viruses [241, 242]. Using this type of screen allied with siRNAs for putative miRNA targets would be a powerful technique for identifying critical roles of the regulation of specific miRNA targets during infection.

A major problem with interpretation of siRNA screen data is highlighted in the variable results obtained from the de-convoluted pool of siRNAs against DSC2. Commercial siRNAs are pre-validated and screened for common biomarkers of off-target effects. However, they are not screened for off-target effects within the context of infection and phenotypically innocuous off-target effects in uninfected cells can have a dramatic effect on infection. As such, one improvement would be to use de-convoluted siRNA pools for every gene within the screen to avoid false positives. However the increased cost of such an approach would have proved prohibitive within the scope of this study.

Finally, the inherent redundancy of eukaryotic processes represents an obstacle when using an siRNA screen to identify novel host-virus interactions. As highlighted earlier, there is evidence that viral miRNAs have the capacity to

target multiple genes within related pathways and it seems likely that these interactions may have evolved to circumvent the redundancy that is prevalent in eukaryotic processes, in order to bring about a change in host-cell phenotype during infection. The importance of targets within these pathways to HCMV biology may therefore not be apparent unless several genes within these pathways are knocked-down. Attempts were made to circumvent this, with the co-transfection of siRNAs against cyclin and nucleobindin family members within the initial siRNA screen. However, until there is a more thorough working knowledge of the host-cellular targets of HCMV miRNAs, this problem will be difficult to overcome.

4. v-ATPase acidification of host-cellular compartments is required for the formation of the HCMV virion assembly compartment

4.1. Differentiating the roles of ATP6VOC and miR-US25-1 in infection

The data presented in the previous chapters demonstrate that ATP6VOC is a target of HCMV miR-US25-1 during infection, that ATP6VOC expression is critical for virus replication, and that it likely has functions in the assembly and egress of HCMV during infection.

However, the role of miR-US25-1 regulation of ATP6VOC during infection is unclear. It seems unlikely that HCMV would encode an miRNA to regulate a host-cellular transcript during infection in order to disrupt HCMV production. As such, it seems likely that the viral phenotype identified in the siRNA screen is not reflective of the role of miR-US25-1 during infection, as it is the result of a complete knock-down of ATP6VOC at early time-points, which is unlikely to occur *via* miRNA mediated regulation of ATP6VOC within the context of infection.

Nevertheless, the loss of function experiments presented in Chapter 3 have revealed ATP6VOC as being a critical host factor in HCMV infection and this has intriguing implications for the roles of the endocytic and secretory pathways in HCMV assembly and egress. These roles are explored further in this chapter.

4.2. The HCMV viral assembly compartment

Herpesvirus assembly is a complex process (as reviewed in [8, 243]). In brief, viral DNA is synthesised in the nucleus and packaged into nucleocapsids. These particles then escape the nuclear lamina and bud through the inner nuclear membrane into the perinuclear space, acquiring a primary envelope in the process. This envelope then fuses with the outer nuclear membrane allowing for egress of the nucleocapsid into the cytoplasm [8].

Once in the cytoplasm, tegument proteins assemble on the capsid, and secondary envelopment occurs as the virion buds into trans-golgi network (TGN) or endoplasmic reticulum (ER) derived plasma membranes that contain viral glycoproteins. The mature virion is then trafficked to the cell surface where it egresses into the extracellular space [8].

During HCMV infection, there are a number of dramatic changes that occur in the cell to facilitate viral assembly. The lytic replication cycle is long, with an initial phase of 96 hours where very few viral progeny are produced. During this time, the cytoskeleton remodels [244], nuclei increase in volume and change in morphology [72], and secretory and endocytic vacuoles reorganise [244, 245].

The most striking result of these changes is the aggregation of elements of the endocytic pathway and secretory apparatus to form a juxtanuclear cytoplasmic inclusion. This inclusion is the HCMV virion assembly compartment (VAC).

The VAC was first described with the use of immunofluorescence microscopy as a region of infected cells where several cytoplasmic virion proteins (pp150, gB,

gH, pp28 and gp65) colocalise late in infection. These proteins also overlap with markers of trans-golgi compartments of the host-cellular secretory apparatus (GM130, Mann II) and this structure lies at the centre of a relocated microtubule organising centre [72, 74]. Since these initial observations, several other host-cellular and viral components have been shown to localise to the site of viral assembly [72, 75-77, 188, 246, 247]. In addition to markers of compartments derived from the trans-golgi network, (TGN46, p230, GM130, and Mann II), compartments derived from the early endosomal (EEA1), late endocytic (VPS4), and ESCRT-III (CHMP1A) pathways colocalise with viral markers within the VAC. While these markers all relocalise to this juxtanuclear inclusion, they each appear to have distinct localisations from one another, leading some to suggest that each compartment may have distinct biological roles in viral assembly [247]. Altogether, the evidence suggests that these host-cellular cytoplasmic compartments are re-organised in a deliberate fashion during HCMV infection to facilitate the recruitment of viral tegument proteins to the nucleocapsid before the mature virus buds into an exocytic vesicle where the virion acquires a final envelope, which contains the requisite quota of viral glycoproteins [80].

Despite evidence of the constituents of the VAC, the host-cellular and viral genes that play roles in the biogenesis of the VAC are poorly understood.

Das *et al* described three HCMV tegument proteins that have been identified as important contributors to VAC biogenesis; UL48, UL94, and UL103 [75]. From previous studies of these proteins and their orthologues in other *Herpesviridae*

family members, UL48 is thought to be a ubiquitin specific protease with roles in capsid transport, UL94 a single stranded DNA binding protein involved in cytoplasmic egress, and UL103 a factor important for late stage replication and egress. Knock-down of these proteins and subsequent infection with HCMV results in a complete loss of progeny virus (for UL94 and UL103 knock-down) or an increase in the number of defective particles and a 2 $\log^{10}$decrease in infectious virus (for UL48 knock-down) [75].

Bughio *et al* [188] described 4 proteins encoded by the UL133-138 locus as being critical for VAC biogenesis in endothelial cells, with a UL133-138^{NULL} strain of TB40E exhibiting defective replication kinetics. Interestingly, this locus is disposable in fibroblast cells. Conversely, Schauflinger *et al* [79] demonstrated that UL71, a viral protein required in fibroblast cells for assembly compartment formation and efficient secondary envelopment, is dispensable in endothelial cells. These examples highlight that the determinants of VAC biogenesis appear to be tropism specific.

In addition to these viral factors, several host factors have been identified whose regulation during infection is essential in VAC biogenesis. Particularly relevant to this study, several of these have been shown to be regulated by HCMV encoded miRNAs.

Hook *et al* demonstrated that VAMP3, RAB5C, RAB11A, SNAP23, and CDC42 are the targets of HCMV encoded microRNAs. Down regulation of these endocytic and secretory pathway genes by miR-UL112-1, US5-1, and US5-2, appear to facilitate the formation of the VAC [172]. It is particularly interesting that the

down-regulation of these genes also reduces the levels of secreted pro-inflammatory cytokines TNFα and IL-6. This highlights that the subjugation of the endocytic and secretory pathways to facilitate VAC biogenesis may also be responsible for reducing the inflammatory response to infected cells *in vivo*, dampening the host immune response to infected cells at late times post infection.

Although VAC formation has not been shown to be explicitly required for functional virion formation, there is an overriding theme that the disruption of factors involved in VAC biogenesis results in a defective viral phenotype. This lends to a hypothesis that VAC formation is required for the efficient assembly of HCMV.

4.3. v-ATPases in the endocytic and secretory pathways

The v-ATPase is a membrane spanning, multi-domain ion pump that is responsible for the regulation of pH in membrane-bound organelles throughout the cell. These channels consist of a luminal V_1 domain, which is responsible for the hydrolysis of ATP, and a trans-membrane V_0 domain which forms the proton channel. ATP6VOC is a critical component within the V_0 domain [248].

The v-ATPase is crucial in the establishment of a low intraluminal pH in vacuoles, and this is pivotal for a variety of processes within the endocytic and secretory pathways. The endocytic pathway is the means by which cells process extracellular cargo. Extracellular macromolecules are transported across the outer cell membrane by receptor/clathrin mediated endocytosis, macropinocytosis, or in caveolae. Once internalised, these macromolecules are sorted in a series of intermediate compartments, and either recycled to the cell surface, or degraded within the lysosome. An acidic intraluminal pH in endosomes facilitates the dissociation of internalised ligand-receptor complexes, which allows cells to selectively internalise extracellular macromolecules and recycle their associated receptors back to the cell membrane [249, 250]. The intracellular sorting of these macromolecules is also dependent on the acidification of vacuoles. Trafficking between early and late endosomes *via* endosomal carrier vesicles, traffic between endosomes and lysosomes, and the fusion of multivesicular bodies with lysosomes are all dependent on the activity of the v-ATPase [251, 252]. Finally, at the terminus of the endocytic pathway, the degradative enzymes within the lysosome require

an acidic pH in order to function, which is again dependent of the v-ATPase [249, 253].

The secretory pathway is the means by which newly synthesised proteins are sorted and trafficked to their final destination within the cell. The intraluminal pH of secretory compartments plays a crucial role in this process. Many newly synthesised proteins are translated by ribosomes that are tethered on the ER surface, and these peptides co-translationally enter the ER lumen [254]. These proteins are then sorted *via* cis-, medial-, and trans-golgi compartments for constitutive or regulated secretion, or for lysosomal degradation. The v-ATPase acidifies these compartments, facilitating the post-translational modification of newly synthesised proteins within trans-golgi vacuoles and for the proper targeting of these proteins to their termini [254-256].

Within the context of infection the possible roles of ATP6VOC and the endocytic and secretory pathways are intriguing. The majority of viruses exploit the endocytic pathway to obtain entry into cells, typically by receptor mediated endocytosis in clathrin coated vesicles. Once internalised, several viruses exploit the acidification of these endosomes to facilitate release of the viral genome into the host cell. One elegant and well-studied example is influenza A virus. Haemaglutinin (HA) molecules on the surface of influenza A virions bind sialic acid receptors on the cell surface which facilitate the internalisation of the virion into the cell. The acidification of virus containing endosomes causes a conformational change in the HA molecules that allow for fusion between the influenza lipid membrane and the endosome membrane, which causes release

of the viral RNPs into the cytoplasm [257, 258]. For some other viruses, such as Ebola virus and SARS coronavirus, acid dependent cleavage of viral glycoproteins by endosomal proteases is required for the penetration of the viral genomes in the cytosol [259, 260]. The roles of acidification in these processes is summarised in Figure 4.1.

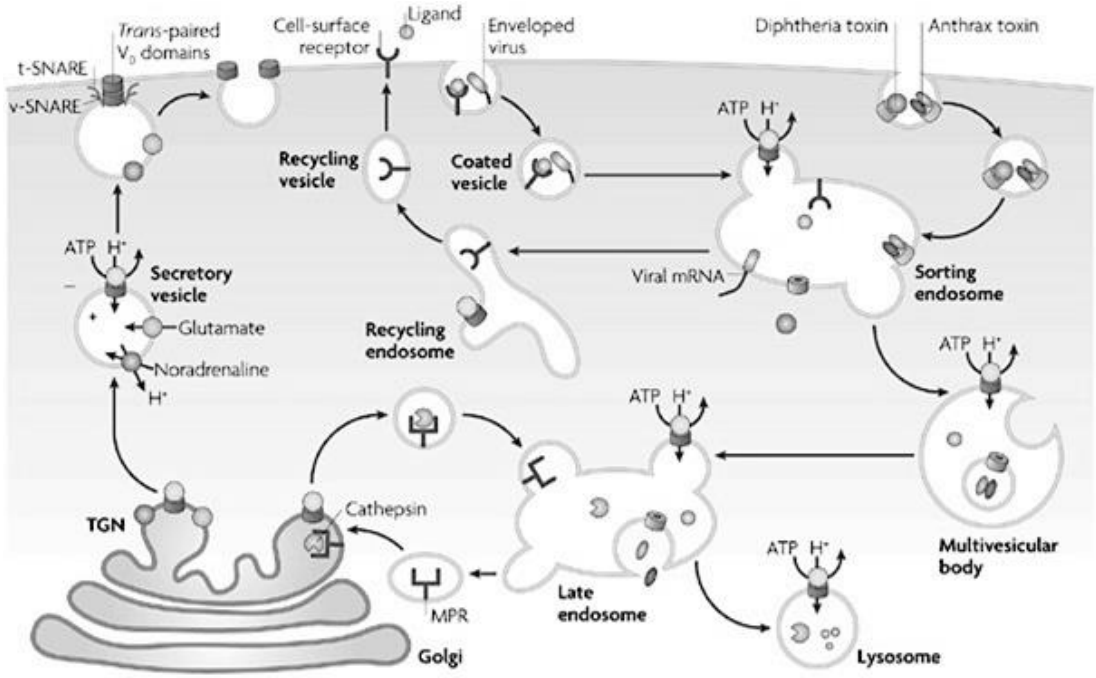

Figure 4.1 Summary of roles of acidification in membrane trafficking processes.
Adapted from Forgac, Nature Reviews Molecular Cell Biology, 2007.

In addition to the role of the v-ATPase in vacuolar acidification, there have also been several observations in a variety of contexts that the V_o domain of the v-ATPase may have an intrinsic membrane fusion activity. In mice, *C. elegans*, and *Drosophila*, the V_o domain has been shown to interact with VAMP-2, syntaxin-1 and Ca^{2+} release channels to directly catalyse the mixing of two lipid bilayers, in an acidification dependent manner [261-265].

Within the context of HCMV infection, the role of ATP6VOC is potentially more complicated due to the distinct methods of entry into different host cell types. In epithelial and endothelial cells, entry predominantly occurs by endocytosis, and penetration by low pH fusion[44]. In fibroblast cells, however, entry predominantly occurs by plasma membrane fusion which allows the naked nucleocapsid to penetrate the cytosol directly [48]. As this process is pH independent, one would predict that v-ATPase activity should not effect HCMV entry into fibroblast cells, and this is supported by the observations presented in Chapter 3. Conversely, v-ATPase activity is likely to be required for entry and penetration of endothelial and epithelial cells.

Post-entry, the endocytic and secretory pathways are subjugated during HCMV infection to facilitate VAC biogenesis. It is possible that an acidic pH within these compartments is required for viral assembly. With the v-ATPase responsible for the acidification of these compartments, it is plausible that the defect that was identified in HCMV replication in fibroblast cells after ATP6VOC knock-down could be the result of a critical defect in VAC biogenesis, or that acidification within the VAC is critical for virion assembly.

4.4. Hypothesis and aims

It was hypothesised that ATP6VOC might be required for the formation of the HCMV virion assembly compartment, and this may be critical for the assembly of functional virions.

The aims of the work presented in this chapter were to:

1. Interrogate HCMV VAC biogenesis in fibroblast cells after knock-down of ATP6VOC.
2. De-convolute the membrane fusogenic and vacuolar acidification effects of ATPVOC within the context of HCMV infection.
3. Characterise and identify defective phenotypes of progeny virus from fibroblast cells lacking the expression of ATP6VOC.

4.5. ATP6VOC is required for HCMV virion assembly compartment biogenesis

Immunofluorescence microscopy was performed to observe the distribution of both host-cellular (TGN46 and EEA1) and viral (pp28) markers of the HCMV VAC in fibroblast cells transfected with an siRNA against ATP6VOC or a negative control siRNA. In cells transfected with a negative control siRNA, host-cellular proteins TGN46 and EEA1 colocalised with the viral tegument protein pp28 in a region adjacent to an enlarged, kidney shape nucleus (Figure 4.2). This staining was primarily diffuse, lacking defined boundaries, and was consistent in localisation and appearance with previous reports of the HCMV VAC [74-76, 188, 246, 247].

In fibroblast cells transfected with ATP6VOC siRNA, there were several observable morphogenic differences when compared with negative control siRNA transfected fibroblasts. The cells were noticeably smaller under low magnification (as can be seen in Figure 3.5), and using high magnification confocal microscopy there was a clear decrease in nuclear volume, and the characteristic kidney shape observed after infection in negative control siRNA transfected fibroblasts was not as apparent. While the host-cellular markers of the VAC appeared to redistribute to a similar juxtanuclear location within the cell, the staining of TGN46 was less diffuse than the pattern observed in negative control siRNA transfected fibroblast cells, and the staining of EEA1 had clear boundaries, indicative of large vesicular compartments. Most strikingly,

pp28 did not colocalise with the host-cellular markers of the VAC (Figure 4.2). Images from a wider field of view are shown in Figure 4.3**A**.

Importantly, these qualitative observations were quantifiable. Scatter plots of pixel intensity from a multi-cell field demonstrated that staining for TGN46 and pp28 overlapped extensively in negative control siRNA transfected fibroblast cells, but did not overlap in fibroblast cells after ATP6VOC knock-down (Figure 4.3**B**). Colocalisation analyses of TGN46, EEA1 and pp28 were performed and Pearson's R scores calculated (1=convergent 0=divergent) from several multi-cell images. The frequency of TGN46 and pp28 staining convergence was high in negative control siRNA transfected fibroblast cells (R=0.58), and low in ATP6VOC siRNA transfected fibroblast cells (R=0.16). Similarly, EEA1 and pp28 staining convergence was high in negative control fibroblast cells (R=0.41) and low in ATP6VOC siRNA transfected fibroblast cells (R=0.17) (Figure 4.3**C**).

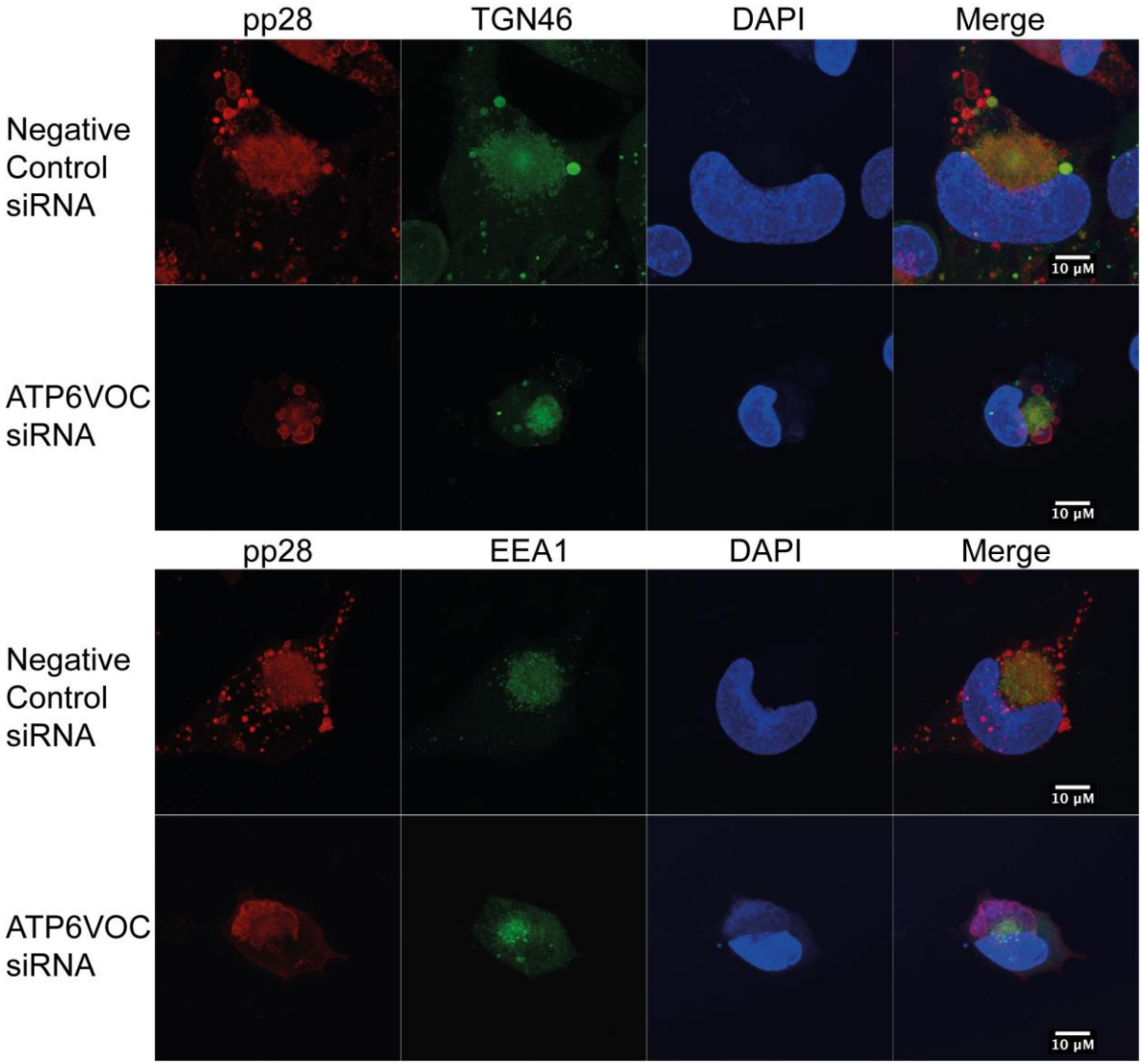

Figure 4.2 Immunofluorescence microscopy of the HCMV viral assembly compartment in fibroblast cells transfected with ATP6VOC siRNA or negative control siRNA (144 hpi) (63X magnification, 2x zoom)
Fibroblast cells were transfected with ATP6VOC siRNA or negative control siRNA and at 72 hours post transfection were infected with AD169. At 144 hpi cells were fixed, permeabilised, and stained for early endosomes or trans golgi vacuoles (EEA1:green or TGN46:green), viral tegument protein (pp28:red), and nuclei (DAPI:blue). Images were acquired on a Zeiss LSM710 confocal microscope. Images presented here are maximum intensity projections compiled from multiple 0.33 µm slices through the Z-axis. 3D renders of these images are provided in

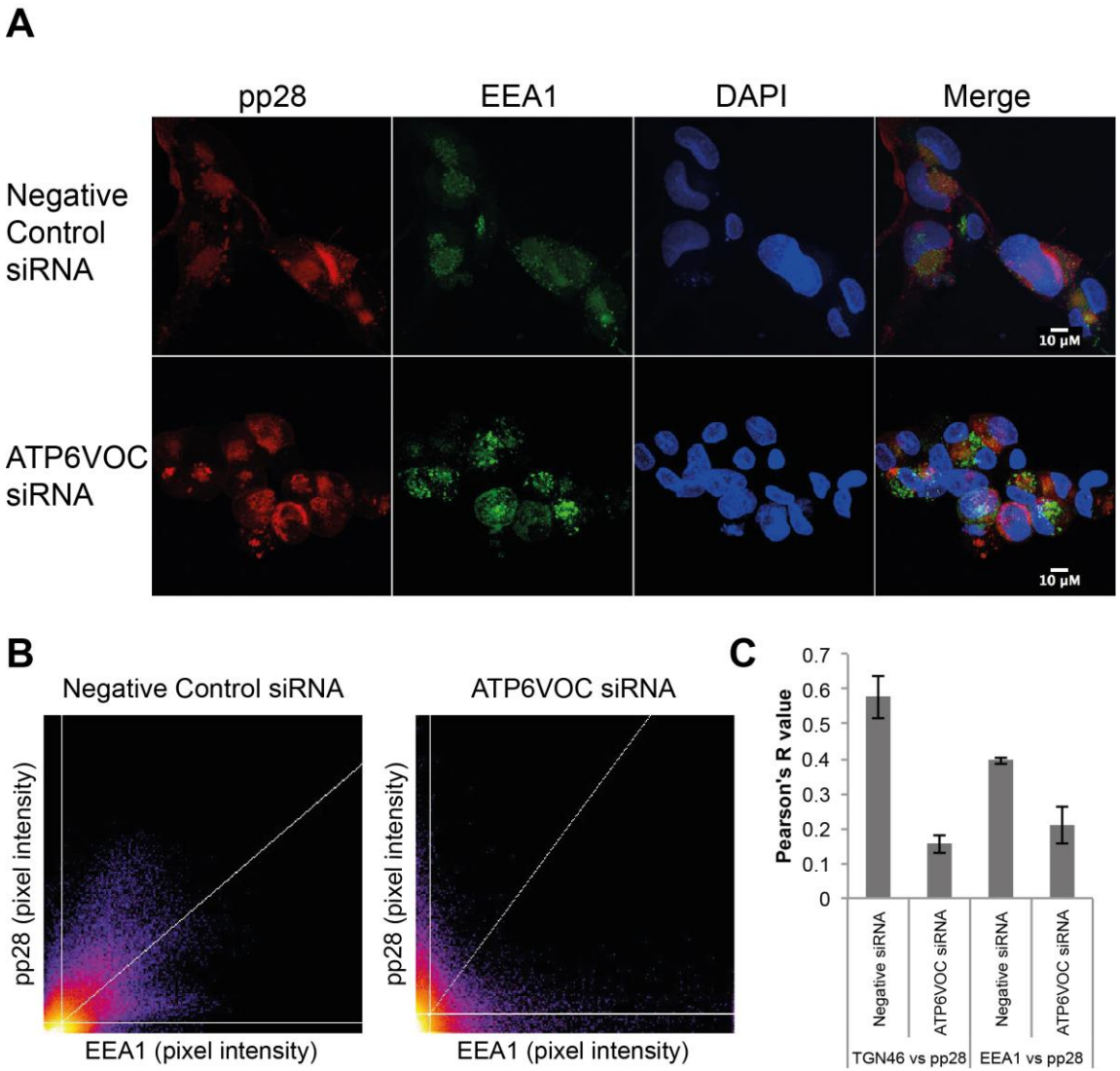

Figure 4.3 Immunofluorescence microscopy of the HCMV viral assembly compartment in fibroblast cells transfected with ATP6VOC siRNA (144 hpi) (63X magnification)
A. Fibroblast cells were transfected with ATP6VOC siRNA or negative control siRNA and at 72 hours post transfection were infected with AD169. At 144 hpi cells were fixed, permeabilised, and stained for early endosomes or trans golgi vacuoles , (EEA1:green or TGN46:green), viral tegument protein (pp28:red) and nuclei (DAPI:blue). Images represent single slices through the Z-axis. **B**. Representative scatter-plot showing average pixel signal intensity in red (pp28) and green (EEA1) channels from multicell images (n=16 for ATP6VOC and n=9 for negative siRNA). Individual images in the Z-field were analysed using Fiji image analysis software. **C**. Pearson's R-value for colocalisation of TGN46 or EEA1 and pp28 in ATP6VOC or negative control siRNA transfected fibroblast cells (n=20).

There was a possibility that this defect was due to the gross disruption of secretory and endocytic pathways as a consequence of ATP6VOC knock-down. To assess whether this was the case, the distribution of these markers in unifected cells was analysed by immunofluorescence microscopy (Figure 4.4**A**) and the abundance of these proteins was analysed by western blot in uninfected cells and infected cells (Figure 4.4**B** and **C**). The distribution of both TGN46 and EEA1 was similar in fibroblast cells after ATP6VOC knock-down when compared with fibroblasts transfected with a negative control siRNA . The abundance of TGN46 and EEA1 proteins were also equivalent in both ATP6VOC siRNA and negative control siRNA transfected fibroblast cells, in uninfected cells and also at 144 hours post infection (Figure 4.4**B** and **C**).

Taken together, the data presented in Figure 4.2, Figure 4.3, and Figure 4.4 demonstrate that ATP6VOC is required for the re-localisation of host-cellular compartments during HCMV VAC biogenesis.

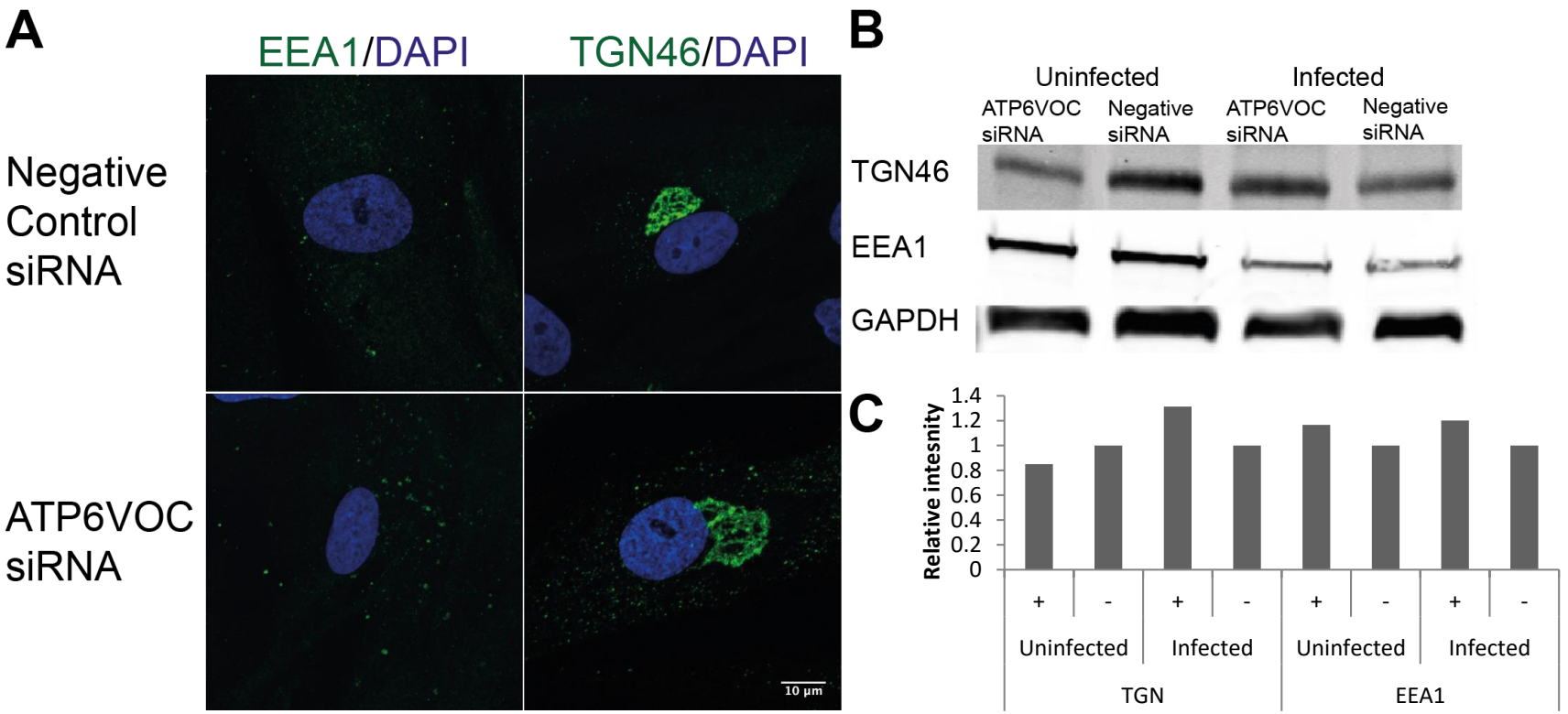

Figure 4.4 Immunofluorescence microscopy of trans-golgi network and early endosomes in fibroblast cells transfected with ATP6VOC siRNA or a negative control siRNA (63 x magnification, 2 x zoom) (72 hours post transfection/hpi)

A. Fibroblast cells were transfected with ATP6VOC siRNA or negative control siRNA. At 72 hours post transfection cells were fixed, permeabilised, and stained for early endosomes or trans golgi vacuoles. Images are maximum intensity projections compiled from multiple 0.33 µM slices through the Z-axis. **B.** Western blot analyses of ATP6VOC siRNA and negative control and transfected fibroblast cells against markers of trans-golgi vacuoles (TGN46), early endosomes (EEA1). Infected cells were harvested at 72 hpi. **C.** Quantification of representative western blot, relative to GAPDH. **+** = ATP6VOC siRNA transfected fibroblast, - = Negative control siRNA.

4.6. v-ATPase acidification activity is required in fibroblast cells for efficient virus production and VAC formation in fibroblast cells

There are two different roles ascribed to ATP6VOC: as a critical component of the v-ATPase responsible for acidifying vacuoles; and as a component of the V_O domain which has acidification independent roles in the fusion of plasma membranes [261-265]. As such, it was important to establish which of these processes was responsible for the defective VAC phenotype that was observed as a consequence of ATP6VOC knock-down.

To ascertain whether inhibiting acidification of endosomal vacuoles resulted in a similar reduction in viral replication, viral growth assays were performed using the TB40E and chemicals that block acidification of vacuoles; chloroquine and bafilomycin. Chloroquine indirectly blocks the acidification of vacuoles. It freely diffuses through cells, but upon reaching an acidic compartment it undergoes a change of conformation that renders it impermeable, causing it to accumulate in these compartments[266]. This acts to buffer any further pH decrease in these vacuoles, inhibiting their functionality. Bafilomycin is a specific inhibitor of acidification, and directly binds ATP6VOC to inhibit the proton channel within the v-ATPase [267]. Fibroblast cells were incubated in media containing chloroquine during infection. Inhibition of acidification of vacuoles within the cell with chloroquine had a dose dependent inhibitory effect on the replication of TB40E as monitored by GFP intensity. At the highest dose of 25 μM the inhibition of TB40E GFP intensity was of a similar magnitude to that observed in cells transfected with ATP6VOC siRNA (Figure 4.5**A**). Again, the

observed inhibition of replication was more apparent by plaque analysis of lysates from treated cells 120 hpi, where a >2 $\log^{10}$ decrease in PFU was observed in fibroblast cells treated with 25 uM chloroquine (Figure 4.5**B**).

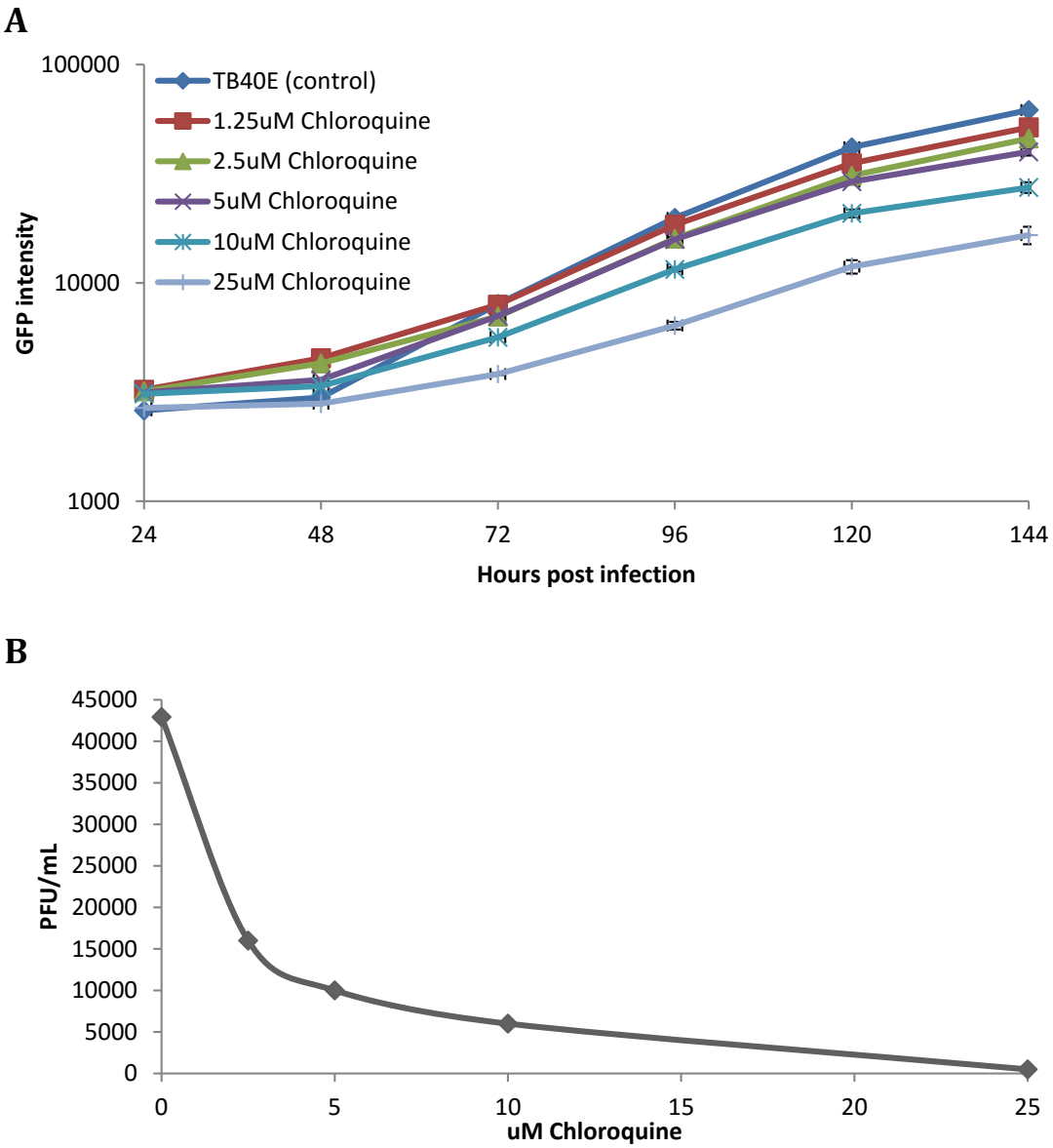

Figure 4.5 TB40E GFP expression profiles and plaque analysis in fibroblast cells treated with chloroquine (N=3)
A. TB40E GFP intensity up to 144 hpi in fibroblast cells treated with 1.25-25 µM chloroquine. **B.** Virus produced from lysates of cells treated with 1.25-25 µM chloroquine at 120hpi. Fibroblast cells were infected and 2 hours later fresh media containing 1.25-25 µM Chloroquine was overlaid. Viral replication and gene expression was monitored by GFP plate reader.

Treatment with bafilomycin was more complicated due to the cytotoxicity associated with prolonged exposure. As a result, treatment over a 7 day infectious time-course was not possible. In order to minimise exposure of the cells to the toxic effects of prolonged exposure to bafilomycin, while maximising the effect of inhibiting v-ATPase activity, fibroblast cells were treated with 0.1 μM bafilomycin at either 72 hpi or 96 hpi. These time-points were selected to have a maximum effect on HCMV VAC biogenesis. Treatment with bafilomycin had a dramatic effect on halting further TB40E replication (Figure 4.6**A**). Inhibition of v-ATPase induced acidification using bafilomycin had profound effects on the infectivity of progeny virus from treated cells, with a 2 $\log^{10}$ decrease in PFU/mL in cells treated at 96 hpi, and a 4 $\log^{10}$decrease in PFU/mL in cells treated from 72hpi. However, despite there being no visible increase in cytopathic effect, it could not be ruled out that these observations were due to these cells no longer being viable as a result of prolonged bafilomycin treatment.

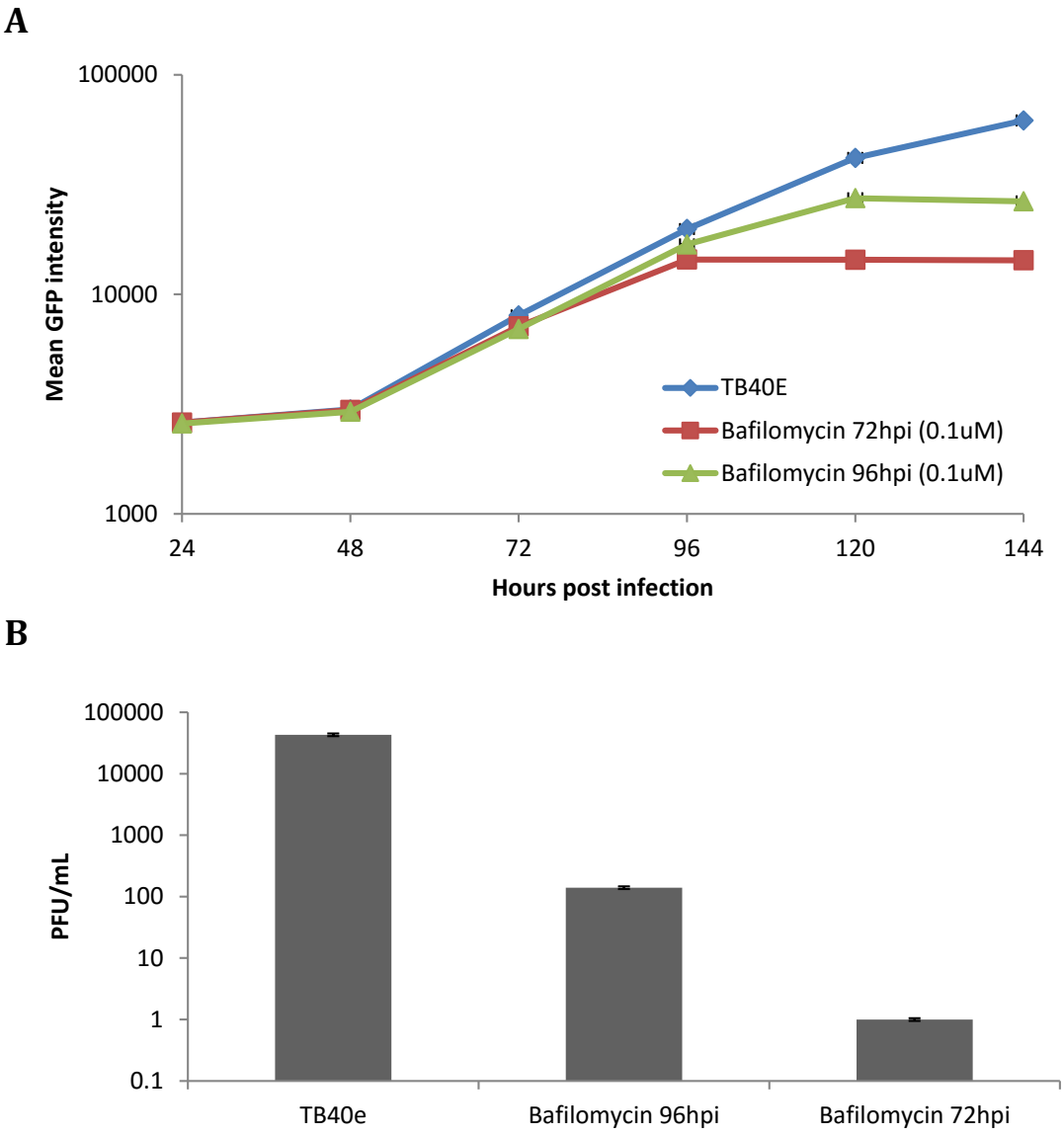

Figure 4.6 TB40E GFP expression profiles and plaque assay in fibroblast cells treated with 0.1 µM bafilomycin at 72 and 96 hpi (N=3)
A. GFP intensity in TB40E infected fibroblast cells treated at 72 or 96 hpi with 0.1 µM bafilomycin. **B.** Plaque assay at 120hpi from cells treated at 72 or 96hpi with 0.1 µM bafilomycin. Note: standard deviation is plotted but was minimal between replicates and is not visible on a $\log^{10}$ scale. For GFP expression profiles, fibroblast cells were infected with TB40E and were overlaid with fresh media containing 0.1 µM bafilomycin at 72 hpi or 96 hpi, and virus replication was monitored by GFP plate reader. For plaque assays, fibroblast cells were treated with 0.1 µM bafilomycin at 72 or 96 hpi. At 120 hpi, infected cells were harvested and plaque assay was performed.

To ascertain whether the defective phenotype observed in Figure 4.2 and Figure 4.3 could be recapitulated when vATPase activity was blocked by another mechanism, siRNAs against other components of the vATPase were used (ATP6V1H and ATP6V1A). ATP6V1H is critical for ATP hydrolysis and vATPase function is dependent upon this activity [268], and although the function of ATP6V1A has not been elucidated, like other components of the v-ATPase it is likely to perform a similarly crucial role . Critically, both of these components lie in the V_1 domain, so the membrane fusion functions of V_0 were not inhibited by their knock-down. TB40E replication was inhibited in fibroblasts after ATP6V1A and ATP61H knock-down when compared with fibroblast cells transfected with negative control siRNA, and the magnitude of this inhibition was almost identical to that observed after ATP6VOC knock-down (Figure 4.7).

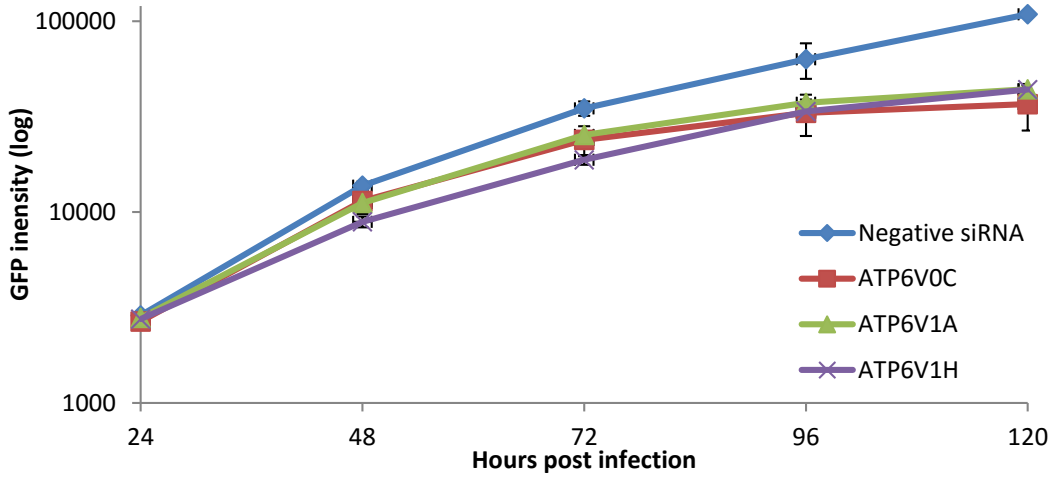

Figure 4.7 TB40E GFP expression profiles in fibroblasts after ATP6VOC, ATP6V1A, or ATP6V1H knock-down
Fibroblasts were transfected with 20 nM AT6VOC, V1H, V1A or a negative control siRNA. 72 hours post transfection cell were infected with TB4OE, and virus growth monitored by GFP plate reader.

This inhibition was analysed by immunofluorescence microscopy in fibroblast cells after ATP6V1H knock-down (Figure 4.8). TGN46 and EEA1 failed to colocalise with pp28 after ATP6V1H knock-down, and the distribution of these markers was very similar to the phenotype observed when ATP6VOC was knocked down (Figure 4.8**A**). Again, these observations were corroborated by quantifying the colocalisation of these markers and Pearson's R scores were calculated (following knock-down of ATP6V1H, TGN46/pp28=0.23 and EEA1/pp28=0.28) (Figure 4.8**B**).

Taken together, the data presented in Figure 4.5, Figure 4.6, Figure 4.7, and Figure 4.8 demonstrate that the role of ATP6VOC in VAC formation is dependent upon its function within the v-ATPase in acidifying vacuoles, rather than any acidification independent membrane fusion activity within the V_O domain.

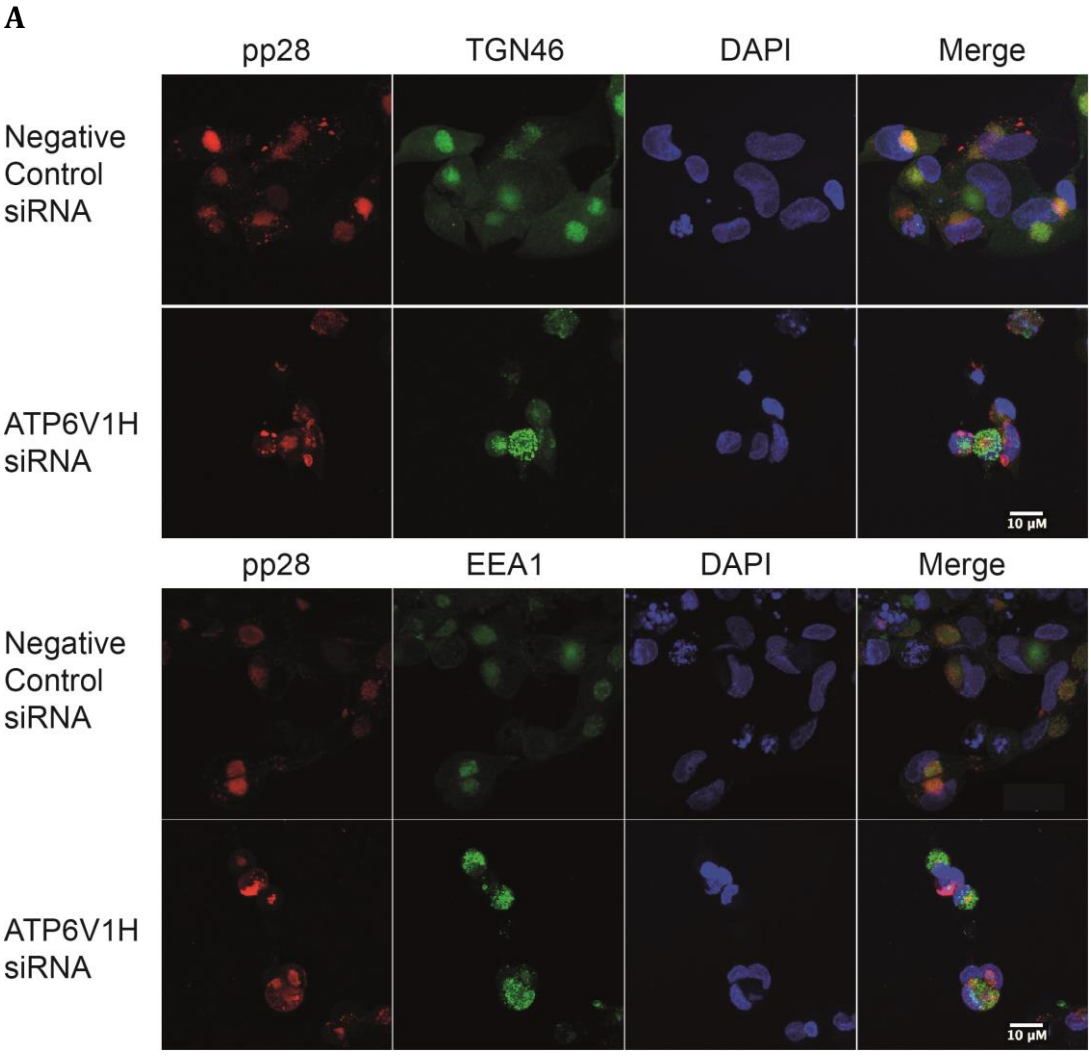

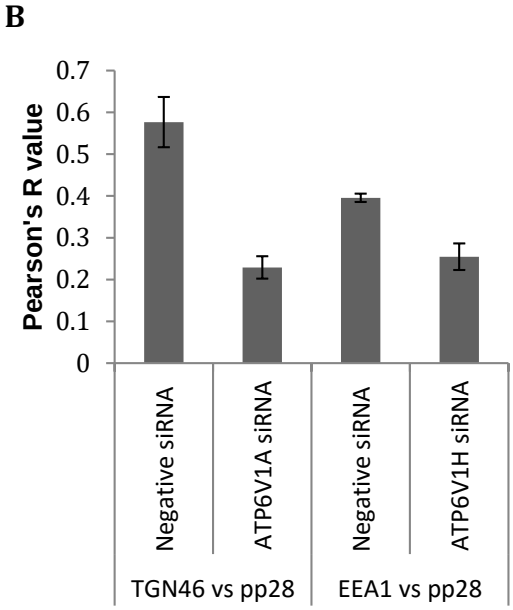

Figure 4.8 Immunofluorescence microscopy of the HCMV viral assembly compartment in fibroblast cells transfected with ATP6V1H siRNA (63 x magnification) (144 hpi)

A. Immunofluorescence microscopy in AD169 infected fibroblast cells transfected with ATP6V1H siRNA and stained for early endosomes (EEA1:green), viral tegument protein (pp28:red) and nuclei (DAPI:blue). Images represent single slices through the Z-axis. **B.** Pearson's R-value for colocalisation of TGN46 or EEA1 and pp28 in ATP6V1H or negative control siRNA transfected fibroblast cells (n=20).

4.7. Characterising progeny virus from fibroblast cells following ATP6VOC knock-down

The data shown in Chapters 4.5 and 4.6 demonstrate that the v-ATPase is required for formation of the HCMV VAC, and this coincides with either defective assembly or egress of the virus (Chapter 3.5). However, the exact nature of the viral defect that occurs as a result of v-ATPase inhibition was unclear. There were several scenarios that could explain these observations:

- Viral assembly was normal, and there was a failure of viral egress;
- Viral assembly was grossly defective, and viral egress was occurring;
- A key stage of viral assembly was specifically defective, and viral egress was occurring;
- Both viral assembly and egress were grossly defective.

In order to establish which of these scenarios was the cause of the assembly defect, intracellular and supernatant virus from fibroblast cells after ATP6VOC knock-down, or negative control siRNA transfected fibroblast cells were isolated and analysed for genome copy number, PFU/mL, and viral protein abundance.

4.7.1. Viral genome copy number and PFU/mL differ in supernatant and cell associated virus after ATP6VOC knockdown compared to the negative control siRNA transfected fibroblast cells

The genome copy number in cell associated virus fractions were strikingly similar after ATP6VOC knock-down in fibroblast cells compared with negative

control siRNA transfected fibroblast cells, with minor differences which were within the margin of error (1.2 fold change) (Figure 4.9**A** and **B**). In the supernatant virus fraction, there was a decrease in genome copy number of 3.4 fold when in fibroblast cells after with ATP6VOC knock-down compared with the negative control transfected fibroblast cells.

The titres of cell associated virus from fibroblast cells after ATP6VOC knock-down were nearly 2 $\log^{10}$ lower than the titres from negative control siRNA transfected fibroblast cells. The titres of supernatant purified virus from fibroblast cells after ATP6VOC knock-down were nearly 3 $\log^{10}$ lower than the titres from negative control siRNA transfected fibroblast cells (Figure 4.9**C** and **D**). These data are consistent with previous results from plaque assay on cell associated and supernatant virus combined, which showed a 2-3 $\log^{10}$ decrease in viral titres (Figure 3.7). However, the data shown in Figure 4.9 demonstrate that there is an order of magnitude difference in the decrease in titres when comparing cell-associated with supernatant purified virus from cells transfected with ATP6VOC siRNA. This is particularly apparent when these data are displayed on a linear scale as a fold change (Negative control siRNA÷ATP6VOC siRNA). There was a 77.3 fold reduction in cell associated and a 727.3 fold reduction in virus titres in supernatant purified virus in fibroblast cells after ATP6VOC knock-down compared with negative control siRNA transfected fibroblast cells (Figure 4.9**D**).

The observation that a dramatic decrease in the infectivity of progeny virus from in fibroblast cells after ATP6VOC knock-down can not be accounted for by

a decrease in genome copy number alone is suggestive of a defect in viral assembly and egress.

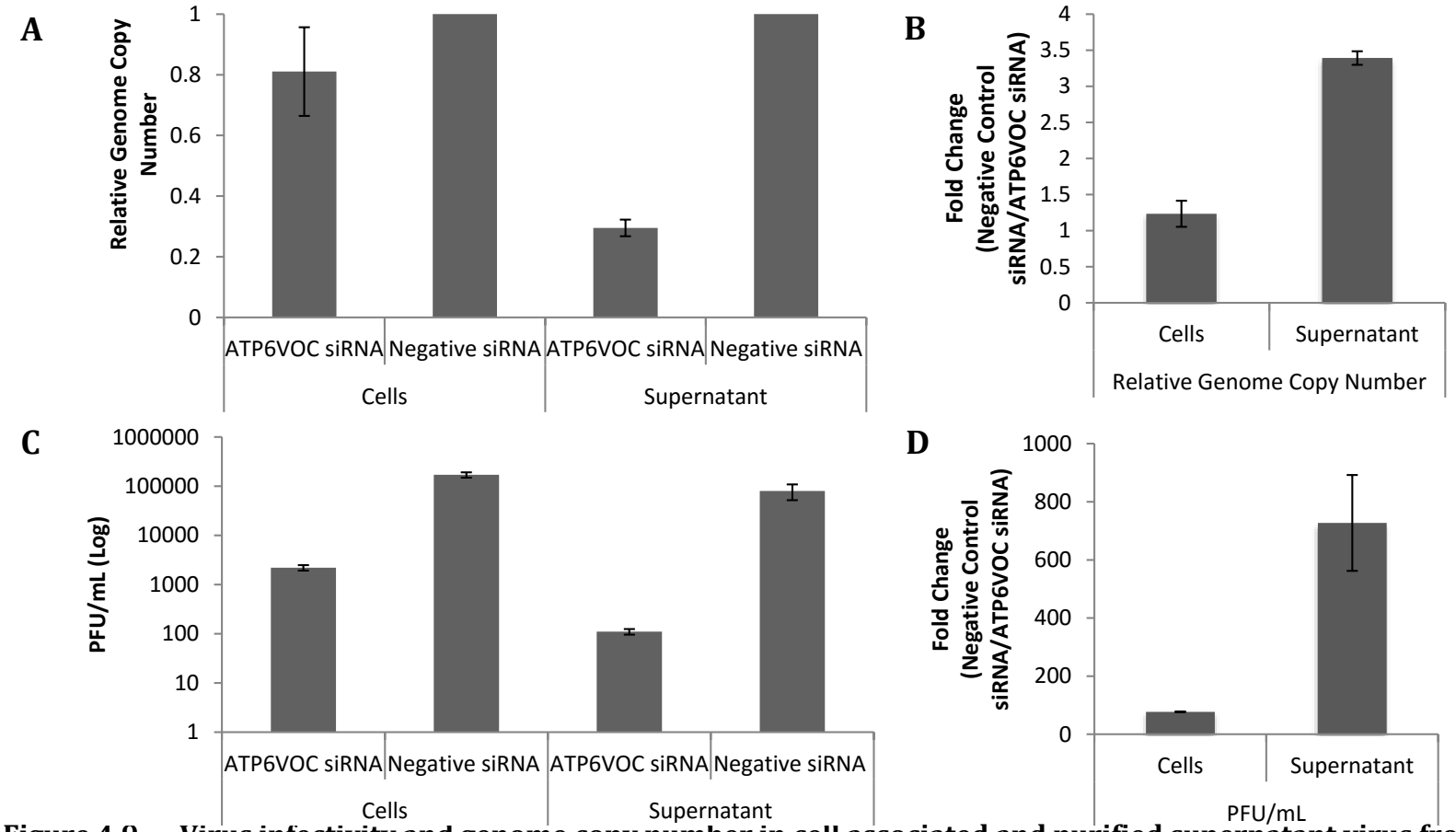

Figure 4.9 Virus infectivity and genome copy number in cell associated and purified supernatant virus from AD169 infected fibroblast cells transfected with ATP6VOC siRNA or negative control siRNA (N=2) (144 hpi

A. Relative genome copy number (relative to negative)**B.** Fold change in genome copy number **C.** PFU/mL **D.** Fold change in PFU/ml. Fibroblasts were transfected with ATP6VOC siRNA, or negative control siRNA and at 72 hours post transfection cells were infected with AD169 at an MOI of 1. At 168 hpi, supernatant virus was purified and infected cells harvested. Supernatant and cell associated virus was analysed for genome copy number by qRTPCR and PFU/mL by plaque assay.

4.7.2. Viral protein levels in fibroblast cells after ATP6VOC knock-down are equivalent in intracellular virus fractions, but dramatically decreased in supernatant virus fractions, compared with negative control transfected fibroblast cells

Western blot analysis was performed to ascertain the abundance of viral proteins in supernatant and cell associated virus from fibroblast cells after ATP6VOC knock-down compared with negative control siRNA transfected fibroblast cells. Immediate early proteins IE72 and IE86, glycoprotein gB, and tegument protein pp28 were assayed. Consistent with the genome copy number analyses (Figure 4.9) and gene expression analyses (Figure 3.6), the levels of protein in the cell associated virus were equivalent, with the exception of IE72 which appeared to be more abundant in fibroblast cells after ATP6VOC knock-down (1.5 fold higher)(Figure 4.10). In the supernatant purified virus, the abundance of viral proteins in fibroblast cells after ATP6VOC knock-down were dramatically decreased compared with supernatant virus from negative control siRNA transfected fibroblast cells. pp28 and gB protein abundance were 16 fold and 12 fold lower, respectively, in supernatant virus from fibroblast cells after ATP6VOC knock-down, with supernatant virus from negative control siRNA transfected fibroblast cells. It should be noted that IE86 and IE72 proteins are not packaged into the progeny virions, and as such were not present in supernatant virus.

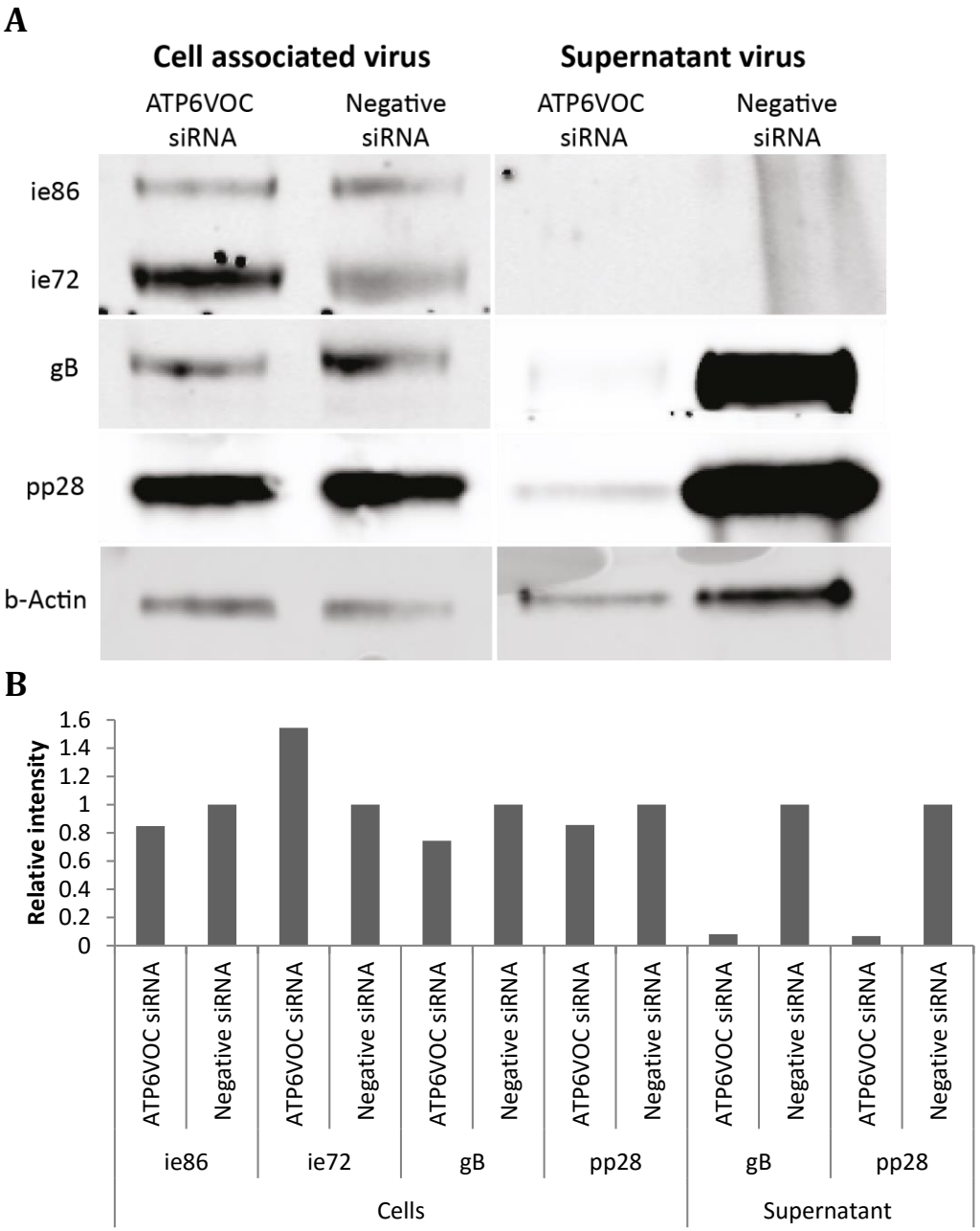

Figure 4.10 Western blot analysis of viral proteins in supernatant and cell associated AD169 in from fibroblast cells transfected with ATP6VOC siRNA or a negative control siRNA (N=1)

A. Fibroblasts were transfected with ATP6VOC siRNA, or negative control siRNA and at 72 hours post transfection cells were infected with AD169 at an MOI of 1. At 168 hpi, supernatant virus was purified and infected cells harvested. Virus samples were lysed in laemmli buffer and western blot analyses were performed using specific primary antibodies, and LiCOR secondary antibodies.
B. Quantification of western blot data, normalised first to b-Actin and then to negative control siRNA transfected fibroblast cells.

The data presented in Figure 4.10 show an increase in the abundance of IE72 in infected cells transfected with ATP6VOC siRNA (at 144 hpi). To explore this phenomenon and the impact, if any, on the HCMV gene expression temporal cascade in more detail, western blot analysis was performed on infected cell lysates against IE72, IE86, gB, and pp28 over a time-course (Figure 4.11). These data demonstrate that there is a greater abundance of IE72 and IE86 protein at 48, 72, and 96 hours post infection in fibroblast cells after ATP6VOC knock-down compared with negative control siRNA transfected fibroblasts. These increases in IE protein abundance were accompanied by increases in the abundance of gB protein (a late protein product) and pp28 (a true late protein product) from 48 and 72 hours post infection, respectively. When these data were quantified, it indicated that the order of magnitude of the increases in protein abundance in fibroblast cells after ATP6VOC knock-down was between 2 and 3 fold at early time-points for all genes tested at the same MOI (Figure 4.12).

The protein abundance data in Figure 4.11 and Figure 4.12 allied with the viral gene expression data in Figure 3.6 indicate that the viral gene expression cascade appears to be initiated more robustly in fibroblast cells after ATP6VOC knock-down, and this appears to translate to a more robust induction of other genes later in the cascade. Logic would suggest that the cause of this phenomenon is likely to be independent of the observations that VAC formation and viral assembly are defective in these cells as: a). it is counter intuitive that an induction in viral gene expression would lead to a defect that results in less

infectious virus, and b). these differences in protein expression occur at a time-point before assembly compartment biogenesis occurs. This suggests that the knockdown of ATP6VOC and subsequent inhibition of v-ATPase activity or V_O induced membrane fusion has other effects early in infection that result in a more robust initiation of the viral gene expression cascade.

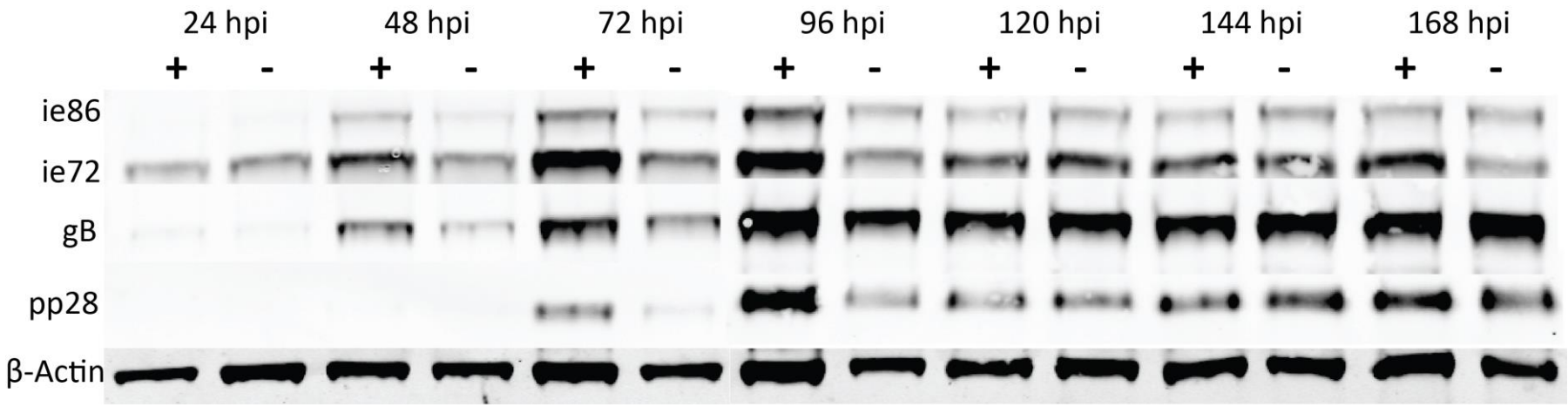

Figure 4.11 Licor western blot analysis of viral proteins in AD169 infected fibroblast cells transfected with ATP6VOC or negative control siRNA (24-168 hpi)

Fibroblasts were transfected with ATP6VOC siRNA, or negative control siRNA and at 72 hours post transfection cells were infected with AD169 at an MOI of 1. At 24 hour time-points, infected cells were harvested in laemmli buffer. Western blot analyses were performed using specific primary antibodies, and LiCOR secondary antibodies.

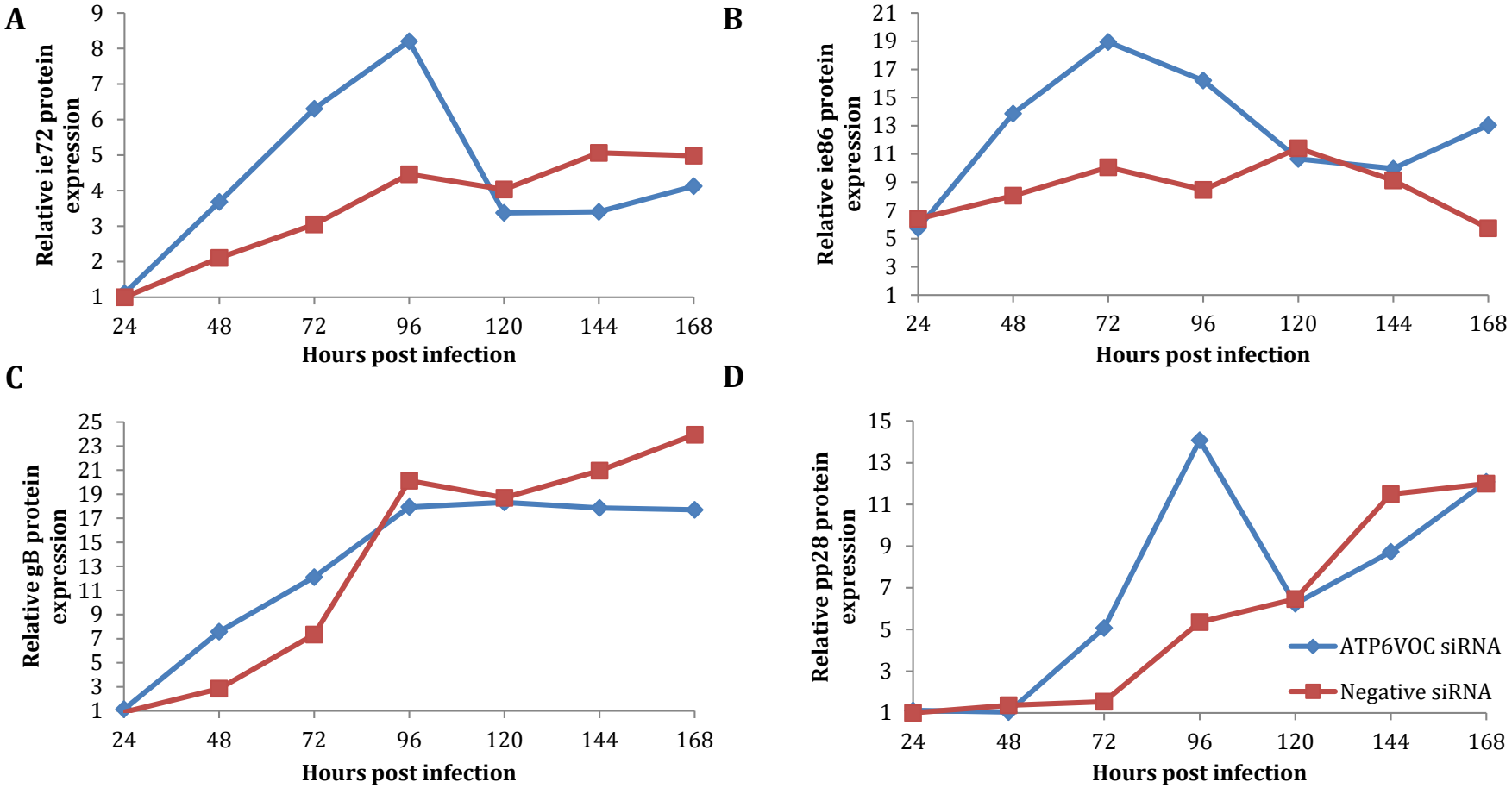

Figure 4.12 Viral protein expression profiles in AD169 infected fibroblast cells transfected with ATP6VOC siRNA or a negative control

A. IE72; **B**. IE86; **C**. gB; **D**. pp28. Relative gene expression normalised to β-Actin. Quantification of western blots shown in Figure 4.11 performed using LiCOR Odyssey software.

4.8. Discussion

In Chapter 3, ATP6VOC was identified as a critical host factor required for HCMV replication. The data in this chapter demonstrate that ATP6VOC activity is required for the proper formation of HCMV VAC, likely as part of the v-ATPase which is responsible for acidification of host-cellular membrane bound compartments. Furthermore, the evidence presented here in combination with that in the literature suggests that the biogenesis of the VAC is required for the efficient production of functional virions [79, 172, 188]. Although it was not directly confirmed, this is likely due to a defect in the acidification of these compartments after ATP6VOC knock-down, as knock-down of another critical component of the vATPase (ATP6V1H) and specific chemical inhibitors of vacuole acidification (chloroquine and bafilomycin) recapitulated these defects in VAC biogenesis and viral replication (Figure 4.8) [79, 172, 188]. However, it was not entirely ruled out that the intrinsic membrane fusion function of ATP6VOC within the V_O domain may also play a role [261-265].

Interestingly, and somewhat counter intuitively, ATP6VOC knockdown was associated with an earlier induction in immediate early protein expression which resulted in a more robust induction of late and true-late protein synthesis (Figure 4.11 and Figure 4.12).

The dysfunction in the formation of the VAC was associated with drastic effects on progeny virions. While there was no decrease in intracellular viral genome copy number or protein abundance in intracellular virus, there was a robust

decrease in both the abundance of viral proteins and the genome copy number in extracellular virus after in fibroblast cells after ATP6VOC knock-down compared with negative control siRNA transfected cells. There was a 4-fold decrease in genomes of progeny virus, yet at least a 20-fold decrease in viral tegument and glycoprotein. Additively these defects do not account for the consistent near 3- $\log^{10}$ decrease in PFU/mL observed in lysates from fibroblast cells after ATP6VOC knock-down, compared with negative control transfected cells. Taken together this indicates that there is a gross defect in viral assembly and egress, and that the majority of viral genomes that are egressing the cell are within defective particles.

4.8.1. Possible roles of vacuole acidification in assembly

While the data presented here demonstrate that ATP6VOC is required for VAC biogenesis and efficient viral replication, they do not identify the exact role of ATP6VOC during viral assembly and egress. It seems likely that the role of ATP6VOC in v-ATPase mediated acidification of endocytic and secretory vacuoles is likely to be central to this role. This begs the question: what role does acidification have within the compartments that make up the VAC?

A characteristic feature, and key determinant, of early to late maturation of endosomes and secretory vesicles is the progressive acidification of these compartments. When v-ATPase activity is inhibited, the maturation of early endosomes is blocked, post translational modification of newly synthesised proteins is inhibited, secretory vesicles are mis-localised, and downstream lysosomal degradation is disrupted [269].

There is evidence that several HCMV miRNAs manipulate the fates of compartments within the endocytic and secretory pathways to facilitate VAC biogenesis [172]: inhibiting the maturation of early endosomes by knocking down Rab5; inhibiting endosomal recycling by knocking down Rab11 [270]; disrupting vesicular membrane anchoring and fusion by knocking down VAMP3 and SNAP23 [271]; and preventing basolateral transport of cargo by knocking down CDC42 [272, 273].

The involvement of v-ATPase activity in almost every step of the endocytic and secretory pathways suggests that ATP6VOC is likely to have a profound effect on these pathways, and this appears to be crucial for VAC biogenesis. Indeed, the observation that knockdown of ATP6VOC inhibits VAC biogenesis indicates that v-ATPase activity is required within these compartments to facilitate their redistribution to the VAC. Due to the diverse effects v-ATPase activity within the secretory and endocytic pathways, dissecting the specific roles of each of these activities in VAC biogenesis, and HCMV biology as a whole, will be difficult to ascertain.

Beyond the biogenesis of the VAC, there are a number of plausible roles for the v-ATPase in the assembly of virions. The sorting of newly synthesised proteins emerging from the endoplasmic reticulum is dependent upon an acidic luminal pH within trans-golgi vacuoles, and it is likely that this machinery is subverted during infection to allow the virus to direct the localisation of viral proteins [274, 275]. Indeed, there are examples of viral glycoproteins being trafficked in this manner in HSV1 [276-278] and in HCMV [279]. The trans-golgi network is

also the site of post-translational glycosylation of newly synthesised proteins. This process is dependent on an acidic luminal pH within these compartments to facilitate the modification of substrates and this has a profound effect on the stability of these proteins [255, 256]. Glycosylation promotes the correct folding of newly synthesised proteins, and this is critical for their stability. There are several examples of herpes viral glycoproteins being heavily glycosylated, including gB, which is a key determinant of viral entry [280, 281]. gB is thought to be the fusion protein trigger required for HCMV cell entry, after gH/gL bind receptors on the cell surface [15]. gB homologues in other herpesviruses have the same activity, and have been shown to change their conformation in response to certain stimuli, including pH. This is important in their functionality in egress of the virus from host cells and in their subsequent entry into new host cells [16, 17, 282, 283]. In addition to gB, there are 6 other glycoproteins that have been identified as being critical in HCMV entry; gH, gL, gO, UL128, UL130, and UL131A. gH/gL/gO form a timer which is sufficient for entry into fibroblast cells and gH/gL/UL128-31 form a pentamer that is required for entry in to epithelial and endothelial cells. It is conceivable that the mis-folding of viral glycoproteins has a major effect on viral assembly and egress, as these events are likely to be closely intertwined. Any disruption to glycoprotein incorporation into progeny virus will also likely have profound effects on their downstream functionality in infection.

4.8.2. Possible roles of miR-US25-1 regulation of ATP6VOC in infection

Based on the data presented in this chapter, there are several valid scenarios by which the inhibition of ATP6VOC mediated vacuolar acidification might disrupt VAC biogenesis and viral assembly. However, it is unclear whether these roles are truly reflective of miR-US25-1 regulation of ATP6VOC during infection.

As described earlier, herpesviruses utilise a variety of mechanisms to restrict their own replication in order to facilitate the establishment and maintenance of latency. It may be that miR-US25-1 regulation of ATP6VOC during infection acts to restrict HCMV lytic gene expression in a similar fashion. However, the viral phenotype evident in fibroblast cells after transfection of ATP6VOC siRNA may be somewhat artificial, as it is the result of an almost complete knock-down of ATP6VOC. In eukaryotes, miRNAs do not typically regulate gene expression by causing this sort of abrupt change in transcript levels. Rather, they facilitate the fine-tuning of gene expression. Current evidence suggests that viral miRNAs likely to act in a similar fashion, 'rheostatitically' fine-tuning host-cellular and viral gene expression during infection. As such, the possibility that marginal expression of ATP6VOC may in fact facilitate lytic replication needs to be taken into account when considering the role of miR-US25-1 during infection.

Restrictive roles

It is possible that ATP6VOC down-regulation by miR-US25-1 at late time-points may act in infection to restrict the lytic cycle and may contribute to the establishment of latency *in vivo*. There is evidence that HCMV regulates lytic gene expression *via* the activity of miRNAs. Two independent studies have

demonstrated that HCMV miR-UL112-1 regulates the expression of the major transcriptional transactivator, IE72 [177, 284]. If the regulation of ATP6VOC by miR-US25-1 had a similar role in HCMV infection, it would be difficult to dissect. A significant hurdle is that *in vitro* latency models available for HCMV do not allow for the establishment of latent infection in lytically infected cells [84] and unlike EBV and KSHV miRNAs, the expression of HCMV miRNAs has not been observed in experimental latency. As such, it would be difficult to ascribe this role to miR-US25-1 regulation of ATP6VOC.

Another possibility is that miRUS25-1 regulation of ATP6VOC might be important in the maintenance of latency, as seen for miRNAs expressed by KSHV and EBV. Again, this possibility will be difficult to dissect as the transcriptional status of miR-US25-1 is unknown during latency [208].

Enhancing roles

There are also a variety of roles potentially attributable to ATP6VOC regulation that would enhance HCMV replication. The acidification of vacuoles is dependent on v-ATPase functionality, and therefore dependent upon ATP6VOC expression. Acidification is critical in the transport of exogenous material *via* the endocytic pathway, and endogenous material *via* the secretory pathway to the lysosome for degradation. Cytoplasmic macromolecules may also be degraded by autophagy. Autophagy is a pathway by which macromolecules in the cell are encased in a double membrane vesicle that fuses with the lysosome resulting in the contents being degraded. v-ATPase activity is likely to have a pivotal role within the autophagic process as acidification of the lysosome is

required for activation of degradative enzymes, and bafilomycin has been shown to be a specific inhibitor of the fusion of the autophagosome and lysosome [285]. Within the context of infection, inhibition of these activities would prevent the breakdown of viral constituents during infection. Potentially, this would facilitate viral assembly, and might prevent the subsequent trafficking of viral epitopes to the cell surface *via* MHC-class I and II and stimulation of an inflammatory response. This would be highly beneficial to the virus in evading the clearance of infected cells by the host cell-mediated immune response. There is evidence that inhibition of endosomal trafficking and lysosomal activity in HIV infection results in an increase in viral replication [286, 287] and there are an increasing number of examples of viral processes that directly subvert autophagy during HCMV, VZV, HSV1, and influenza A virus infection [288-300]. This indicates that autophagy may play an important role in the host immune response to virus infection. Consistent with this hypothesis, preliminary data from fibroblast cells transfected with ATP6VOC siRNA or a miR-US25-1 mimic demonstrate an accumulation of autophagy biomarker LC3BII within the cell, which is likely to be the result of an accumulation of autophagosomes. This highlights the possibility that the subversion of autophagy may be a role of the miRUS25-1 regulation of ATP6VOC during infection (personal communication, Dr Finn Grey, Roslin Institute, Edinburgh).

There is a possibility that the apparent induction of immediate-early gene expression in fibroblasts after ATP6VOC knock-down may be connected with the inhibition of autophagy and other lysosomal degradation pathways. It is

conceivable that endocytic and autophagic pathways might divert internalised virions and their components towards lysosomes for degradation, and that inhibiting these processes *via* ATP6VOC knock-down allows for more viral genomes to reach the nucleus, effectively altering the MOI.

5. Concluding remarks

5.1. Future directions

In the data presented in Chapters 1.9 and 2, hundreds of host-cellular targets of HCMV miRNAs were identified which potentially represent novel host-virus interactions. In future, it would be useful to expand these global analyses in order to improve our understanding of the HCMV miRNA 'targetome'.

HCMV has a broad tropism *in vivo*, and it is likely that some host-cellular targets of HCMV miRNAs will be cell type specific. Within the scope of the work presented here, it was only possible to investigate miRNA targets in fibroblast cells. It is plausible that performing similar studies in other cell types, such as endothelial and epithelial cells would yield a distinct subset of miRNA targets that are important for HCMV propagation in these cell types, and this would be an interesting route of future study.

It should also be noted that the *in vitro* model of infection in fibroblast cells only supports the lytic phase of the HCMV lifecycle. As such, in this study it was not possible to identify any targets transcripts that are specifically regulated by HCMV miRNAs during latent infection. There is growing evidence that miRNA regulation of host and viral genes in HSV-1 and 2, EBV, and KSHV infection play important roles during latency (see Chapter 1.8), and it would be of great interest to investigate these potential roles during HCMV latency, both *in vitro* and *in vivo*.

With regards to the approach used in the miRNA target screen, it would be interesting in future to use biochemical techniques that allow for the identification of transcripts that are rapidly degraded, or those that do not form stable interactions with RISC. While RISC-IP is clearly a powerful tool in identifying the targets of viral miRNAs, cutting-edge techniques such as CLASH allow for the identification of not only the target transcript, but the miRNA responsible, and the target site with the transcript. This information would be of great benefit to viral miRNA researchers, would make target validation more straight-forward, and has the potential to dramatically advance our understanding of viral miRNA targets in the near future.

With regards to the siRNA screen of HCMV miRNA targets, it is likely that several genes that play crucial roles were discounted due to an apparent lack of effect on viral replication based on the criteria that were used for establishing a viral phenotype. The true role of these genes may have been masked within the siRNA screen due to redundant co-factors, tropism specific roles, or effects that don't impact viral replication as monitored by GFP expression in TB40E infected cells. To circumvent these possibilities, it would be of interest in future to screen progeny virus from cells transfected with these siRNAs for the capacity to infect naive cells. Indeed, observations from others who have used this technique for screening endocytic pathway genes have demonstrated that the knock-down of certain genes can cause a dramatic decrease in progeny viral fitness, while having no effect on viral replication as monitored by GFP (personal communication, Dr. Oliver Lin, Roslin Institute, Edinburgh). There is

also a likelihood that the critical role of the regulation of some genes in HCMV biology may only become apparent after their over-expression, and this is particularly relevant with regards to regulation by miRNAs. As such it would be of interest to develop a lenti-viral library for the over-expression of miRNA target genes in order to better understand the effect of their regulation during infection.

Finally, in addition to ATP6VOC several other potentially interesting targets of HCMV miR-US25-1 were identified in this study; CCNE2, BCKDHA, and LGALS3. While these genes were not selected for further characterisation based on the results of the siRNA screen, they may still have a crucial role in HCMV biology. With possible roles in cell cycle manipulation, autophagy, and mTOR signaling, each represents a potentially interesting avenue of future research.

This study demonstrated that miR-US25-1 is the sole miRNA responsible for regulating several host cellular genes during infection, and identified ATP6VOC as a critical host factor in HCMV VAC biogenesis and assembly. However, it stopped short of identifying the specific role of miR-US25-1 regulation of ATP6VOC during infection. Clearly this would be an interesting avenue of future research, and the work presented here is a prelude to ongoing studies to establish these roles. As discussed in Chapter 4, the potential subjugation of autophagy by miR-US25-1 during infection, and the possible effect of this on the immune response to HCMV may be of particular interest in this regard.

5.2. Conclusions

In this study, hundreds of host-cellular transcripts were identified as being potentially regulated by HCMV encoded miRNAs during lytic infection. Using a combination of bioinformatics and further biochemical techniques, the regulation of 13 host cellular-transcripts by HCMV miRNAs were independently validated, and miR-US25-1 was identified as the sole HCMV miRNA responsible for the regulation of ATP6VOC, BCKDHA, CCNE2, and LGALS3 at the RNA and protein level during infection. The regulation of each of these genes by miR-US25-1 represent novel-host virus interactions, which the exception of CCNE2 which was identified as a prelude to the work presented here [165]. As a first step to ascertaining the roles that these genes play in HCMV biology a phenotypic screen was performed, and this identified ATP6VOC as a critical factor that is required for HCMV replication *in vitro*. ATP6VOC was subsequently shown to be critical in the formation of the HCMV VAC, the failure of which has repercussions on the formation of progeny virus. The disruptive effect of ATP6VOC knock-down on the formation of the HCMV VAC is likely the result of the inhibition of v-ATPase induced acidification of host-cell secretory and endocytic vacuoles.

In conclusion, this work has greatly increased the number of validated host-cellular HCMV miRNA targets that have been identified to date, and this acts as a platform to achieve a better understanding of the role of HCMV miRNA regulation of host-cellular gene expression during infection. Improving our understanding of the complex virus-host interactions that take place during

HCMV infection will be critical in future as we look forward to developing novel therapeutics to tackle this clinically important human pathogen.

6. Materials and Methods

6.1. General Methods

6.1.1. Cell lines and culture

Human primary normal human dermal fibroblast cells (NHDF) (Clonetics), and human embryonic kidney 293 (HEK 293) cells were cultured in Dulbecco's modified Eagle's medium (DMEM) supplemented with 10% fetal calf serum (FCS) and penicillin-streptomycin-L-glutamine (PSG), and incubated at 37°C in 5% CO_2.

6.1.2. Virus strains

Wild type AD169 was obtained from the American Type Culture Collection (Rockville, MD). BAC derived AD169 pAD CRE was provided by Thomas Shenk [209]. TRTF was provided by Professor Jay Nelson and TB40E BAC4 eGFP was provided by Felicia Goodrum [47, 301]. Purified virus was generated as follows: Sub-confluent NHDFs were infected at low MOI. Infected cells were scraped into media at 168 hpi and dounced. Cellular debris was cleared from the supernatant by low speed centrifugation (2000 g for 30 minutes). Purified virus was obtained from infected supernatant by ultracentrifugation over a 20% sorbitol cushion (40000 g for 1 hour). Purified virus was re-suspended in DMEM containing 10% FCS, and stored at -80°C.

6.2. Chapter 1 methods

6.2.1. RISC-IP and microarray

RISC-IP analysis was performed as described in [139]. NHDFs were seeded to a density of 80% in tissue culture grade 10 cm dishes. Cells were infected at a MOI of 3 with AD169 or TR HCMV strains. Media was removed from the cells, cells were washed twice with PBS, and harvested into 1 mL of lysis buffer (20 mM Tris pH7.5, 2.5 mM $MgCl_2$, 200 mM NaCl, 0.05% Nonidet P40, 1mM DTT, 1x proteinase inhibitor, 1:50 RNasin 40 U/ μL. Lysates were vortexed, and centrifuged at 12000 g for 15 minutes at 4°C. 50 μL of lysate was added to 500 μL of Trizol® reagent for total RNA.

25 μL of protein-A sepharose (for Ago-2 antibody pull-down), streptavidin-agar (for biotin pull-down) or myc-ago (for myc-Ago pull-down) beads were prepared in advance. Beads were pelleted (1000 g), washed in lysis buffer (without RNasin), and re-suspended to a final volume of 100 μL per sample. Beads were blocked with 100 mg tRNA and 100 mg BSA for 2 hours at 4°C, and washed twice in 300 μL lysis buffer (without RNasin). Beads were resuspended to a final volume of 100 μL per sample.

For myc and biotin pull-downs, lysates were added straight onto the blocked beads. For antibody pull-downs, lysate fractions were incubated with Ago-2 antibody or with pre-bleed serum for 1 hour at 4°C. Lysates were then incubated with beads for 2 hours at 4°C. Beads were pelleted (1000 g), and washed twice with 500 μL of lysis buffer. Beads were then resuspended in

500 µL Trizol® reagent. RNA fractions were isolated according to the manufacturer's instructions (www.lifetechnologies.com/trizol).

Ago-2 specific antibody was generated by immunisation of rabbits with a peptide corresponding to the N-terminal region of Argonaute-2 (5-MYSGAGPALAPPAPPPPIQGYAFKPPPRPD-3').

RNA samples were analyzed for quality using Agilent Bioanalyser. Transcript levels were determined using the Illumina HumanRef-8 microarray platform.

6.2.2. Bioinformatic analyses

HCMV miRNA targets sites within host-cellular genes were ascertained by scanning 5'UTR, ORF, and 3'UTR sequences (obtained from www.ncbi.nlm.nih.gov) for target sites of HCMV miRNAs (obtained from www.mirbase.org) using the RNA-hybrid online tool (bibiserv.techfak.uni-bielefeld.de/rnahybrid). Parameters were selected to include Watson-Crick base pairing between nucleotides 1 to 7 or 2 to 8.

6.3. Chapter 2 methods

6.3.1. RISC-IP

RISC-IPs were performed and RNA isolated as described in Chapter 6.2.1. RNA was quantified by spectrophotometer, and 200ng was reverse-transcribed, using the high capacity cDNA reverse transcription kit and poly-dT primers according to the manufacturer's instructions (Life Technologies). This cDNA was then used for subsequent qRTPCR analyses.

The efficacy of RISC-IP was assessed using primer-probe qRTPCR against SOCS1, a transcript that is readily regulated by host-cellular miRNAs, and as such was enriched equivalently in each RISC-IP sample, infected and uninfected.

6.3.2. miRNA and siRNA transfections

miRNAs and siRNAs were transfected into NHDF or HEK 293 cells using lipofectamine RNAiMax® reagent according to the manufacturer's instructions (Life Technologies). For NHDFs and HEK 293s, cells were seeded to 60-80% confluence and transfected with 20 nM siRNA or miRNA mimic in Optimem® serum free medium (Life Technologies). NHDFs were double transfected a minimum of 6 hours apart, and HEK 293s were single transfected.

6.3.3. qRTPCR

Validated primer probe assays were selected for best coverage from Life Technologies. qRTPCR was carried out using Taqman® gene specific primer probe sets (Life Technologies) on a Rotor gene 3000 thermal cycler (Corbet

Research). The thermal cycler was programmed as follows: **1x HOLD**; 2 minutes at 50°C; **1x HOLD** 10 minutes at 95°C; **40x CYCLE** 15 seconds at 95°C, 1 minute at 60°C. Fluorescent signal acquisition occurred after each cycle at the required wavelengths. For more information see: http://www3.appliedbiosystems.com/cms/groups/mcb_support/documents/generaldocuments/cms_042996.pdf.

Relative gene expression levels were ascertained using the ΔΔct method. Statistical significance was analysed using Mann Whitney U-test. The calculative method can be found in Table 7.4. An arbitrary significance threshold of 0.01 was used.

Table 6.1 qRTPCR primer probe assays

Assay ID	Accession No.	Source
ATP6VOC	Hs00798308_sH	Life technology
BCKDHA	Hs00958109_m1	Life technology
CCNE2	Hs00180319_m1	Life technology
LGALS3	Hs00173587_m1	Life technology
NUCB2	Hs00172851_m1	Life technology
SGSH	Hs00164924_m1	Life technology
CCNE1	Hs01026536_m1	Life technology
BSG	Hs00936295_m1	Life technology
PIGH	Hs00762253_s1	Life technology
LEPRE1	Hs00223565_m1	Life technology
NUCB1	Hs00939167_m1	Life technology
LIN28B	Hs01013729_m1	Life technology
GRN	Hs00963707_g1	Life technology
COMMD10	Hs00211680_m1	Life technology
ACTB	Hs01060665_g1	Life technology
SOCS1	Hs00705164_s1	Life technology

6.3.4. Western blot analysis

Protein lysates were obtained from NHDFs infected with either AD169, AD169 25-1/2KO, mock infected NHDFs, or NHDFs transfected with specific siRNAs as negative controls for protein expression. NHDF for infection were seeded at a density of $1x10^6$ cells in 100 mm^2 tissue culture coated dishes and 24h later were infected at an MOI of 3. At 72 hpi the media was removed, cells were washed twice with PBS, and protein lysates were harvested in 1 mL of 2X laemmli buffer (BioRad). NHDFs for transfection were seeded at 60-80% confluence, $4x10^4$ cells per 24 well. NHDFs were double transfected as described previously, and protein lysates harvested at 72 hours post transfection in 65 µL 2X laemmli buffer (BioRad).

For the majority of proteins, PAGE separation was performed on 4-12% Mini-Protean TGX® pre-cast gradient gels (BioRad), using 1X Tris-Glycine SDS running buffer (0.025M, 0.192M, 0.1%, respectively). ATP6VOC PAGE separation was performed on 12% Novex® pre cast gel (Life technologies) using a dedicated MES running buffer, due to it's small size (16 kda). 30 µL of each sample was loaded, and PAGE gels were run at 150 V until the dye front exited the gel. PAGE gels were blotted onto either nitrocellulose (pore size of 45 micron with the exception of ATP6VOC, which required pore size of 20 micron) were wet transferred in 1X Tris-Glycine transfer buffer with 20% methanol on ice at 100 V for 1 hr. Protein size was ascertained using 10-250 kd pre-stained protein marker (Life technologies).

Membranes were blocked for 1 hour at room temperature using 1X ECL advanced blocking reagent (Amersham). Primary antibodies were diluted appropriately and left to hybridise with membranes for 12 hours at 4°C. Membranes were then washed twice in 1X PBS-Tween 1% three times for 20 minutes. Secondary fluorescent antibodies (IR800 or IR680 dye conjugated anti-rabbit IgG or anti-mouse IgG secondary antibodies from LiCOR®) were diluted 1:1000 in 1X PBS-Tween 1%, and left to hybridise with membranes in the dark for 45 minutes at room temperature. Membranes were washed three times for 5 minutes before fluorescent image acquisition.

Membranes were imaged using infrared fluorescence and quantified using LiCOR® Odyssey scanner and software.

Table 6.2 List of primary antibodies and dilutions for western blot analysis

Gene ID	Species	Lot no.	Accession No.	Dilution	Supplier
ATP6V0C	Rb monoclonal	QC15184	ARP45161_P050	1in250	Aviva
BCKDHA	Rb monoclonal	SH091020TAV	AP6830b	1in250	Cambridge/Aviva
CCNE2	Rb monoclonal	405485	AB40890-100	1in2000	Abcam
LGALS3	Rb monoclonal	SA110628A01	AP13725b	1in250	Cambridge/Aviva
NUCB2	Rb polyclonal	059K4783	N6789-25UL	1in500	Sigma
SGSH	Rb polyclonal		GTX101700	1in1000	Genetex
GAPDH	Ms monoclonal		ab9485	1 in 10000	Abcam

6.3.5. Luciferase assay

The region containing the predicted miR-US25-1 target site (GAGCGGT starting at nucleotide 186) within the ATP6V0C ORF was created using custom oligonucleotides (146-226 nucleotides downstream of the ATG). For the ATP6V0C seed mutant construct, nucleotides 186-191 were replaced with a BAMHI restriction site. Inserts were cloned downstream of the renilla luciferase reporter gene in the pSicheck 2® dual luciferase construct (Promega).

BCKDHA, CCNE2, LGALS3, NUCB2, and SGSH 5'UTR regions were amplified by PCR from genomic DNA. The primers used to clone these regions and the length of amplicons are shown in Figure 6.1. These amplicons were cloned upstream of the firefly luciferase reporter gene in the pGL4 luc2® construct (Promega). The pRL® renilla luciferase construct (Promega) was used as a control.

For luciferase assay, HEK-293 cells were seeded at 60-80% confluence in 96 well tissue culture coated plates. Luciferase constructs (200 ng) were co-transfected with miR-US25-1 seed mutant mimic (20 nM), miR US25-1 mimic (20 nM) (both IDT) or negative control siRNA mimic (Qiagen) using Lipofectamine 2000 reagent in accordance with the manufacturer's instructions (Life technologies). At 48 hours post transfection, cells lysate were harvested, and luciferase levels analysed using luciferase Dual-Glo® reagents and a GloMax plate reader (Promega).

A schematic representation of the predicted target sites that were cloned into luciferase constructs for each of these genes is provide in Figure 6.1.

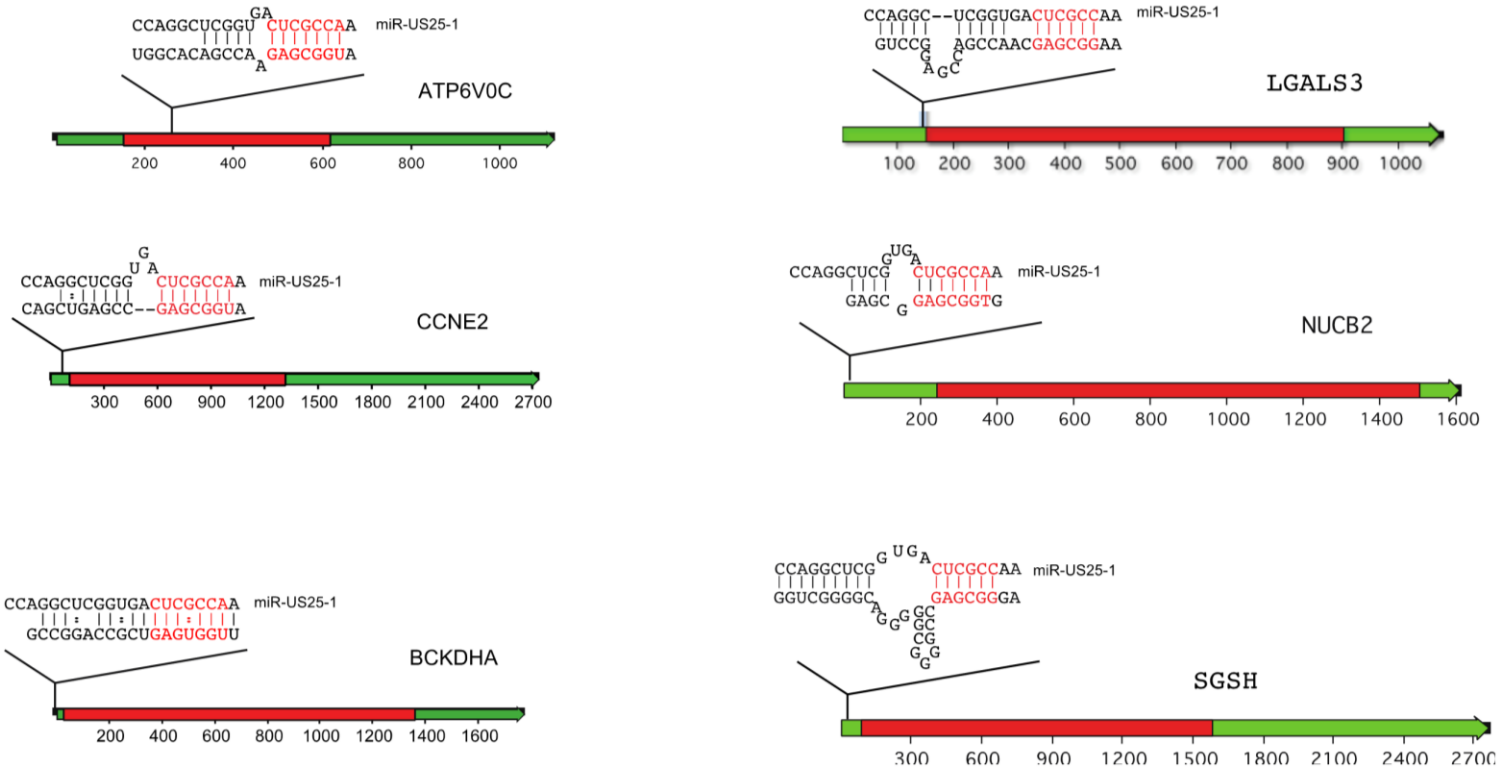

Figure 6.1 Schematic representation of the bioinformatically predicted target sites for ATP6VOC, BCKDHA, CCNE2, LGALS2, NUCB2, and SGSH

ORFs are designated in red, with 5' and 3' UTRs designated in green. Blown up regions show individual miR-US25-1 targets sites and predicted miRNA binding according to RNA hybrid.

Table 6.3 Primers for amplification of genomic regions for luciferase assay

Forward Primer	Sequence	Reverse Primer	Sequence Reverse Primer	Amplicon Length (bp)	Vector
BCKDHA_xhoI_genomic_FP	AGCTCGAGAGAGACAGGGTTTCGCCATG	BCKDHA_genomic_RP	AGAGTAAAGCGGATCAATGCCAAG	1161	pGL4
LGALS3_xhoI_genomic_FP	AGCTCGAGAGTGAGTCCTTCACAGGAAC	LGALS3_genomic_RP	CTCCGAGCCTCAAATACTCC	230	pSiCheck2
NUCB2_kpnI_genomic_FP	AGGGTACCAGTAGCTGGGACTACAGATGTG	NUCB2_xhoI_genomic_RP	AGCTCGAGGCACAAACCTGTCCTCCAGC	1119	pGL4
SGSH_kpnI_genomic_FP	AGGGTACCGTCAGGAGAGGTCACTATGG	SGSH_nheI_genomic_RP_mk2	AGGCTAGCAGGAGCAGCAGTGCGTTCC	587	pGL4
CCNE2 FP	AGCTCGAGCGGCCTATATATTGGGTTGG	CCNE2 RP	ATGCGGCCGCTCTTGGCCTGGATTATCTGG	1196	pSiCheck2

6.3.6. Mutant virus strains

miR-US25-1/2 pre-miRNA coding region was deleted from AD169 pAD CRE BAC clone using BAC technology as previously described [302]. A PCR amplified cassette containing FRT flanked kanamycin was recombined into AD169 BAC genome replacing the miR-US25-1 coding region using primers listed below.

Table 6.4 Primer sequences for BAC mutagenesis

Primer	Sequence
miR-US25-1 KO forward	GACGTCGGGACCGACGGACGCGACTCGGGGTCCT TCGGTT*CAGGAACACTTAACGGCTGA*
miR-US25-1 KO reverse	ACCGACCTAGCGTTCGGACCGGTGCGCAGAAACA GCCGGC*GAAAAGTGCCACCTGCAGAT*
miR-US25-2 KO reverse	TCGAACGTCTCTCCGGTAACTATCGGCGGCCGGG GCTGTG*CAGGAACACTTAACGGCTGA*

Sequence in *italics* indicate regions homologous to an FRT flanked Kanamycin cassette, with the remaining sequence homologous to recombination sites within the HCMV genome. The Kanamycin cassette was then removed by recombining the FRT sites through inducible FLIP recombinase. The resulting BAC was isolated and electroporated into NHDFs, which were then propagated to produce infectious virus.

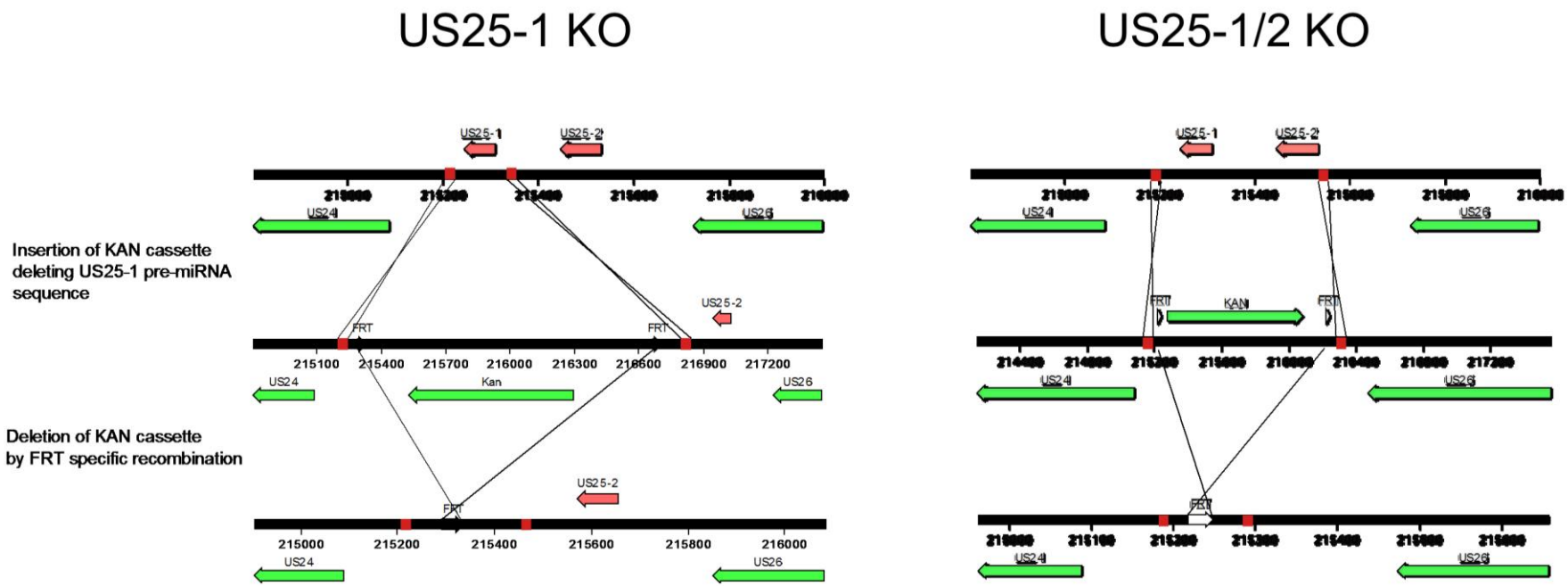

Figure 6.2 Schematic representation of AD169 miR-US25-1 knock-out virus cloning strategies
US25-1 and US25-2 pre-miRNA coding sequences are designated by the red arrows. Homologous flanking regions are designated by the red blocks.

6.4. Chapter 3 methods

6.4.1. siRNA transfections and GFP plate reading

For TB40E GFP expression analyses, NHDFs were seeded at 60-80% confluence in 96 well and double transfected as previously described. At 72 hours post transfection, cells were with TB40E at an MOI of 1. At 24 hpi, the infectious inoculum was removed, and cells were washed three times with PBS. Cells were then overlaid with phenol red free DMEM, and eGFP monitored using a Biotech Synergy HT plate reader (excitation 485 nm: emission 525 nm).

siRNA details for miR-US25-1 targets and for miRNA mimics are provided in Table 6.5.

The screen of the top 30 miRNA targets was performed using pre-validated Silencer Select® (Life Technologies) siRNAs. Assay IDs, accession numbers, and target sites are provided in Table 6.6.

Table 6.5 List of miR-US25-1 target siRNA mimic sequences

Gene ID	Accession No.	Sense
Negative Control	1027310	UUCUCCGAACGUGUCACGUdTdT
ATP6V0C S80	S80	ACUGGAUGUUUAUUUAUAATT
ATP6V0C stealth 1	HSS141330(3	GCCTATGGCACAGCCAAGAGCGGTA
ATP6V0C stealth 2	HSS141332(3	TCGTCGCCCTCATCCTCTCCACAAA
ATP6V0C stealth 3	HSS182300	CGGAGCAGATCATGAAGTCCATCAT
ATP6V1A	s1791	GGUAAGGUAGAGUCAAUUATT
ATP6V1H	s28403	GGCUAUGAUUCAGUGCAAATT
BCKDHA	s1909	UGACACUGCUUAACACCAUTT
CCNE2	s17449	CCAUUGAAGUGGUUAAGAATT
LGALS3	s8148	GGAGAGUCAUUGUUUGCAATT
NUCB2	s9773	GGAUUCCCUUCAAGAUAUATT
SGSH	HSS109691	CCTTTCCCATCGACCAGGACTTCTA
SGSH Pool	M-009053-01-0003	CCGCAUGGACCAAGGAGUU
		GAGAGUGGCGCGUACAACA
		CGGAACAUCACUAGAAUUA
		ACAAGGACCUCCGUCAUUA
US25-1		AACCGCUCAGUGGCUCGGACCGC
US25-1mut		AAGGAUCCAGUGGCUCGGACCGC
US25-2-3p		GCGGGAGCUCUCCAAGUGGCUAG
US25-2-5p		AGCGGUCUGUUCAGGUGGAUGA

Table 6.6 List of siRNAs for putative targets of HCMV miRNAs

Gene ID	Accession No.	Primary NCBI Refseq siRNA target nucleotide location
ACP2	s930	451
ATP1A3	s1724	230
ATP6VOC	s79	892
BCKDHA	s1909	373
BSG	s194316	2055
C1ORF35	s35664	1229
CCNE1	s2524	1052
CCNE2	s17449	1029
COL1A1	s375	343
CTRB2	s196535	795
DSC2	s4309	3062
FAC1	s197300	1452
FAM38	s226181	4296
FLJ39061	s46554	509
GRN	s6149	552
KRTAP107	s196174	1063
LEPRE1	s34536	1054
LGALS3	s8148	599
LIN28B	s52477	612
NUCB1	s9770	1659
NUCB2	s9773	619
PD1A5	n313465	1842
PIGH	117257	544
PRSS8	s11273	1079
SGSH	s12778	479
SPRB	s13378	158
STX10	137195	409
TMEM74	s45992	590

6.4.2. Cell viability analysis

NHDFs were seeded at 60-80% confluence double transfected with ATP6VOC siRNAs or negative control siRNA using Lipofectamine RNAimax in accordance with the manufacturer's recommendations. Cell viability was assessed using Cell

Titer-Glo® luminescent cell viability assay (Promega) in accordance with the manufacturer's instructions.

6.4.3. Viral plaque analysis

Viral plaque analyses were performed as described in [303]. NHDFs were transfected as previously described. At 72 hours post transfection, cells were infected at an MOI of 1. At 24 hpi, cells were washed three times with PBS and overlaid with fresh media. Infected cells were harvested, scraped into media, at 24 hpi, and at every subsequent 24 hour time-point. Samples were snap frozen at -80°C to lyse the cells. These lysates were then serially diluted, and used to infect sub-confluent NHDFs. At 24 hpi, cells were overlaid with 0.5% carboxymethyl-cellulose (CMC) diluted in DMEM +10% FBS+PSG. At 168 hpi, the CMC was removed, monolayers were stained with toluidine blue, and plaques counted.

6.4.4. Viral genome copy analysis

Infected cells were harvested at designated time-points and applied to DNEasy® blood and tissue kit columns (Qiagen). DNA was extracted following the manufacturer's protocol.

6.4.5. qRTPCR

Specific primer and probe sequences were kindly provided by Lauren Hook. IE86, UL83 and gH primer and probes were synthesised by Life Technologies. Sequences are provided in Table 6.7.

Table 6.7 List of primer and probe sequences for viral genes

Assay ID	Primer Forward	Probe/Dye	Primer Reverse
HCMV gH (UL75)	TTGCTAGCTC ATCCGCACC	CAGCGACCTGTACACACCCTGTT CCAGTAG / FAM	AAGAGACGCG TAAGGCGTTC
HCMV IE86	ATGTCCTGGC AGAACTCGGT	CCAGTAGCACCGGCCCCACG / FAM	GCTGCAAGAG TGGGTTGTCA
HCMV UL83	TGGAGAACGT GTCGGTCAAC	AGCCAGGAGCCCATGTCGATCTA TGTGTAC / FAM	GGATGTTCAGC ATCTTGAGCG

6.5. Chapter 4 methods

6.5.1. Immunofluorescence and confocal microscopy

Round glass 14mm cover slips were sterilised and placed in a tissue culture coated 24-well plate. NHDFs were seeded for siRNA transfection, and double-transfected as previously described. At 72 hours post transfection, cells were infected with AD169 at an MOI of 1. At 144 hpi, cover slips were washed with PBS, and fixed for 15 minutes with freshly prepared 4% paraformaldehyde in Dulbecco's PBS (DPBS). Coverslips were then washed 3 times with DPBS. Coverslips were then permeabilised for 5 minutes (DPBS + 3% FBS + 0.2% TX100), and then washed 3 times with DPBS + 3%FBS. Coverslips were then blocked for 1 hour at room temperature (DPBS + 3% FBS + 0.5% Tween 20), before the addition of primary antibodies, diluted as specified in Table 6.8. Coverslips were incubated with primary antibodies overnight at 4°C. Coverslips were washed 3 times with DPBS + 3% FBS before the addition of secondary fluorescent antibodies (AlexaFluor® anti-mouse 647 and anti-rabbit 488 [Life Technologies]). Coverslips were incubated for 1 hour at room temperature, and washed 3 times with DPBS+3% FBS. Finally, coverslips were nuclear stained using 1:1000 DAPI before mounting to slides using 5 μL Prolong Gold® anti-fade reagent (Life Technologies).

Images were acquired using a Zeiss LSM 710 confocal microscope in accordance with the manufacturer's instructions. Images were compiled and analysed using Fiji open source image processing software (http://www.fiji.sc).

6.5.2. Supernatant and cell associated virus purification

AD169 was propagated as previously described. Cells were scraped into infected supernatant at 7 days post infection. Cell associated virus was isolated from the supernatant by centrifugation (1000 x g for 1 hour). Supernatant was removed from the cell pellet. Virus was then pelleted from the supernatant by ultra-centrifugation following the method outlined previously. Supernatant purified virus was then re-suspended in DPBS. Fractions of purified virus were then added to either DMEM for plaque analysis, laemmli buffer for western blot analysis, or added directly to DNEasy blood and tissue DNA isolation columns (Qiagen). Plaque and western blot analyses were then performed as previously outlined, and viral DNA was isolated in accordance the manufacturer's instructions. Viral DNA was assayed using the gH primer probe assay (Table 6.7), and relative copy number calculated using the ΔΔct method.

6.5.3. Western blot analyses

Western blot analyses were performed as previously outlined, using Novex 4-12% and MOPS running buffer. Primary antibodies and dilution for western blot are shown in Table 6.8.

Table 6.8 Antibodies for immunofluorescence microscopy and western blot

Gene ID	Species	Accession No.	Dilution	Supplier
TGN46	Rabbit	PA5-23068	1:500 IF 1:1000 WB	Pierce
EEA1	Rabbit	ab2900	1:500 IF 1:1000 WB	Abcam
pp28	Mouse	CH19	1:500 IF 1:1000 WB	Santa Cruz
gB	Mouse	2F12	1:1000 WB	Abcam
IE72/86	Mouse		1:2000 WB	

IF = immunfluorescence, WB = western blot

7. Appendices

7.1. Appendix I: Supplemental Data

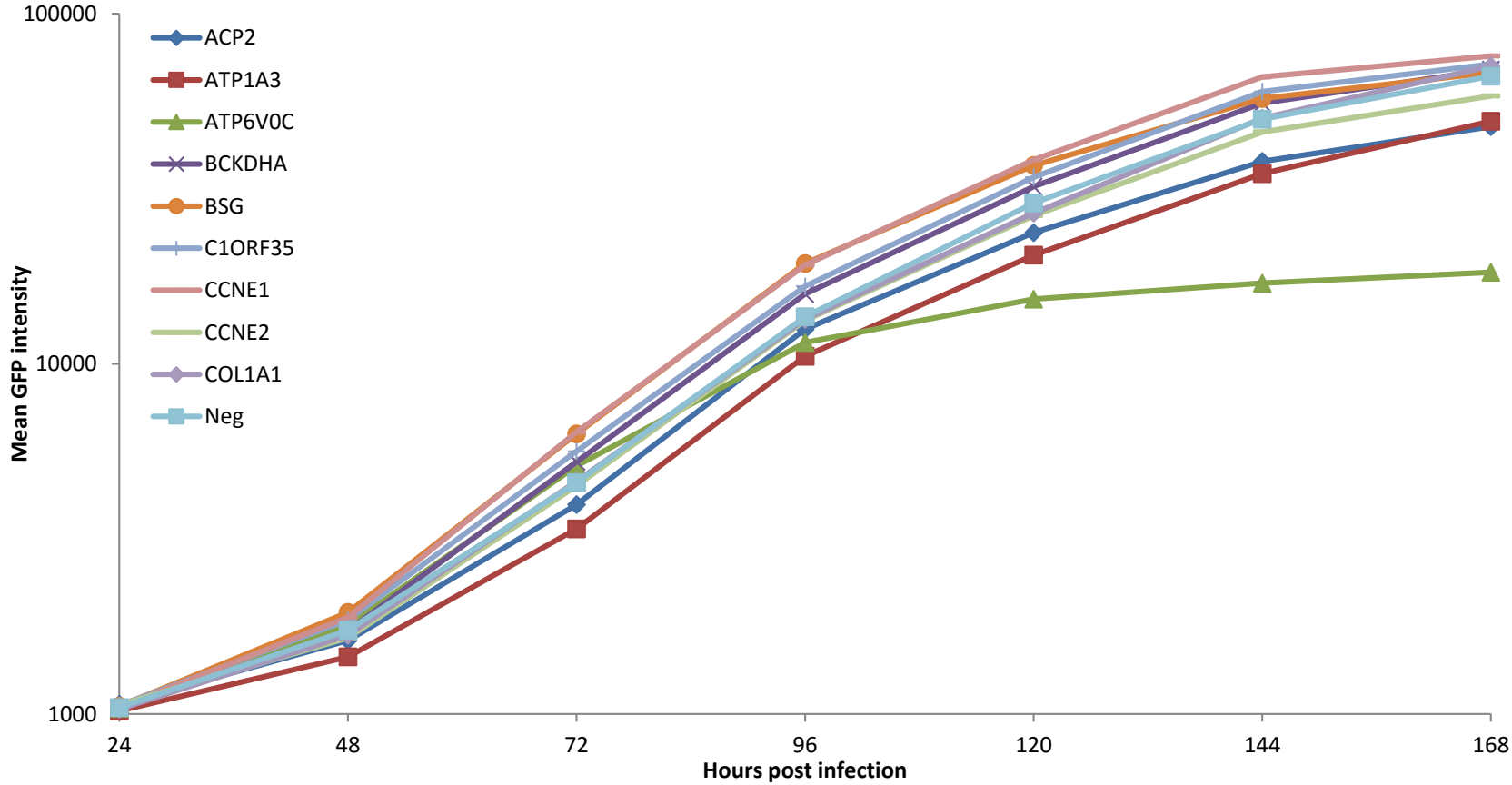

Figure 7.1 siRNA screen: GFP intensity in fibroblast cells transfected with siRNAs against the top 30 host-cellular targets of HCMV miRNAs (20 nM) (N=3)

Fibroblast cells were transfected with siRNAs and 72 hours post transfection were infected with TB40E. Virus replication was monitored *via* GFP plate reader.

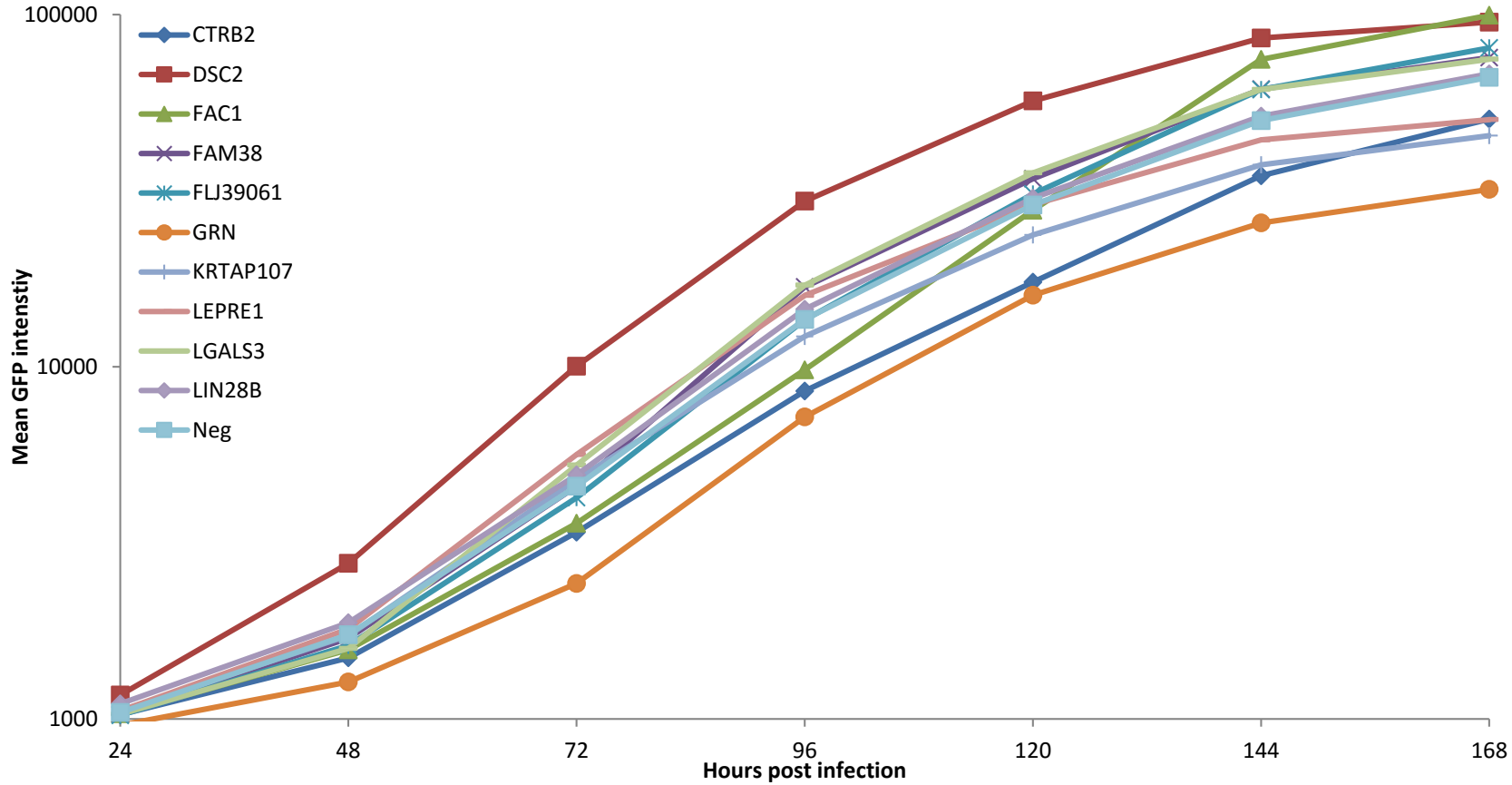

Figure 7.2 siRNA screen: GFP intensity in fibroblast cells transfected with siRNAs against the top 30 host-cellular targets of HCMV miRNAs (20 nM) (N=3)

Fibroblast cells were transfected with siRNAs and 72 hours post transfection were infected with TB40E. Virus replication was monitored *via* GFP plate reader.

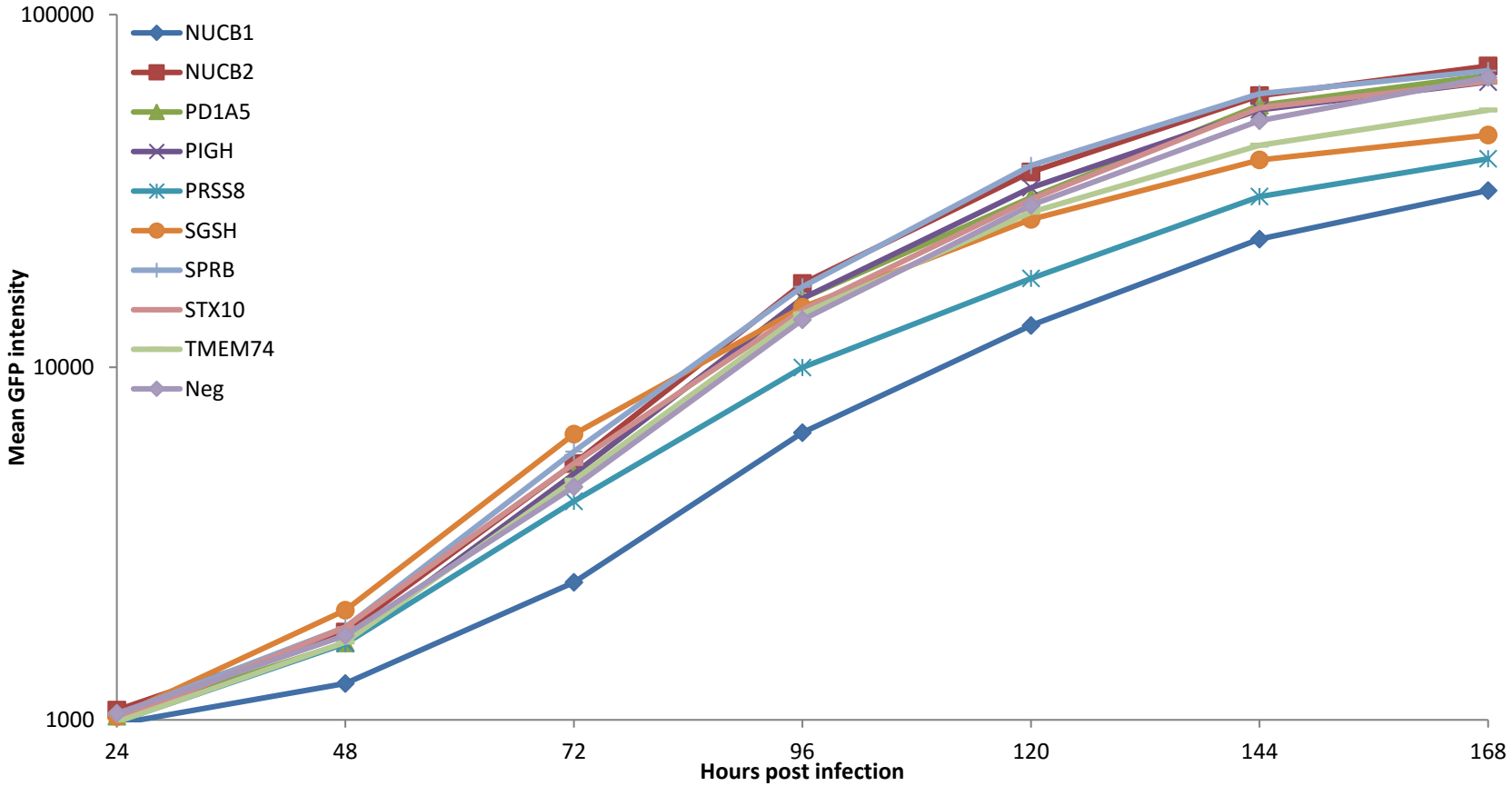

Figure 7.3 siRNA screen: GFP intensity in fibroblast cells transfected with siRNAs against the top 30 host-cellular targets of HCMV miRNAs (20 nM) (N=3)

Fibroblast cells were transfected with siRNAs and 72 hours post transfection were infected with TB40E. Virus replication was monitored *via* GFP plate reader.

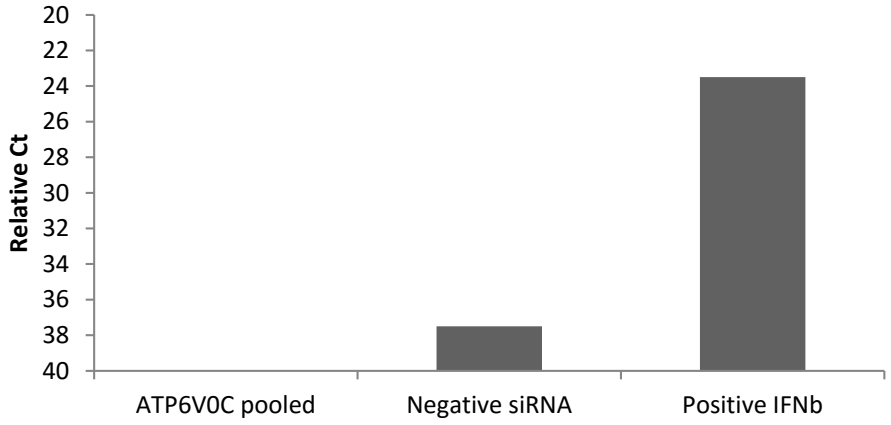

Figure 7.4 IFN-β expression in fibroblast cells transfected with pooled ATP6VOC siRNA (20 nM) (N=1)
Fibroblast cells were transfected with ATP6VOC, Negative control siRNA, or a IFNb positive control siRNA. 72 hour post transfection, RNA was extracted and expression levels assayed by qRTPCR.

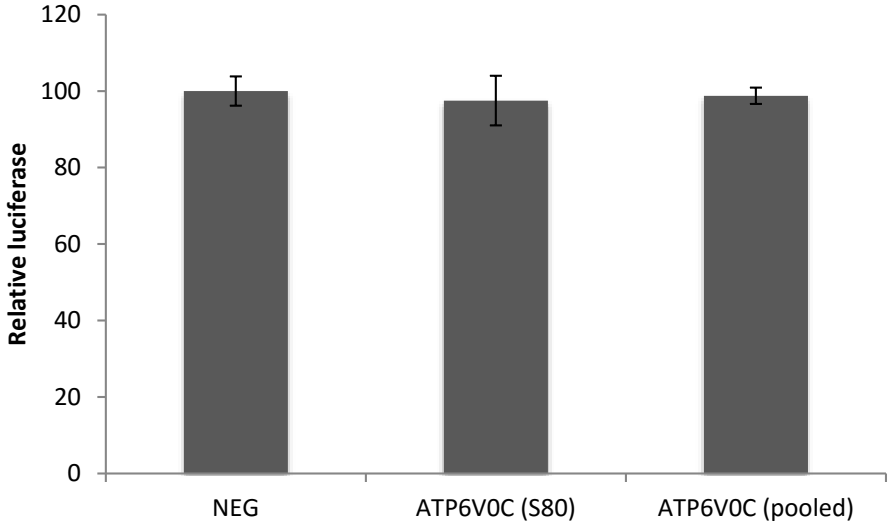

Figure 7.5 Cell viability in fibroblast cells transfected with pooled ATP6VOC siRNA (20 nM) (N=3)
Fibroblast cells were transfected with ATP6VOC, or a Negative control siRNA. 72 hour post transfection, cells were lysed and cell viability measured using a luciferase based system.

7.2. Appendix 2: List and description of electronic supplemental data

Table 7.1 Microarray dataset from RISC-IP of AD169 infected fibroblast cells

Table 7.2 Microarray dataset from RISC-IP of TR infected fibroblast cells

Table 7.3 Microarray from RISCIP in pUS25-1 and b-US25-1 transfected HEK 293 cells

Table 7.4 Raw data from RISC-IP and qRTPCR in fibroblasts infected with AD169, AD169 miR-US25-1KO, AD169 miR-US25-1/2KO, and uninfected fibroblast cells

Table 7.5 RNA hybrid target prediction data for miR-US25-1 targeting

Figure 7.6 3D renders of VAC in fibroblast cells after ATP6VOC knock-down compared with negative control siRNA transfected fibroblast cells

7.3. Appendix 3: Publications, conference presentations, and posters

Oral Presentations

2013 - Society for general microbiology annual meeting, Manchester UK

2013 - International Herpesvirus Workshop, Grand Rapids, Michigan, USA

2014 - Society for general microbiology annual meeting, Liverpool, UK

Poster Presentations

2014 - International Herpesvirus workshop, Kobe, Japan.

OPEN ACCESS Freely available online

PLOS | PATHOGENS

Systematic MicroRNA Analysis Identifies ATP6V0C as an Essential Host Factor for Human Cytomegalovirus Replication

Jon Pavelin[1], Natalie Reynolds[1], Stephen Chiweshe[1], Guanming Wu[2], Rebecca Tiribassi[3], Finn Grey[1]*

1 Division of Infection and Immunity, The Roslin Institute, University of Edinburgh, Easter Bush, Midlothian, United Kingdom, **2** OCTRI, Health Sciences University, Portland, Oregon, United States of America, **3** Vaccine and Gene Therapy Institute, Health Sciences University, Portland, Oregon, United States of America

Abstract

Recent advances in microRNA target identification have greatly increased the number of putative targets of viral microRNAs. However, it is still unclear whether all targets identified are biologically relevant. Here, we use a combined approach of RISC immunoprecipitation and focused siRNA screening to identify targets of HCMV encoded human cytomegalovirus that play an important role in the biology of the virus. Using both a laboratory and clinical strain of human cytomegalovirus, we identify over 200 putative targets of human cytomegalovirus microRNAs following infection of fibroblast cells. By comparing RISC-IP profiles of miRNA knockout viruses, we have resolved specific interactions between human cytomegalovirus miRNAs and the top candidate target transcripts and validated regulation by western blot analysis and luciferase assay. Crucially we demonstrate that miRNA target genes play important roles in the biology of human cytomegalovirus as siRNA knockdown results in marked effects on virus replication. The most striking phenotype followed knockdown of the top target ATP6V0C, which is required for endosomal acidification. siRNA knockdown of ATP6V0C resulted in almost complete loss of infectious virus production, suggesting that an HCMV microRNA targets a crucial cellular factor required for virus replication. This study greatly increases the number of identified targets of human cytomegalovirus microRNAs and demonstrates the effective use of combined miRNA target identification and focused siRNA screening for identifying novel host virus interactions.

Citation: Pavelin J, Reynolds N, Chiweshe S, Wu G, Tiribassi R, et al. (2013) Systematic MicroRNA Analysis Identifies ATP6V0C as an Essential Host Factor for Human Cytomegalovirus Replication. PLoS Pathog 9(12): e1003820. doi:10.1371/journal.ppat.1003820

Editor: William J. Britt, University of Alabama at Birmingham, United States of America

Received April 17, 2013; **Accepted** October 21, 2013; **Published** December 26, 2013

Funding: This work was supported by funding from The Wellcome Trust (088308/z/09/z and Institute Strategic Programme Grant Funding from the U.K. Biotechnology and Biological Sciences Research Council [grant number BB/J004324/1]. The funders had no role in study design, data collection and analysis, decision to publish, or preparation of the manuscript.

Competing Interests: The authors have declared that no competing interests exist.

* E-mail: finn.grey@roslin.ed.ac.uk

Introduction

Human cytomegalovirus (HCMV) is a highly prevalent infectious disease, infecting greater than 30% of the population. Although normally asymptomatic in healthy individuals, HCMV infection is a significant cause of morbidity and mortality in immunocompromised populations, individuals with heart disease and recipients of solid organ and bone marrow transplants [1–8]. HCMV is also the leading cause of infectious congenital birth defects resulting from spread of the virus to the unborn fetus. Reactivation of virus from a latent infection, rather than primary infection, is often responsible for HCMV associated pathologies [9–13].

The capacity of HCMV to strictly regulate the expression of its own genes and to manipulate host gene expression is crucial to the virus's ability to replicate and its success in maintaining a persistent infection [14]. Studies in our lab and others have demonstrated that herpesviruses have evolved to encode microRNA (miRNA) genes, enabling regulation of the virus's gene expression profile as well as altering the host environment by targeting cellular transcripts. Recent reports have demonstrated roles for viral miRNAs in suppressing apoptosis, immune evasion and regulation of viral replication through targeting of both cellular and viral gene expression [15].

HCMV encodes at least 14 pre-miRNAs corresponding to a total of 27 mature miRNA species [16–20]. Clear functions have not been shown for the majority of HCMV miRNAs. However, these regulatory RNAs have been shown to target genes involved in viral latency, immune evasion, and cell cycle control [21]. We previously demonstrated that the HCMV miRNA, UL112-1, restricted viral acute replication through targeting of the major immediate early gene IE72, suggesting this miRNA may play a role in establishing and maintaining viral latency [22]. Others have since shown that targeting of immediate early genes by viral miRNAs may be a fundamental mechanism involved in herpesvirus latency regulation [23–26]. UL112-1 has also been shown to target the major histocompatibility complex class I-related chain B (MICB) resulting in reduced killing by NK cells [27].

Despite these advances, identification of miRNA targets remains challenging. Until we have a greater understanding of the rules governing miRNA target interaction, bioinformatic strategies alone continue to produce unreliable results, especially for viral miRNAs, which in most cases do not display significant evolutionary conservation.

Author Summary

Human cytomegalovirus is a prevalent pathogen. Like other herpesviruses, human cytomegalovirus expresses small regulatory RNAs called microRNAs. The focus of this study was to understand the role of these RNAs in the context of viral infection and to use this information to identify novel host factors involved in human cytomegalovirus biology. We used a biochemical approach that allowed us to systematically identify cellular genes targeted by virus microRNAs. Because the virus targets these genes, it is reasonable to propose that these genes play an important role during infection. We confirmed this hypothesis using a second screen in which we knocked down expression of a number of the identified targets of the virus microRNAs. Knock down of one of the targets, a cellular factor called ATP6V0C, resulted in an almost complete block in production of infectious virus. These data suggest that endosomal acidification is crucial to HCMV replication, and the virus targets this process by microRNA regulation.

Biochemical approaches have provided an alternative means for the identification of miRNA targets. One such approach, RISC immunoprecipitation (RISC-IP) has proved effective in identifying both cellular and viral targets [28]. Recently, we used a RISC-IP approach to identify multiple cellular targets of US25-1, an HCMV miRNA expressed at high levels during acute infection [29]. Here we use a combined approach of RISC-IP profiling in infected cells combined with focused siRNA screening to identify host targets of HCMV miRNAs that have significant effects on virus replication. Our results, using a laboratory strain as well as a clinical strain of virus greatly increases the number of identified and validated HCMV miRNA targets. Furthermore, the results show that the V-ATPase complex, involved in acidification of endosomal compartments, is essential for HCMV virus replication and is targeted by the HCMV miRNA US25-1.

Results

RISC-IP techniques have recently been used to identify targets of viral miRNAs [29,30]. The approach relies on the stable interaction of the miRNA associated RISC protein complex with the targeted transcript. Following lysis of cells the RISC complexes are immunoprecipitated using direct antibodies that recognize Argonaute 2. RNA is then isolated, labeled and analysed by microarray to identify transcripts which are significantly enriched due to miRNA targeting. In a previous study we used this technique to identify targets of a single miRNA, US25-1, in the context of HEK293 cells [29]. Here we used the same basic approach to identify targets in primary human fibroblast cells infected with either the laboratory adapted AD169 strain of HCMV or the clinical strain TR. In both cases cells were infected at a high multiplicity of infection (MOI) of three and cells harvested three days post infection. Following lysis and immunoprecipitation, RNA was isolated by trizol extraction and analysed by microarray using the Illumina HumanRef-8 platform which contains probes for approximately 24,000 well annotated genes (Figure 1A). In addition to uninfected cells, RNA was analysed from infected cells immunoprecipitated with pre-immune serum instead of anti-Argonaute 2 antibody. To determine the level of enrichment, lysate was sampled before immunoprecipitation to establish total levels of transcript expression. Enrichment was then calculated as the transcript level of the IP sample divided by the total RNA sample. To determine transcripts specifically targeted by HCMV miRNAs, the level of enrichment from infected samples was divided by the level of enrichment in uninfected samples. However, infection with HCMV results in significant perturbation of total levels of many cellular transcripts through mechanisms unrelated to miRNA expression. False positive enrichment attributed to viral miRNA targeting can therefore occur due to down regulation of total RNA levels in the infected sample, where IP background levels remain relatively unchanged. To overcome this, a correction calculation was introduced using the results from the control IP using the pre-immune serum pull down. As enrichment values in this sample would only occur through changes in total levels due to AD169 infection, rather than any effective enrichment through specific immunoprecipitation, false enrichment could be effectively subtracted from the data sets generated with anti-Argonaute 2 pull downs. Example calculations are shown in supplemental figure S1.

The results indicate that greater than 96% of transcripts showed little or no enrichment in infected cells compared to uninfected cells, as would be expected if virus miRNAs are targeting a specific subset of transcripts (Figure 1B). In cells infected with AD169, 686 transcripts were enriched two fold or more with enrichment levels as high as 28.9 fold for the top target ATP6V0C. Enrichment levels were slightly lower for TR infected cells with 442 genes enriched 2 fold or higher with the highest level of enrichment for COMMD10 at 19.8 fold (Figure 1C). The lower enrichment in TR infected cells was expected as the clinical strain replicates less efficiently than AD169 in primary fibroblast cells, resulting in lower levels of miRNA expression (data not shown). Given that HCMV miRNAs are completely conserved between TR and AD169, with the exception of miR-148D-1, which is deleted from AD169 due to genome rearrangements, a similar suite of enriched genes would be expected from each pull down experiment. Indeed, 222 of the 442 genes enriched by two fold or more in cells infected with TR, were also enriched in the AD169 sample. This is a highly significant level of correlation ($P = 3.2 \times 10^{-233}$ as determined by hypergeometric distribution analysis) (Figure 1D) that validates the biological reproducibility of the system. Of the top 30 most highly enriched transcripts from AD169 infected cells, 26 were also enriched at least two fold in pull downs from TR infected cells, giving a high level of confidence that these genes are specifically enriched due to HCMV miRNA targeting. Table 1 lists the top 30 most highly enriched genes from cells infected with AD169 with corresponding enrichment values for TR. The complete data sets are shown in supplemental tables S1 and S2.

As pull down experiments were performed in the context of viral infection, any one, or a combination of, HCMV encoded miRNAs could target the identified transcripts. It is also possible that transcripts could be enriched through targeting by an induced cellular miRNA. Target interaction between miRNAs and transcripts rely heavily on binding between the 5′ end of miRNAs, specifically nucleotides 1 through 8, known as the seed sequence. To define which HCMV miRNA has the potential to target the identified transcripts we predicted seed match sites using the online algorithm RNAHybrid for the 14 most abundant HCMV miRNAs. Stringent parameters of full Watson Crick base pairing with bases 1–7 or 2–8 were employed with the top 30 putative targets analysed. All but three of the transcripts contained at least one seed match to the major HCMV encoded miRNAs, with most transcripts containing targets sites for multiple HCMV miRNAs (Figure 2). The majority of target sites reside within the open reading frame of the transcripts with only 14 of the 30 transcripts containing predicted seed matches for HCMV miRNAs within the 3′UTR. Although there is evidence that cellular miRNA targeting

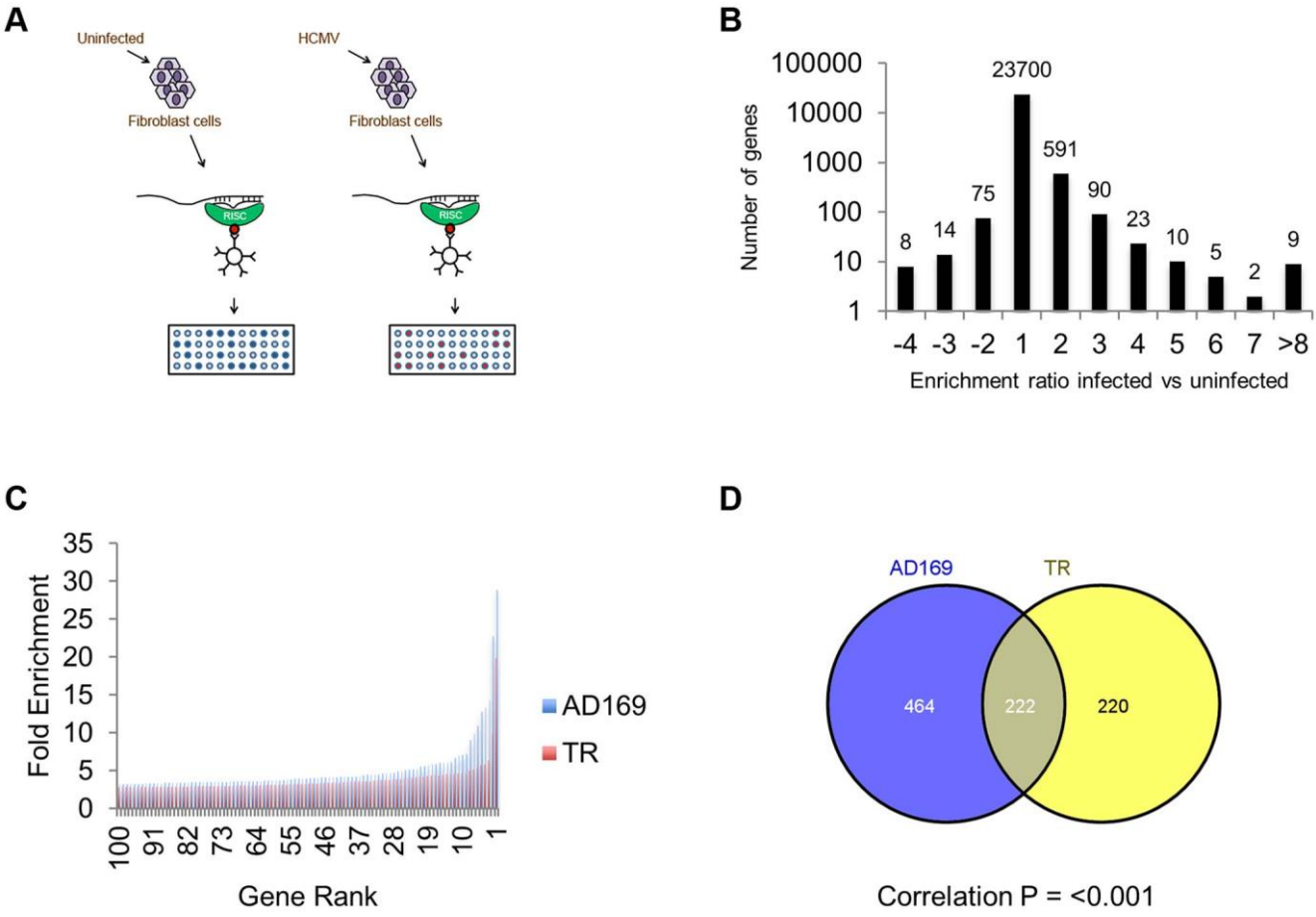

Figure 1. Systematic analysis of RISC-IP from HCMV infected fibroblast cells. (A) Schematic representation of RISC-IP procedure in HCMV infected and uninfected fibroblast cells. (B) Enrichment profile of all genes from AD169 infected cells. Genes were binned according to the enrichment ratio of infected vs uninfected. For example genes with an enrichment ratio from supplemental table 1 of between 0.5 and <2.0 were binned to 1 whereas genes with an enrichment profile of <0.5 but >0.33 were binned to −2. Total number of genes are shown above each bar. Values are skewed towards positive enrichment indicating effective enrichment of HCMV miRNA targets (C). Enrichment profile of the top 100 genes from cells infected with AD169 or TR. (D) Overlap of genes enriched greater than two fold between AD169 infected cells and TR infected cells. Correlation between the enriched profiles was highly significant as determined by Chi Squared test.
doi:10.1371/journal.ppat.1003820.g001

is heavily constrained to the 3′UTR region of transcripts [31–33], a number of studies, including our own, suggest that these constraints may not always be applied to viral miRNA targeting. In fact targeting by US25-1 was shown to predominantly target sites within the 5′UTR [29]. Full analysis of transcripts is shown in Supplemental Table S3.

To delineate the miRNA target interactions, we compared the RISC-IP data from infected cells with the previous published study generated from cells transfected with US25-1 [29]. Figure 3A represents heat map analysis comparing enrichment profiles from the top 30 enriched transcripts of cells infected with AD169 or TR, with cells transfected with either a plasmid expressing US25-1 or immunoprecipitations using a synthetic US25-1 mimic containing a biotin moiety. The majority of transcripts show clear enrichment with AD169 and TR as would be expected. In addition, highly enriched genes from infected cells were also significantly enriched in cells only expressing US25-1, demonstrating that these transcripts are targeted by US25-1 in the context of viral infection. Six genes, including the top target from the previous study, CCNE2, and the top target from this study, ATP6V0C, were in the top 30 enriched genes from cells infected with AD169 or cells transfected with US25-1 (Figure 3B and C).

Although the combined data sets provide strong evidence that these six genes are targeted by US25-1 in the context of virus infection, it is possible that other viral miRNAs may also target these genes, potentially complicating further validation. To determine whether this was the case, additional RISC-IP analysis was carried out comparing wild type AD169 virus to two recombinant AD169 viruses in which either US25-1 had been deleted, or the entire US25 region, encoding both US25-1 and 2, was deleted. Enrichment levels for each of the six genes identified from the previous analysis was determined by direct RT-PCR using specific primer probe sets (Figure 4). To allow direct comparison, enrichment values for wild type pull downs were set at 100% (actual enrichment values are displayed above each bar for reference). All six targets showed significant enrichment in infected cells compared to uninfected cells, validating the results from the original microarray experiments. Four of the six genes, ATP6V0C, CCNE2, BCKDHA and LGALS3, also showed a near complete loss of enrichment from cells infected with either US25 knock out viruses, indicating that US25-1 is required for enrichment of these transcripts. The results were less clear-cut for NUCB2 and SGSH. Although the levels of enrichment were reduced, the reduction was not statistically significant, suggesting

Table 1. Summary table of the top 30 most enriched genes following infection with AD169.

Gene	AD169	TR	DEFINITION
ATP6V0C	28.9	9.8	ATPase, H+ transporting, lysosomal
GRN	22.8	2.4	granulin
COMMD10	14.3	19.9	COMM domain containing 10
CTRB2	13.3	6.4	chymotrypsinogen B2
SGSH	12.8	3.4	N-sulfoglucosamine sulfohydrolase
LGALS3	10.9	3.6	galactoside-binding, soluble, 3 (galectin 3)
PIGH	9.9	3.7	phosphatidylinositol glycan anchor biosynthesis
BSG	9.0	1.7	basigin
LEPRE1	7.2	2.4	leucine proline-enriched proteoglycan
LIN28B	7.1	2.9	lin-28 homolog B
SRPRB	7.0	3.8	signal recognition particle receptor
PDIA5	6.6	4.2	protein disulfide isomerase family A
CCNE1	6.1	5.7	cyclin E1
FLJ39061	6.1	3.2	FLJ39061
NUCB1	6.0	0.9	nucleobindin 1
PRSS8	6.0	4.6	protease, serine, 8
BCKDHA	5.9	1.8	branched chain keto acid dehydrogenase E1
C1ORF35	5.9	4.7	chromosome 1 open reading frame 35
TMEM74	5.7	2.4	transmembrane protein 74
NUCB2	5.6	3.1	nucleobindin 2
DSC2	5.5	2.0	desmocollin 2
FALZ	5.2	2.1	fetal Alzheimer antigen
CCNE2	5.2	2.6	cyclin E2
STX10	5.1	3.5	syntaxin 10
COL1A1	5.0	3.4	collagen, type I
KRTAP10-7	4.9	4.1	keratin associated protein 10-7
FAM38A	4.9	2.3	family with sequence similarity 38
ACP2	4.7	1.8	acid phosphatase 2, lysosomal
ATP1A3	4.7	4.2	ATPase, Na+/K+ transporting
PROK2	4.7	4.4	prokineticin 2

Corresponding enrichment levels are shown for TR infected cells.
doi:10.1371/journal.ppat.1003820.t001

that other viral miRNAs may be involved in targeting these genes. Additional validation of genes from the top 30 most enriched transcripts also showed significant enrichment in infected samples compared to uninfected samples, again validating the original microarray data (Supplemental Figure S2). However, no other genes showed a complete loss of enrichment in the knock out viruses. Transcripts that were not predicted to be targeted by US25-1, such as LIN28B, showed enrichment in both wild type and knock out virus, confirming that successful enrichment from the knock out virus infected cells had occurred. In addition no enrichment was detected in control transcripts such as beta actin (data not shown). No significant enrichment was observed following transfection with mimics corresponding to US25-2-3p, US25-2-5p or a US25-1 mimic containing a mutated seed region, demonstrating that neighboring miRNAs do not play a role in the enrichment of the six identified targets and that the seed region of US25-1 is necessary for effective enrichment (Supplemental Figure S3A).

Although these results confirmed that US25-1 RISC complexes bind to the identified transcripts it remained necessary to determine whether these interactions were functional and resulted in effects on gene expression. In our previous study we demonstrated that targeting of CCNE2 by US25-1 resulted in reduced cyclin E2 expression and conversely deletion of US25-1 from the virus resulted in increased expression of cyclin E2 in the context of virus infection. Using the same approach the effect of US25-1 on the expression levels of all six identified genes was investigated. Primary human fibroblast cells were infected at high MOI with either wild type AD169 or US25-1 KO virus and protein levels for the six genes compared by western blot analysis (Figure 5A). Uninfected cell lysates were also included as well as cells transfected with a siRNA specific for the target gene, to confirm the specificity of the antibody. As has been shown before, CCNE2 levels were higher in the knock out virus infected cells compared to the wild type infected cells. In addition, ATP6V0C, BCKDHA, LGALS3 all showed increased levels of expression in cells infected with the US25-1 knock out virus, whereas NUCB2 and SGSH did not show significant difference between wild type infected cells and knockout infected cells. Representative western blots are shown in Figure 5A with direct quantitation from three biological repeats shown in Figure 5B. These results correspond well with the RISC-IP data, indicating that ATP6V0C, CCNE2, BCKDHA and LGALS3 are targeted by US25-1 and deletion of this miRNA results in near complete abrogation of the inhibitory effects, whereas NUCB2 and SGSH may be targeted by additional viral miRNAs, or other virally induced mechanisms. Further supporting the role of US25-1 in targeting of these cellular genes, transfection of fibroblast cells with US25-1 mimic RNA results in significant knockdown at RNA levels of the putative US25-1 targets. The exception to this is SGSH, where transfection of US25-1 reproducibly resulted in a two-fold increase in total RNA levels. Whether this is due to a direct effect of US25-1 binding to the SGSH transcript or secondary effects from regulation of other US25-1 targets is unclear and will require further study. In addition, transfection of US25-2-3p and US25-2-5p did not result in significant knockdown of ATP6V0C, again supporting the role of US25-1 alone in targeting these genes (Supplemental Figure S3B).

Our previous study showed that US25-1 predominantly targets the 5′UTR of transcripts and five of the six genes (including the previously identified CCNE2) have potential target sites within the 5′UTR for US25-1 (Supplemental Figure S5). However, ATP6V0C contains a 7mer target site for US25-1 downstream of the 5′UTR within the open reading frame. To determine whether the US25-1 target within the open reading frame is responsible for the observed knockdown in ATP6V0C protein expression we carried out luciferase assays using a construct containing the target site from ATPV0C cloned into the 3′UTR of the reporter construct psiCheck2 (Figure 6A). The construct was co-transfected into HEK293 cells with either US25-1 mimic, or a non-targeting control siRNA. A CCNE2 luciferase construct was included as a positive control. US25-1 mimic induced a significant reduction in luciferase expression, compared to the negative control siRNA for both constructs (Figure 6C). Furthermore, mutation of the ATP6V0C target seed region to a BamHI restriction site resulted in restoration of the luciferase activity, indicating that the target site identified in ATP6V0C is both sufficient and necessary for US25-1 specific inhibition of gene expression. Transfection of a US25-1 mimic with a mutated seed sequence that corresponds to the mutated ATP6V0C luciferase construct did not reduce expression of the wild type ATP6V0C

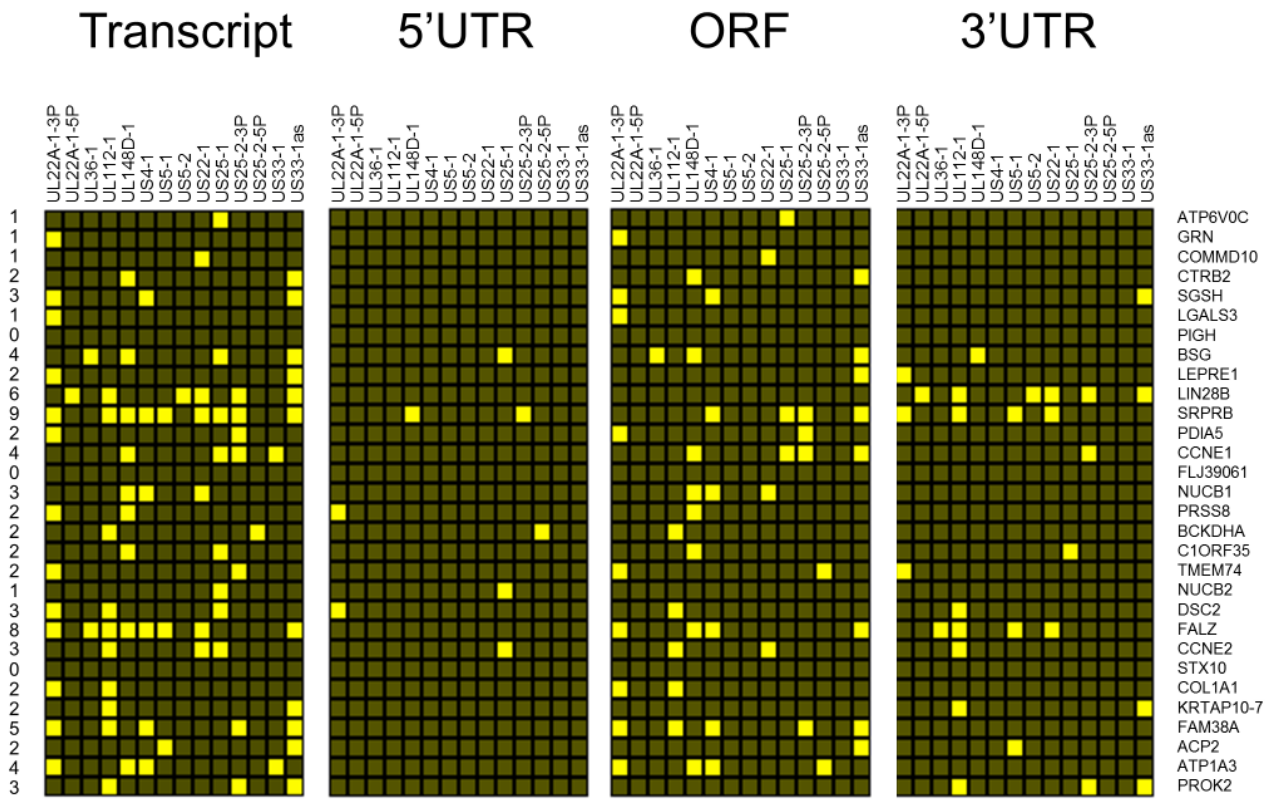

Figure 2. Top 30 enriched genes contain multiple target sites for HCMV miRNAs. Sequences for the top 30 enriched transcripts were analysed for HCMV miRNA targets using RNA Hybrid algorithm. Figure shows hit matrix where a yellow square indicates at least one target site for the indicated HCMV miRNA. Independent hit matrices shown for targets either within the whole transcript, or within the CDS, 5′UTR and 3′UTR. Total number of potential miRNAs targeting a transcript shown in the far left column.
doi:10.1371/journal.ppat.1003820.g002

luciferase construct, but did inhibit expression of the mutated ATP6V0C construct (Figure 6B and C).

Although it is clear that US25-1 targets and regulates the identified genes in the context of viral infection it is less clear whether these targets are functionally relevant. It is possible that viral miRNAs target many genes, but only a few are important to the virus while other targets represent fortuitous or irrelevant targets in the context of infection. Previous studies have established that cell cycle control and expression of cyclin E proteins are intimately involved in HCMV biology. However, the potential role of the remaining 5 targets is unclear, as they have not been reported as host factors involved in HCMV replication. To investigate their potential role, replication of HCMV was analysed following siRNA knockdown of each of the individual US25-1 targets in primary human fibroblast cells. Knock down of each gene was confirmed by RT-PCR (Supplemental figure S4A). Cells were infected, post siRNA transfection, at an MOI of 1 with the clinical strain TB40E, which expresses GFP fluorescence protein under control of the SV40 promoter. This allows continuous monitoring of virus levels through GFP fluorescence. As can be seen from Figure 7A, knockdown of SGSH resulted in a modest increase in virus replication. In contrast knockdown of ATP6V0C resulted in significant reduction in virus replication at all time points. To rule out the possibility that the effects on virus replication were caused by artifactual or non-targeting effects, the assay was repeated using three additional independent siRNAs targeting different regions of the ATP6V0C transcript (Figure 7B). All three siRNAs resulted in the same reduction of GFP fluorescence. To determine the effect on production of infectious virus, plaque assays were conducted following transfection of fibroblast cells with siRNA pools targeting ATP6V0C, SGSH or a negative control siRNA. The results support and confirm the GFP screen with a modest but statistically significant increase in replication in cells transfected with SGSH siRNA (Mann-Whitney U Test: $p = 0.0039$) and a more dramatic reduction in virus production in cells transfected with ATP6V0C siRNA (Figure 7C). In fact, knock down of ATP6V0C resulted in almost complete block in virus production, indicating that expression of ATP6V0C is essential for HCMV virus production and suggests that acidification of endosomal compartments is required for HCMV acute replication. Cell viability assays demonstrate that the reduction in virus replication was not due to cellular toxicity caused by ATP6V0C knockdown and transfection of the small RNAs did not induce an interferon response (Supplemental Figure S4B and C). However, previous reports have indicated that ATP6V0C may have functions independent of endosomal acidification [34]. To determine whether the observed inhibition of virus replication is due to a defect in endosomal acidification, fibroblast cells were transfected with siRNAs targeting ATP6V1A and ATP6V1H, components of the same vacuolar ATPase complex. Disruption of any of the essential components has been shown to be sufficient to destabilize the complex. Knockdown of either ATP6V1A or ATP6V1H resulted in a similar reduction in HCMV replication compared to cells in which ATP6V0C had been knocked down (Figure 7D). These results support the conclusion that acidification of the endosomal compartments by V- ATPase is essential for efficient HCMV replication and this gene is targeted by the HCMV miRNA US25-1.

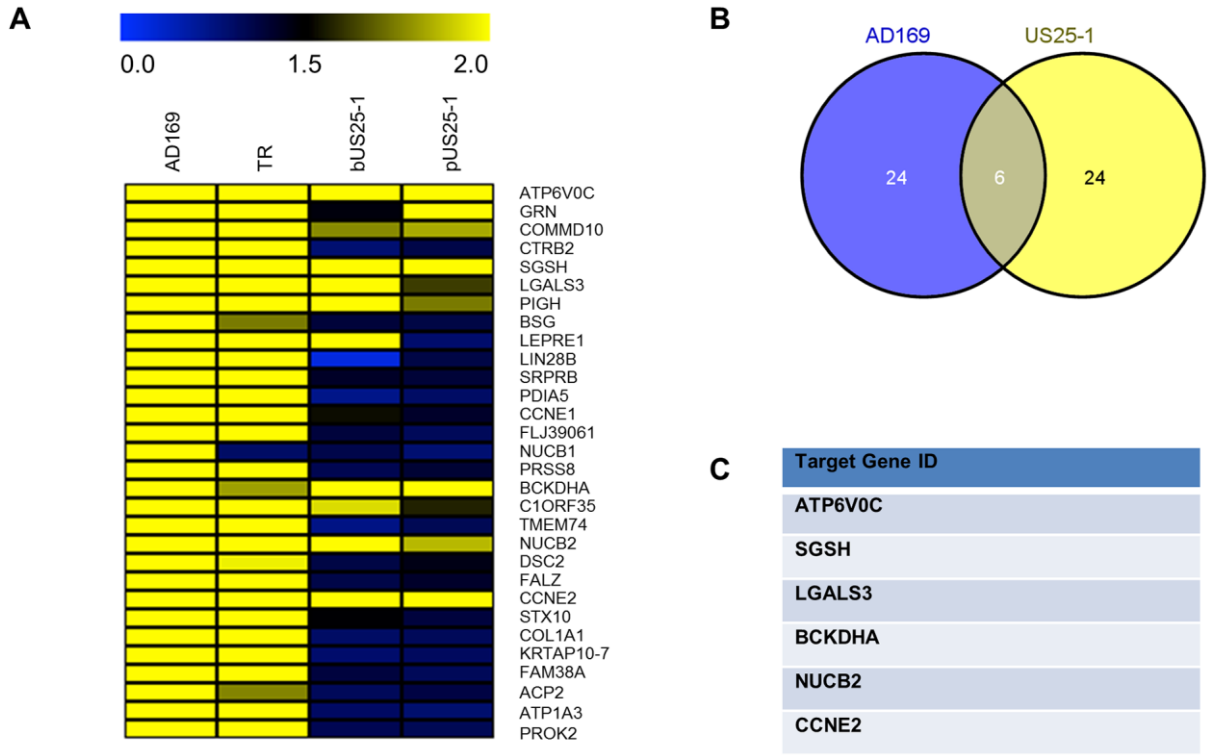

Figure 3. Comparison of RISC-IP profiles from infected fibroblast cells and HEK293 cells transfected with US25-1. (A) Heat map comparing the enrichment levels from fibroblast cells infected with HCMV or HEK293 cells transfected with either a plasmid expressing US25-1 (pUS25-1) or a US25-1 mimic (bUS25-1). (B) Venn diagram showing the overlap between the top 30 enriched genes from AD169 infected cells and combined enrichment data from cells transfected with US25-1. List of overlapping genes shown in (C).
doi:10.1371/journal.ppat.1003820.g003

Discussion

Despite recent advances in our understanding of miRNA transcript interaction, identification of valid targets remains challenging. The nature of miRNA targeting, where functional effects may rely on multiple miRNAs targeting a single transcript or multiple genes within single pathways being targeted, requires a system wide approach to elucidate the functions of miRNAs. Recent studies have used such approaches to identify targets of gamma-herpesvirus miRNAs [30,35–38]. However, no systematic screening approach has been presented for HCMV in the context of viral infection. Here we use a RISC-IP approach to identify putative targets of HCMV miRNAs in the context of viral infection, an important step towards generating a global understanding of the role these small regulatory RNAs play in the biology of HCMV and herpes viruses in general.

Using a laboratory strain of HCMV and clinical strain we identified a total of 906 transcripts that were enriched by at least two fold over immunoprecipitations from uninfected cells, 222 of which were enriched by both viruses. Relatively few cellular targets of HCMV miRNAs have been previously published [27,39,40]. Of those, BclAF1 and RANTES did not show significant enrichment in infected cells. In the case of RANTES and BclAF1 it is possible that the effects are cell type specific or the complex formed between the transcript and RISC is not stable and therefore does not result in enrichment. MICB was significantly enriched in both uninfected and infected cells correlating well with previous studies indicating that both cellular and viral miRNAs target this gene.

Many of the targets identified in this study have not previously been linked to HCMV, and in many cases, have not been linked to virus infections in general. Only a fraction of host genes have been investigated for potential roles in viral infections. Systematic analysis of viral miRNA targets can effectively exploit target identification for the discovery of novel host factors that play important roles in the biology of HCMV. Here we verify the effectiveness of this approach with the identification of at least two genes that have significant effects on HCMV replication. Knockdown of ATP6V0C resulted in attenuation of viral replication, while knockdown of SGSH resulted in an increase in viral replication.

The most highly enriched target identified in this study, ATP6V0C, is a component of the Vacuolar ATPase, which is responsible for acidification of endosomal compartments [41]. Knockdown of this gene resulted in striking inhibition of virus replication with almost no infectious virus detected during growth curve analysis. Acidification of endosomes has previously been shown to be required for HCMV entry into endothelial and epithelial cells through receptor mediated endocytosis. However, infection of fibroblast cells occurs through direct fusion with the plasma membrane and has been demonstrated to be pH independent [42]. The attenuation of HCMV replication through siRNA targeting of ATP6V0C is therefore unlikely to be due to a defect in viral entry. In support of this, although GFP levels were reduced in siRNA knockdown experiments, all cells were clearly GFP positive 24 hours post infection (Supplemental Figure S6). An alternative explanation could involve the marked reorganization of intracellular membranous organelles during the formation of HCMV assembly compartment [43]. A block in endosomal

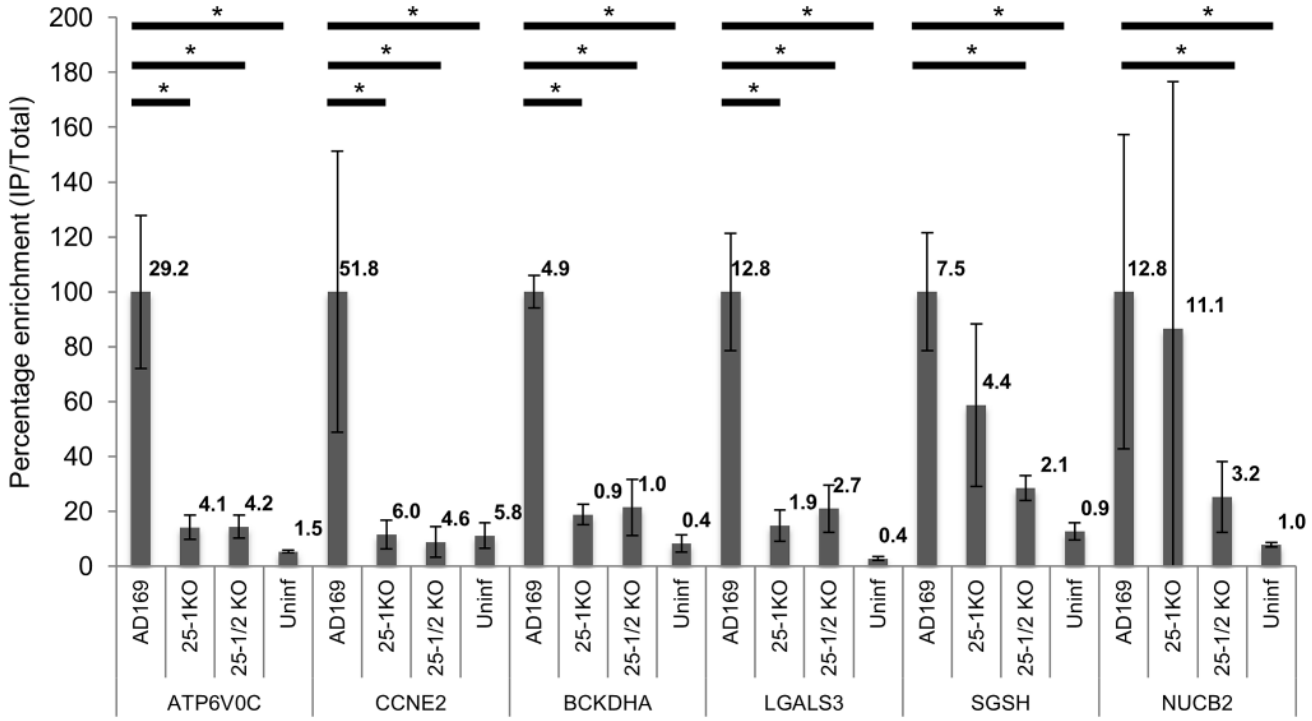

Figure 4. Deletion of US25-1 from HCMV results in loss of enrichment of identified targets. Enrichment of the six US25-1 targets was determined by RT-PCR following RISC-IP from cells infected with wild type virus or cells infected with US25 knock out viruses. Enrichment levels converted to percentage with enrichment from AD169 infected cells set at 100%. Raw enrichment values shown above each bar. Expression levels were corrected against GAPDH and each bar represents 3 biological repeats. * = statistically significant difference ($p = <0.01$). Statistics were performed on raw data using the Mann-Whitney non-parametric U-test.
doi:10.1371/journal.ppat.1003820.g004

acidification may interfere with this process resulting in attenuation of virus replication and virion assembly. Interestingly, a previous report indicated that US25-1 expression has a negative effect on acute replication of HCMV [44]. This effect was not specific, as adenovirus replication was also inhibited, suggesting targeting of a cellular factor was responsible for the phenotypic effects. Our findings suggest this cellular factor may be ATP6V0C and acidification of endosomal compartments may be a necessary process for efficient replication of DNA viruses in general.

SGSH is involved in heparin sulphate degradation in the lysosomal compartment. Initial attachment of HCMV virions to target cells has been shown to occur through binding of viral glycoprotein B with heparin sulphate moieties on the cell surface [41]. However, it is unlikely that disruption of this pathway would result in higher levels of heparin sulphate on the cell surface. Western blot analysis in this study shows that infection with HCMV results in significant reduction in SGSH levels, and although this reduction appears to occur independently of US25-1, the result suggests targeting of this gene plays an important role in the replication of the virus.

The question remains as to why the virus would target a cellular gene, such as ATP6V0C, required for efficient replication. We previously demonstrated that UL112-1 attenuates HCMV replication through direct targeting of the immediate early gene IE72 and suggested that this represents a mechanism of establishing or maintaining viral latency [22]. Targeting of ATP6V0C may represent a similar mechanism, possibly blocking assembly and release of virions during latent infection. Alternatively, targeting by US25-1 may be unrelated to viral replication, but rather serve a different function such as immune evasion. Acidification has been shown to be required for efficient signaling by endosomal resident toll like receptors and for efficient MHC class II presentation [45,46]. Blocking acidification of endosomes through targeting of ATP6V0C may be an effective way for the virus to interfere with both innate and adaptive immune response.

In conclusion, this study greatly increases the number of putative and validated targets of HCMV miRNAs. The use of systematic miRNA target analysis with focused siRNA screening is an effective strategy for the identification of novel host virus interactions. Finally the V-ATPase complex is an essential host factor in HCMV replication and is targeted by the HCMV miRNA US25-1.

Materials and Methods

Cells and viruses

Normal human dermal fibroblast (NHDF) cells (Clonetics) were cultured in Dulbecco's modified Eagle's medium supplemented with 10% fetal calf serum and penicillin-streptomycin-L-glutamine. HCMV strain AD169 was obtained from the American Type Culture Collection (Rockville, Md.). TR HCMV was obtained from Dr Jay Nelson. TB40E GFP was obtained from Dr Goodrum [47]. All HCMV strains were grown on primary fibroblast cells following infection at low MOI. Virus preps were purified over 10% sorbitol gradients.

RISC-IP analysis

RISC-IP analysis was carried as out previously described [28,48]. In brief for systematic analysis of HCMV miRNA targets,

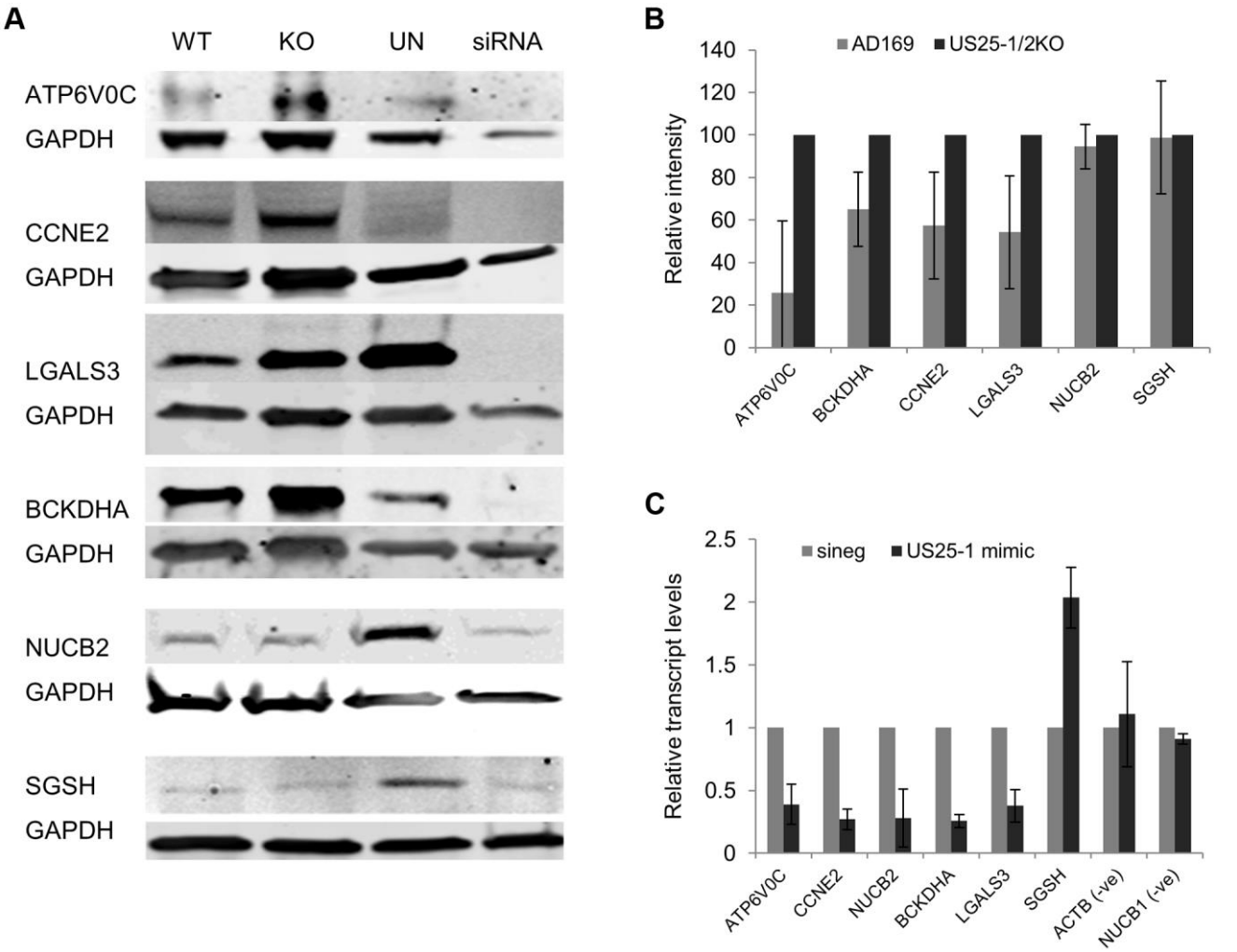

Figure 5. Deletion of US25-1 results in increased expression of identified targets in context of virus infection. (A) Fibroblast cells were infected at an MOI of 3 with either wild type virus or US25-1 knockout virus and harvested 72 hours post infection. Western blot analysis was performed using antibodies against identified US25-1 targets. Uninfected cells and cells transfected with siRNA against the gene being analysed are included for comparison. (B) Band intensities for three independent biological repeats were determined and corrected for GAPDH levels with relative intensities shown as a percentage with the uninfected value set to 100%. As data represents the ratio between wild type and infected protein levels the error of the ratio is incorporated into the error bars shown for the KO virus protein levels. (C) Fibroblast cells were transfected with either US25-1 mimic or a negative control mimic (40 nM). Cells were harvested 48 h post infection and RNA levels for each of the indicated transcripts determined by real time RT-PCR analysis. Relative levels of RNA for US25-1 mimic transfected cells compared to negative control transfected cells are shown with results normalized to GAPDH. Results represent 3 biological repeats.
doi:10.1371/journal.ppat.1003820.g005

primary human fibroblast cells were infected at a MOI of three with either AD169 or TR. Three days post infection cells were lysed, samples taken for total RNA and miRNP complexes immunoprecipitated using anti Ago2 antibody followed by streptavidin bead pull down. RNA was isolated using Trizol and analyzed for quality using an Agilent Bioanalyzer and transcript levels determined on the Illumina HumanRef-8 platform. Microarray data was analyzed using Gene sifter software. Enrichment of specific transcripts, through association with miRNP complexes was determined by dividing the immunoprecipitated levels of transcripts by the total levels. Analysis of specific genes by RT-PCR was conducted using the same protocol and parameters, except specific primer probe sets were used instead of microarray analysis. Primer probe sets were purchased from Lifetechnologies. For mimic RISC-IPs the same procedure was followed except 293T cells were transfected with 40 nM of mimic RNA and cells were harvested 48 hours post transfection.

Argonaute specific antibody was generated by immunization of rabbits with a peptide corresponding to the N terminal region of Argonaute 2 (5-MYSGAGPALAPPAPPPPIQGYAFKPPPRPD3′).

Sequence analysis

Transcript sequences were down loaded from NCBI using RefSeq ID's. Predicted binding between HCMV miRNAs and putative target transcripts were determined using the online algorithm RNAhybrid (http://bibiserv.techfak.uni-bielefeld.de/rnahybrid/) [49]. Parameters were selected to include Watson-Crick base pairing between either nucleotides 1 to 7 or 2 to 8. Full transcript data was searched for seed sequence matches using a Java based script program.

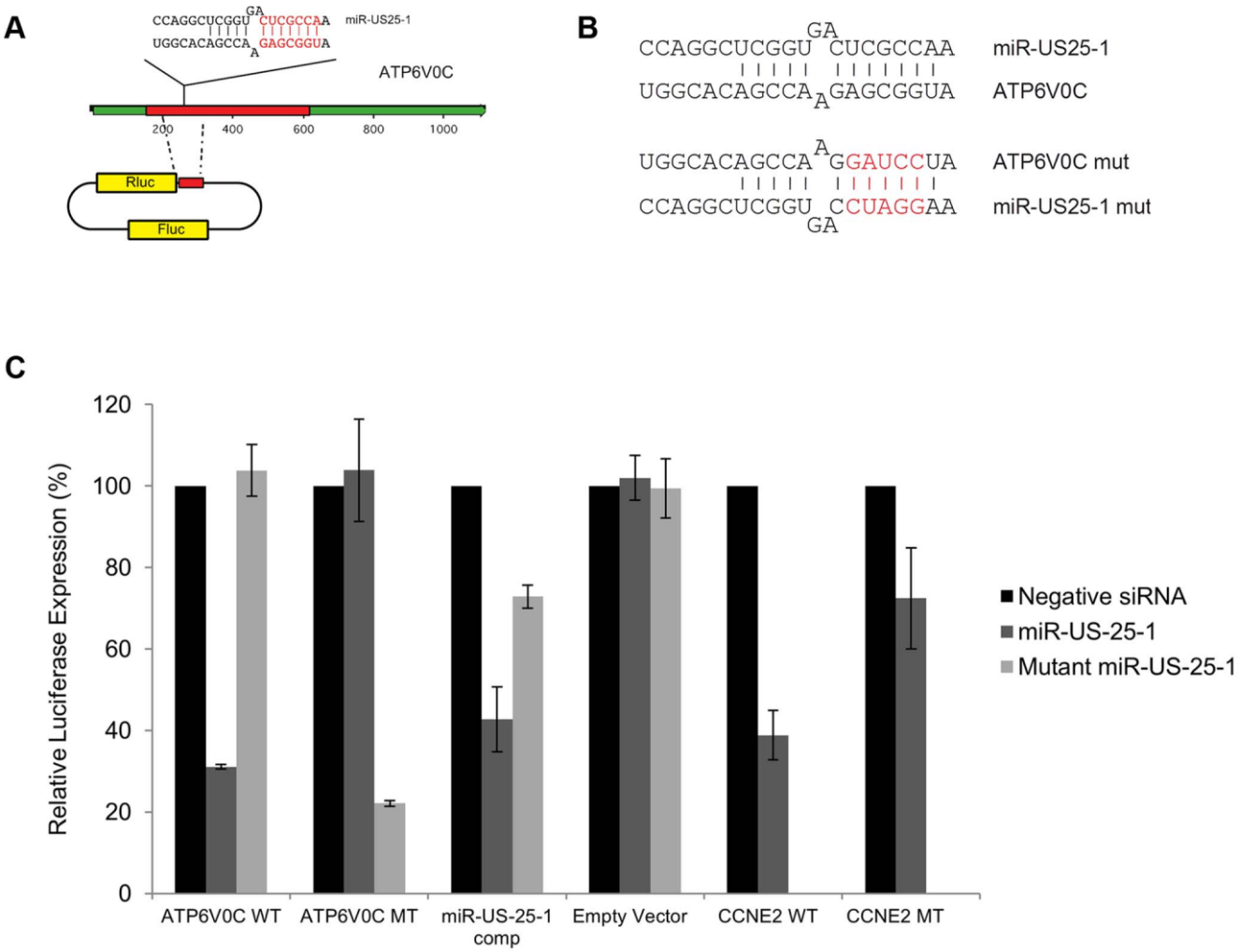

Figure 6. US25-1 targeting of ATP6V0C occurs through the predicted target site within the ORF. (A) The predicted US25-1 target site from ATP6V0C was cloned downstream of the luciferase reporter construct psiCheck2. The schematic shows the cloning strategy for ATP6V0C. (B) Schematic representation of sequence changes within the target site of ATP6V0C and the corresponding mutation in US25-1 mimic (sequence alterations in the US25-1 mimic are shown in red). (C) Constructs were co-transfected into HEK293 cells with US25-1 mimic, negative control siRNA or a US25-1 mimic with a mutated seed sequence at 40 nM. Data represents 3 biological replicates with standard deviation.
doi:10.1371/journal.ppat.1003820.g006

miR-US25-1 and miR-US25-1/2 KO viruses

miR-US25-1 pre-miRNA coding region was deleted from AD169 BAC clone using BAC technology as previously described [50]. Briefly a PCR amplified cassette containing FRT flanked Kanamycin was recombined into AD169 BAC genome replacing the miR-US25-1 coding region using primers listed in Supplemental table S4.

Sequence in italics indicates regions homologous to FRT flanked Kanamycin cassette with remaining sequence homologous to recombination site in HCMV genome. The Kanamycin cassette was then removed by recombining the FRT sites through inducible FLIP recombinase. The resulting BAC was isolated and electroporated into human primary fibroblast cells to produce infectious virus. Schematic representations of recombination strategies are shown in Supplemental Figure S7.

Small RNA transfections

Cells were transfected with small RNAs using RNAiMAX lipofectamine reagent (Life technologies) according to manufacturer's guidelines with the following modifications. Fibroblast cells were double transfected with 20 pmol (40 nM) of small RNA per 24 well 8 hours apart. Cells were either infected or harvested 24 hours post transfection for siRNAs or 48 hours post transfection for mimics. Control cells were transfected with a non-targeting negative control siRNA (Qiagen – cat 1027310). The sequence and siRNA IDs are listed in Supplemental Table S5.

RT-PCR analysis

Total RNA was harvested using Trizol with concentrations and RNA quality determined by nano-drop spectrophotometer analysis. 100 ng of total RNA was DNAse treated (Promega) then reverse transcribed using high capacity cDNA reverse transcription kit (ABI). Real time PCR was carried out using gene specific primer probe sets from ABI on a Rotor gene 3000 (Corbet Research). Relative expression levels were determined by delta delta Ct calculation with levels corrected to GAPDH levels.

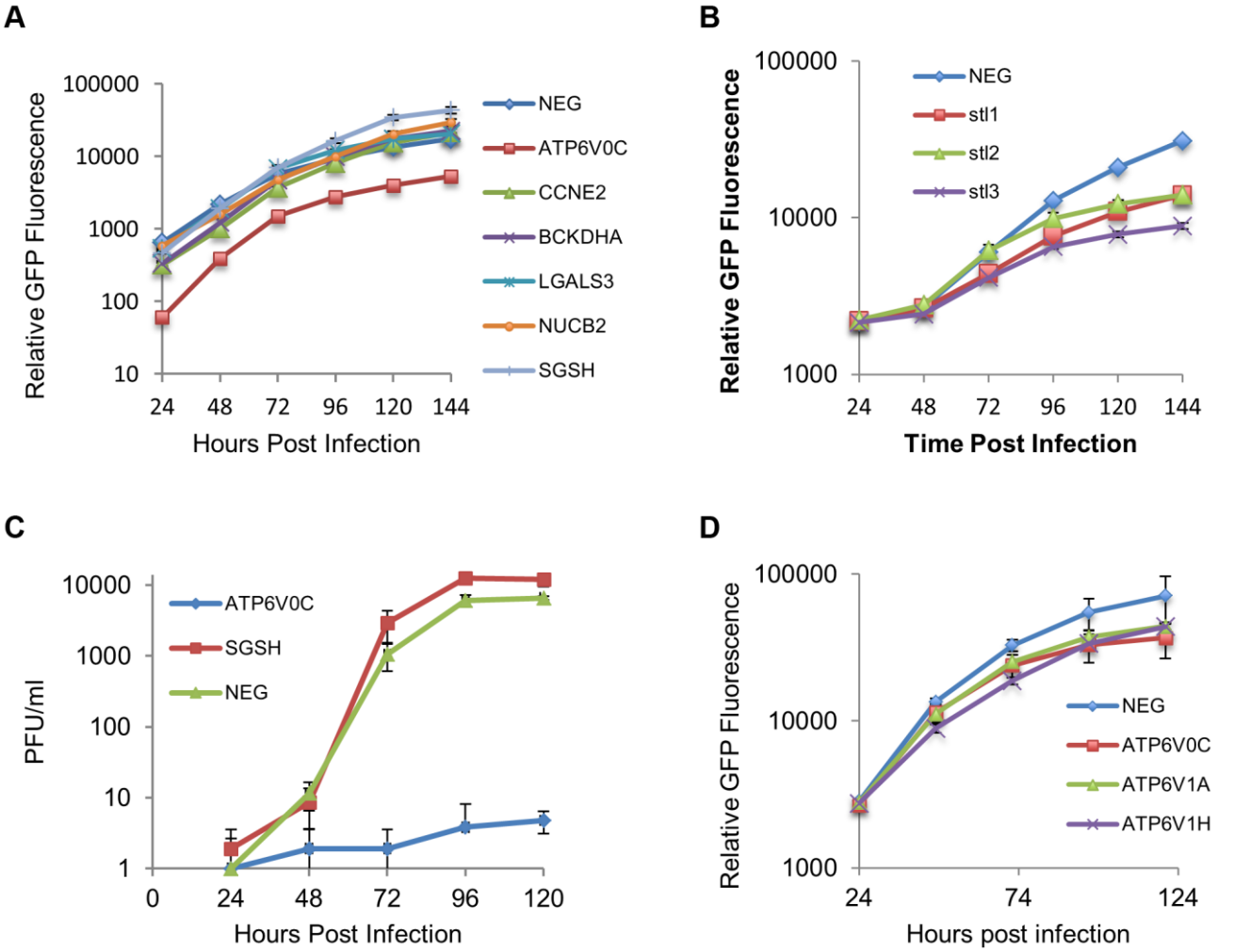

Figure 7. ATP6V0C is an essential host factor for HCMV replication. (A) Human Fibroblast cells were transfected with siRNAs (40 nM) against each of the six HCMV miRNA targets previously identified. Cells were then infected with a GFP tagged HCMV virus at an MOI of one, 16 hours post transfection. GFP levels were monitored during the course of infection and compared to determine the effect of knock down of the miRNA targets on HCMV replication. Data represents 4 biological repeats. (B) Fibroblast cells were transfected with three independent siRNAs targeting ATP6V0C (stl1, 2 and 3) as above. Each siRNA resulted in reduced virus growth as determined by GFP fluorescence. Data represents 4 biological repeats. (C) Cells were transfected with pooled siRNAs and infected as above with cells and supernatant harvested at the indicated time points and analysed for infectious virus by plaque assay. Data represents 3 biological repeats (D) Fibroblast cells were transfected with siRNAs as above targeting ATP6V1A or ATP6V1H, components of the V-ATPase complex and HCMV replication analysed by GFP fluorescence. Replication was inhibited by similar levels as observed for knockdown of ATP6V0C. Data represents 4 biological repeats.
doi:10.1371/journal.ppat.1003820.g007

Western blot analysis

Human primary fibroblast cells were grown in either 10% serum supplemented DMEM before infection at a multiplicity of 3 with either wild type AD169, miR-US25-1, or miR-US25-1/2 knock out virus. 72 hours post infection, cells were harvested using SDS sample loading buffer. 30 ul of protein sample were loaded and proteins were probed using primary antibodies to ATP6V0C (Aviva), BCKDHA (Cambridge Biosciences), CCNE2 (Abcam), LGALS3 (Cambridge Biosciences), NUCB2 (Sigma), and SGSH (Genetex) according to manufacturer's specifications. Protein loading was normalised to GAPDH (Sigma). IR800 or IR680 dye conjugated anti-rabbit IgG and anti-mouse IgG secondary antibodies were purchased from LiCor. Blots were imaged using infrared fluorescence of appropriately tagged secondary antibodies and quantified using a LiCOR Odyssey scanner and software.

Luciferase assay

ATP6V0C luciferase constructs were created using custom oligonucleotides corresponding to the genomic region between nucleotides 146 and 226 downstream of the transcriptional start site, flanking the bioinformatically predicted miR US25-1 target site (GAGCGGT starting at nucleotide 186). For the ATP6V0C mutant construct, the miR US25-1 target site was replaced with a BAMHI restriction site. These inserts were cloned downstream of the renilla luciferase reporter gene of the pSicheck 2 dual luciferase construct (Promega). Cloning oligonucleotides are shown in Supplemental table S4 Luciferase constructs were co-transfected with miR US25-1 mimic or control mimic (IDT) into HEK293 cells using Lipofectamine 2000 reagent according to the manufacturer's instructions. Cells were harvested 48 hours post transfection and luciferase levels measured using Promega's dual

luciferase reporter kit. CCNE2 luciferase constructs were created and assays were performed as described previously [29].

Virus growth curves

For virus growth curve analysis by GFP fluorescence 96 well plates seeded with primary human fibroblast cells were transfected with siRNAs at a final concentration of 2 nM using RNAiMAX transfection reagent (Life Technologies). Specific siRNAs for ATP6V0C (S80), ATP6V1A, ATP6V1H BCKDHA, CCNE2, LGALS3, NUCB2, and SGSH were obtained from Life Technologies. 24 hours post transfection, cells were infected at a MOI of 1. The MOI was empirically determined to provide robust signal without inducing extensive cell death through CPE. Twenty-four hours post infection cells were washed three times and overlayed with fresh complete DMEM media without phenol red pH indicator (Lonza) and GFP levels monitored using Biotech Synergy HT plate reader. For plaque assays 24 well plates seeded with HCMV were transfected with pooled siRNAs for ATP6V0C (Life Technologies) and SGSH (Thermo Scientific). 24 hours post transfection, cells were infected at an MOI of 1. 24 hours post infection cells were washed three times and at indicated time points the cell monolayer was scraped into the media and the media and cells collected and frozen. Standard plaque assays were carried out on human primary fibroblast cells overlayed with carboxy methyl cellulose.

Supporting Information

Figure S1 Example calculation of corrected enrichment of miRNA target transcripts. PSG6 gives a false positive because, although IP levels remain the same for both Uninfected and infected, total levels are reduced drastically in infected sample resulting in false enrichment. As total levels are also reduced in the Pre-Serum sample this counters the false enrichment through the correction calculation.
(TIF)

Figure S2 Validation of RISC-IP enrichment by RT-PCR. Enrichment of selected top 30 targets was determined by RT-PCR following RISC-IP from cells infected with wild type virus or cells infected with US25 knock out viruses. Enrichment levels converted to percentage with enrichment from AD169 infected cells set at 100%. Raw enrichment values shown above each bar. Expression levels were corrected against GAPDH and each bar represents 3 biological repeats. * = statistically significant difference ($p = <0.01$). Statistics were performed on raw data using the Mann-Whitney non-parametric U-test.
(TIF)

Figure S3 US25-2-3p and US25-2-5p do not target ATP6V0C. (A) Enrichment of selected top 30 targets was determined by RT-PCR following RISC-IP from cells transfected with indicted miRNA mimics (40 nM), including US25-1 mutant seed mimic. Enrichment levels converted to percentage with enrichment from AD169 infected cells set at 100%. Raw enrichment values shown above each bar. Expression levels were corrected against GAPDH and each bar represents 3 biological repeats. * = statistically significant difference ($p = <0.01$). Statistics were performed on raw data using the Mann-Whitney non-parametric U-test. (B) RNA levels were determined for ATP6V0C by RT-PCR, following transfection of fibroblast cells with US25-1, US25-2-3p or US25-2-5p. RNA levels were normalized to GAPDH and compared to cells transfected with a US25-1 seed mutant mimic.
(TIF)

Figure S4 Confirmation of siRNA activity. (A) Percentage knock down of each of the target transcripts is shown following transfection of human fibroblast cells with 40 nM of siRNA. Cells were harvested 24 hours post transfection and RT-PCR analysis performed as previously described. Percent knockdown versus cells transfected with negative control siRNA is shown. All assays were normalized against GAPDH levels and assays performed in triplicate. Stl1, 2 and 3 represent the independent siRNAs from the STL pool, targeting ATP6V0C (B) Human fibroblast cells were transfected with 40 nM siRNA or mimic and cells harvest 48 hours post transfection. Total RNA was harvested and IFN beta levels determined by RT-PCR. Positive control was RNA from cells transfected with non-infectious viral RNA. ND indicates not detected. (C) Cytotoxic effects on cells transfected with ATP6V0C siRNAs was measured using CytoTox-Glo according to manufacturer's instructions. Fibroblast cells were transfected at 40 nM and harvested 48 hours post transfection. Results are shown as relative percentage of luciferase.
(TIF)

Figure S5 Schematic representation of US25-1 targets. Untranslated regions of transcripts are shown in red, with translated region of transcript shown in green. Seed region of miRNA target interaction highlighted in red.
(TIF)

Figure S6 Reduction of HCMV replication from ATP6V0C knock down is not due to block in viral entry. GFP fluorescence is shown 24 hours post infection of primary fibroblast cells with GFP tagged HCMV. Cells were transfected with either negative control siRNA (A) or ATP6V0C siRNA (B) and infected 16 hours post transfection.
(TIF)

Figure S7 Schematic diagram of knock virus construction. Deletion of US25-1 or US25-1 and 2 sequence regions are shown as well as the recombination event removing the KAN cassette resulting in the final BAC constructs. Red boxes indicate the homologous regions of sequence where recombination occurs. Flanking transcripts US24 and US26 are shown in green.
(TIF)

Table S1 Full data set for RISC-IP analysis of AD169 infected cells. Signal levels for total RNA and IP RNA levels are shown from uninfected and infected pull down experiments. Final enrichment level represents analysed data after correction for false enrichment as explained in supplemental figure S1.
(ZIP)

Table S2 Full data set for RISC-IP analysis of TR infected cells. Data analyzed as for supplemental table S1.
(ZIP)

Table S3 Full analysis of transcripts for HCMV miRNA seed targets. Transcript sequences were down loaded from NCBI using RefSeq ID's. Transcript data sets were searched for seed sequence matches using a Java based script program. Seed matches for either 1 to 7 or 2 to 8 nucleotides are given. Results are shown for either the ORF, 5′ or 3′ UTR regions of the transcripts. The position of the target site is given as nucleotide coordinates.
(XLSX)

Table S4 Summary of cloning oligonucleotides. The US25-1 target seed region for ATP6V0C is highlighted in yellow and the sequence changes to create the mutant seed region are indicated in red.
(DOCX)

Table S5 Small RNA sequences. Sequences of siRNA and mimics are shown along with assay ID numbers. For SGSH, a Dharmacon smart pool was used and target sequence is shown under sense strand column. The seed mutation in US25-1 is indicated in red.
(DOCX)

Acknowledgments

We would like to thank Paul Digard, Mike Clinton and Amy Buck for comments and critical review of the manuscript. We thank Jeroen Witteveldt for assistance with interferon assays.

Author Contributions

Conceived and designed the experiments: JP NR FG. Performed the experiments: JP NR SC FG. Analyzed the data: JP NR FG GW. Contributed reagents/materials/analysis tools: RT. Wrote the paper: JP FG.

References

1. Nelson JA, Gnann JW, Jr., Ghazal P (1990) Regulation and tissue-specific expression of human cytomegalovirus. Curr Top Microbiol Immunol 154: 75–100.
2. Boehler A, Schaffner A, Salomon F, Keusch G (1994) Cytomegalovirus disease of late onset following renal transplantation: a potentially fatal entity. Scand J Infect Dis 26: 369–373.
3. Ballard RA, Drew WL, Hufnagle KG, Riedel PA (1979) Acquired cytomegalovirus infection in preterm infants. Am J Dis Child 133: 482–485.
4. Adler SP (1983) Transfusion-associated cytomegalovirus infections. Rev Infect Dis 5: 977–993.
5. Einhorn L, Ost A (1984) Cytomegalovirus infection of human blood cells. J Infect Dis 149: 207–214.
6. Macher AM, Reichert CM, Straus SE, Longo DL, Parrillo J, et al. (1983) Death in the AIDS patient: role of cytomegalovirus. N Engl J Med 309: 1454.
7. Neiman P, Wasserman PB, Wentworth BB, Kao GF, Lerner KG, et al. (1973) Interstitial pneumonia and cytomegalovirus infection as complications of human marrow transplantation. Transplantation 15: 478–485.
8. Tegtmeier GE (1988) The use of cytomegalovirus-screened blood in neonates. Transfusion 28: 201–203.
9. Larsson S, Soderberg-Naucler C, Wang FZ, Moller E (1998) Cytomegalovirus DNA can be detected in peripheral blood mononuclear cells from all seropositive and most seronegative healthy blood donors over time. Transfusion 38: 271–278.
10. Soderberg-Naucler C, Fish KN, Nelson JA (1997) Reactivation of latent human cytomegalovirus by allogeneic stimulation of blood cells from healthy donors. Cell 91: 119–126.
11. Stanier P, Kitchen AD, Taylor DL, Tyms AS (1992) Detection of human cytomegalovirus in peripheral mononuclear cells and urine samples using PCR. Mol Cell Probes 6: 51–58.
12. Taylor-Wiedeman J, Sissons JG, Borysiewicz LK, Sinclair JH (1991) Monocytes are a major site of persistence of human cytomegalovirus in peripheral blood mononuclear cells. J Gen Virol 72 (Pt 9): 2059–2064.
13. Myerson D, Hackman RC, Nelson JA, Ward DC, McDougall JK (1984) Widespread presence of histologically occult cytomegalovirus. Hum Pathol 15: 430–439.
14. Goodrum F, Caviness K, Zagallo P (2012) Human cytomegalovirus persistence. Cell Microbiol 14: 644–655.
15. Grundhoff A, Sullivan CS (2011) Virus-encoded microRNAs. Virology 411: 325–343.
16. Dunn W, Trang P, Zhong Q, Yang E, van Belle C, et al. (2005) Human cytomegalovirus expresses novel microRNAs during productive viral infection. Cell Microbiol 7: 1684–1695.
17. Grey F, Antoniewicz A, Allen E, Saugstad J, McShea A, et al. (2005) Identification and characterization of human cytomegalovirus-encoded microRNAs. J Virol 79: 12095–12099.
18. Meshesha MK, Veksler-Lublinsky I, Isakov O, Reichenstein I, Shomron N, et al. (2012) The microRNA Transcriptome of Human Cytomegalovirus (HCMV). Open Virol J 6: 38–48.
19. Pfeffer S, Sewer A, Lagos-Quintana M, Sheridan R, Sander C, et al. (2005) Identification of microRNAs of the herpesvirus family. Nat Methods 2: 269–276.
20. Stark TJ, Arnold JD, Spector DH, Yeo GW (2012) High-resolution profiling and analysis of viral and host small RNAs during human cytomegalovirus infection. J Virol 86: 226–235.
21. Tuddenham L, Pfeffer S (2011) Roles and regulation of microRNAs in cytomegalovirus infection. Biochim Biophys Acta 1809: 613–622.
22. Grey F, Meyers H, White EA, Spector DH, Nelson J (2007) A Human Cytomegalovirus-Encoded microRNA Regulates Expression of Multiple Viral Genes Involved in Replication. PLoS Pathog 3: e163.
23. Bellare P, Ganem D (2009) Regulation of KSHV lytic switch protein expression by a virus-encoded microRNA: an evolutionary adaptation that fine-tunes lytic reactivation. Cell Host Microbe 6: 570–575.
24. Lei X, Bai Z, Ye F, Xie J, Kim CG, et al. (2010) Regulation of NF-kappaB inhibitor IkappaBalpha and viral replication by a KSHV microRNA. Nat Cell Biol 12: 193–199.
25. Lu F, Stedman W, Yousef M, Renne R, Lieberman PM (2010) Epigenetic regulation of Kaposi's sarcoma-associated herpesvirus latency by virus-encoded microRNAs that target Rta and the cellular Rbl2-DNMT pathway. J Virol 84: 2697–2706.
26. Murphy E, Vanicek J, Robins H, Shenk T, Levine AJ (2008) Suppression of immediate-early viral gene expression by herpesvirus-coded microRNAs: implications for latency. Proc Natl Acad Sci U S A 105: 5453–5458.
27. Stern-Ginossar N, Elefant N, Zimmermann A, Wolf DG, Saleh N, et al. (2007) Host immune system gene targeting by a viral miRNA. Science 317: 376–381.
28. Karginov FV, Conaco C, Xuan Z, Schmidt BH, Parker JS, et al. (2007) A biochemical approach to identifying microRNA targets. Proc Natl Acad Sci U S A 104: 19291–19296.
29. Grey F, Tirabassi R, Meyers H, Wu G, McWeeney S, et al. (2010) A viral microRNA down-regulates multiple cell cycle genes through mRNA 5′UTRs. PLoS Pathog 6: e1000967.
30. Dolken L, Malterer G, Erhard F, Kothe S, Friedel CC, et al. (2010) Systematic analysis of viral and cellular microRNA targets in cells latently infected with human gamma-herpesviruses by RISC immunoprecipitation assay. Cell Host Microbe 7: 324–334.
31. Farh KK, Grimson A, Jan C, Lewis BP, Johnston WK, et al. (2005) The widespread impact of mammalian MicroRNAs on mRNA repression and evolution. Science 310: 1817–1821.
32. Lewis BP, Burge CB, Bartel DP (2005) Conserved seed pairing, often flanked by adenosines, indicates that thousands of human genes are microRNA targets. Cell 120: 15–20.
33. Lim LP, Lau NC, Garrett-Engele P, Grimson A, Schelter JM, et al. (2005) Microarray analysis shows that some microRNAs downregulate large numbers of target mRNAs. Nature 433: 769–773.
34. Lim JH, Park JW, Kim SJ, Kim MS, Park SK, et al. (2007) ATP6V0C competes with von Hippel-Lindau protein in hypoxia-inducible factor 1alpha (HIF-1alpha) binding and mediates HIF-1alpha expression by bafilomycin A1. Mol Pharmacol 71: 942–948.
35. Gottwein E, Corcoran DL, Mukherjee N, Skalsky RL, Hafner M, et al. (2011) Viral microRNA targetome of KSHV-infected primary effusion lymphoma cell lines. Cell Host Microbe 10: 515–526.
36. Haecker I, Gay LA, Yang Y, Hu J, Morse AM, et al. (2012) Ago HITS-CLIP expands understanding of Kaposi's sarcoma-associated herpesvirus miRNA function in primary effusion lymphomas. PLoS Pathog 8: e1002884.
37. Riley KJ, Rabinowitz GS, Yario TA, Luna JM, Darnell RB, et al. (2012) EBV and human microRNAs co-target oncogenic and apoptotic viral and human genes during latency. EMBO J 31: 2207–2221.
38. Skalsky RL, Corcoran DL, Gottwein E, Frank CL, Kang D, et al. (2012) The viral and cellular microRNA targetome in lymphoblastoid cell lines. PLoS Pathog 8: e1002484.
39. Kim Y, Lee S, Kim S, Kim D, Ahn JH, et al. (2012) Human cytomegalovirus clinical strain-specific microRNA miR-UL148D targets the human chemokine RANTES during infection. PLoS Pathog 8: e1002577.
40. Lee SH, Kalejta RF, Kerry J, Semmes OJ, O'Connor CM, et al. (2012) BclAF1 restriction factor is neutralized by proteasomal degradation and microRNA repression during human cytomegalovirus infection. Proc Natl Acad Sci U S A 109: 9575–9580.
41. Forgac M (2007) Vacuolar ATPases: rotary proton pumps in physiology and pathophysiology. Nat Rev Mol Cell Biol 8: 917–929.
42. Ryckman BJ, Jarvis MA, Drummond DD, Nelson JA, Johnson DC (2006) Human cytomegalovirus entry into epithelial and endothelial cells depends on genes UL128 to UL150 and occurs by endocytosis and low-pH fusion. J Virol 80: 710–722.
43. Sanchez V, Greis KD, Sztul E, Britt WJ (2000) Accumulation of virion tegument and envelope proteins in a stable cytoplasmic compartment during human cytomegalovirus replication: characterization of a potential site of virus assembly. J Virol 74: 975–986.
44. Stern-Ginossar N, Saleh N, Goldberg MD, Prichard M, Wolf DG, et al. (2009) Analysis of human cytomegalovirus-encoded microRNA activity during infection. J Virol 83: 10684–10693.
45. Benaroch P, Yilla M, Raposo G, Ito K, Miwa K, et al. (1995) How MHC class II molecules reach the endocytic pathway. EMBO J 14: 37–49.
46. Macfarlane DE, Manzel L (1998) Antagonism of immunostimulatory CpG-oligodeoxynucleotides by quinacrine, chloroquine, and structurally related compounds. J Immunol 160: 1122–1131.
47. Umashankar M, Petrucelli A, Cicchini L, Caposio P, Kreklywich CN, et al. (2011) A novel human cytomegalovirus locus modulates cell type-specific outcomes of infection. PLoS Pathog 7: e1002444.

48. Easow G, Teleman AA, Cohen SM (2007) Isolation of microRNA targets by miRNP immunopurification. Rna 13: 1198–1204.
49. Rehmsmeier M, Steffen P, Hochsmann M, Giegerich R (2004) Fast and effective prediction of microRNA/target duplexes. Rna 10: 1507–1517.
50. Rue CA, Jarvis MA, Knoche AJ, Meyers HL, DeFilippis VR, et al. (2004) A cyclooxygenase-2 homologue encoded by rhesus cytomegalovirus is a determinant for endothelial cell tropism. J Virol 78: 12529–12536.

8. Bibliography

1. Alba, M.M., et al., *Genomewide function conservation and phylogeny in the Herpesviridae.* Genome Res, 2001. **11**(1): p. 43-54.

2. Viruses, I.C.o.T.o. *Virus Taxonomy: 2014 Release*. 2014; Available from: http://www.ictvonline.org/virusTaxonomy.asp.

3. Davison, A.J., *Herpesvirus systematics.* Vet Microbiol, 2010. **143**(1): p. 52-69.

4. Luitweiler, E.M., et al., *Interactions of the Kaposi's Sarcoma-associated herpesvirus nuclear egress complex: ORF69 is a potent factor for remodeling cellular membranes.* J Virol, 2013. **87**(7): p. 3915-29.

5. Sharma, M., et al., *Human cytomegalovirus UL50 and UL53 recruit viral protein kinase UL97, not protein kinase C, for disruption of nuclear lamina and nuclear egress in infected cells.* J Virol, 2014. **88**(1): p. 249-62.

6. Sharma, M., et al., *Human cytomegalovirus UL97 phosphorylates the viral nuclear egress complex.* J Virol, 2015. **89**(1): p. 523-34.

7. Milbradt, J., et al., *Proteomic analysis of the multimeric nuclear egress complex of human cytomegalovirus.* Mol Cell Proteomics, 2014. **13**(8): p. 2132-46.

8. Mettenleiter, T.C., B.G. Klupp, and H. Granzow, *Herpesvirus assembly: An update.* Virus Research, 2009. **143**(2): p. 222-234.

9. Guo, H., et al., *Role of tegument proteins in herpesvirus assembly and egress.* Protein Cell, 2010. **1**(11): p. 987-98.

10. Brock, I., et al., *Nuclear targeting of human cytomegalovirus large tegument protein pUL48 is essential for viral growth.* J Virol, 2013. **87**(10): p. 6005-19.

11. Kalejta, R.F., *Functions of human cytomegalovirus tegument proteins prior to immediate early gene expression.* Curr Top Microbiol Immunol, 2008. **325**: p. 101-15.

12. Kalejta, R.F., *Tegument proteins of human cytomegalovirus.* Microbiol Mol Biol Rev, 2008. **72**(2): p. 249-65, table of contents.

13. Tomtishen, J.P., 3rd, *Human cytomegalovirus tegument proteins (pp65, pp71, pp150, pp28).* Virol J, 2012. **9**: p. 22.

14. Vanarsdall, A.L., M.C. Chase, and D.C. Johnson, *Human cytomegalovirus glycoprotein gO complexes with gH/gL, promoting interference with viral entry into human fibroblasts but not entry into epithelial cells.* J Virol, 2011. **85**(22): p. 11638-45.

15. Wille, P.T., et al., *Human cytomegalovirus (HCMV) glycoprotein gB promotes virus entry in trans acting as the viral fusion protein rather than as a receptor-binding protein.* MBio, 2013. **4**(3): p. e00332-13.

16. Roche, S., et al., *Structure of the prefusion form of the vesicular stomatitis virus glycoprotein G.* Science, 2007. **315**(5813): p. 843-8.

17. Gillet, L., S. Colaco, and P.G. Stevenson, *Glycoprotein B switches conformation during murid herpesvirus 4 entry.* J Gen Virol, 2008. **89**(Pt 6): p. 1352-63.

18. Mocarski, E. and C. Courcelle, *Cytomegalovirus and their replication*, in *Fields Virology*. 2007, Wolters Kluwer Health/Lippincott Williams & Wilkins: Philadelphia.

19. Britt, W., *Manifestations of human cytomegalovirus infection: proposed mechanisms of acute and chronic disease.* Curr Top Microbiol Immunol, 2008. **325**: p. 417-70.

20. Weller, T.H., *The cytomegaloviruses: ubiquitous agents with protean clinical manifestations. II.* N Engl J Med, 1971. **285**(5): p. 267-74.

21. Weller, T.H., *The cytomegaloviruses: ubiquitous agents with protean clinical manifestations. I.* N Engl J Med, 1971. **285**(4): p. 203-14.

22. Dogan, K., et al., *Seroprevalence and Seroconversion Rates of Cytomegalovirus pp65 Antigen and Cord Blood Screening of Pregnant Women in Malatya, Turkey.* Eurasian J Med, 2013. **45**(2): p. 88-91.

23. Patrick, E.J., et al., *A cohort study in university students: investigation of risk factors for cytomegalovirus infection.* Epidemiol Infect, 2014. **142**(9): p. 1990-5.

24. Michaelis, M., H.W. Doerr, and J. Cinatl, *The story of human cytomegalovirus and cancer: increasing evidence and open questions.* Neoplasia, 2009. **11**(1): p. 1-9.

25. Vescovini, R., et al., *Massive load of functional effector CD4+ and CD8+ T cells against cytomegalovirus in very old subjects.* J Immunol, 2007. **179**(6): p. 4283-91.

26. Louise McCormick, A. and E.S. Mocarski, *The immunological underpinnings of vaccinations to prevent cytomegalovirus disease.* Cell Mol Immunol, 2015. **12**(2): p. 170-179.

27. Bissinger, A.L., et al., *Human cytomegalovirus as a direct pathogen: correlation of multiorgan involvement and cell distribution with clinical and pathological findings in a case of congenital inclusion disease.* J Med Virol, 2002. **67**(2): p. 200-6.

28. Sinzger, C., et al., *Fibroblasts, epithelial cells, endothelial cells and smooth muscle cells are major targets of human cytomegalovirus infection in lung and gastrointestinal tissues.* J Gen Virol, 1995. **76 (Pt 4)**: p. 741-50.

29. Emery, V.C., et al., *The dynamics of human cytomegalovirus replication in vivo.* J Exp Med, 1999. **190**(2): p. 177-82.

30. Jacobson, M.A. and J. Mills, *Serious cytomegalovirus disease in the acquired immunodeficiency syndrome (AIDS). Clinical findings, diagnosis, and treatment.* Ann Intern Med, 1988. **108**(4): p. 585-94.

31. Slobedman, B. and E.S. Mocarski, *Mechanisms modulating immune clearance during human cytomegalovirus latency.* Proc Natl Acad Sci U S A, 2012. **109**(36): p. 14291-2.

32. Wiley, C.A. and J.A. Nelson, *Role of human immunodeficiency virus and cytomegalovirus in AIDS encephalitis.* Am J Pathol, 1988. **133**(1): p. 73-81.

33. Mehra, M.R., *Contemporary concepts in prevention and treatment of cardiac allograft vasculopathy.* Am J Transplant, 2006. **6**(6): p. 1248-56.

34. Hubscher, S.G., et al., *Vanishing bile-duct syndrome following liver transplantation--is it reversible?* Transplantation, 1991. **51**(5): p. 1004-10.

35. Vazquez-Martul, E., et al., *Histological features with clinical impact in chronic allograft nephropathy: review of 66 cases.* Transplant Proc, 2004. **36**(3): p. 770-1.

36. Cannon, M.J. and K.F. Davis, *Washing our hands of the congenital cytomegalovirus disease epidemic.* Bmc Public Health, 2005. **5**.

37. Deere, J.D. and P.A. Barry, *Using the Nonhuman Primate Model of HCMV to Guide Vaccine Development.* Viruses-Basel, 2014. **6**(4): p. 1483-1501.

38. Britt, W., et al., *Formulation of an immunogenic human cytomegalovirus vaccine: responses in mice.* J Infect Dis, 1995. **171**(1): p. 18-25.

39. Britt, W., *Controversies in the natural history of congenital human cytomegalovirus infection: the paradox of infection and disease in offspring of women with immunity prior to pregnancy.* Med Microbiol Immunol, 2015.

40. Schreiber, A., et al., *Antiviral treatment of cytomegalovirus infection and resistant strains.* Expert Opin Pharmacother, 2009. **10**(2): p. 191-209.

41. Ahmed, A., *Antiviral treatment of cytomegalovirus infection.* Infect Disord Drug Targets, 2011. **11**(5): p. 475-503.

42. Borst, E.M., et al., *Cloning of the human cytomegalovirus (HCMV) genome as an infectious bacterial artificial chromosome in Escherichia coli: a new approach for construction of HCMV mutants.* J Virol, 1999. **73**(10): p. 8320-9.

43. Pignatelli, S., et al., *Genetic polymorphisms among human cytomegalovirus (HCMV) wild-type strains.* Reviews in Medical Virology, 2004. **14**(6): p. 383-410.

44. Ryckman, B.J., et al., *Human cytomegalovirus entry into epithelial and endothelial cells depends on genes UL128 to UL150 and occurs by endocytosis and low-pH fusion.* Journal of Virology, 2006. **80**(2): p. 710-722.

45. Ryckman, B.J., M.C. Chase, and D.C. Johnson, *HCMV gH/gL/UL128-131 interferes with virus entry into epithelial cells: evidence for cell type-specific receptors.* Proc Natl Acad Sci U S A, 2008. **105**(37): p. 14118-23.

46. Dolan, A., et al., *Genetic content of wild-type human cytomegalovirus.* J Gen Virol, 2004. **85**(Pt 5): p. 1301-12.

47. Sinzger, C., et al., *Cloning and sequencing of a highly productive, endotheliotropic virus strain derived from human cytomegalovirus TB40/E.* J Gen Virol, 2008. **89**(Pt 2): p. 359-68.

48. Compton, T., R.R. Nepomuceno, and D.M. Nowlin, *Human Cytomegalovirus Penetrates Host-Cells by Ph-Independent Fusion at the Cell-Surface.* Virology, 1992. **191**(1): p. 387-395.

49. Compton, T., D.M. Nowlin, and N.R. Cooper, *Initiation of human cytomegalovirus infection requires initial interaction with cell surface heparan sulfate.* Virology, 1993. **193**(2): p. 834-41.

50. Kari, B. and R. Gehrz, *Structure, composition and heparin binding properties of a human cytomegalovirus glycoprotein complex designated gC-II.* J Gen Virol, 1993. **74 (Pt 2)**: p. 255-64.

51. Dunn, W., et al., *Functional profiling of a human cytomegalovirus genome.* Proc Natl Acad Sci U S A, 2003. **100**(24): p. 14223-8.

52. Roberts, A.P., et al., *Differing roles of inner tegument proteins pUL36 and pUL37 during entry of herpes simplex virus type 1.* J Virol, 2009. **83**(1): p. 105-16.

53. Ogawa-Goto, K., et al., *Microtubule network facilitates nuclear targeting of human cytomegalovirus capsid.* J Virol, 2003. **77**(15): p. 8541-7.

54. Yu, D., M.C. Silva, and T. Shenk, *Functional map of human cytomegalovirus AD169 defined by global mutational analysis.* Proc Natl Acad Sci U S A, 2003. **100**(21): p. 12396-401.

55. Rode, K., et al., *Uncoupling uncoating of herpes simplex virus genomes from their nuclear import and gene expression.* J Virol, 2011. **85**(9): p. 4271-83.

56. Pasdeloup, D., et al., *Herpesvirus capsid association with the nuclear pore complex and viral DNA release involve the nucleoporin CAN/Nup214 and the capsid protein pUL25.* J Virol, 2009. **83**(13): p. 6610-23.

57. Murphy, E., et al., *Reevaluation of human cytomegalovirus coding potential.* Proceedings of the National Academy of Sciences of the United States of America, 2003. **100**(23): p. 13585-13590.

58. Gatherer, D., et al., *High-resolution human cytomegalovirus transcriptome.* Proc Natl Acad Sci U S A, 2011. **108**(49): p. 19755-60.

59. Weekes, M.P., et al., *Quantitative Temporal Viromics: An Approach to Investigate Host-Pathogen Interaction.* Cell, 2014. **157**(6): p. 1460-1472.

60. Fortunato, E.A. and D.H. Spector, *Regulation of human cytomegalovirus gene expression.* Adv Virus Res, 1999. **54**: p. 61-128.

61. Stenberg, R.M., P.R. Witte, and M.F. Stinski, *Multiple spliced and unspliced transcripts from human cytomegalovirus immediate-early region 2 and evidence for a common initiation site within immediate-early region 1.* J Virol, 1985. **56**(3): p. 665-75.

62. Stenberg, R.M., et al., *Regulated expression of early and late RNAs and proteins from the human cytomegalovirus immediate-early gene region.* J Virol, 1989. **63**(6): p. 2699-708.

63. Stenberg, R.M., *The human cytomegalovirus major immediate-early gene.* Intervirology, 1996. **39**(5-6): p. 343-349.

64. Stenberg, R.M., *Separation of Functional Domains within the Human Cytomegalovirus Major Immediate Early 72kd Protein.* Journal of Cellular Biochemistry, 1987: p. 150-150.

65. Mocarski, E.S., *Immune escape and exploitation strategies of cytomegaloviruses: impact on and imitation of the major histocompatibility system.* Cellular Microbiology, 2004. **6**(8): p. 707-717.

66. Mocarski, E.S., *Immunomodulation by cytomegaloviruses: manipulative strategies beyond evasion.* Trends in Microbiology, 2002. **10**(7): p. 332-339.

67. Britt, B., *Maturation and egress*, in *Human Herpesviruses: Biology, Therapy, and Immunoprophylaxis*, A. Arvin, et al., Editors. 2007: Cambridge.

68. Borst, E.M., et al., *The human cytomegalovirus UL51 protein is essential for viral genome cleavage-packaging and interacts with the terminase subunits pUL56 and pUL89.* J Virol, 2013. **87**(3): p. 1720-32.

69. Wang, J.B., et al., *Changes in subcellular localization reveal interactions between human cytomegalovirus terminase subunits.* Virol J, 2012. **9**: p. 315.

70. Tandon, R. and E.S. Mocarski, *Cytomegalovirus pUL96 is critical for the stability of pp150-associated nucleocapsids.* J Virol, 2011. **85**(14): p. 7129-41.

71. Dai, X., et al., *The smallest capsid protein mediates binding of the essential tegument protein pp150 to stabilize DNA-containing capsids in human cytomegalovirus.* PLoS Pathog, 2013. **9**(8): p. e1003525.

72. Buchkovich, N.J., T.G. Maguire, and J.C. Alwine, *Role of the endoplasmic reticulum chaperone BiP, SUN domain proteins, and dynein in altering nuclear*

morphology during human cytomegalovirus infection. J Virol, 2010. **84**(14): p. 7005-17.

73. Johnson, D.C. and J.D. Baines, *Herpesviruses remodel host membranes for virus egress.* Nat Rev Microbiol, 2011. **9**(5): p. 382-94.

74. Sanchez, V., et al., *Accumulation of virion tegument and envelope proteins in a stable cytoplasmic compartment during human cytomegalovirus replication: characterization of a potential site of virus assembly.* J Virol, 2000. **74**(2): p. 975-86.

75. Das, S., et al., *Identification of human cytomegalovirus genes important for biogenesis of the cytoplasmic virion assembly complex.* J Virol, 2014. **88**(16): p. 9086-99.

76. Das, S., A. Vasanji, and P.E. Pellett, *Three-dimensional structure of the human cytomegalovirus cytoplasmic virion assembly complex includes a reoriented secretory apparatus.* J Virol, 2007. **81**(21): p. 11861-9.

77. Alwine, J.C., *The human cytomegalovirus assembly compartment: a masterpiece of viral manipulation of cellular processes that facilitates assembly and egress.* PLoS Pathog, 2012. **8**(9): p. e1002878.

78. Meissner, C.S., et al., *A leucine zipper motif of a tegument protein triggers final envelopment of human cytomegalovirus.* J Virol, 2012. **86**(6): p. 3370-82.

79. Schauflinger, M., et al., *The tegument protein UL71 of human cytomegalovirus is involved in late envelopment and affects multivesicular bodies.* J Virol, 2011. **85**(8): p. 3821-32.

80. Schauflinger, M., et al., *Analysis of human cytomegalovirus secondary envelopment by advanced electron microscopy.* Cellular Microbiology, 2013. **15**(2): p. 305-314.

81. Smith, R.M., S. Kosuri, and J.A. Kerry, *Role of human cytomegalovirus tegument proteins in virion assembly.* Viruses, 2014. **6**(2): p. 582-605.

82. Goodrum, F., et al., *Human cytomegalovirus sequences expressed in latently infected individuals promote a latent infection in vitro.* Blood, 2007. **110**(3): p. 937-45.

83. Sinclair, J., *Human cytomegalovirus: Latency and reactivation in the myeloid lineage.* J Clin Virol, 2008. **41**(3): p. 180-5.

84. Sinclair, J.H. and M.B. Reeves, *Human cytomegalovirus manipulation of latently infected cells.* Viruses, 2013. **5**(11): p. 2803-24.

85. Jarvis, M.A. and J.A. Nelson, *Human cytomegalovirus tropism for endothelial cells: not all endothelial cells are created equal.* J Virol, 2007. **81**(5): p. 2095-101.

86. Pampou, S., et al., *Cytomegalovirus genome and the immediate-early antigen in cells of different layers of human aorta.* Virchows Arch, 2000. **436**(6): p. 539-52.

87. Reeves, M.B., et al., *Vascular endothelial and smooth muscle cells are unlikely to be major sites of latency of human cytomegalovirus in vivo.* J Gen Virol, 2004. **85**(Pt 11): p. 3337-41.

88. Simmons, P., K. Kaushansky, and B. Torok-Storb, *Mechanisms of cytomegalovirus-mediated myelosuppression: perturbation of stromal cell*

function versus direct infection of myeloid cells. Proc Natl Acad Sci U S A, 1990. **87**(4): p. 1386-90.

89. Jarvis, M.A. and J.A. Nelson, *Molecular basis of persistence and latency*, in *Human Herpesviruses: Biology, Therapy, and Immunoprophylaxis*, A. Arvin, et al., Editors. 2007: Cambridge.

90. Soderberg-Naucler, C., K.N. Fish, and J.A. Nelson, *Reactivation of latent human cytomegalovirus by allogeneic stimulation of blood cells from healthy donors.* Cell, 1997. **91**(1): p. 119-26.

91. Goodrum, F., et al., *Differential outcomes of human cytomegalovirus infection in primitive hematopoietic cell subpopulations.* Blood, 2004. **104**(3): p. 687-95.

92. Powers, C. and K. Fruh, *Rhesus CMV: an emerging animal model for human CMV.* Med Microbiol Immunol, 2008. **197**(2): p. 109-15.

93. Schleiss, M.R., *Nonprimate models of congenital cytomegalovirus (CMV) infection: gaining insight into pathogenesis and prevention of disease in newborns.* ILAR J, 2006. **47**(1): p. 65-72.

94. Reddehase, M.J., J. Podlech, and N.K. Grzimek, *Mouse models of cytomegalovirus latency: overview.* J Clin Virol, 2002. **25 Suppl 2**: p. S23-36.

95. Orloff, S.L., et al., *Cytomegalovirus latency promotes cardiac lymphoid neogenesis and accelerated allograft rejection in CMV naive recipients.* Am J Transplant, 2011. **11**(1): p. 45-55.

96. Berges, B.K. and A. Tanner, *Modelling of human herpesvirus infections in humanized mice.* J Gen Virol, 2014. **95**(Pt 10): p. 2106-17.

97. Hakki, M., et al., *HCMV infection of humanized mice after transplantation of G-CSF-mobilized peripheral blood stem cells from HCMV-seropositive donors.* Biol Blood Marrow Transplant, 2014. **20**(1): p. 132-5.

98. Smith, M.S., et al., *Granulocyte-colony stimulating factor reactivates human cytomegalovirus in a latently infected humanized mouse model.* Cell Host Microbe, 2010. **8**(3): p. 284-91.

99. Wightman, B., I. Ha, and G. Ruvkun, *Posttranscriptional regulation of the heterochronic gene lin-14 by lin-4 mediates temporal pattern formation in C. elegans.* Cell, 1993. **75**(5): p. 855-62.

100. Olsen, P.H. and V. Ambros, *The lin-4 regulatory RNA controls developmental timing in Caenorhabditis elegans by blocking LIN-14 protein synthesis after the initiation of translation.* Dev Biol, 1999. **216**(2): p. 671-80.

101. Lee, R.C., R.L. Feinbaum, and V. Ambros, *The C. elegans heterochronic gene lin-4 encodes small RNAs with antisense complementarity to lin-14.* Cell, 1993. **75**(5): p. 843-54.

102. Friedman, R.C., et al., *Most mammalian mRNAs are conserved targets of microRNAs.* Genome Research, 2009. **19**(1): p. 92-105.

103. Saini, H.K., S. Griffiths-Jones, and A.J. Enright, *Genomic analysis of human microRNA transcripts.* Proc Natl Acad Sci U S A, 2007. **104**(45): p. 17719-24.

104. Ha, M. and V.N. Kim, *Regulation of microRNA biogenesis.* Nat Rev Mol Cell Biol, 2014. **15**(8): p. 509-24.

105. Chendrimada, T.P., et al., *TRBP recruits the Dicer complex to Ago2 for microRNA processing and gene silencing.* Nature, 2005. **436**(7051): p. 740-4.

106. Tetreault, N. and V. De Guire, *miRNAs: Their discovery, biogenesis and mechanism of action.* Clinical Biochemistry, 2013. **46**(10-11): p. 842-845.

107. Hutvagner, G. and P.D. Zamore, *A microRNA in a multiple-turnover RNAi enzyme complex.* Science, 2002. **297**(5589): p. 2056-60.

108. Hammond, S.M., et al., *Argonaute2, a link between genetic and biochemical analyses of RNAi.* Science, 2001. **293**(5532): p. 1146-1150.

109. Mourelatos, Z., et al., *miRNPs: a novel class of ribonucleoproteins containing numerous microRNAs.* Genes Dev, 2002. **16**(6): p. 720-8.

110. Helwak, A., et al., *Mapping the human miRNA interactome by CLASH reveals frequent noncanonical binding.* Cell, 2013. **153**(3): p. 654-65.

111. Guo, H., et al., *Mammalian microRNAs predominantly act to decrease target mRNA levels.* Nature, 2010. **466**(7308): p. 835-40.

112. Wilczynska, A. and M. Bushell, *The complexity of miRNA-mediated repression.* Cell Death Differ, 2015. **22**(1): p. 22-33.

113. Baek, D., et al., *The impact of microRNAs on protein output.* Nature, 2008. **455**(7209): p. 64-U38.

114. Fabian, M.R., N. Sonenberg, and W. Filipowicz, *Regulation of mRNA Translation and Stability by microRNAs.* Annual Review of Biochemistry, Vol 79, 2010. **79**: p. 351-379.

115. Farazi, T.A., et al., *Identification of distinct miRNA target regulation between breast cancer molecular subtypes using AGO2-PAR-CLIP and patient datasets.* Genome Biology, 2014. **15**(1).

116. Jacobsen, A., et al., *Analysis of microRNA-target interactions across diverse cancer types.* Nat Struct Mol Biol, 2013. **20**(11): p. 1325-32.

117. Reinhart, B.J., et al., *The 21-nucleotide let-7 RNA regulates developmental timing in Caenorhabditis elegans.* Nature, 2000. **403**(6772): p. 901-6.

118. Abrahante, J.E., et al., *The Caenorhabditis elegans hunchback-like gene lin-57/hbl-1 controls developmental time and is regulated by microRNAs.* Dev Cell, 2003. **4**(5): p. 625-37.

119. Lee, R.C. and V. Ambros, *An extensive class of small RNAs in Caenorhabditis elegans.* Science, 2001. **294**(5543): p. 862-4.

120. Pfeffer, S., et al., *Identification of virus-encoded microRNAs.* Science, 2004. **304**(5671): p. 734-6.

121. Bentwich, I., et al., *Identification of hundreds of conserved and nonconserved human microRNAs.* Nat Genet, 2005. **37**(7): p. 766-70.

122. Xie, Z., et al., *Expression of Arabidopsis MIRNA genes.* Plant Physiol, 2005. **138**(4): p. 2145-54.

123. Morin, R.D., et al., *Application of massively parallel sequencing to microRNA profiling and discovery in human embryonic stem cells.* Genome Res, 2008. **18**(4): p. 610-21.

124. Mendes, N.D., A.T. Freitas, and M.F. Sagot, *Current tools for the identification of miRNA genes and their targets.* Nucleic Acids Research, 2009. **37**(8): p. 2419-2433.

125. Lim, L.P., et al., *The microRNAs of Caenorhabditis elegans.* Genes & Development, 2003. **17**(8): p. 991-1008.

126. Lai, E.C., et al., *Computational identification of Drosophila microRNA genes.* Genome Biology, 2003. **4**(7).

127. Nam, J.W., et al., *Human microRNA prediction through a probabilistic co-learning model of sequence and structure.* Nucleic Acids Research, 2005. **33**(11): p. 3570-3581.

128. Kozomara, A. and S. Griffiths-Jones, *miRBase: annotating high confidence microRNAs using deep sequencing data.* Nucleic Acids Research, 2014. **42**(D1): p. D68-D73.

129. John, B., et al., *Human MicroRNA targets.* PLoS Biol, 2004. **2**(11): p. e363.

130. Betel, D., et al., *Comprehensive modeling of microRNA targets predicts functional non-conserved and non-canonical sites.* Genome Biol, 2010. **11**(8): p. R90.

131. Krek, A., et al., *Combinatorial microRNA target predictions.* Nature Genetics, 2005. **37**(5): p. 495-500.

132. Lewis, B.P., et al., *Prediction of mammalian microRNA targets.* Cell, 2003. **115**(7): p. 787-98.

133. Lewis, B.P., C.B. Burge, and D.P. Bartel, *Conserved seed pairing, often flanked by adenosines, indicates that thousands of human genes are microRNA targets.* Cell, 2005. **120**(1): p. 15-20.

134. Miranda, K.C., et al., *A pattern-based method for the identification of microRNA binding sites and their corresponding heteroduplexes.* Cell, 2006. **126**(6): p. 1203-1217.

135. Kertesz, M., et al., *The role of site accessibility in microRNA target recognition.* Nature Genetics, 2007. **39**(10): p. 1278-1284.

136. Kiriakidou, M., et al., *A combined computational-experimental approach predicts human microRNA targets.* Genes Dev, 2004. **18**(10): p. 1165-78.

137. Rehmsmeier, M., et al., *Fast and effective prediction of microRNA/target duplexes.* Rna-a Publication of the Rna Society, 2004. **10**(10): p. 1507-1517.

138. Alexiou, P., et al., *Lost in translation: an assessment and perspective for computational microRNA target identification.* Bioinformatics, 2009. **25**(23): p. 3049-3055.

139. Karginov, F.V., et al., *A biochemical approach to identifying microRNA targets.* Proc Natl Acad Sci U S A, 2007. **104**(49): p. 19291-6.

140. Easow, G., A.A. Teleman, and S.M. Cohen, *Isolation of microRNA targets by miRNP immunopurification.* Rna-a Publication of the Rna Society, 2007. **13**(8): p. 1198-1204.

141. Hafner, M., et al., *Transcriptome-wide identification of RNA-binding protein and microRNA target sites by PAR-CLIP.* Cell, 2010. **141**(1): p. 129-41.

142. Chi, S.W., et al., *Argonaute HITS-CLIP decodes microRNA-mRNA interaction maps.* Nature, 2009. **460**(7254): p. 479-86.

143. Helwak, A. and D. Tollervey, *Mapping the miRNA interactome by cross-linking ligation and sequencing of hybrids (CLASH).* Nat Protoc, 2014. **9**(3): p. 711-28.

144. Bellutti, F., et al., *Identification of RISC-Associated Adenoviral MicroRNAs, a Subset of Their Direct Targets, and Global Changes in the Targetome upon Lytic Adenovirus 5 Infection.* Journal of Virology, 2015. **89**(3): p. 1608-1627.

145. Harwig, A., A.T. Das, and B. Berkhout, *Retroviral microRNAs.* Current Opinion in Virology, 2014. **7**: p. 47-54.

146. Whisnant, A.W., et al., *Identification of Novel, Highly Expressed Retroviral MicroRNAs in Cells Infected by Bovine Foamy Virus.* Journal of Virology, 2014. **88**(9): p. 4679-4686.

147. Imperiale, M.J., *Polyomavirus miRNAs: the beginning.* Current Opinion in Virology, 2014. **7**: p. 29-32.

148. Stark, T.J., et al., *High-Resolution Profiling and Analysis of Viral and Host Small RNAs during Human Cytomegalovirus Infection.* Journal of Virology, 2012. **86**(1): p. 226-235.

149. Walz, N., et al., *A Global Analysis of Evolutionary Conservation among Known and Predicted Gammaherpesvirus MicroRNAs.* Journal of Virology, 2010. **84**(2): p. 716-728.

150. Grey, F., et al., *Identification and characterization of human cytomegalovirus-encoded microRNAs.* J Virol, 2005. **79**(18): p. 12095-9.

151. Nachmani, D., et al., *Diverse herpesvirus microRNAs target the stress-induced immune ligand MICB to escape recognition by natural killer cells.* Cell Host Microbe, 2009. **5**(4): p. 376-85.

152. Stern-Ginossar, N., et al., *Host immune system gene targeting by a viral miRNA.* Science, 2007. **317**(5836): p. 376-81.

153. Stern-Ginossar, N., et al., *Analysis of human cytomegalovirus-encoded microRNA activity during infection.* J Virol, 2009. **83**(20): p. 10684-93.

154. Pegtel, D.M., M.D. van de Garde, and J.M. Middeldorp, *Viral miRNAs exploiting the endosomal-exosomal pathway for intercellular cross-talk and immune evasion.* Biochim Biophys Acta, 2011. **1809**(11-12): p. 715-21.

155. Brandstadter, J.D. and Y. Yang, *Natural killer cell responses to viral infection.* J Innate Immun, 2011. **3**(3): p. 274-9.

156. Yokoyama, W.M., *Specific and non-specific natural killer cell responses to viral infection.* Adv Exp Med Biol, 2005. **560**: p. 57-61.

157. Jonjic, S., et al., *Immune evasion of natural killer cells by viruses.* Current Opinion in Immunology, 2008. **20**(1): p. 30-38.

158. Kim, Y., et al., *Human cytomegalovirus clinical strain-specific microRNA miR-UL148D targets the human chemokine RANTES during infection.* PLoS Pathog, 2012. **8**(3): p. e1002577.

159. Everett, H. and G. McFadden, *Apoptosis: an innate immune response to virus infection.* Trends in Microbiology, 1999. **7**(4): p. 160-165.

160. Abend, J.R., T. Uldrick, and J.M. Ziegelbauer, *Regulation of tumor necrosis factor-like weak inducer of apoptosis receptor protein (TWEAKR) expression by Kaposi's sarcoma-associated herpesvirus microRNA prevents TWEAK-induced apoptosis and inflammatory cytokine expression.* J Virol, 2010. **84**(23): p. 12139-51.

161. Ziegelbauer, J.M., C.S. Sullivan, and D. Ganem, *Tandem array-based expression screens identify host mRNA targets of virus-encoded microRNAs.* Nat Genet, 2009. **41**(1): p. 130-4.

162. Lee, S.H., et al., *BclAF1 restriction factor is neutralized by proteasomal degradation and microRNA repression during human cytomegalovirus infection.* Proceedings of the National Academy of Sciences of the United States of America, 2012. **109**(24): p. 9575-9580.

163. Kong, S., et al., *The type III histone deacetylase Sirt1 protein suppresses p300-mediated histone H3 lysine 56 acetylation at Bclaf1 promoter to inhibit T cell activation.* J Biol Chem, 2011. **286**(19): p. 16967-75.

164. Saffert, R.T. and R.F. Kalejta, *Inactivating a cellular intrinsic immune defense mediated by Daxx is the mechanism through which the human cytomegalovirus pp71 protein stimulates viral immeiate-early gene expression.* Journal of Virology, 2006. **80**(8): p. 3863-3871.

165. Grey, F., et al., *A Viral microRNA Down-Regulates Multiple Cell Cycle Genes through mRNA 5 ' UTRs.* Plos Pathogens, 2010. **6**(6).

166. Salvant, B.S., E.A. Fortunato, and D.H. Spector, *Cell cycle dysregulation by human cytomegalovirus: influence of the cell cycle phase at the time of infection and effects on cyclin transcription.* J Virol, 1998. **72**(5): p. 3729-41.

167. Hertel, L. and E.S. Mocarski, *Global analysis of host cell gene expression late during cytomegalovirus infection reveals extensive dysregulation of cell cycle gene expression and induction of Pseudomitosis independent of US28 function.* J Virol, 2004. **78**(21): p. 11988-2011.

168. Wolf, D., K. Hug, and S.P. Goff, *TRIM28 mediates primer binding site-targeted silencing of Lys1,2 tRNA-utilizing retroviruses in embryonic cells.* Proc Natl Acad Sci U S A, 2008. **105**(34): p. 12521-6.

169. Wolf, D. and S.P. Goff, *TRIM28 mediates primer binding site-targeted silencing of murine leukemia virus in embryonic cells.* Cell, 2007. **131**(1): p. 46-57.

170. Bunch, H., et al., *TRIM28 regulates RNA polymerase II promoter-proximal pausing and pause release.* Nat Struct Mol Biol, 2014. **21**(10): p. 876-83.

171. Perng, Y.C., et al., *Human Cytomegalovirus pUL79 Is an Elongation Factor of RNA Polymerase II for Viral Gene Transcription.* Plos Pathogens, 2014. **10**(8).

172. Hook, L.M., et al., *Cytomegalovirus miRNAs target secretory pathway genes to facilitate formation of the virion assembly compartment and reduce cytokine secretion.* Cell Host Microbe, 2014. **15**(3): p. 363-73.

173. Lin, X., et al., *miR-K12-7-5p encoded by Kaposi's sarcoma-associated herpesvirus stabilizes the latent state by targeting viral ORF50/RTA.* PLoS One, 2011. **6**(1): p. e16224.

174. Lu, F., et al., *Epigenetic regulation of Kaposi's sarcoma-associated herpesvirus latency by virus-encoded microRNAs that target Rta and the cellular Rbl2-DNMT pathway.* J Virol, 2010. **84**(6): p. 2697-706.

175. Lu, C.C., et al., *MicroRNAs encoded by Kaposi's sarcoma-associated herpesvirus regulate viral life cycle.* EMBO Rep, 2010. **11**(10): p. 784-90.

176. Bellare, P. and D. Ganem, *Regulation of KSHV lytic switch protein expression by a virus-encoded microRNA: an evolutionary adaptation that fine-tunes lytic reactivation.* Cell Host Microbe, 2009. **6**(6): p. 570-5.

177. Grey, F., et al., *A human cytomegalovirus-encoded microRNA regulates expression of multiple viral genes involved in replication.* PLoS Pathog, 2007. **3**(11): p. e163.

178. Umbach, J.L., et al., *MicroRNAs expressed by herpes simplex virus 1 during latent infection regulate viral mRNAs.* Nature, 2008. **454**(7205): p. 780-3.

179. Tang, S., A. Patel, and P.R. Krause, *Novel Less-Abundant Viral MicroRNAs Encoded by Herpes Simplex Virus 2 Latency-Associated Transcript and Their Roles*

in Regulating ICP34.5 and ICP0 mRNAs. Journal of Virology, 2009. **83**(3): p. 1433-1442.

180. Riaz, A., et al., *Ovine herpesvirus-2-encoded microRNAs target virus genes involved in virus latency.* J Gen Virol, 2014. **95**(Pt 2): p. 472-80.

181. Li, Q., et al., *Genetic disruption of KSHV major latent nuclear antigen LANA enhances viral lytic transcriptional program.* Virology, 2008. **379**(2): p. 234-44.

182. Lei, X., et al., *Regulation of NF-kappaB inhibitor IkappaBalpha and viral replication by a KSHV microRNA.* Nat Cell Biol, 2010. **12**(2): p. 193-9.

183. Skalsky, R.L., et al., *Kaposi's sarcoma-associated herpesvirus encodes an ortholog of miR-155.* J Virol, 2007. **81**(23): p. 12836-45.

184. Gottwein, E., et al., *A viral microRNA functions as an orthologue of cellular miR-155.* Nature, 2007. **450**(7172): p. 1096-9.

185. Sin, S.H., Y.B. Kim, and D.P. Dittmer, *Latency locus complements MicroRNA 155 deficiency in vivo.* J Virol, 2013. **87**(21): p. 11908-11.

186. Boss, I.W., et al., *A Kaposi's sarcoma-associated herpesvirus-encoded ortholog of microRNA miR-155 induces human splenic B-cell expansion in NOD/LtSz-scid IL2Rgammanull mice.* J Virol, 2011. **85**(19): p. 9877-86.

187. Zhao, Y., et al., *Critical role of the virus-encoded microRNA-155 ortholog in the induction of Marek's disease lymphomas.* PLoS Pathog, 2011. **7**(2): p. e1001305.

188. Bughio, F., D.A. Elliott, and F. Goodrum, *An endothelial cell-specific requirement for the UL133-UL138 locus of human cytomegalovirus for efficient virus maturation.* J Virol, 2013. **87**(6): p. 3062-75.

189. Smith, J.L., et al., *Induction of the cellular microRNA, Hs_154, by West Nile virus contributes to virus-mediated apoptosis through repression of antiapoptotic factors.* J Virol, 2012. **86**(9): p. 5278-87.

190. Bellutti, F., et al., *Identification of RISC-Associated Adenoviral MicroRNAs, a Subset of Their Direct Targets, and Global Changes in the Targetome upon Lytic Adenovirus 5 Infection.* J Virol, 2015. **89**(3): p. 1608-27.

191. Lee, S.H., et al., *BclAF1 restriction factor is neutralized by proteasomal degradation and microRNA repression during human cytomegalovirus infection.* Proc Natl Acad Sci U S A, 2012. **109**(24): p. 9575-80.

192. Wang, H., et al., *CD147 deficiency blocks IL-8 secretion and inhibits lung cancer-induced osteoclastogenesis.* Biochem Biophys Res Commun, 2015.

193. Park, B., et al., *Granulin is a soluble cofactor for toll-like receptor 9 signaling.* Immunity, 2011. **34**(4): p. 505-13.

194. Chung, A.W., et al., *Galectin-3 regulates the innate immune response of human monocytes.* J Infect Dis, 2013. **207**(6): p. 947-56.

195. Ferraz, L.C., et al., *Lack of galectin-3 alters the balance of innate immune cytokines and confers resistance to Rhodococcus equi infection.* Eur J Immunol, 2008. **38**(10): p. 2762-75.

196. Yu, C., et al., *TMEM74, a lysosome and autophagosome protein, regulates autophagy.* Biochem Biophys Res Commun, 2008. **369**(2): p. 622-9.

197. Makrypidi, G., et al., *Mannose 6 dephosphorylation of lysosomal proteins mediated by acid phosphatases Acp2 and Acp5.* Mol Cell Biol, 2012. **32**(4): p. 774-82.

198. Ganley, I.G., E. Espinosa, and S.R. Pfeffer, *A syntaxin 10-SNARE complex distinguishes two distinct transport routes from endosomes to the trans-Golgi in human cells.* Journal of Cell Biology, 2008. **180**(1): p. 159-172.

199. Skalsky, R.L., et al., *The viral and cellular microRNA targetome in lymphoblastoid cell lines.* PLoS Pathog, 2012. **8**(1): p. e1002484.

200. Malterer, G., L. Dolken, and J. Haas, *The miRNA-targetome of KSHV and EBV in human B-cells.* RNA Biol, 2011. **8**(1): p. 30-4.

201. Haecker, I. and R. Renne, *HITS-CLIP and PAR-CLIP advance viral miRNA targetome analysis.* Crit Rev Eukaryot Gene Expr, 2014. **24**(2): p. 101-16.

202. Gottwein, E., et al., *Viral microRNA targetome of KSHV-infected primary effusion lymphoma cell lines.* Cell Host Microbe, 2011. **10**(5): p. 515-26.

203. Dolken, L., et al., *Systematic analysis of viral and cellular microRNA targets in cells latently infected with human gamma-herpesviruses by RISC immunoprecipitation assay.* Cell Host Microbe, 2010. **7**(4): p. 324-34.

204. Pavelin, J., et al., *Systematic microRNA analysis identifies ATP6V0C as an essential host factor for human cytomegalovirus replication.* PLoS Pathog, 2013. **9**(12): p. e1003820.

205. Riley, K.J., T.A. Yario, and J.A. Steitz, *Association of Argonaute proteins and microRNAs can occur after cell lysis.* RNA, 2012. **18**(9): p. 1581-5.

206. Baek, D., et al., *The impact of microRNAs on protein output.* Nature, 2008. **455**(7209): p. 64-71.

207. Hsu, C.Y., et al., *The Epstein-Barr virus-encoded microRNA MiR-BART9 promotes tumor metastasis by targeting E-cadherin in nasopharyngeal carcinoma.* PLoS Pathog, 2014. **10**(2): p. e1003974.

208. Shen, Z.Z., et al., *Comprehensive analysis of human cytomegalovirus microRNA expression during lytic and quiescent infection.* PLoS One, 2014. **9**(2): p. e88531.

209. Yu, D., et al., *Construction of a self-excisable bacterial artificial chromosome containing the human cytomegalovirus genome and mutagenesis of the diploid TRL/IRL13 gene.* J Virol, 2002. **76**(5): p. 2316-28.

210. Livak, K.J. and T.D. Schmittgen, *Analysis of relative gene expression data using real-time quantitative PCR and the 2(T)(-Delta Delta C) method.* Methods, 2001. **25**(4): p. 402-408.

211. Carroll, A.P., et al., *Alternative mRNA fates identified in microRNA-associated transcriptome analysis.* BMC Genomics, 2012. **13**: p. 561.

212. Shimakami, T., et al., *Stabilization of hepatitis C virus RNA by an Ago2-miR-122 complex.* Proc Natl Acad Sci U S A, 2012. **109**(3): p. 941-6.

213. Cipriano, D.J., et al., *Structure and regulation of the vacuolar ATPases.* Biochim Biophys Acta, 2008. **1777**(7-8): p. 599-604.

214. Lynch, C.J. and S.H. Adams, *Branched-chain amino acids in metabolic signalling and insulin resistance.* Nat Rev Endocrinol, 2014. **10**(12): p. 723-36.

215. Martin, S., B. Saha, and J.L. Riley, *The battle over mTOR: an emerging theatre in host-pathogen immunity.* PLoS Pathog, 2012. **8**(9): p. e1002894.

216. Clippinger, A.J., T.G. Maguire, and J.C. Alwine, *Human cytomegalovirus infection maintains mTOR activity and its perinuclear localization during amino acid deprivation.* J Virol, 2011. **85**(18): p. 9369-76.

217. Clippinger, A.J., T.G. Maguire, and J.C. Alwine, *The changing role of mTOR kinase in the maintenance of protein synthesis during human cytomegalovirus infection.* J Virol, 2011. **85**(8): p. 3930-9.

218. Payton, M. and S. Coats, *Cyclin E2, the cycle continues.* Int J Biochem Cell Biol, 2002. **34**(4): p. 315-20.

219. Jault, F.M., et al., *Cytomegalovirus infection induces high levels of cyclins, phosphorylated Rb, and p53, leading to cell cycle arrest.* J Virol, 1995. **69**(11): p. 6697-704.

220. Kalejta, R.F. and T. Shenk, *Manipulation of the cell cycle by human cytomegalovirus.* Front Biosci, 2002. **7**: p. d295-306.

221. Garner, O.B., et al., *Timing of galectin-1 exposure differentially modulates nipah virus entry and syncytium formation in endothelial cells.* J Virol, 2015. **89**(5): p. 2520-9.

222. Yang, M.L., et al., *Galectin-1 binds to influenza virus and ameliorates influenza virus pathogenesis.* J Virol, 2011. **85**(19): p. 10010-20.

223. Thurston, T.L., et al., *Galectin 8 targets damaged vesicles for autophagy to defend cells against bacterial invasion.* Nature, 2012. **482**(7385): p. 414-8.

224. Mercier, S., et al., *Galectin-1 promotes HIV-1 infectivity in macrophages through stabilization of viral adsorption.* Virology, 2008. **371**(1): p. 121-9.

225. Paz, I., et al., *Galectin-3, a marker for vacuole lysis by invasive pathogens.* Cell Microbiol, 2010. **12**(4): p. 530-44.

226. Chen, S.S., et al., *Downregulating galectin-3 inhibits proinflammatory cytokine production by human monocyte-derived dendritic cells via RNA interference.* Cell Immunol, 2015. **294**(1): p. 44-53.

227. Zhang, H., et al., *High expression of nucleobindin 2 mRNA: an independent prognostic factor for overall survival of patients with prostate cancer.* Tumour Biol, 2014. **35**(3): p. 2025-8.

228. de Alba, E. and N. Tjandra, *Structural studies on the Ca2+-binding domain of human nucleobindin (calnuc).* Biochemistry, 2004. **43**(31): p. 10039-49.

229. Panda, D., et al., *RNAi screening reveals requirement for host cell secretory pathway in infection by diverse families of negative-strand RNA viruses.* Proc Natl Acad Sci U S A, 2011. **108**(47): p. 19036-41.

230. Suratanee, A., et al., *Detecting host factors involved in virus infection by observing the clustering of infected cells in siRNA screening images.* Bioinformatics, 2010. **26**(18): p. i653-8.

231. Kolokoltsov, A.A., et al., *Small interfering RNA profiling reveals key role of clathrin-mediated endocytosis and early endosome formation for infection by respiratory syncytial virus.* J Virol, 2007. **81**(14): p. 7786-800.

232. Wen, X., et al., *An siRNA screen of membrane trafficking genes highlights pathways common to HIV-1 and M-PMV virus assembly and release.* PLoS One, 2014. **9**(9): p. e106151.

233. Kilcher, S., et al., *siRNA screen of early poxvirus genes identifies the AAA+ ATPase D5 as the virus genome-uncoating factor.* Cell Host Microbe, 2014. **15**(1): p. 103-12.

234. Lavanya, M., et al., *siRNA screen for genes that affect Junin virus entry uncovers voltage-gated calcium channels as a therapeutic target.* Sci Transl Med, 2013. **5**(204): p. 204ra131.

235. Panda, D., et al., *Genome-wide RNAi screen identifies SEC61A and VCP as conserved regulators of Sindbis virus entry.* Cell Rep, 2013. **5**(6): p. 1737-48.

236. Su, W.C., et al., *Pooled RNAi screen identifies ubiquitin ligase Itch as crucial for influenza A virus release from the endosome during virus entry.* Proc Natl Acad Sci U S A, 2013. **110**(43): p. 17516-21.

237. Baril, M., et al., *Genome-wide RNAi screen reveals a new role of a WNT/CTNNB1 signaling pathway as negative regulator of virus-induced innate immune responses.* PLoS Pathog, 2013. **9**(6): p. e1003416.

238. Karlas, A., et al., *Genome-wide RNAi screen identifies human host factors crucial for influenza virus replication.* Nature, 2010. **463**(7282): p. 818-22.

239. Cao, D., et al., *Combined proteomic-RNAi screen for host factors involved in human hepatitis delta virus replication.* RNA, 2009. **15**(11): p. 1971-9.

240. Hao, L., et al., *Drosophila RNAi screen identifies host genes important for influenza virus replication.* Nature, 2008. **454**(7206): p. 890-3.

241. Schoggins, J.W., et al., *Pan-viral specificity of IFN-induced genes reveals new roles for cGAS in innate immunity.* Nature, 2014. **505**(7485): p. 691-5.

242. Schoggins, J.W., et al., *A diverse range of gene products are effectors of the type I interferon antiviral response.* Nature, 2011. **472**(7344): p. 481-5.

243. Johnson, D.C. and J.D. Baines, *Herpesviruses remodel host membranes for virus egress.* Nature Reviews Microbiology, 2011. **9**(5): p. 382-394.

244. Sanchez, V., et al., *Accumulation of Virion Tegument and Envelope Proteins in a Stable Cytoplasmic Compartment during Human Cytomegalovirus Replication: Characterization of a Potential Site of Virus Assembly.* Journal of Virology, 2000. **74**(2): p. 975-986.

245. Das, S., A. Vasanji, and P.E. Pellett, *Three-Dimensional Structure of the Human Cytomegalovirus Cytoplasmic Virion Assembly Complex Includes a Reoriented Secretory Apparatus.* Journal of Virology, 2007. **81**(21): p. 11861-11869.

246. Das, S. and P.E. Pellett, *Members of the HCMV US12 family of predicted heptaspanning membrane proteins have unique intracellular distributions, including association with the cytoplasmic virion assembly complex.* Virology, 2007. **361**(2): p. 263-73.

247. Das, S. and P.E. Pellett, *Spatial relationships between markers for secretory and endosomal machinery in human cytomegalovirus-infected cells versus those in uninfected cells.* J Virol, 2011. **85**(12): p. 5864-79.

248. Boesen, T. and P. Nissen, *V for victory--a V1-ATPase structure revealed.* EMBO Rep, 2009. **10**(11): p. 1211-2.

249. Mellman, I., *Endocytosis and molecular sorting.* Annu Rev Cell Dev Biol, 1996. **12**: p. 575-625.

250. Reaves, B. and G. Banting, *Vacuolar ATPase inactivation blocks recycling to the trans-Golgi network from the plasma membrane.* FEBS Lett, 1994. **345**(1): p. 61-6.

251. Clague, M.J., et al., *Vacuolar ATPase activity is required for endosomal carrier vesicle formation.* J Biol Chem, 1994. **269**(1): p. 21-4.

252. van Weert, A.W., et al., *Transport from late endosomes to lysosomes, but not sorting of integral membrane proteins in endosomes, depends on the vacuolar proton pump.* J Cell Biol, 1995. **130**(4): p. 821-34.

253. Maxfield, F.R. and T.E. McGraw, *Endocytic recycling.* Nat Rev Mol Cell Biol, 2004. **5**(2): p. 121-32.

254. Paroutis, P., N. Touret, and S. Grinstein, *The pH of the secretory pathway: measurement, determinants, and regulation.* Physiology (Bethesda), 2004. **19**: p. 207-15.

255. Hassinen, A., et al., *Functional organization of Golgi N- and O-glycosylation pathways involves pH-dependent complex formation that is impaired in cancer cells.* J Biol Chem, 2011. **286**(44): p. 38329-40.

256. Wang, W., et al., *pH dependent effect of glycosylation on protein stability.* Eur J Pharm Sci, 2008. **33**(2): p. 120-7.

257. Carr, C.M. and P.S. Kim, *A spring-loaded mechanism for the conformational change of influenza hemagglutinin.* Cell, 1993. **73**(4): p. 823-32.

258. Huang, Q., et al., *Early steps of the conformational change of influenza virus hemagglutinin to a fusion active state: stability and energetics of the hemagglutinin.* Biochim Biophys Acta, 2003. **1614**(1): p. 3-13.

259. Chandran, K., et al., *Endosomal proteolysis of the Ebola virus glycoprotein is necessary for infection.* Science, 2005. **308**(5728): p. 1643-5.

260. Simmons, G., et al., *Inhibitors of cathepsin L prevent severe acute respiratory syndrome coronavirus entry.* Proc Natl Acad Sci U S A, 2005. **102**(33): p. 11876-81.

261. Sun-Wada, G.H., et al., *The a3 isoform of V-ATPase regulates insulin secretion from pancreatic beta-cells.* J Cell Sci, 2006. **119**(Pt 21): p. 4531-40.

262. Peters, C., et al., *Trans-complex formation by proteolipid channels in the terminal phase of membrane fusion.* Nature, 2001. **409**(6820): p. 581-8.

263. Peri, F. and C. Nusslein-Volhard, *Live imaging of neuronal degradation by microglia reveals a role for v0-ATPase a1 in phagosomal fusion in vivo.* Cell, 2008. **133**(5): p. 916-27.

264. Liegeois, S., et al., *The V0-ATPase mediates apical secretion of exosomes containing Hedgehog-related proteins in Caenorhabditis elegans.* J Cell Biol, 2006. **173**(6): p. 949-61.

265. Hiesinger, P.R., et al., *The v-ATPase V0 subunit a1 is required for a late step in synaptic vesicle exocytosis in Drosophila.* Cell, 2005. **121**(4): p. 607-20.

266. Gonzaleznoriega, A., et al., *Chloroquine Inhibits Lysosomal-Enzyme Pinocytosis and Enhances Lysosomal Enzyme-Secretion by Impairing Receptor Recycling.* Journal of Cell Biology, 1980. **85**(3): p. 839-852.

267. Bowman, B.J. and E.J. Bowman, *Mutations in subunit c of the vacuolar ATPase confer resistance to bafilomycin and identify a conserved antibiotic binding site.* Journal of Biological Chemistry, 2002. **277**(6): p. 3965-3972.

268. Ho, M.N., et al., *Vma13 Encodes a 54-Kda Vacuolar H+-Atpase Subunit Required for Activity but Not Assembly of the Enzyme Complex in Saccharomyces-Cerevisiae.* Journal of Biological Chemistry, 1993. **268**(24): p. 18286-18292.

269. Baravalle, G., et al., *Transferrin recycling and dextran transport to lysosomes is differentially affected by bafilomycin, nocodazole, and low temperature.* Cell Tissue Res, 2005. **320**(1): p. 99-113.

270. Trischler, M., W. Stoorvogel, and O. Ullrich, *Biochemical analysis of distinct Rab5- and Rab11-positive endosomes along the transferrin pathway.* J Cell Sci, 1999. **112 (Pt 24)**: p. 4773-83.

271. Hu, C., D. Hardee, and F. Minnear, *Membrane fusion by VAMP3 and plasma membrane t-SNAREs.* Exp Cell Res, 2007. **313**(15): p. 3198-209.

272. Kroschewski, R., A. Hall, and I. Mellman, *Cdc42 controls secretory and endocytic transport to the basolateral plasma membrane of MDCK cells.* Nat Cell Biol, 1999. **1**(1): p. 8-13.

273. Harris, K.P. and U. Tepass, *Cdc42 and vesicle trafficking in polarized cells.* Traffic, 2010. **11**(10): p. 1272-9.

274. Kane, P.M., *The where, when, and how of organelle acidification by the yeast vacuolar H+-ATPase.* Microbiol Mol Biol Rev, 2006. **70**(1): p. 177-91.

275. Henkel, J.R., et al., *Selective perturbation of early endosome and/or trans-Golgi network pH but not lysosome pH by dose-dependent expression of influenza M2 protein.* J Biol Chem, 1999. **274**(14): p. 9854-60.

276. Potel, C., et al., *Herpes simplex virus type 1 glycoprotein B sorting in hippocampal neurons.* J Gen Virol, 2003. **84**(Pt 10): p. 2613-24.

277. Wisner, T.W. and D.C. Johnson, *Redistribution of cellular and herpes simplex virus proteins from the trans-golgi network to cell junctions without enveloped capsids.* J Virol, 2004. **78**(21): p. 11519-35.

278. Alconada, A., et al., *Intracellular traffic of herpes simplex virus glycoprotein gE: characterization of the sorting signals required for its trans-Golgi network localization.* J Virol, 1999. **73**(1): p. 377-87.

279. Theiler, R.N. and T. Compton, *Distinct glycoprotein O complexes arise in a post-Golgi compartment of cytomegalovirus-infected cells.* J Virol, 2002. **76**(6): p. 2890-8.

280. Glorioso, J., et al., *Inhibition of glycosylation of herpes simplex virus glycoproteins: identification of antigenic and immunogenic partially glycosylated glycopeptides on the cell surface membrane.* Virology, 1983. **126**(1): p. 1-18.

281. Sharma, S., et al., *HCMV gB shares structural and functional properties with gB proteins from other herpesviruses.* Virology, 2013. **435**(2): p. 239-49.

282. Roche, S., et al., *Crystal structure of the low-pH form of the vesicular stomatitis virus glycoprotein G.* Science, 2006. **313**(5784): p. 187-91.

283. Dollery, S.J., et al., *Low-pH-dependent changes in the conformation and oligomeric state of the prefusion form of herpes simplex virus glycoprotein B are separable from fusion activity.* J Virol, 2011. **85**(19): p. 9964-73.

284. Murphy, E., et al., *Suppression of immediate-early viral gene expression by herpesvirus-coded microRNAs: implications for latency.* Proc Natl Acad Sci U S A, 2008. **105**(14): p. 5453-8.

285. Mijaljica, D., M. Prescott, and R.J. Devenish, *V-ATPase engagement in autophagic processes.* Autophagy, 2011. **7**(6): p. 666-8.

286. Wei, B.L., et al., *Inhibition of lysosome and proteasome function enhances human immunodeficiency virus type 1 infection.* J Virol, 2005. **79**(9): p. 5705-12.

287. Fredericksen, B.L., et al., *Inhibition of endosomal/lysosomal degradation increases the infectivity of human immunodeficiency virus.* J Virol, 2002. **76**(22): p. 11440-6.

288. Beale, R., et al., *A LC3-interacting motif in the influenza A virus M2 protein is required to subvert autophagy and maintain virion stability.* Cell Host Microbe, 2014. **15**(2): p. 239-47.

289. Zhao, J., et al., *Manipulation of autophagy by HCMV infection is involved in mTOR and influences the replication of virus.* Acta Biochim Biophys Sin (Shanghai), 2013. **45**(11): p. 979-81.

290. Wen, H.J., et al., *Enhancement of autophagy during lytic replication by the Kaposi's sarcoma-associated herpesvirus replication and transcription activator.* J Virol, 2010. **84**(15): p. 7448-58.

291. Tovilovic, G., et al., *mTOR-independent autophagy counteracts apoptosis in herpes simplex virus type 1-infected U251 glioma cells.* Microbes Infect, 2013. **15**(8-9): p. 615-24.

292. Richetta, C., et al., *Sustained autophagy contributes to measles virus infectivity.* PLoS Pathog, 2013. **9**(9): p. e1003599.

293. Mohl, B.P., et al., *Hepatitis C virus-induced autophagy is independent of the unfolded protein response.* J Virol, 2012. **86**(19): p. 10724-32.

294. McFarlane, S., et al., *Early induction of autophagy in human fibroblasts after infection with human cytomegalovirus or herpes simplex virus 1.* J Virol, 2011. **85**(9): p. 4212-21.

295. Leidal, A.M., et al., *Subversion of autophagy by Kaposi's sarcoma-associated herpesvirus impairs oncogene-induced senescence.* Cell Host Microbe, 2012. **11**(2): p. 167-80.

296. Huang, J., et al., *Coordinated regulation of autophagy and apoptosis determines endothelial cell fate during Dengue virus type 2 infection.* Mol Cell Biochem, 2014. **397**(1-2): p. 157-65.

297. Chiramel, A.I., N.R. Brady, and R. Bartenschlager, *Divergent roles of autophagy in virus infection.* Cells, 2013. **2**(1): p. 83-104.

298. Campbell, G.R. and S.A. Spector, *Inhibition of human immunodeficiency virus type-1 through autophagy.* Curr Opin Microbiol, 2013. **16**(3): p. 349-54.

299. Buckingham, E.M., et al., *Autophagy and the effects of its inhibition on varicella-zoster virus glycoprotein biosynthesis and infectivity.* J Virol, 2014. **88**(2): p. 890-902.

300. Alexander, D.E., et al., *Analysis of the role of autophagy in replication of herpes simplex virus in cell culture.* J Virol, 2007. **81**(22): p. 12128-34.

301. Umashankar, M., et al., *A novel human cytomegalovirus locus modulates cell type-specific outcomes of infection.* PLoS Pathog, 2011. **7**(12): p. e1002444.

302. Rue, C.A., et al., *A cyclooxygenase-2 homologue encoded by rhesus cytomegalovirus is a determinant for endothelial cell tropism.* J Virol, 2004. **78**(22): p. 12529-36.

303. Britt, W.J., *Human cytomegalovirus: propagation, quantification, and storage.* Curr Protoc Microbiol, 2010. **Chapter 14**: p. Unit 14E 3.